Final Report

Personal Air Transportation
DSE Team 5
DID-10

Technische Universiteit Delft

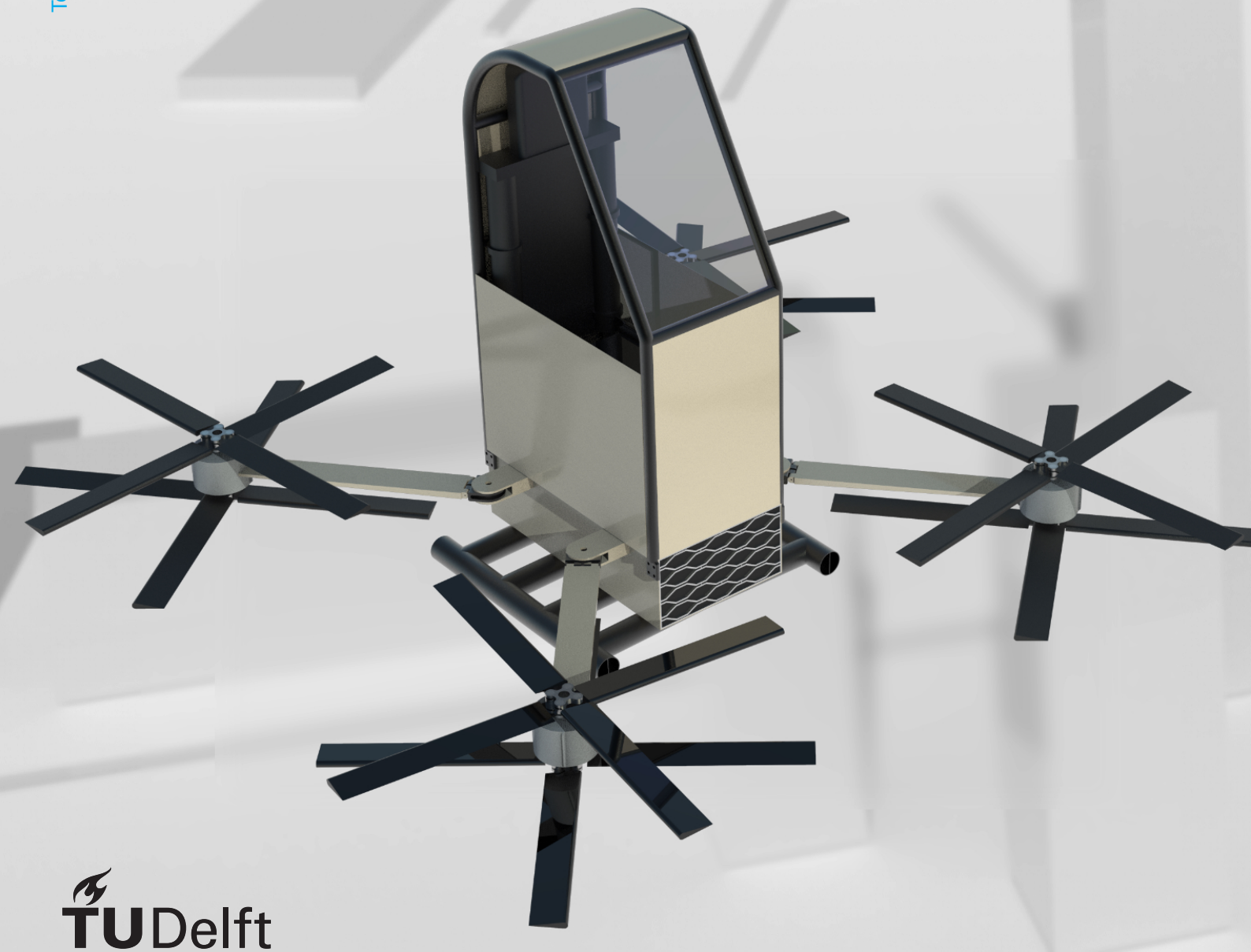

TU Delft

- This page is intentionally left blank -

Final Report

Personal Air Transportation

by

DSE Team 5

Students:	Aida van de Wetering	4665090
	Aslan Bagirov	4668820
	Derin Ulcay	4562836
	Dirk de Fuijk	4562968
	Josephine Siebert Pockelé	4644425
	Johan Nicolaas van As	4540735
	Julius Caron	4653548
	Martijn van Roij	4670183
	Maurits Rietveld	4546458
	Muhammad Sebtain	4532589
Project duration:	*November 9, 2020 – January 28, 2021*	
Tutor:	Dr. Dimitrios Zarouchas,	TU Delft
Coaches:	Dr. Wei Yu,	TU Delft
	Dr. Ing. Christoph Bode	TU Braunschweig
TA:	Robert Coenen	TU Delft

TU Delft

Preface

Delft, January 26, 2021

This report is the final design report by group 5 of the 2020 fall Design Synthesis Exercise of the TU Delft, Faculty of Aerospace Engineering. The conceptual design process is outlined for a personal air transportation system.

The team would like to acknowledge the help from the teaching staff, external experts and companies to achieve the presented design. In no particular order, we would like to thank:

Dr. Dimitrios Zarouchas,	*TU Delft*
Dr. Wei Yu,	*TU Delft*
Dr. Ing. Christoph Bode,	*TU Braunschweig*
Robert Coenen,	*TU Delft*
Dr. Bruno Santos,	*TU Delft*
Dr. Irene Fernandez Villegas,	*TU Delft*
Novita Saraswati,	*TNO*
Sanne Castro,	*Joulz*
Mr. Kovářiček,	*MGM Compro*
Mr. Švec,	*MGM Compro*

Executive Overview

Market research

A market analysis was performed, looking at research on urban air mobility (UAM). The advantages of UAM, which are mainly the decrease in transportation time and reduced pressure on other transportation methods. Estimations on market demand range between 0.3% and 5.5% of the transportation market, showing there is a potential need in the order of thousands vehicles. Vehicle sharing is discussed, showing a strong growth in this market.Estimates for the UAM market of 15.54 billion in 2027 and 74 billion in 2035. Competitors were described, showing that competitors have generally high air speeds (+100km/h) compared to cars and show many companies planning their products' launch into market in the next decade. A survey on UAM showed that the public is generally enthusiastic, preferring rental over retail vehicles and showing a high willingness to use UAM, given the user feels safe.

Market analysis showed that the vehicle designed in this project is specifically advantageous in its compact size and personal use. While regulations, noise and reluctance towards automation are disadvantages in the potential consumers. The project may use the opportunity that there are for now few competitors, and that Europe consists of many dense urban regions where traffic congestion is an issue.

System functions and requirements

From the client needs, risk management, market research, the functionality of the vehicle. Requirements are generated and presented in Table 3.1 and 3.2. Some requirements on the system influence the design more than others, leading to labels on requirements, which are killer requirements (important for the mission and hard to comply with), key requirements (important to the mission) and finally driving requirements (which drive the design process more than other requirements do).

Table 1: Killer and Key Requirements Table

Requirement ID	Requirement	Source	Urgency
PAT-UR-PERF-04	The operational range shall be 30km.	Client	Killer
PAT-UR-PERF-03	The system shall not exceed a volume of 1 m3 in undeployed state.	Client	Killer
PAT-UR-PERF-02	The system shall be able to transport a user mass of 100kg	Client	Killer
PAT-UR-PERF-12	The system shall be controllable via a smartphone or a tablet.	Fun. 1.1	Key
PAT-UR-PERF-08	The cruise altitude of the system shall not exceed 20m.	Client	Key
PAT-UR-05	The system shall be piloted by the user.	Fun. 4.2.3	Key
PAT-UR-01	The system shall be rent-able by the user.	Client, Market analysis	Key
PAT-SYS.O-FUNC-02	The system shall support daily operation for 5 consecutive days.	Client	Key
PAT-SYS-FUNC-10	The system shall self-diagnose its structural state.	Fun. 1.1.1	Key
PAT-SYS-FUNC-03	The system shall report structural state and system state to the user.	Fun. 1.4	Key
PAT-SYS-CONS-05	The system shall have a smaller environmental footprint than its competitors	Sustainability	Key

Concept trade-off

From the requirements and functionality of the design, three concepts were generated, shown in the Figure 1:

The first concept is the battery-powered quadcopter concept. Its advantage are good dynamics and controllability and relatively low noise production, while fitting it in a $1m^3$ volume is a challenge.

The second concept is the helipack concept. Advantage is the relative simplicity and higher potential to meet the volume requirement. It has some major noise and safety concerns that would be impossible to overcome.

The last concept is called the ice cream cone, due to its original shape. The main advantage of this concept is that the volume requirement can easily be met with the foldable structure of the cabin. Due

to the hydrogen fuel cell system, the energy storage mass is also easily kept under the required 30% of the total mass. The big downside is the almost non-existent infrastructure for hydrogen refuelling and the safety concerns surrounding the use of hydrogen.

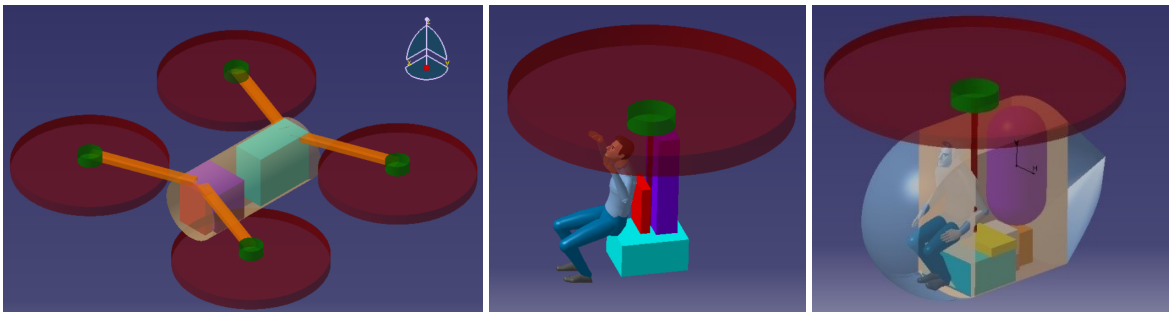

(a) Quadcopter (b) Helipack (c) Ice Cream Cone

Figure 1: Overview of the design concepts in their most worked out form.

The next step was to conduct a trade-off between the three concepts, with the following trade-off criteria: the cost of the system, the use of public space, the range and endurance, sustainability, noise, safety, interaction, stability and control and maintenance.

The trade-off had the following outcome: the helipack ended as the best design. However, the helipack had some fatal flaws, which came up during design analysis. Therefore, a combination of all concepts was considered. Mixing and matching resulted in a quadcopter at its core with coaxial counter-rotating propellers from the helipack. The ice cream cone concepts contributes its full encapsulation. It turned out that the new generated concept scored considerably better than the initial concepts. the configuration is shown in the Figure 2.

Figure 2: The final concept resulting from the trade-off.

Propulsion, Power and Performance

The power to rotate the propeller is electrical power and provided by the battery. The propeller needed to be modelled and the battery needed to be sized.

Modelling the propellers is a study on its own, so the decision was made to focus on statistical models. Next to that, the focus was on the folding mechanism and counter-rotating coaxial configuration. The axle-brake power is determined by assuming both the propellers act on the same disc and are operating at the same RPM. In this way, the interaction of the two propellers is taken into account. Four sets of propellers are needed in the design, with the resulting total power of $56.7kW$. To meet the volume requirement, the propellers need to be foldable. The blades are attached to a hub in sets of two opposing blades. These pairs of blades fold into overlapping positions. Automated actuators are used to fold the blades and secure the locking. The material of the propellers will be Aluminum 6061-T6, considering its mechanical properties, shaping properties and cost effectiveness. Similar size CFRP propellers are found, as data on Aluminum propellers was not available and estimation methods were not applicable due to the size and loading combination. The radius of the propeller turned out to be $1.3m$ as optimal value, concerning foldability and performance. The volume of the CFRP blades were used, in

combination with the density of Aluminum 6061-T6 and resulted in a hub weight of $0.35kg$ per propeller.

DC motors are used, as a DC configuration outweighs the drawbacks of the added weight and space of a power inverter, although a DC motor is slightly heavier and more expensive. The voltage, efficiency and other parameters need to be known to design and size the rest of the system, a statistical model is used to estimate the mass and size of a motor based on its output power. Several companies were contacted in search for a motor that fit the requirements and constraints. MGM Compro was very helpful and helped with the selection of the motor and provided details for a slightly customised configuration that would make the motor of better use for the vehicle and the interface with other components such as the controller and batteries. The RET30 fits the requirements. Other than technical information, experimental data was provided by MGM Compro. The motor controller was provided by MGM Compro as well, and it turned out that no gearbox was required for this configuration.

Licerion lithium metal cells provided by Sion power are used to design the propulsion battery system. These cells provide $3.82V$, have a capacity of $20Ahr$ and can provide a discharge rate of 2C. Furthermore the cell mass is equal to $158g$. Using these cells, the battery system is sized according to the voltage requirement of motors and capacity requirement for maximum power and endurance. The final configuration calculated to meet these requirements consists of 16 cells in series and 40 cells in parallel. A total of 4 battery packs connected in parallel are designed to fit in the structural battery casing. Each pack consist of 16 cells in series and 10 cells in parallel. Furthermore, each battery pack is connected to the Battery Management System (BMS) as well. The BMS consists of a monitoring unit and a control unit. The cooling is done by fans protected with filters, provided by Johnson electric and controlled by the BMS.

The horizontal thrust will counter the drag force, whereas the vertical thrust force will counter the weight. The power draw for hover equals $64.475kW$ and the energy required to cover the distance of 30 kilometers is $1.626MJ$. This leaves $174.08MJ$ for hovering. As a result, the 45 minutes endurance is met.

To charge the vehicle, a low-power infrastructure is created. An ACDC converter is required, which adds a little weight to the system, but is cheaper and fast-charging damages the battery. It weighs $1.2kg$ and has dimensions $14 * 25 * 4cm$.The ACDC converter communicates with the battery controller to ensure the right voltage and currents are supplied. If a DC source is directly connected to the system, it shall detect this and relay the power and communications directly to the battery controller.

Structures and Materials

The detailed design of structures and materials consisted mainly of sizing and designing the specific structural components of the vehicle. The components that were analysed are the rotor beams, the beam hinges, the load-carrying battery casing, the landing gear and the user module frame.Before the design, a material consideration was performed. The trade-off between Aluminium and a CFRP Composite was done, and based on sustainability and the ease and flexibility in production, Aluminium was chosen for the final design. AL7075-T6 is to be used for the landing gear and user module frame due to its higher strength properties and AL6061-T6 for the rest of the structure.

The different structural components were designed for strength and deflection. For the beams this meant: the stress due to bending, shear stress and in the end the von Mises stress. In the hinge design, there are two nodes, for the two hinging points, Node A and Node B. At those nodes the hinge is designed for axial stress, shear stress and bearing stress. In the load carrying battery design the main loads in the structure are shear forces and bending moments due to thrust introduced into the structure through the beams and hinges. The landing gear was designed to a $0.33m$ drop test from CS27 small rotorcraft regulations. It is a typical skid landing gear with 8 struts and 2 skids.

Lastly the user module frame. It is made out of aluminium tubes like the landing gear. This element is also sized for the $0.33m$ drop test criteria as its main function is to protect the user in a crash. The shape of the frame is seen in Figure 3.

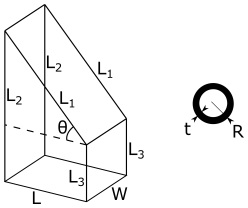

Figure 3: User module frame configuration

In the end dimensions were obtained for all these parts and components. The dimensions and angles are shown in

Table 2: Structural component dimensions overview

Hinge property	Value	Battery casing	Value	Beam property	Value	Landing gear property	Value	User module dimension	Length
Diameter 1 D_1	$4.2mm$	Thickness	$2.0mm$	Length R	$0.76m$	Beam Length L	$0.419m$	Length L	0.840
Diameter 2 D_2	$20mm$	Clearance top/bottom	$4.5mm$	Wall thickness t	$0.002m$	Placement Angle θ	$1.37°$	Width W	0.500
Thickness A t_A	$40.8mm$	Clearance sides	$13.5mm$	Height at root	$0.021m$	Cross-section Radius R	$40mm$	Angled Beam Length L_1	1.288
Thickness B t_B	$8mm$	Mass	$9.5kg$	Height at end	$0.008m$	Wall thickness t	$11.0mm$	Long Beam Length L_2	1.775
Hinge Mass	$0.44kg$			Mass	$1.009kg$	Landing gear mass	$24.43kg$	Short Beam Length L_3	0.778

Aerodynamics

As determined from the start of the project, the aerodynamic analysis of the vehicle would be minimal. However aerodynamics cannot be completely dismissed so a small drag and centre of pressure analysis was done. In comparison to the midterm, the analysis was not done in all directions and not just from the front side of the vehicle. The vehicle shape was simplified into a combination of multiple smaller simple shapes of which the drag is easily calculated. So the concept was estimated as a combination of spheres, cuboids, disks and cylinders in the drag and centre of pressure estimation. In the end rough estimates for the drag coefficient and centre of pressure were obtained in three flow directions. It was concluded that due to the low flow velocities the drag can be neglected for now, but in the future more elaborate aerodynamic analysis is necessary. This will be done using computational fluid dynamics and possibly wind tunnel testing.

Stability and Control

The means of control were first identified, from these thrust vectoring was chosen. In order to facilitate control in 6DOF the lower rotors spin clockwise while the upper rotors spin counterclockwise. Rolling and pitching motion is provided by thrust differential between the relevant coupled rotor sets. Yawing motion is achieved by an RPM differential of the lower rotors with respect to the upper rotors.

The plant of the control system consists of the motor and propeller model, the coaxial quadcopter dynamics model, and the sensor model. The motor and propeller model is linearly approximated for simplicity of control input. The nonlinear coaxial quadcopter dynamics model is built by setting up the equations of motion in MATLAB and Simulink. The input to the system are the individual thrust forces originating from the 8 rotors. In order to exploit well-developed linear control theories, this model is linearised about two trimming points: hover condition and cruise condition. In order to perform simulation, the centre of gravity limits and the mass moments of inertia are approximated. The open-loop systems are determined to be unstable.

In order to gain full observability, research on sensors is done and a selection is made. Besides the sensors available in the smart device, it was decided to include an IMU (including a magnetometer), a barometer, a LIDAR sensor, and a GPS sensor.

The system makes use of two different control schemes: VTOL and cruise. The former allows for positional control of the vehicle, while facilitating landing and takeoff in cross-wind situations. The latter implements velocity control throughout the operational speed envelope by means similar to gain scheduling.

For the controller type selection, a simple trade-off was made between Proportional–Integral–Derivative (PID) control, Model-predictive control (MPC), and a Linear Quadratic Regulator (LQR). For the hover control scheme a cascading control design with an LQR controller and a PID controller was chosen. For the cruise control scheme only an LQR controller was chosen.

A processor is required to run the flight control system. A general purpose microcontroller along with a digital signal processor (DSP) was used. After maturity of the design, an application specific integrated circuit (ASIC) processor may be developed.

The controller design parameters are found through trial-and-error until simulation results were deemed satisfactory. The closed-loop systems (hover and cruise) are stable with a worst case disk margin of greater than 2.5 dB and a phase margin 16^o.

Finally, a sensitivity analysis to the controller design parameters is performed and verification and validation procedures are discussed.

Operations

Operations aims to describe operational aspects of the design, which are communications, no-fly zones, interface with user, flight training, charging and finally vertiports, For communications, VHF radiois used in order to communicate with the ground-pilot, who keeps an eye on multiple vehicles. VHF radio is widely used in aviation and is reliable, therefore it is used for critical subsystems.

The requirement that the vehicle should avoid no-fly zones is fulfilled by a combination of warnings and a link to the control system that makes flying near these zones physically impossible. The safe-guarding system contains a GPS sensor in combination with a system that checks pre-defined no-fly locations with the GPS signal Interface with the user consists of a user panel, where the smartphone can be clicked in.

The user must be able to use a smartphone for user interaction and the user must be able to control the device. Controlling the vehicle requires the following information: airspeed, navigation(including location), altitude, communication options to ground pilot, system diagnosis information, and VTOL activation. The reliability of the smartphone is doubtful, therefore the vehicle must be controllable by the user panel for back-up in case of smartphone failure. The user panel will have a size of 40x14x5 cm to be legible. To have a view downward during VTOL, a camera is installed underneath the vehicle.

Since only direct flight control is automated and the user controls the vehicle in person, flight training is needed for user tasks such as deployment of vehicle, authentication, system start-up, route planning, VTOL procedures, safety procedures and communication procedures. These tasks have to be learned in user training, with a preferred focus on knowledge and procedural related learning goals, as skills are automated as much as possible. Learning methods are videos, mock vehicles and flight simulators.

The charging will take place while the vehicles are parked, requiring overnight charging as an option. Low-power charging is demanded as high-power charging is not good for battery-lifetime. Low-power charging is also advantageous in costs as no transformation house is needed to lower the voltage.

Vertiports are constructed to allow the user to VTOL to and from the destination. A number of 200 vehicles per vertiport is chosen. From the expected dimensions of VTOL pads, parking and charging, a vertipad concept can be constructed. A centre for maintenance is created, operating multiple vertiports. To transport the vehicle from the VTOL site, a platform with wheels big enough for supporting the bottom structure is needed, in combination with a elevation system to elevate the vehicle from the ground.

Other than vertiports, urban VTOL locations are created. Examples are sites on roofs of big shopping centres or other big buildings. For sites not on top of a building, bystander safety is important to take into account. The vehicle does this by sounds and lights. A total of 9 meters in diameter is needed as the diameter of the vehicle is 3.8 meters and it can stay in a radius of 1.5 meters.

Risk management

It is unavoidable that components in the vehicle have the risk to fail. Therefore, risk management is required. The procedure starts by identifying and assessing the risks. The risks are categorised between technical performance, safety, cost, and scheduling. A Failure Modes and Effect Analysis (FMEA) is done by the departments.

The costs are broken down into manufacturing, development and operational costs. For manufacturing, a margin is added to the inventory cost to account for uncertainties For development costs, the growth of the team is taken into account and a margin is added per person. To estimate the operational

costs risk, several profit scenarios are made, where the worst case scenario should comply with the requirements.

Other than specific subsystem failure, additional failure modes are present. Some risks are used to generate requirements, others became irrelevant after performing the trade-off, as preliminary design choices were made, or performing the FMEA already identified more specific subsystem risks. Mitigation plans are devised by the departments originating from the FMEA and for the general technical risk log. After the mitigation plans, the risks are decreased significantly.

Sustainability

With designing the rent-a-copter, sustainability has to be kept in mind. A balance between environmental, economic and social sustainability is needed to assure general sustainability. All three aspects are considered and discussed. For the environmental sustainability, a LCA is performed using OpenLCA to quantify the impact of one vehicle on the environment throughout one life cycle. Components that have the biggest impact on the environment have been identified. The potential that is directly related to the enhanced greenhouse effect is the global warming potential (GWP) and defines the carbon dioxide exhausted by a product. Figure 4 shows the components that have the largest GWP, hence are the bottlenecks of the rent-a-copter regarding CO_2 emissions.

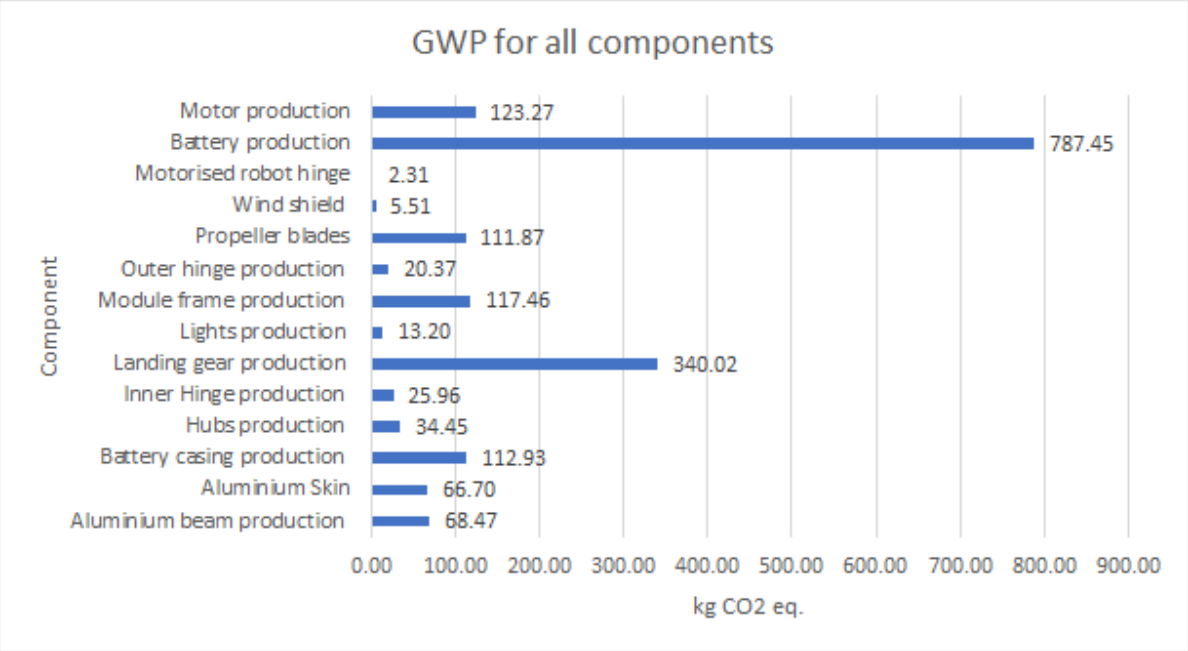

Figure 4: The GWP of the components present in the rent-a-copter.

Comparing the total GWP of rent-a-copter with a conventional car and an electric car, it can be concluded that, with some assumptions, the rent-a-copter exhaust 76% and 52% less carbon dioxide emissions per kilometer, respectively.

As the rent-a-copter is a one-of-a-kind product in a relatively new niche market, it is attractive for investors to invest money in it. With zero direct emissions produced during flight, which will be the standard in the (far) future, so it is not only investing in a product, but more in the future as well. Investing now will pay off in the future. These features make the rent-a-copter economically sustainable for the long term.

Social sustainability is achieved with the low noise level of the vehicle, the self-diagnosing system assuring that failures are detected before taking-off and the protection of the user against environmental conditions.

Final design

The individual design is finally integrated into a final design. Firstly, the compliance with the requirements is checked.

Requirement compliance

The killer and driving requirements mentioned earlier are all complied with. Table 1 shows the killing and driving requirements of the design. The weight requirements are complied with and taken into account as seen in Table 3. With this weight the system was designed for an operational range of 30km and the structural design was done such that the final design fits within $1m^3$. In the operations plan of the vehicle it becomes clear that the device is controllable with a mobile device, it is piloted by the user who has received some flight training and the vehicle is rent-able by the user for 5 consecutive days. In the control system design a maximum altitude of 20m is implemented. To recognise damage early on, the system has a self diagnosis system in place that reports to the user. Lastly from the LCA and the rest of the sustainability analysis the vehicle was found to have a very low environmental footprint compared to (electric) cars.

Mass budget

A mass budget has been set up to guide the sizing process of the vehicle and to give an overview of the distribution of mass in the finished product. The final mass budget can be found below in Table 3.

Table 3: The mass budget for the final vehicle configuration

Component	Mass [kg]
Contingency	17.4
Main motors	30.4
Battery	100.2
Landing gear	24.43
User + Luggage	110
ACDS and Sensors	2
Flight computer	2
Seat	7
Cabling	2.5
Wind shield	4.5
Propellers	5.76
Load-carrying battery casing	9.5
Battery auxiliary systems	9.5
Propeller connection beam	5.71
Vehicle skin	5.64
Hinges and connectors	4.9
Vehicle frame	8.56

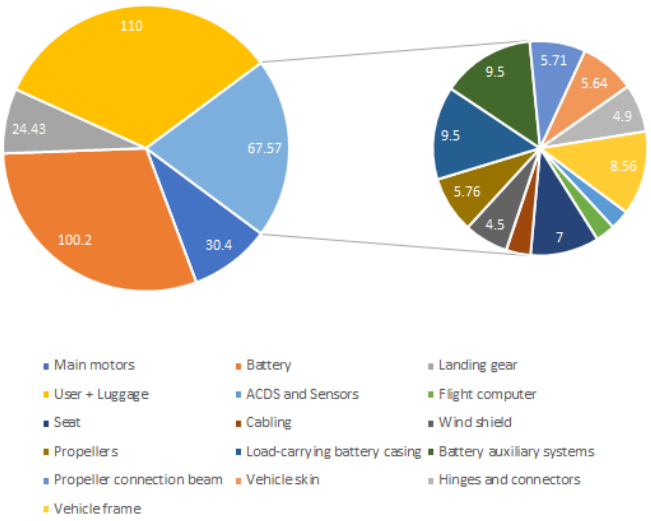

The final system features various mechanical and electrical components. in order to get an overview of the final system an electrical block diagram, a data handling diagram, a hardware diagram, and a software diagram are generated. In these diagrams the components and their interactions are presented. Finally, the configuration of the system and the external lay-out are found in the technical drawings of the system.

Before producing the product, it is vital to perform an analysis for the Reliability, Availability, Maintainability, and safety (RAMS analysis).

Self Diagnosis

In currently operational safety-critical systems the overwhelming design strategy to combat risk and uncertainty involves the allocation of sufficiently large safety margins in calculations, the use of redundant components, and the design of fail-operational systems. The high performance required (especially relating to mass) from aerospace systems limits the use of the mentioned strategies and lead to the

operational approaches of scheduling frequent inspections and periodic replacement of parts. With the current improvements in sensing technology and computation, a real-time self monitoring vehicle can be designed to replace the need for frequent inspections, to identify faults when they occur, to predict failure into the future, and to integrate with a degradation aware part replacement schedule. Resulting in a less costly, more sustainable, and safer system overall.

Production plan

The future production process has already been determined. The general flow is shown in Figure 5. The light green shows that some components and parts like the motors, battery cells and actuators are bought from external suppliers and are integrated in the product in the sub-assembly phase. The ”A” symbol shows the extensive inspection and testing between every stage of production. Also at the end full system quality control is performed.

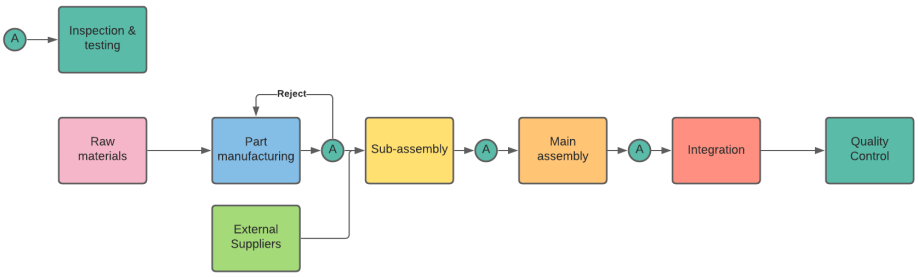

Figure 5: General production plan

For the different parts the part manufacturing methods were determined. To limit the environmental impact, some research was done on sustainability of specific manufacturing methods. Casting and hot forming were two processes that were preferred to be avoided. For the main assembly, the production of the complete arms with propulsion system attached will be a separate process, to ensure modularity in the design. The arms are not produced as being a specific arm for the front left part of the vehicle. The same is true for the battery modules. There are 4 compartments in the casing where 4 identical battery modules are installed. The integration phase in Figure 5 consists of installing and connecting the final cabling and hooking up all electronic systems.

Cost breakdown and Return on Investment

The costs are estimated by finding one-time costs, such as vertiport and development costs, and yearly costs, such as staff and value reduction of vehicles. The cost breakdown is given as follows:

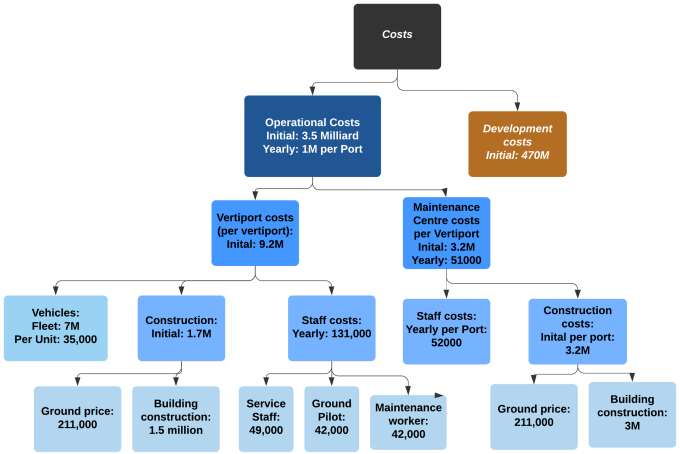

Figure 6: The Cost Breakdown structure.

Assuming a certain use of vehicle and distribution of payment plans of costumers, a plan was made to make profit. In this plan, vertiports keep getting build, as the production of 1000 vehicles per year keeps going on. Following this, it is estimated that break-even is reached after 12 years.

Future of the project

After this project, the system has some steps to be run through to get to a product in service. This is presented in Figure 7.

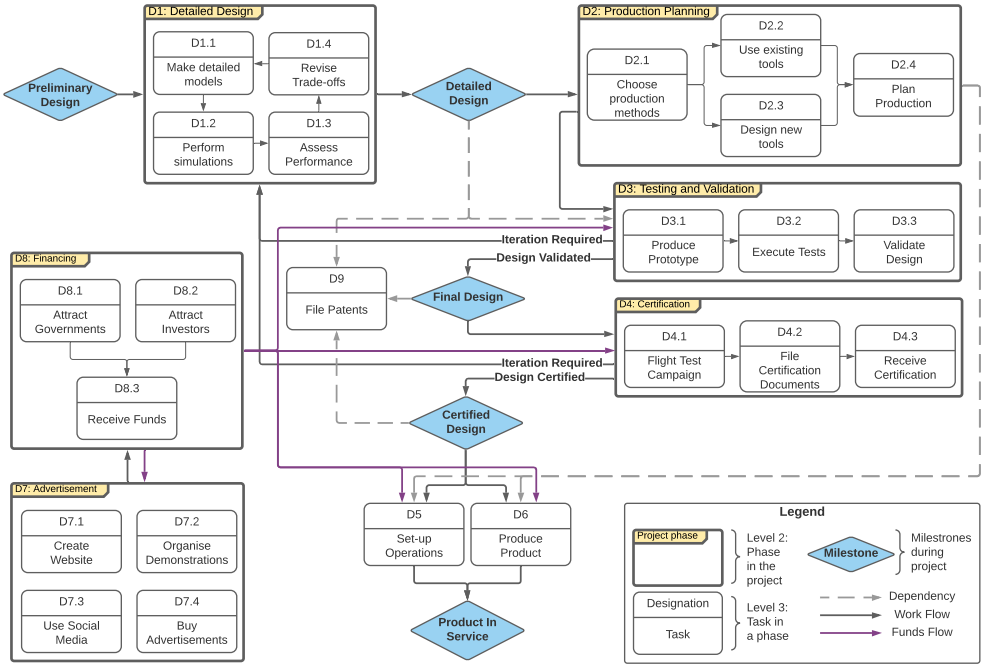

Figure 7: Flow diagram of the design and development logic.

Contents

List of Figures

List of Tables

Nomenclature

Abbreviations

V_{ce}	Vehicle-carried Earth reference frame
A	Acceptance
AMR	Add margins of redundancy
AP	Acidification Potential
ASIC	Application-specific instruction set processor
B	Body reference frame
BMS	Battery Management System
CAD	Computer-aided design
CATIA	Computer-aided three-dimensional interactive application
CMO	Change manner of operating
COG	Centre of gravity
CTC	Change technology choice
DimitriOS	Diagnostic Intelligent Maintenance Inference Test-Referencing Interface Operating System
DSP	Digital signal processor
EASA	European Aviation Safety Agency
EOL	End Of Life
FATO	Final Approach and Take-Off Area
fEP	freshwater Eutrophication Potential
fETP	freshwater Eco-toxicity Potential
FMEA	Failure Modes and Effects Analysis
FRU	Fossils Resource Use
GWP	Global Warming Potential
HTP	Human Toxicity Potential
ICAO	International Civil Aviation Organisation
IMU	Inertial measurement unit
LCA	Life Cycle Analysis
LCI	Life Cycle Inventory
LCIA	Life Cycle Impact Assessment
LIDAR	Light Detection And Ranging of Laser Imaging Detection And Ranging
LQR	Linear–quadratic regulator
LTI	Linear time-invariant (system)
LUP	Land Use Potential
MCU	Microcontroller unit
MMOI	Mass Moment Of Inertia
MPC	Model predictive control
ODP	Ozone Depletion Potential
PEF	Product Environmental Footprint
PID	Proportional–integral–derivative (controller)
POFP	Photo-chemical Ozone Formation Potential
PWM	Pulse-width modulation
RoI	Return of Investment
SHM	Strucutral Health Monitoring
TOW	Take-off weight
UAM	Urban Air Mobility
VHF	Very High Frequency
VR	Vehicle reference frame
VTOL	Vertical Take-Off and Landing
WSP	Water Scarcity Potential

Symbols

δ	Deformation	m
κ_{int}	Co-axial thrust inference factor	$[-]$
μ	Dynamic viscosity	kg/ms
ω	Rotational velocity	rad/s
ϕ	Angle of rotation around x-axis	rad
ψ	Angle of rotation around z-axis	rad
ρ	Density	kg/m^3

σ	Normal stress	Pa
τ	Shear stress	Pa
θ	Angle of rotation around y-axis	rad
θ	Deformation angle	rad
θ	Placement angle	rad
$C\vec{O}P$	Centre of pressure location vector	
$\vec{p}$	Position vector	
A	Area	m^2
B	Beam width	m
C	Battery C-rating	$[-]$
c	Maximum distance from normal axis	m
C_b	Noise correction factor	dB
C_D	Drag coefficient	$[-]$
$CTRL$	Controllability matrix	
D	Diameter	m
D	Drag force	N
D	Risk detection level	$[-]$
E	Energy	J
E	Young's modulus	Pa
F	Force	N
g	Gravitational acceleration	m/s^2
h	Altitude	m
h	Height	m
I	Area moment of inertia	m^4
I	Electrical current	A
I	Mass moment of inertia	kgm^2
J	Cost function	$[-]$
L	Length	m
L	Lift force	N
L	Risk likelihood	$[-]$
M	Mach number	$[-]$
M	Moment	Nm
m	Mass	kg
N	Number of what is in the subscript	$[-]$
Obs	Observability matrix	
P	Power	W
p	Rotational velocity around x-axis	rad/s
Q	Energy capacity	Ah
Q	First moment of area	m^3
Q	State weighting matrix	$[-]$
q	Rotational velocity around y-axis	rad/s
q	Shear flow	N/m
R	Control weighting matrix	$[-]$
R	Radius	m
r	Rotational velocity around z-axis	rad/s
S	Propeller disk area	m^2
S	Risk severity	$[-]$
SPL	Sound pressure level	dB
T	Thrust	N
T	Torque	Nm
t	Thickness	m
t	time	s
u	Velocity component in x-direction	m/s
V	Shear force	N
V	Velocity	m/s
v	Velocity	m/s
v	Velocity component in y-direction	m/s
W	Width	m
w	Deflection in z-direction	m
w	Velocity component in z-direction	m/s
X	Ground position x-coordinate	m
x	Distance along the x-axis	m
Y	Ground position y-coordinate	m
y	Distance along the y-axis	m
z	Distance along the z-axis	m

1 Introduction

Over the last few years, pressure on road infrastructure and public transportation has been steadily increasing due to increasingly rising demand. On average, a US worker spends 27 minutes per day, or 9 days per year, in transit. This results in a large amount of social, economical and health issues. Examples are more stress, leading to health problems, and loss of time, leading to loss of money.

During the COVID-19 pandemic, the popularity of utilisation of public transportation has decreased due to the increased health risks it might pose. There is no single consensus on what the future holds, but all major predictions point towards an even higher expected time in transit in the coming years.

One way to solve this issue is by alleviating the road infrastructure by taking to the skies. To solve the traffic issue, many concepts have been proposed for urban air transportation. Most of these consist of an air taxi type vehicle, where a trained pilot takes to user from point A to B. Both Airbus and Uber have made leaps in the development of their air taxis, but both still have many challenges to overcome.

Combining the need to alleviate traffic and to provide an independent mode of transport void of social contact leads to the concept of a personal air transportation system. This project aims to develop an early design for such a system over the course of 10 weeks.

At the start of the project, the mission and objectives were set out by the team to have a general guide through the project. The mission need statement reads as follows: *"The system will transfer a single person through an urban environment for daily applications."* From this mission need, the project objective is created: *"Make a conceptual design for an urban, user controllable air transportation system, that is self-diagnosing, by ten students in ten weeks."* [1]

The report consists of 3 large parts. First are 3 introductory chapters, which introduce the first steps taken in the project. They go over the market research, the system functions and requirements and a summary of the previously executed concept trade-off.

Next is the technical work done by the different departments of the team. First is the power, propulsion and performance; followed by structures and materials. The aerodynamics are also discussed, which closely ties in with the stability and control of the system. Then the operations of the system are presented. Lastly, the risk management and sustainable development are discussed.

The last chapters tie all this department work together. First is an overview of the entire system, followed by a suggested system for self-diagnosis. The production and business plans are also elaborated on, after which the future is discussed as a closing.

2
Market Research

In order to explore the world of personal urban air transportation and to know what is needed in such a vehicle, a market analysis makes sense. Such a market analysis aims to find market gaps and may generate some requirements on the design. This chapter covers the following subjects in order of appearance: Value of Urban air mobility, Focus Markets, Prediction of Market, Competition, Societal influences, Target Audience and finally market gap discussion with SWOT Analysis, where this project is discussed with respect to the market.

2.1. The Value of Urban Air Mobility

Urban air mobility (UAM) promises various advantages such as decongest road traffic, improve mobility, reduce transport time and reduce the load on public transport. Additionally, designing new transportation methods allows the use of new sustainable technologies, decreasing effects on pollution and the environment . The congestion of road traffic is of particular importance in the Netherlands. One of the most effective solutions is to make people use the road less [2], offering a big benefit for UAM. One major contributor to road congestion is the very low efficiency in terms of passengers per car, making a compact vehicle better in space utility. In the Netherlands for example, cars are occupied by on average 1.4 persons [3], using a big amount of unnecessary space for transport. Public transport experience huge pressure in the Netherlands as well, asking for load reduction[0]. Hence,

2.2. Focus Markets

As the system is a rental system, various uses of the system can be thought of, making clear the focus markets for personal, urban air transportation. Simply put, uses are categorised as commute, sightseeing and airport transit, also allowing the user to use it for daily transportation, for example groceries or shopping. An important question is how big these markets are and to what extend UAM might get a part in it.

Much research can be found on the possible market demands of UAM compared to other means of transportation being most predominantly cars and public transport. These researches have estimated the demand by means of elaborate tools, assuming certain costs per km and comparing that with cars and public transport. As the costs per km vary greatly per research however, the market shares vary greatly unfortunately. Looking at these results may give an indication of market demand.

Table 2.1: Demand estimates Netherlands, using number of cars in NL = 7200000 CBS[4]

% Market estimation	Vehicle buy demand	Demand Vehicle Sharing	Source
5.5	396000	16500	[5]
0.3	21600	900	[5]
0.7	50400	2100	[5]
4	288000	12000	[6]

This table uses the percentage of market, the number of personal cars in the Netherlands and the number of persons sharing a vehicle, to come to a number of vehicles on which is demand in The Netherlands. This might be underestimated as public transport is not taken into account.

One important side note is that often a new method of transportation generates new demand. This is the case for Uber, where 12 percent of rides is expected to not have occurred without Uber.(The impact of ride-hailing on vehicle miles travelled) This is hard to predict however. Still, one should keep in mind that demand may increase after the inception of UAM.

2.3. Market Prediction

This section aims to predict how the markets of vehicle sharing and urban air mobility will evolve over the years.

2.3.1. Prediction Vehicle Sharing

Road use has grown enormously from the 1950's, the stark increase in traffic jams show that is infrastructure is struggling to allow for more cars. Car and scooter sharing is rising in popularity over the past years, expecting more grow in this market, some suggesting a 9% market grow each year[7]. Car users become more accustomed to vehicle sharing and better see the values in terms of sustainability and economics. A survey on UAM also showed a high willingness for vehicle sharing in UAM [8].

2.3.2. Prediction Urban Air Mobility

Predicting the market size in the future is naturally highly complex, yet there are companies that have done some research on it. A market research of Porsche estimates the possibility of 74 billion in 2035 [9]. Other research presents a possible UAM market size of 15.54 Billion by 2027 [10].

The market share of this company is hard to estimate, but due to the small amount of UAM start-ups (explained in the next section), this can be a significant amount and be close to the values found in section 2.2.

In the end, a big market might be available. Transportation is an indispensable part of today's society, meaning a big market is definitely possible.

2.4. Competition

For this section, a list of competitors similar to our project are named. The list of options show that there are already many concepts and start-ups out there, promising to commercially start in the next decade. It becomes clear that only the Volocopter has an option for personal (1 person) transportation, and all others can transport more passengers. In addition, competitors have a significantly higher airspeed. Much research presents high air speeds as favourable. A motion efficiency comparison can be made, analysing the motion efficiency by dividing the speed over the required power. For cars, the required power depends on drag and ground friction, while for VTOL aircraft depends on drag and power to lift the device. Cars are hence much more motion efficient unless the speed increases, as then the power to lift the VTOL is needed for less time. Hence, urban air transport is much more feasible compared to cars at speeds higher than approximately 100km/h [11].

Looking at the competition, a rotorcraft is not uncommon, meaning there are competitors close to the configuration this project chose, as explained in chapter 4. Critical characteristics to fit a gap in the market are therefore that the vehicle must be highly compact, as the competitors use much more space than the volume requirement in Table 3.1.

Table 2.2: Market Competitors with important characteristics

Competitors	**Markets**	**Cruise speed [km/h]**	**Range [km]**	**First take-off**	**Comm. Intro**	**Pax**	**Flight control**
Airbus Vahana	Air taxi	190	50	2018	-	1	Autonomous
Airbus CityAirbus	Air taxi	120	30	2019	2023	4	Autonomous or Pilot
Jaunt Air Mobility	Air taxi	108	130	2020	2030	4	-
Lilium Jet	Air taxi	300	300	2019	2025	5	
Volocopter	Air taxi, personal	-	-	2016	2022	2	-
Ehang 216	Air taxi	130	35	2018	2020	2	Autonomous
AirspaceX MoBi	Air taxi	241	104	Unknown	2026	5	Pilot assisted, autonomous

(a) Airbus Vahana

(b) CityAirbus

(c) Jaunt Air

(d) Lilium Jet

(e) Volocopter

(f) Ehang 216

(g) AirspaceX MoBi

Figure 2.1: Market Competitors

2.5. Societal Analysis

A 1700 person survey showed much insight in societal views to many aspects of UAM [8]. Many showed excited by UAM (32%), with younger people (mid twenties) more excited that older. In addition, males were slightly more often excited than women about UAM. Willingness to fly was bout 55%, while 36% would feel safe and secure. Half of participants were neutral, most likely influenced by the lack of personal experience. Many views on UAM are that is a premium service, with a desire for affordable, inter-regional trips. After hearing concepts of vehicle sharing, many participants reacted positively. Some specific consideration might be given to security, vertiports, noise, ownership and pilots.

Security A 1700 person survey showed that there is a great preference for security screening before every urban air flight. 76% of participants would be willing to being subject to some security screening in advance of every flight, and 80% would prefer that passengers are screened before every flight.

Vertiport travel The same survey showed that people are willing to travel a maximum of 30 minutes to a vertiport, with car and public transport as the most preferred method of transportation to the vertiport.

Noise Noise concerns were highest for noise at home during morning hours and night, hence noise at those times is not preferred.

Ownership or rental Most participants were not interested in owning a UAM vehicles with only 17% interested. When owning a vehicle, they however did show interest in making their vehicle part of a fleet.

Pilot or automation When asked whether participants preferred pilots, ground pilots or automation, pilots were by far preferred, while automation was disliked. Hence, effort needs to be made for acceptance of automation if used.

Concluding, it can be said that there is a generally excited view on UAM, however showing that many are in need of more information on UAM. Taking a look at security is recommended, and making sure vertiports are not closer than 30min from home. Noise is already an important requirement. Rental is actually preferred by the public, hence is a good choice and might be a market gap, as no competitors employ this method. Finally, some kind of professorial piloting is definitely recommended for the costumer to fly with a feeling of safety.

2.6. Target Audience and Demographics

The characteristics of this transportation method together with the requirements go together with some specific audiences, and might be more applicable to certain regions than others. This led to a number of user personas and regions applicable to the system.

First of all, some requirements already constraint the user type and regions. The rental price of €20

a day is a low price, comparing to renting a car. Next, Since the product is an air transportation device controllable by the user itself, the user must use the product with responsibility, in other words, the user must be sufficiently mature.

The weight requirement is an important one, since the product only allows for a small extra amount of weight and not much volume to store it. Hence, the target audience must comply with this. The product is operated by the user, via a tablet, smartphone or smartwatch requiring the user to have some experience with them.

To give form to an understanding of the target audience, a number of persona's are described. These make up the audience for which the design will be made.

- **Daily Commuters**: The daily commuter travels between work and home, preferably not being bothered by car traffic jams. He/she flies to work in the morning during the working week, stores the vehicle somewhere close to the office and flies home at the end of the afternoon. He/She carries some small luggage such as a suitcase or small backpack.
- **Parent with baby**: The parent with the small child drops off the child to day-care and subsequently goes to work. He/She also does not want to be bothered by traffic.
- **Travellers**: The traveller generally comes from some transportation into the urban area, and hence wishes to travel between airports/train stations and various parts of the urban area, for example city centre. They often carry big backpacks or bigger suitcases. When they travel from airports, they might have cabin luggage already subject to specific dimensions.
- **Tourists**: Tourists wants to go sightseeing, hence travel between famous sites in the area. Having special lookout views over the city, doing something exciting or perhaps visit an attraction will be appealing. Flying in a vehicle might already be exciting for tourists. Taking photos is a big need for them.
- **Groups / Couples**: Small groups of people or couples might like flying together, for example as a group activity or to travel together. This means that they appreciate staying together in the air, hence flying in formation can be nice for this group.
- **Shopping Civilian**: Lastly, shopping civilians want to travel from home to the city centre, store it close to shopping areas and fly home. Most need for them shall be in the evening and weekends. Room should be available for shopping bags.

As discussed in section 2.5, males are more likely to use UAM than females, as well as younger people more likely than older people. This might be important as an addition for the target audience.

Next, a look can be taken in the demographics of the possible urban areas. The population of the Randstad and Ruhr-area has a sufficient degree of education and a high degree of middle-aged people. The same can be said for the education level of Paris and London. However, the mission in Paris and London is limited to within the city. Northern-Spain, Austria and Swiss suit the target audience as well. For Northern-Italy and North-East France, distances are larger between cities and hence are not favourable. [1]. Furthermore, the average weight of Europeans suits the weight requirement[2]. The people who live in the areas mentioned above are aware of the need to become more sustainable. As the product will be a sustainable way of commuting, this matches the target audience. Looking at regions, the range of the vehicle is 30km. This means that, assuming the vehicle can be charged at destination, a radius of 30km can be achieved.

2.7. Market Gap and Strengths, Weaknesses, Opportunities and Threats

Looking at the market research thus far, conclusions can be made on whether this project fits the market, and what characteristics are important for this market. This section is started with stating

[1] Eurostat. *Quick facts on European regions*. URL: `https://ec.europa.eu/eurostat/web/regions/statistics-illustrated` (visited on 11/17/2020)

[2] Worlddata. *Average sizes of men and women*. URL: `https://www.worlddata.info/average-bodyheight.php` (visited on 11/17/2020)

strengths, weaknesses, opportunities and threats towards the inception of the project's personal urban air vehicle.. They are given in the following graphic:

Table 2.3: SWOT analysis for product in market

Strengths		**Weaknesses**
Product is fit for large part of population, due to controllability and price		Audience reluctant to fly in automated vehicle without professional pilot
Compact vehicle advantageous as solution to road congestion		Audience reluctant about noise
One person is almost unheard of in current UAM projects		No regulations and infrastructure for UAM exist yet
Compact vehicle is good for storage and VTOL sites		
Not many professional pilots needed due to automation		
Emission free during operation, while much present-day transport is not emission free		
Air transportation allows for direct routes, making it fast		
Low cruise speed makes collisions easier to prevent		
Opportunities		**Threats**
Few Competitors		Requirement of low rental price per vehicle is low (5000 euro/year)
Dense Urban Regions in Europe		Low cruise speed is hard to compete with against other means of transport (40 km/h)
Pandemic generates need for personal travel		An accident may severely reduce credibility and willingness to use vehicle
Overflooded transport infrastructue calls for other transportation means		Development costs high and hard to predict
Car charging infrastructure already exists, energy infrastructure very good in urban areas		

After the established SWOT analysis, the weak and strong points become apparent.

Firstly, only one one-person urban air project is known, which means the design is a very specific vehicle. It is compact and thus making it possible to VTOL on more locations than its competitors, additionally being more compact than the one-person urban air competitor. It also means little volume is needed for storage of the vehicle, allowing for a larger number of stored vehicles in the same place. Another aspect is that the user can fly the device independently with only some training, being uncommon as other vehicles are automated or require a professional pilot. Looking at the user persona's, a luggage area is needed to comply with all persona's, with the need for luggage used by airplane travellers. On another note though, a discussion can be held whether the requirement of 40 km/h is disadvantageous for motion efficiency, making it harder to fit the market better than cars. Low speed does have advantages however, such as less piloting skills needed allowing the user to fly the vehicle. Users show a preference for pilot controlled instead of complete automation. This is satisfied by the quadcopter by allowing for easy control and possible take-over and guidance from ground pilots. In addition, looking at security and specifically pre-flight screenings are preferred by the public.

Finally, a rental system is actual preferred over retail, according to the discussed UAM survey.

3
System Functions and Requirements

The first step after the market analysis is to analyse the functions the system should execute under normal operation. This functional breakdown is described in section 3.1. Next, a set of requirements can be derived that the system has to meet. This combination of user, functional, risk and other requirements is discussed in section 3.2.

3.1. Functional Flow and Breakdown diagrams

A functional flow diagram visualises the chronological order of functions the system should provide to conduct a successfully mission. These functions have also been used to set up additional requirements. This chart can be found after Table 3.2 onwards. The diagram has a top level, which has been broken down to two levels further. Breaking this diagram down a level deeper and grouping tasks results in the functional breakdown structure, which can be found behind the functional flow diagram.

3.2. Requirements

During the previous phases of the project, an extensive analysis was done to determine the requirements of the system. Part of the requirements were given by the client for which this system is being designed. Others were found from the market analysis, the risk analysis and the functional breakdown of the system. The final set of requirements for the system to adhere to are presented in Table 3.1 and Table 3.2. These tables are updated with the updated functional breakdown.

Table 3.1: The Requirements Table, Part 1 of 2

Requirement ID	Requirement	Source	Urgency
PAT-UR-PERF-04	The operational range shall be 30km.	Client	Killer
PAT-UR-PERF-03	The system shall not exceed a volume of 1 m3 in undeployed state.	Client	Killer
PAT-UR-PERF-02	The system shall be able to transport a user mass of 100kg	Client	Killer
PAT-UR-PERF-12	The system shall be controllable via a smartphone or a tablet.	Fun. 1.1	Key
PAT-UR-PERF-08	The cruise altitude of the system shall not exceed 20m.	Client	Key
PAT-UR-05	The system shall be piloted by the user.	Fun. 4.2.3	Key
PAT-UR-01	The system shall be rent-able by the user.	Client, Market analysis	Key
PAT-SYS.O-FUNC-02	The system shall support daily operation for 5 consecutive days.	Client	Key
PAT-SYS-FUNC-10	The system shall self-diagnose its structural state.	Fun. 1.1.1	Key
PAT-SYS-FUNC-03	The system shall report structural state and system state to the user.	Fun. 1.4	Key
PAT-SYS-CONS-05	The system shall have a smaller environmental footprint than its competitors	Sustainability	Key
PAT-SYS.O-CONS-03	The landing and take-off clearance shall not exceed a circular area with a diameter smaller than 9.5m.	Fun. 3.1	Key
PAT-SYS-FUNC-16	The system shall transport maximum 10 kg of luggage in addition to the user.	Market Analysis	Key
PAT-UR-SUST-07	Energy used by the system shall be generated by sustainable means.	Sustainability	
PAT-UR-SUST-01	The maximum noise level of the system shall not exceed 75 dB.	Client	
PAT-UR-SAFE-06	The system shall shield the user from rain	Risk Analysis	
PAT-UR-SAFE-07	The system shall shield the user from wind	Risk Analysis	
PAT-UR-SAFE-08	The system shall shield the user from flying obstacles	Risk Analysis	
PAT-UR-SAFE-04	The system shall fulfill its functions without maintenance for 2 years.	Client	
PAT-UR-SAFE-01-02	The system shall update storage of no-fly zone data.	Risk Analysis	
PAT-UR-SAFE-01-01	The system shall store no-fly zone data.	Fun. 4.2.2.2	

Table 3.2: The Requirements Table, Part 2 of 2

PAT-UR-PROD-01	1000 units of the system shall be produced per year.	Client	
PAT-UR-PERF-13	The system shall be able to conduct flights 5 days a week.	Client	
PAT-UR-PERF-12-02	An electronic device shall be used to interface input from the user to the system.	Fun. 3.3.2	
PAT-UR-SAFE-09	The system shall be self-desinfecting	Risk Analysis	
PAT-UR-PERF-09	The power supply shall weigh less than 30% of the system weight.	Client	
PAT-UR-PERF-06-02	System self-check prior to flight shall take less than 2 minutes.	Fun. 3.2	
PAT-UR-PERF-06	Time of deployment shall take less than 2 minutes.	Client	
PAT-UR-PERF-05	The maximum airspeed of the system shall be 40 km/hr	Client	
PAT-UR-PERF-01	The system shall transport 1 person with a baby	Client	
PAT-UR-COST-01-01	The development cost of the control software shall be included in the cost of the system.	Client	
PAT-UR-COST-01	The system shall not exceed a rental cost of 5000 euro's per year.	Client	
PAT-UR-07	The system shall be able to achieve 500 flights a year.	Client	
PAT-UR-06	The system shall charge the battery of the user's controlling electronic device.	Fun. 1.1.1	
PAT-UR-04	The system shall verify its users' authorization to fly	Fun. 1.2	
PAT-UR-02	The system shall be applicable for air transportation.	Fun. 4.0	
PAT-SYS.S-FUNC-02	The system shall protect the user in case of total system failure.	Risk Analysis	
PAT-SYS.S-FUNC	The load-bearing structures shall be able to withstand the system loading.	Risk Analysis	
PAT-SYS.S-CONS-05	The load-bearing structures shall withstand a peak static load of 1545 Newton.	Risk Analysis	
PAT-SYS.S-CONS-04	The load-bearing structures shall withstand a continuous loading cycle of 1 flight.	Risk Analysis	
PAT-SYS.S-CONS-03	The structural subsystems deformations shall be kept low enough to ensure nominal operation.	Risk Analysis	
PAT-SYS.P-FUNC-01	The system shall not pose a threat to its environment.	Risk Analysis	
PAT-SYS.P-FUNC-02	The power subsystem shall provide 58550 Watt.	Fun. 4.1, Fun. 4.2, Fun. 4.3	
PAT-SYS.O-FUNC-01	The system shall announce take-off to its environment.	Fun. 4.1.1.2	
PAT-SYS.O-CONS-04	The system shall be able to VTOL on a slope of 5 degrees.	Market Analysis	
PAT-SYS.O-CONS-02	The system shall not be explosive under normal usage conditions.	Risk Analysis	
PAT-SYS.O-CONS-01	the system shall keep a safe distance of 2.5 meters from obstacles.	Risk Analysis	
PAT-SYS.C-FUNC-11	The system shall stop ascending at an altitude of 20m.	Risk Analysis	
PAT-SYS.C-FUNC-10	The system shall be able to measure its altitude.	Fun. 4.1.4	
PAT-SYS.C-FUNC-09	The system shall have altitude control.	Fun. 4.1.4	
PAT-SYS.C-FUNC-07	The control subsystem shall have 3 axis velocity determination.	Fun. 4.2.2	
PAT-SYS.C-FUNC-03	The system shall be aware of its current position.	Fun. 1.3	
PAT-SYS.C-FUNC-01	The system shall be stable.	Risk Analysis	
PAT-SYS-PROD-04	Decomissioning shall be sustainable	Sustainability	
PAT-SYS-PROD-03	The system shall be modular.	Sustainability, Market analysis	
PAT-SYS-PROD-01	The manufacturing process shall be sustainable.	Sustainability	
PAT-SYS-FUNC-23	The system shall analyse payload weight before flight.	Fun. 1.2	
PAT-SYS-FUNC-22	The system shall analyse the weather conditions before flight.	Risk Analysis	
PAT-SYS-FUNC-20	The system shall lift itself.	Fun. 4.1	
PAT-SYS-FUNC-19	The system shall monitor when maintenance is required.	Client	
PAT-SYS-FUNC-18	The state of the system shall be tracked in real time.	Client	
PAT-SYS-FUNC-12	The system shall propel itself forwards.	Fun. 4.2	
PAT-SYS-FUNC-09	the system shall cease operation safely when further operations are not safe.	Fun. 2.4	
PAT-SYS-FUNC-02	The system shall be controllable.	Fun. 4.2.1	
PAT-SYS-FUNC-01	The system shall perform emergency procedures in case of subsystem failure.	Risk analysis	
PAT-SYS-CONS-03	ground maneouvres shall only be performed with 9 meters of clearance.	Fun. 3.1, Risk Analysis	
PAT-SYS-CONS-04	The system shall not exceed a load factor higher than 4 g's	Risk Analysis	
PAT-UR-SAFE-06	The user shall be trained to safely pilot the system.	Risk Analysis	
PAT-SYS-PROD-04-02	61 % of the materials of the system shall have an End-Of-Life purpose	Sustainability	
PAT-SYS-PROD-08-01	The packaging material shall be made bio degradable materials	Sustainability	
PAT-SYS-PROD-08-02	The use of ceramics for materials shall be minimized	Sustainability	
PAT-SYS-PROD-08-03	The labels that will be used shall be made of biodegradable material.	Sustainability	
PAT-UR-SUST-03-01	The system shall have zero local emissions during operation	Sustainability	

Functional flow block diagram

START

1.0 Pre-flight check

S1.0 Continuous self-diagnosis

2.0 Prepare operation

3.0 Start air transportation system

4.0 Perform air transportation

5.0 Park system

END

T

T1.7.1 Activate safety protocol

T1.7.2 Communicate sensor data to ground control

T1.7.3 Communicate faliure causes to pilot

1.0 *Ref* Pre-flight check

1.1 Connect mobile device

1.2 Collect passenger data

1.3 Analyze flight plan

1.3 *Ref* Analyze flight plan

1.3.1 Receive destination

1.3.2 Check destination is within range

IF YES

IF NOT

AND

1.4 Initial control & simulation fault diagnosis

1.5 Initial hardware damage diagnosis

1.4 *Ref* Initial system fault diagnosis

1.6 Make start decision

No GO

GO

T

2.0 *Ref* Prepare operation

2.0 *Ref* Prepare operation

2.1 Deploy system preparation

2.2 Accomodate passenger

2.3 Deploy to flight mode

2.1 *Ref* Deploy system preparation

2.1.1 Alarm enviroment of deployment

2.1.2 Deploy to pre-flight mode

2.2 *Ref* Accomodate passenger

2.2.1 Allow for easy access

2.2.2 Secure pilot and luggage

2.2.3 Perform safety check

NOT SECURE (3x)

UNSUCCESFUL

SECURE

T

2.3 *Ref* Deploy to flight mode

2.3.1 Final deployment operations

2.3.2 Notify pilot of succesful deployance

3.0 *Ref* Start air transportation system

3.0 *Ref* Start air transportation system

3.1 Activate subsystems

3.2 Check successful activation

UNSUCCESFUL

T

SUCCESFUL

3.3 Provide interaction with system control

3.1 *Ref* Activate subsystems

3.1.1 Alert ground control of activity

3.1.2 Activate propulsion system

3.1.3 Activate stability & control system

AND

3.2 *Ref* Check successful activation

3.3 *Ref* Provide interaction with system control

3.3.1 Communicate operational information to the user

3.3.2 Provide user interface to issue system commands

4.0 *Ref* Perform air transportation

4.0
Ref
Perform air transportation

4.1
Lift-off

4.1
Ref
Lift-off

4.1.1
Prepare lift-off procedure

4.1.2
Execute lift-off procedure

4.1.3
Reach cruise altitude

ADJUST

4.1.4
Check altitude

4.2
Ref
Cruise

4.2
Cruise

4.3
Land system

4.3.1
Prepare landing procedure

4.3.2
Execute landing procedure

5.0
Ref
Park system

4.2
Ref
Cruise

4.2.1
Maintain communication with ground control

4.2.2
Check control input feasibility

4.2.3
Respond to pilot control input

4.3
Ref
Land system

5.0
Ref
Park system

5.1
Deactivate subsystems

5.2
Report final diagnosis

5.3
Allow for user exit

5.4
Confirm correct docking

5.5
Enter rest mode

END

5.1
Ref
Deactivate subsystems

AND

5.1.1
Deactivate propulsion system

5.1.2
Deactivate stability & control system

5.2
Ref
Report final diagnosis

AND

5.2.1
Deactivate real time system fault diagnosis

5.2.2
Deactivate real time structural damage diagnosis

5.2.3
Collect final diagnosis data

5.3
Ref
Allow for user exit

5.3.1
Retract to pre-park mode

5.3.2
Release pilot and luggage safety devices

5.3.3
Retract to park mode

5.4
Ref
Confirm correct docking

5.4.1
Pre-charging operations

5.4.2
Charge battery

5.5
Ref
Enter rest mode

S1.0
Ref
Continuous self-diagnosis

S1.1
Monitor hardware health

S1.2
Monitor stability & control faults

S1.1
Ref
Structural damage

S1.1.1
Run structural health test

S1.1.2
Collect sensor data

Assess health

S1.3
continue

S1.4
Alert company of maintenance trespass

5.2
Ref
Report final diagnosis

T

S1.2
Monitor stability & control faults

AND

S1.2.1
Monitor processor fault

S1.2.2
Monitor sensors output

LEGEND

Top level function

Second level function

Third level function

Function breakdown structure

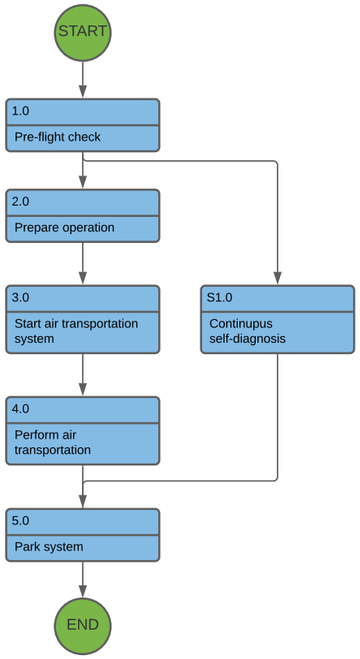

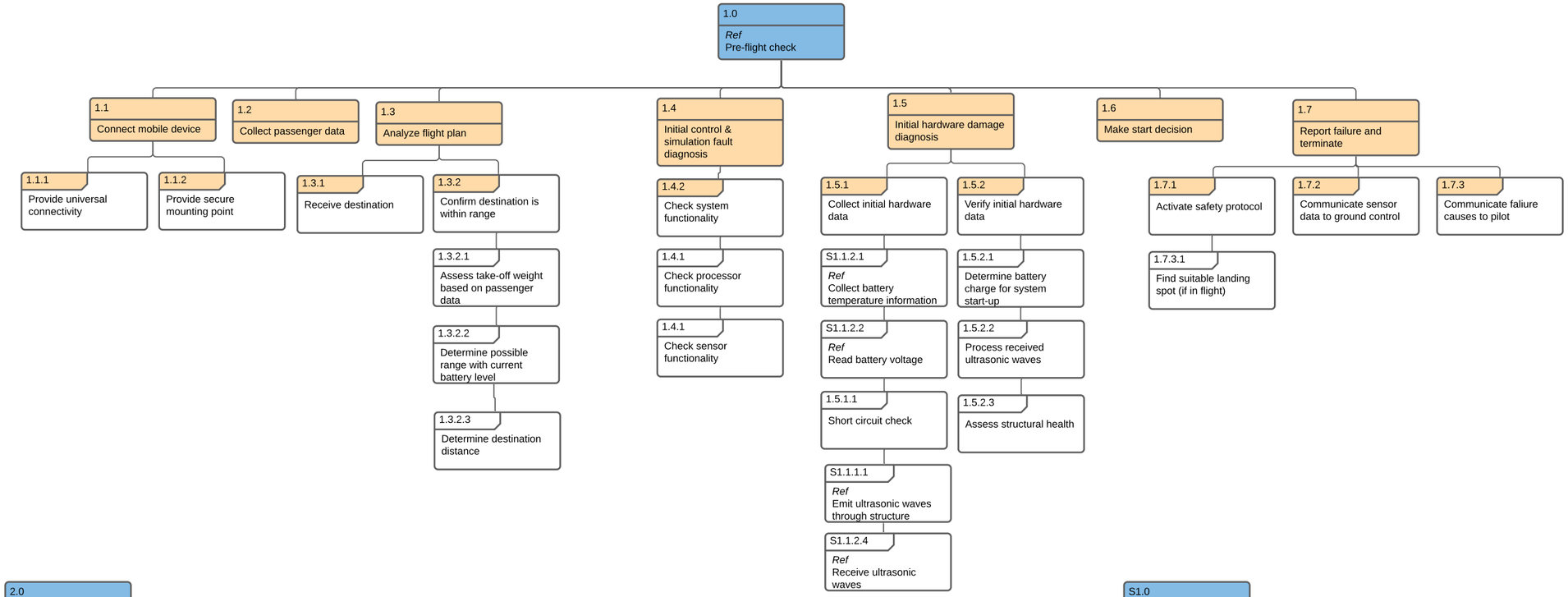

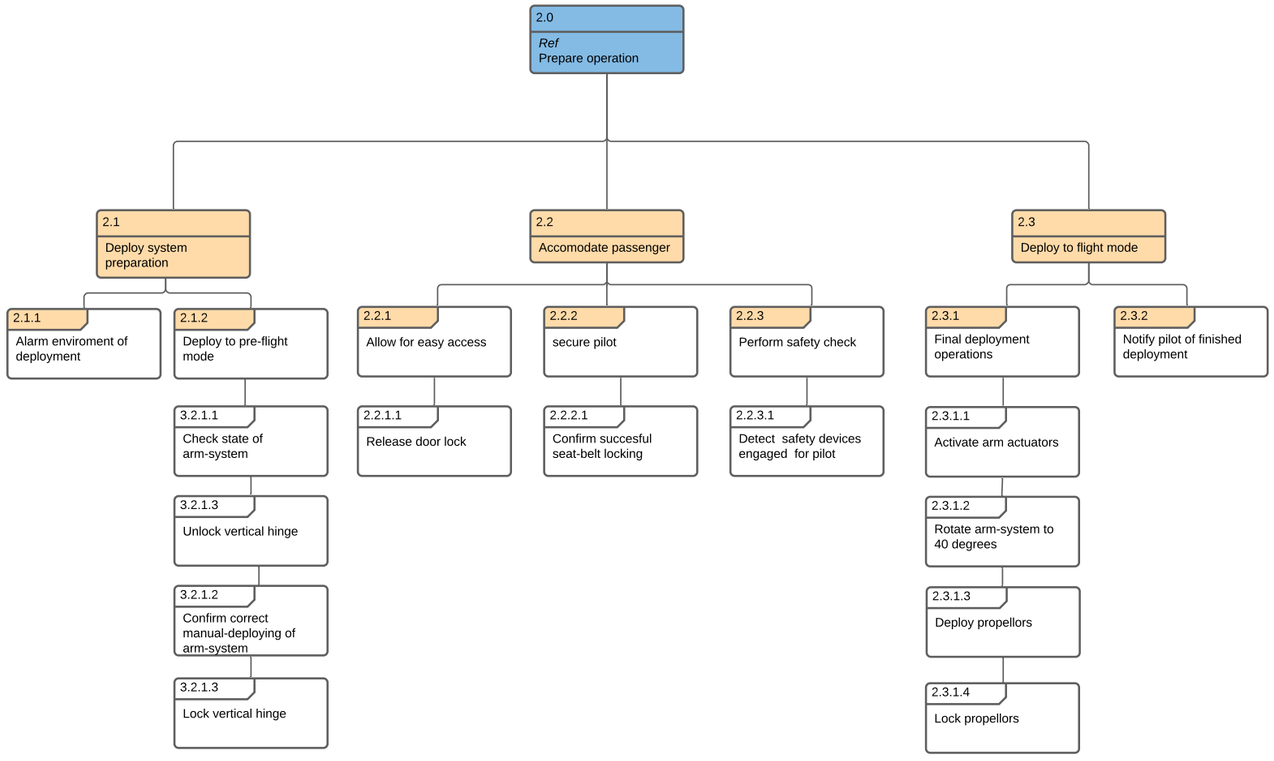

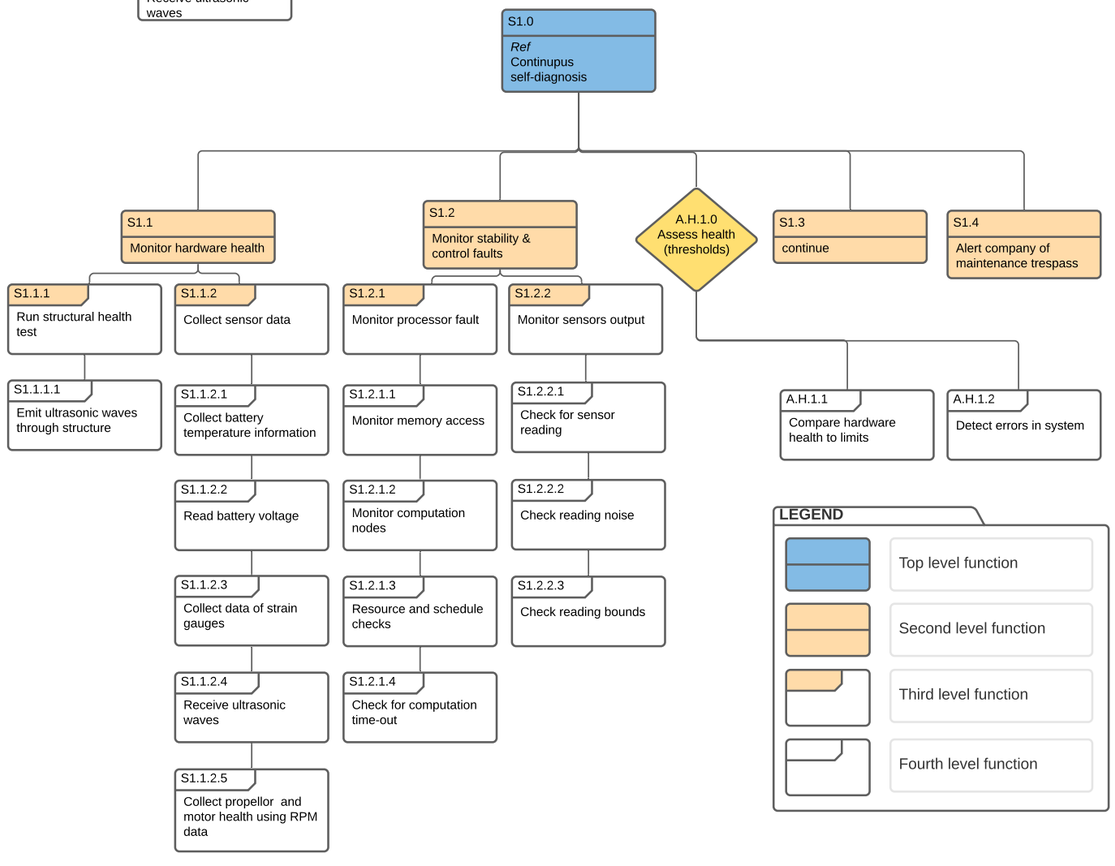

- 3.0 *Ref* Start air transportation system
  - 3.1 Activate subsystems
    - 3.1.1 Alert ground control of activity
      - 3.1.1.1 Send radio signal to ground control
    - 3.1.2 Activate propulsion system
      - 3.1.2.1 Turn-on motors
      - 3.1.2.2 Check for obstructions using voltage dipping
      - 3.1.2.3 Spin-up propellors
      - S1.1.2.5 *Ref* Self-diagnosis: Assess propellor and motor health using RPM data
    - 3.1.3 Activate stability & control system
      - 3.1.3.1 Activate sensory devices
      - 3.1.3.2 Calibrate control sensors
      - 3.1.3.3 Determine lift-off weight
      - 3.1.3.4 Determine flight conditions
      - 3.1.3.5 Activate hover control program
  - 3.2 check successful activation
  - 3.3 Provide interaction with system control
    - 3.3.1 Communicate operational information to the user
    - 3.3.2 Provide user interface to issue system commands

- 4.0 *Ref* Perform air transportation
  - 4.1 Lift-off
    - 4.1.1 Prepare lift-off procedure
      - 4.1.1.1 Receive pilot lift-off order
      - 4.1.1.2 Notify surroundings of lift-off
    - 4.1.2 Execute lift-off procedure
      - 4.1.2.1 Communicate flight parameters to pilot
      - 4.1.2.2 increase thrust for controlled ascent
      - 4.1.2.3 Run control system
    - 4.1.3 Reach cruise altitude
      - 4.1.3.1 Monitor flight conditions
    - 4.1.4 Check altitude
  - 4.2 Cruise
    - 4.2.1 Maintain communication with ground control
      - 4.2.1.1 Receive ground control radio signal
      - 4.2.1.2 Take over controls if required by ground control
    - 4.2.2 Check control input feasibility
      - 4.2.2.1 Track location
      - 4.2.2.2 Analyze nearby no-fly zones
      - 4.2.2.3 Verify control input
    - 4.2.3 Respond to pilot control input
      - 4.2.3.1 Receive control input
      - 4.2.3.2 Communicate control input to subsystems
      - 4.2.3.3 Reach cruise condition
      - 4.2.3.4 Switch to cruise control system
  - 4.3 Land system
    - 4.3.1 Prepare landing procedure
      - 4.3.1.1 Reach hover condition
      - 4.3.1.2 Switch to hover control program
      - 4.3.1.3 Receive ground control clearance for landing
      - 4.3.1.4 Communicate landing to ground control
      - 4.3.1.5 Find suitable place to land
      - 4.3.1.6 Check system ability to land
      - 4.3.1.7 Notify surrounding of landing procedure
    - 4.3.2 Execute landing procedure
      - 4.3.2.1 Receive user control input to decrease altitude
      - 4.3.2.2 Decrease thrust for controlled descent

- 5.0 *Ref* Park system
  - 5.1 Deactivate subsystems
    - 5.1.1 Deactivate propulsion system
      - 5.1.1.1 Decrease thrust to zero
      - 5.1.1.2 Turn off motors
      - 5.1.1.3 Wait for spin-out
      - 5.1.1.4 Wait for power down of all auxiliary units
      - 5.1.1.5 Cut off power source
    - 5.1.2 Deactivate stability & control system
      - 5.1.2.1 Deactivate user control interaction
      - 5.1.2.2 Deactivate hover control program
      - 5.1.2.3 Deactivate sensory devices
  - 5.2 Report final diagnosis
    - 5.2.1 Deactivate real time system fault diagnosis
    - 5.2.2 Deactivate real time structural damage diagnosis
    - 5.2.3 Collect final diagnosis data
      - 5.2.3.1 Collect flight data
      - 5.2.3.2 Collect final real time data
      - 5.2.3.3 Report final diagnosis to ground control via Wi-Fi
  - 5.3 Allow for user exit
    - 5.3.1 Retract to pre-park mode
      - 5.3.1.1 Release propellor lock
        - 5.3.1.1 Fold propellors
      - 5.3.1.2 Rotate arm-system back with 40 degrees
      - 5.3.1.3 Release vertical hinge lock
    - 5.3.2 Release pilot and luggage safety devices
      - 5.3.2.1 Release secure mobile device mounting point
      - 5.3.2.2 Allow for mobile device disconnection
    - 5.3.3 Retract to park-mode
      - 5.3.3.1 Wait for user manual vertical folding of arm-system
      - 5.3.3.2 Check final retraction configuration
  - 5.4 Confirm correct docking
    - 5.4.1 Pre-charging operations
      - 5.4.1.1 Communicate vehicle ID
      - 5.4.1.2 Communicate current battery charge
      - 5.4.1.3 Communicate desired battery voltage
      - 5.4.1.4 Notify surrounding of correct docking
    - 5.4.2 Charge battery
      - 5.4.2.1 Receive power from docking station
      - 5.4.2.2 Communicate charging progress with docking station
  - 5.5 Enter rest mode

LEGEND

- Top level function
- Second level function
- Third level function
- Fourth level function

4
Concept Trade-off

In the initial phases of this project, the requirements and functional breakdown from chapter 3 are used to come up with 3 initial concepts. The concepts are shown in Figure 4.1. An analysis of these concepts was executed and a trade-off was done to determine the best suited to meet the requirements. In the end, a hybrid between concepts 1 and 2 was created, which lead to the design as it will be further detailed in the rest of the report. This chapter gives an overview of this analysis and trade-off process, which gave way to the starting point of this report.

4.1. Concepts

Three concepts have been created and analysed. This section is aimed at introducing the most important features of all three and to indicate some of the pitfalls that were identified early on. In Figure 4.1, the initial sketches of the concepts are presented.

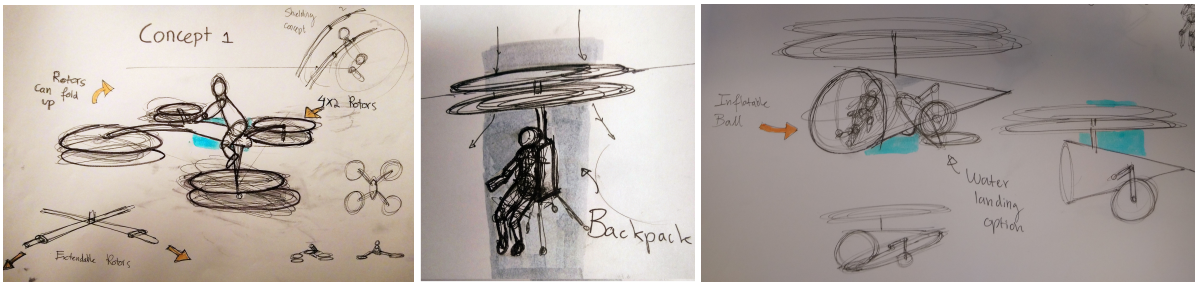

(a) Quadcopter (b) Helipack (c) Ice Cream Cone

Figure 4.1: Overview of the initial design concepts.

The first concept is the battery-powered quadcopter concept, which is based on current drone models. Its main features are a central body to accommodate the user, batteries and other systems. Attached to this body are 4 arms which transfer the lift from the propellers to the main body. These propellers have a diameter of $1.3m$ and are powered by one electric motor each.

The main advantage of this concept are its good controllability. It also has potential for redundancy for the lift generation. Another advantage is in terms of noise, as these multiple smaller rotors have lower tip speeds. In terms of disadvantages, the main concern is the ease of complying to the volume requirements, while also complying to other requirements. This requires multiple folding mechanisms, which increase the amount of parts to be maintained and thus makes maintenance more demanding.

The second concept is the helipack concept. This one is based on a combination of a helicopter and a backpack. Its main structure is the backpack part that houses all main subsystems. During flight, the entire system hangs from the coaxial propeller that is powered by a single electric motor. A seat would be mounted to the structure for user comfort and safety.

The advantage of this concept is the relative simplicity compared to the other concepts. It also has the best potential to meet the volume requirement. Due to this simplicity, it also has the most potential to have the lowest maintenance requirement. It does have some significant safety and comfort concerns, however. In terms of stability and control, it also has a large disadvantage, due to its single propeller system. It also has the worst noise potential due to its large, counter-rotating propeller.

The last concept is called the ice cream cone, due to its original shape being very similar. It has a spacious user cabin, that houses the user and the hydrogen fuel cell system. Most of this cabin would

be a collapsible structure to meet the volume requirement. This concept has a single large, electrically powered rotor and a small tail rotor.

The main advantage of this concept is that the volume requirement can easily be met with the foldable structure of the cabin. Due to the hydrogen fuel cell system, the energy storage mass is also easily kept under the required 30% of the total mass. The big downside is the almost non-existent infrastructure for hydrogen refuelling and the safety concerns surrounding the use of hydrogen. A fuel cell system also requires intensive maintenance and is more complex than a battery. There are also some challenges to combine a tail rotor with the collapsible tail in terms of structure.

Before any analysis, the concepts are worked out more to obtain information for the trade-off. The most important aspects are the propeller performance, battery or fuel cell sizing and the sizing of other electrical components. Other aspects are the deployment mechanisms and user positioning. Some of the major structural components are also designed preliminary to get better weight estimations. The worked out forms of these concepts is shown in Figure 4.2.

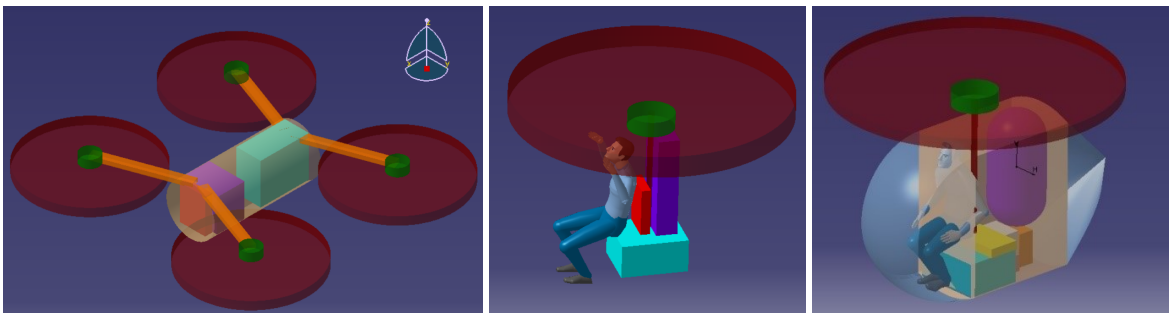

(a) Quadcopter (b) Helipack (c) Ice Cream Cone

Figure 4.2: Overview of the design concepts in their most worked out form.

4.2. Criteria

This section discusses the main trade-off criteria and briefly overviews the important findings. The details of the calculations to achieve these results can be found in the midterm report [12].

The first criterion is the cost of the system. This is one of the defining criteria of the system, as a rental price is defined in the requirements of the system. The cost criterion is split in 2 sub-criteria: the manufacturing cost and the energy cost. This cost has initially been given a high weight. This is significantly lowered, due to the high uncertainty of the determination of this factor.

This manufacturing cost is defined only by the relative cost of materials and powertrain components, as it is hard to detail the other aspects of manufacturing in the conceptual phase of the design. These are also the largest costs to occur, that can be influenced by the design of the system. The energy cost criterion, on the other, is based on the cost per delivered kWh of energy for the different power sources. This does not take into account the need for difference in energy capacities between the systems, but forms a good differentiating factor.

The next criterion is the use of public space, determined by the used floor projected area. This criterion is used as an indicator of how easily the volume requirement can be met. It is determined instead of an exact storage volume as that is hard to obtain for the quadcopter and ice cream cone without a detailed structural design. This is another criterion for which the weight is lowered significantly, as the uncertainty in the result is very high.

The third criterion under consideration is the range and endurance performance of the system. Although there is an exact requirement for both, this factor is considered for the indirect influence on size and weight of the system. The drag and propulsive efficiency are used as the determining factors of this criterion, as they are the main contributors to this factor that can be determined in this phase. The weight is not set very high, as it is not deemed very important in differentiating the concepts.

Sustainability is one of the core design factors and is deemed a major factor of the trade-off. It is also expected to have differentiating power that is important to consider. There are 2 sub-criteria for sustainability: indirect emissions and end-of-life. This criterion is another one with a lowered weight compared to the one initially set, due to the inexact nature of the determination of the sub-criteria.

Indirect emissions are determined with the emissions caused by production and energy generation. This sub-criterion is determined in a more relative fashion, as the concept designs are still very unpolished. The end-of-life criterion is on its own determined by 2 parameters: end-of-life purposes and modularity. The end-of-life purposes is an indicator of how easily the system's components can be reused for other usages. This is again a relative indication, as it is hard to quantify this parameter numerically. The modularity is a factor that determines how easily components can be swapped to get a device back into service after a failure. This is again a relative indication.

Noise is a parameter that comes directly from the requirements. Due to the different propeller configurations, there will be large differences in this parameter. The trade-off is only based on the tip mach number, as this is the only major factor that can be found during this design phase.

Safety is another important criterion for the trade-off, as it is a major requirement of the system. Both the safety of the user and of bystanders is considered. This criterion is given a high weight, mainly for its differentiating power combined with the importance of safety in any aerospace system.

The bystander safety, is determined by the size of the safety area from authority standards. It is considered that a larger safety area leads to a less safe design for bystanders. The user safety is split in a stability and a structures component. The more stable the system, the lower the probability of a crash by loss of control. The structures aspect is considered more by the potential of a concept leading to a survivable crash.

The interaction between the user and the system is taken under consideration, for the fact that this ties directly into user satisfaction. Both the user comfort and the user field of view are taken into consideration for this criterion. For the user comfort, there are some major differences between the concept, as the user is in different seating position for each one. The visibility is also important, as it makes flying the device around easier for the user. It also makes the device more suited for tourists, which widens the user base of the system.

The stability and control of the concepts is also taken into consideration, by comparing the level of control automation between the concepts. This is determined on the basis of the required control means and the actuators requirements. Control automation is put in place to ease the controls for the user and to keep the system in a stable situation. If the level of automation is higher, a more complex flight control system is required with an increased cost and development time as a result.

The last criterion is the maintenance of the system. This criterion mainly indicates the feasibility of meeting the requirement on the maintenance-free period. Part of determining this period is done by the count of moving parts. These moving parts are the main drivers of maintenance of a system and thus less of these raises the maintenance-free period. The powertrain is also taken into account, as a more complex power system, such as hydrogen fuel cells, require more checks and have a lower potential to remain without maintenance for long periods.

4.3. Trade-Off

Doing the final trade-off required determining all the above criteria, which is done by the different design departments. To get a meaningful result, the analysis results are all normalised and filled into a table. The sub-criteria scores are added up to the criteria scores using small weighted sums. These criteria scores are then also summed with a weighted sums.

From the trade-off in Table 4.1, the helipack concept turns out the best overall concept. It does have some fatal flaws that also came up during the analysis. These flaws consist of the high noise and low safety. The quadcopter is a close second, with its worst flaws being the public space usage, user interaction and maintenance.

Table 4.1: Trade-off table with weights and results for all criteria. Criteria are divised in main criteria (bold), sub-criteria (normal text) and sub-sub-criteria (italic).

Criteria	Weight	Quadcopter	Helipack	Ice Cream Cone	Final Concept
Cost	**8**	**431**	**579**	**214**	**431**
Manufacturing	5	26	56	2	26
Energy	3	100	100	68	100
Public Space	**5**	**-500**	**-221**	**-221**	**-500**
Floor projected area	5	-100	-44	-44	-100
Performance	**5**	**347**	**400**	**299**	**411**
Drag	0.5	-78	-100	-19	-78
Propulsive Efficiency	4.5	86	100	69	100
Sustainability	**10**	**30**	**60**	**-79**	**30**
Indirect Emissions	5	-82	-86	-100	-82
End-of-life	5	88	98	84	88
Noise	**10**	**-620**	**-1000**	**-882**	**-620**
Propulsion	10	-62	-100	-88	-62
Safety	**15**	**-128**	**-477**	**-272**	**-100**
Bystander	8	-100	-85	-85	-100
User	7	672	203	408	700
User Interaction	**5**	**158**	**180**	**474**	**478**
Comfort	4	20	20	100	100
Visibility	1	78	100	74	78
Stability & Control	**8**	**-264**	**-400**	**-800**	**-264**
Level of control automation	8	-33	-50	-100	-33
Maintenance	**10**	**-750**	**-281**	**-719**	**-750**
Number of moving parts	*5*	*-100*	*-6*	*-44*	*-100*
Powertrain	*5*	*-50*	*-50*	*-100*	*-50*
Result		**-1296**	**-1161**	**-1986**	**-884**

Comparison on an element basis in this table shows that all of the concepts have very defined strong- and weak sides. The overall winner, the helipack, was severely lacking in its noice generation and safety, while other concepts had these as their strong sides. It was hence ultimately decided to create a combination of all concepts, where the best aspects are combined to score better overall.

4.4. Final Design Concept

This final concept is a quadcopter at its core, taking the concept of a main body and 4 propeller arms from that concept. Instead of 4 single propellers, it is decided to have 4 sets of coaxial counter-rotating propellers for extra redundancy in yaw controls and for the performance benefits. The ice cream cone concepts contributes its full encapsulation of the user to offer higher comfort and safety. The final concept is presented in Figure 4.3.

To check whether this solution is actually better than the presented concepts, a simplified trade-off is done by taking the aspects from the other concepts that have been transferred. This is shown in the rightmost column of Table 4.1. It can be seen that it scores better overall with a significant margin. The only criteria for which it scores badly, are the use of public space and the maintenance potential. Especially the public space usage turns out to be an issue and is solved before any other design work is done, to assure the requirements are met.

Figure 4.3: The final concept resulting from the trade-off.

4.5. Next steps

Having come up with a final concept, the detailed design phase can be started,presented in the next part of the report. Here, the design is further analysed in terms of power and propulsion, some aerodynamics, structures, stability and control and finally operations. Sustainability and risks related to the design were as well analysed. In the end, all domains came together in the final design, presented in chapter 12.

5
Propulsion, Power and Performance

This chapter presents the processes followed to detail the power, propulsion and performance systems of the vehicle. This chapter builds on top of the previous reports in this series, and hence will re-use some procedures and knowledge. Where relevant, this is specifically stated. Resulting from this is the vehicle configuration: The vehicle will be powered by batteries. Its main propulsion system consists of 4 pairs of coaxial rotors driven by separate electrical motors. These motors are controlled by separate motor controllers, and the batteries are controller by battery controllers per set. These power management systems work closely together with the flight computer: They receive instructions from it, and update it on their current states. The auxiliary systems and support systems in the vehicle are also to be driven by batteries. Since the main user interface with the vehicle is a smartphone, this device will be charged by the auxiliary power system as well.

Several components and processes are modelled in more detail in this chapter. The electric motors, which up until this point have largely been considered on statistics for weight and performance, are replaced by actual motors which fit the requirements. The same processes is done for the propeller, although its result opens up many more research questions. To reduce battery weight, the batteries are integrated into the load-carrying structures. The power and propulsion subsystems must also allow for self-diagnosis: The required components and techniques for this are outlined in subsection 13.2.2. An analysis of how requirements specific to the power and propulsion subsystem are met follows; this details the noise generation, range, endurance, modularity, and the vehicle's ability for consecutive operation over a longer period of time with minimal idle time in between.

5.1. Propellers and Thrust Generation

Up until this point, the propellers for the vehicle were based on statistics. In the early stages of design only a few characteristics of the propeller were key: its weight, and its power-to-thrust factor. Finding full propellers for all these configurations was overkill at this stage and suboptimal management of resources. In this detail design stage, several other factors become important: The noise generated by the propellers, their folding mechanisms, and their layout. This requires the propellers to be expressed more specifically. A logical final step for this would be to substitute the theoretical propeller with an actual propeller. This could mean either designing a completely new propeller, or finding one based on the requirements as an already existing product. This process is not as straightforward as it seems however: The propeller required would be a propeller designed for counter-rotating coaxial use at a scale that is very small for a helicopter, but large for a quadcopter, all the while remaining foldable. These are very specific criteria, which would make finding a propeller that suits all very time consuming. The other option would then be to design a propeller specifically fit for this purpose. The field of propeller design however is vast, and worthy of a series of reports of its own entirely. This would also not be an option. A hybrid approach was considered as well: Finding an existing propeller, and adapting it for the specific needs of the vehicle. This would also add up the downsides of both approaches: First, a suitable comparable design has to be found, after which a complete analysis needs to be performed anyway to determine the propeller characteristics as small changes in propeller geometry can have very large effects. Data on existing propellers is not always readily available either, so this would be even harder.

It became apparent that getting a propeller for this vehicle was an even larger undertaking than it was originally estimated to be. For the amount of extra clarity it would give on the total design of the vehicle, fully designing a propeller was simply not worth the expenditure of resources. Hence, the difficult decision was made to not fully work out the propellers, but to elaborate on the statistical models currently in place. A follow-up study needs to be performed to find the exact details applicable propellers for the design. In this report, the general characteristics of the propellers are worked out

in more detail, but aerofoils, chord profiles, and other highly specific propeller properties will not be considered. Instead, the focus will be on the aspects that make this propeller unique: Its foldability and its counter-rotating coaxial configuration. This sacrifices exactness of the values of the exact lift generation under a specific power as parametric function of RPM, the interactions and aerodynamics of horizontal translation with vertical thrust generation, but ultimately does give all the answers required to determine if and how the PAT shall function and perform and allows to focus more on other aspects of the design.

This leads to the points where the propellers will be further detailed: Firstly, its thrust generation based on power consumption is improved by taking into consideration the coaxial thrust generation on a disk basis by using a coaxial interference factor. The folding mechanism for the propeller is detailed by showing and analysing the mechanism and shape of the propeller in stowed configuration. Finally, the propellers' weight estimation is also changed to reflect the use of more compact propellers used for vertical application instead of the full-metal, high-speed design based on aeroplanes.

The folding mechanism is also detailed further. This has its own text dedicated to it in subsection 5.1.2.

The top-level configuration of the propeller stays the same: 4 blades, with a diameter of 1.3 metres.

5.1.1. Co-Axial Thrust Modeling

The main goal of using these propellers is to generate thrust. This is done by transferring the rotary motion or the propeller (and in extension, the axle driven by a motor) to the air. This transfer is not without losses however, and needs to be modeled. For the sake of computational brevity, the propellers' performance is modeled as having an input of a specific power, yielding a certain thrust. This process has been estimated several times before in previous reports in this series, but with more clarity on the propeller configuration, a more accurate model can be implemented. When using two vertically distanced coaxially counter-rotating propellers to generate a thrust, it is impossible to asses the two propellers separately: They interact to some degree with each other by accelerating the same air. To properly model this using disk actuator theory, the two propellers must hence be considered to act in the same disk [13]. This can be modeled by using Equation 5.1 [14]. This gives the power required for both propellers combined, assuming the propellers operate at the same RPM. The input T is the total thrust over the disk, and hence also the combined propeller thrust. It does take into consideration the difference in thrust per propeller due to interference while the propellers run at the same power levels. The exact distribution in thrust depends on the propeller geometry, but as a rule of thumb a ratio of $T_{lower} = 0.86T_{upper}$ based on statistics is used [15]. This results in a value of $\kappa_{int} = 1.26$ [14].

$$P_{br} = \kappa_{int} \frac{T^{\frac{3}{2}}}{2\sqrt{\rho S}} \tag{5.1}$$

Using this relationship, the axle brake power can be determined for every propeller-actuated disk- for every set of propellers. Taking into consideration that a total of four sets or coaxially counter-rotating propellers are used, the total power to be delivered by the eight motors is equal to $56.7kW$.

This method was verified by setting up mock cases using the examples given in the paper. The resulting powers were compared to those in the paper. Validation was done by comparing the model to a DZP30 off-the-shelf contra-rotating coaxial model aircraft propeller and to the Rotorschmiede VA115. The DZP30 is much smaller in scale, but resembles the type of propeller to be used in this vehicle better. The VA115 is larger in scale, uses traditional propeller rotors, and is driven by a combustion engine, but it gives a good indicator of how performance would look like on with the more scaled-up approach. For both comparisons, it was estimated that the data given by their manufacturers were done under standard conditions. The DZP30 returned an error of -8%, and the VA115 an error of -21%. Thus for both verification cases, the thrust generated was slightly lower than the model estimates. This should be taken into consideration when developing the concept further.

5.1.2. Folding Mechanism

To meet the volume requirement in stowed state, it is decided to fold the propeller to a compact state. Inspiration is taken from aircraft carrier helicopters, which have folding rotors. A conceptual design based on this is made. No sizing is done, however, as there is too little information available on the blade loading.

To achieve compact folding, the blades are attached to a hub part in 2 pairs of opposing blades. The blades on these hubs both fold in the same direction. These pairs of blades then rotate 90 degrees to have the blades overlap. The unfolded and folded states of the mechanism is shown in Figure 5.1.

In further design stages, actuators have to be designed to achieve folding and locking of the blades and to achieve the rotation of the 2 pairs of blades. It is preferable for this folding to be automated, as this is a complex set of operations that would require checks for proper locking.

(a) The propeller in the unfolded state.

(b) The propeller in the folded state.

Figure 5.1: Conceptual propeller folding mechanism.

It is preliminarily determined that the folding mechanism should be made from a high strength metal, preferably stainless steel. Although the loading of the mechanism is not known, it is known that this will be a highly loaded part, which steel is best suited for. Due to its outdoor usage, it should be stainless to resist any type of corrosion. Coatings are not deemed an option, as these would wear of over the large amount of required deployment cycles.

5.1.3. Weight Estimation

A preliminary weight estimation of the propellers is done. Due to cost considerations, it is decided to use aluminium 6061-T6 for the construction of the blades, because of its good strength and shaping properties.

Weight data on aluminium propellers of this size category is not readily available. Estimation methods are also not applicable to this propeller design, due to the combination of small size and high disk loading that falls out of range of these methods. For this reason, similarly sized CFRP propellers are found. The most similar is the Mejzlik 48 x 16.4 inch propeller, of which the weight is doubled for it having only 2 blades [1]. Using the density of CFRP material [16], the volume of these propellers is determined and subsequently multiplied by the density of the aluminium [16]. This results in a blade mass of $1.215kg$ per propeller. Due to the differences in design between CFRP and aluminium propellers, this assimilation would not hold, it is however the best available method for a first estimation.

Since the hub is made from a different material, its weight is estimated separately. Using a density of $7860kg/m^3$, a realistic value for stainless steel alloys [16], and the model used in the conceptual folding mechanism, it is found that the hub weighs $0.35kg$ per propeller. Margins should be taken into account for further design stages, as this is a very preliminary estimation of the mass of the hub mechanism.

5.2. Motors

The propellers described in section 5.1 cannot rotate by themselves. There should be an energy conversion to generate mechanical energy to drive the propellers. Electrically powered motors are to be used to convert electrical energy into mechanical energy.

As the power supply for the propulsion systems operates on a reference voltage DC current, either DC motors have to be used or a DC-AC converter (inverter) must be used. In the previous reports, it was established that DC motors were slightly heavier and more expensive than their AC counterparts, but a DC configuration still outweighs the drawbacks of the added weight and space of a power inverter, which at the order of magnitude of power it is to be operated on in this vehicle makes it well over double the size of a DC motor, notwithstanding cost and weight. Hence, DC motors were settled on. So far, a statistical model was used to estimate the mass and size of a motor based on its output power. To properly design and size the rest of the power system, it was important that the actual voltage, efficiency,

[1] Mejzlík Propellers s.r.o. *Technical data*. URL: `https://www.mejzlik.eu/technical-data` (visited on 01/12/2021)

and other parameters were known. Finding relationships to keep the motor design parametric was not feasible anymore at this point, so instead it was decided that enough certainty was in place to swap out the theoretical motor for an actual motor. Several companies were contacted in search for a motor that fit our requirements and constraints, and in the end one was found that was settled for. The company is called MGM Compro and is located in Zlin, Czech Republic. Their goal is ”focusing on development and production of special, custom electronics[2].” Based on first estimation mission and performance requirements, Mr. Kováříček (Account Manager) and Mr. Švec helped with the selection of the motor and provided details for a slightly customised configuration that would make the motor of better use for the vehicle and the interface with other components, such as the controller and batteries. High performance and power peaks in combination with low vehicle weight were important criteria for selecting the motor. The RET30 perfectly suits these touchstones and is mainly used for ambitious projects, drones and multirotor applications[3]. Table 5.1 shows the general operating ranges of the motor[4]. Furthermore, Figure 5.2 shows the dimensions of the RET30.

Table 5.1: General technical characteristics of the selected motor

Type	Voltage [V]	Continuous / peak power [kW]	Working rotation [rpm]	Max Torque [Nm]	Weight [kg]	Cooling
RET30	63	8-12/15	2000-8000	35	4	Air

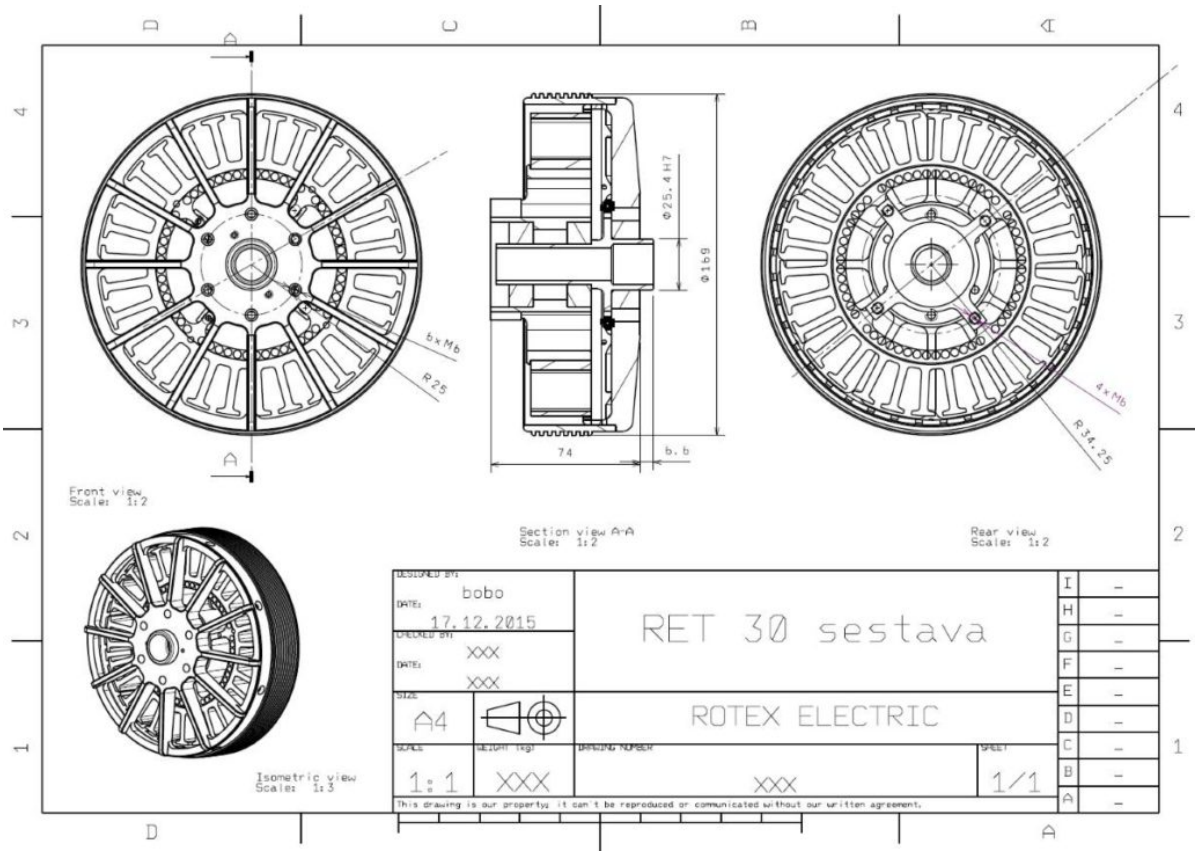

Figure 5.2: Dimensions of the selected motor RET30

Aside form the technical information, experimental data was supplied as well. This experimental data was used to determine performance at the vehicle’s operation points, as well as several other charac-

[2]MGM compro. *About us*. URL: `https://www.mgm-compro.com/` (visited on 01/08/2021)

[3]MGM compro. *Electric Motors*. URL: `https://www.mgm-compro.com/kategorie-produktu/electric-motors/` (visited on 01/08/2021)

[4]MGM compro. *Electric Motors*. URL: `https://www.mgm-compro.com/kategorie-produktu/electric-motors/` (visited on 01/08/2021)

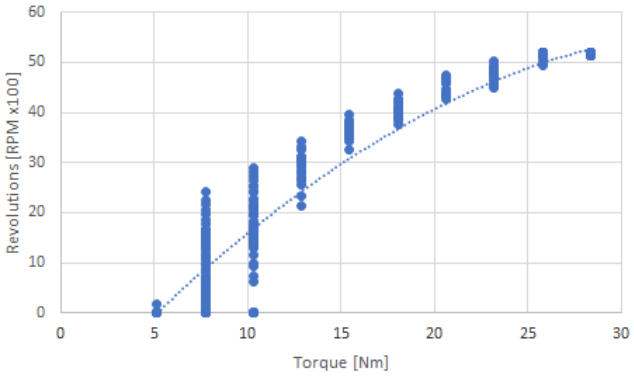

Figure 5.3: The performance graph of the MGM Compro electromotor based on experimental data

teristics. The most important of these was the torque-rpm curve, shown in Figure 5.3. It is known that $P = \omega * \tau$, and hence the operational point for the vehicle is determined using this graph at a point of 28 Nm of torque and 2400 RPM. It can be noted that there are several data points spread over different RPMs at a specific torque; this has to do with the fact that the spin-up phase and spin-down phase of the motor is also included in this diagram. For operation, the topmost values (the highest RPM for a given torque) are therefore considered as the nominal operation conditions. In reality there will be some latency before these values are attained, but the exact characteristics of this cannot be modeled yet, and have to be determined experimentally when the propeller is finalised.

The motor controller, also provided by mgm compro, modulates the current to control the supplied power to the motor. This system will receive an input power setting, which for all intents and purposes can be considered a simple scalar value. The resulting thrust from this increase in power is not so linear, but this can be more accurately determined in specific tests when the system is built to be used as reference for the flight controller.

Using this motor also made something else apparent: The gearbox that had been designed previously to meet the relatively low RPM and high torque would not be necessary with this motor: It has much more power than what was anticipated, and with a near constant performance efficiency it can just be limited directly to ensure lower noise levels during operation, which is the root for the rpm requirements. This means that the gearbox can be scrapped from the design, alleviating weight, space, and system complexity. This removes one common point of failure, which aids massively in meeting the maintenance requirement (PAT-UR-SAFE-04).

5.3. Power Budget

The power budget for the system remains largely unchanged compared to the budget that was assessed in the earlier stages of design. The propulsive power usage differs slightly however. The updated power budget can be found in Table 5.2. Note that this only covers the components that are active at all times: variable or incidentally loaded components such as the actuators are averaged and omitted accordingly.

Table 5.2: The updated power budget

Component	Power draw [W]
Propulsive Electromotors	56700
Battery management system	30
Motor controllers	25
Flight computer	60
ACDS	30
Communications	50
User phone	5
Self-diagnosis systems	80
Lights and visbility	20
Headroom for vriable load	1550

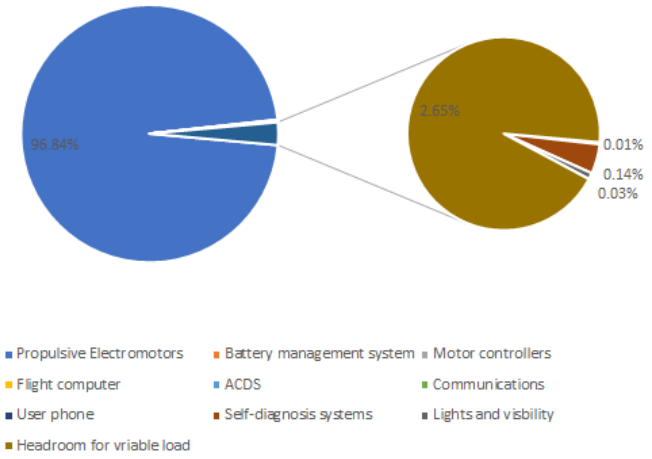

5.4. Batteries

To ensure sufficient power is provided to the system to complete the mission, a detailed sizing of the propulsive battery system is done. The emphasises of this sizing is the battery system power output and endurance performances. This sizing method first solves for the number of cells needed in series to meet the system voltage requirement, then it solves for the number of cells needed in parallel for the capacity requirement.

5.4.1. Lithium Battery Properties

For batteries to be used in aviation, two performance indexes are of importance; power density and energy density. Licerion lithium metal cells made by Sion power are selected to be used as they have both high power density and energy density.

Lithium metal battery production first started in 1980's by Moil energy. At that point of time it was seen as the future of rechargeable batteries as it provided high specific energy and good loading capability. However, uncontrolled lithium deposition on the electrodes cause dendrite growth which not only decreases the amount of use able lithium in the battery but also induces safety hazards. As dendrite penetrates the separator between the anode and cathode causing a short circuit[17]. This failure mode has been addressed and solved by Sion power. Licerion lithium metal cells make use of protected lithium anode along with chemically stable ceramic separator to ensure that no dendrite growth is possible[18].

After battery energy density and power density, an other important property of lithium batteries is the C rating. Battery cells with different chemistry have different C rating. C rating is the amount of time it takes for a battery cell to charge and discharge. If a battery can be discharged fully in one hour then the C rate of this battery is $1C$. This property provides an easy method to estimate the amount of time required to fully discharge a battery at maximum current. All relevant battery properties needed for sizing the battery pack are given in Table 5.3.

Table 5.3: Licerion Cell Properties

Licerion®Cell Properties	
Dimensions(mm)	80 x 91 x 10
Mass(g)	158
Capacity(Ah)	20
Discharge rate(C)	2C
Voltage(V)	3.82

5.4.2. Series Cells Sizing

Each cell has a nominal output voltage that it can provide.The nominal output voltage for the cells being used is $3.82V$ as mentioned in Table 5.3. When the cells are connected in series configuration in a battery the total output voltage of the battery V_b is given by Equation 5.2 where N_s is the number of cells in series and V_c is the nominal voltage of each cell.

$$V_b = N_s \cdot V_c \tag{5.2}$$

The output voltage of the battery has to comply with the maximum and minimum acceptance voltage of the electric motor. As the motors has already been sized in section 5.2 and the maximum voltage that is required is $63V$ so the battery is sized for this voltage point using Equation 5.3 where V_{motor} is the motor voltage.

$$N_s = \frac{V_{motor}}{V_c} \tag{5.3}$$

Furthermore as all the motors are connected in parallel configuration so the total voltage required by 8 motor system is the same as voltage required by a single motor. Hence a total of 16 cells are required in series to provide sufficient voltage to all the motors.

5.4.3. Parallel Cells Sizing

Cell capacity Q_{cell} is given in ampere hours is the amount of charge that the cell can provide at rated voltage. The cell being used have a capacity of 20 ampere hours as given in Table 5.3. In parallel configuration the total battery capacity Q_{batt} is calculated by Equation 5.4.

$$Q_{batt} = N_p \cdot Q_{cell} \tag{5.4}$$

The maximum C rating of the battery cells as given in subsection 5.4.1 can be then used to relate the maximum output current of the battery I_{max} and the battery capacity as given in Equation 5.5.

$$I_{batt} = C_{max} \cdot Q_{batt} \tag{5.5}$$

To size the battery for maximum power, the power output of battery P_{batt} should be equal to the maximum power required by the motor system P_{motor} where η is the cumulative efficiency of the motor ($\eta = 0.95$), battery ($\eta = 0.98$) and power electronics ($\eta = 0.97$)[19]:

$$P_{batt} = \frac{P_{motor}}{\eta} \tag{5.6}$$

Further more the battery power can be calculated using Equation 5.7 where V_{batt} is the battery voltage, as calculated in subsection 5.4.2.

$$P_{batt} = I_{batt} \cdot V_{batt} \tag{5.7}$$

Now combining Equation 5.6 and Equation 5.7 the battery output current can be given by Equation 5.8.

$$I_{batt} = \frac{P_{motor}}{V_{batt} \cdot \eta} \tag{5.8}$$

Finally, using Equation 5.4, Equation 5.5 and Equation 5.8 a parallel sizing relation is formed as given in below:

$$N_p = \frac{P_{motor}}{V_{batt} \cdot Q_{cell} \cdot C_{max} \cdot \eta} \tag{5.9}$$

Using this relation and the maximum power required by all the motor, a total of 26 cells are needed in parallel to satisfy the power requirement.

Now to size the battery for endurance, the battery energy should be equal to the total energy need by the motors during the entire mission. The total energy needed by the motors during the entire mission has already been calculated and is equal to $43912.5Wh$. Furthermore the battery energy is given by Equation 5.10.

$$E_{batt} = V_{batt} \cdot Q_{batt} \tag{5.10}$$

Using Equation 5.10 and Equation 5.4 the following relation can be derived:

$$N_p = \frac{E_{mission}}{Q_{cell} \cdot V_{batt} \cdot \eta} \tag{5.11}$$

Using this relation it is calculated that a total of 39 cells in parallel are needed to satisfy the endurance requirement. Instead a total 40 cells are connected in parallel as this increases the total capacity of the battery pack by 1.225 kWh hence providing a safety margin incase the mission duration is exceeded.

5.4.4. Total Battery Pack Configuration

The total number of cells needed and the configuration that these cells are to be connected can now be calculated using Equation 5.12.

$$N_t = N_s \cdot max(N_{p_E}, N_{p_p}) \tag{5.12}$$

N_t is the total number of cells needed, N_{p_E} is the number of cells needed in parallel to meet the endurance requirement and N_{p_p} is the number of cells needed in parallel to meet the maximum power requirement. According to the calculations 40 cells are to be connected in parallel configuration to ensure that the battery can provide sufficient power and energy through out the mission. A total of 640 cells are used in the battery pack with 16 cells in series and 40 cells in parallel.

5.4.5. Battery System Sizing

Now as the cells configuration is determined, the sizing of the battery system can be performed. Figure 5.4 provides an overview of the components present in the battery system. First the cells are connected together to make battery modules, these modules are then connected to make battery packs which are then housed in a battery casing and connected to a battery management system to complete the battery system.

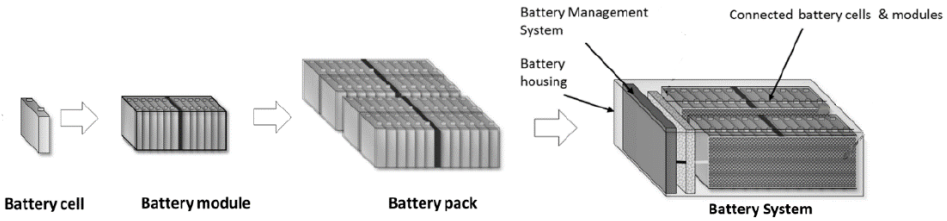

Figure 5.4: Schematic of the major components of the battery system.

As the battery casing is also used as a load carrying structure, which will be later discussed in section 6.4, so the battery casing is first designed and sized to meet the volume requirement PAT-UR-PERF-03 and the loading requirement. The battery casing design as given in section 6.4 comprise of 4 hollow aluminium beams connected together in a 2x2 grid. So a total of 4 battery packs are designed to fit in the hollow beams. As calculated in subsection 5.4.4 a total of 16 cells in series and 40 cells in parallel are needed. Using the battery cell dimensions as given in Table 5.3 and the available space in the beams, the battery modules are sized. The resulting battery module, after this sizing process, consists of 16 cells all connected in series configuration which can be seen in Figure 5.5a.

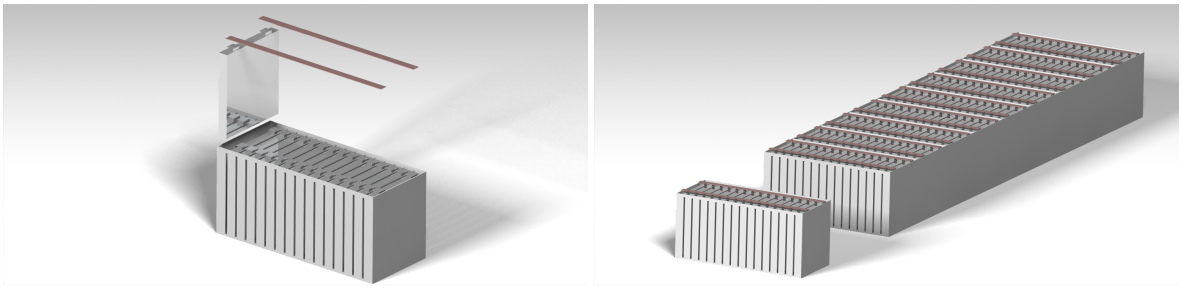

(a) Battery module containing Licerion cells

(b) Battery pack consisting of 10 battery modules

Figure 5.5: Conceptual propeller folding mechanism.

10 of these modules are then connected in parallel to create a battery pack as seen in Figure 5.5b. Furthermore all 4 battery packs are also connected in parallel to satisfy the 16Sx40P battery system configuration. Each battery pack is also connected to battery management system provided by Lithium balance[5]. The BMS (battery management system) consists of a monitoring unit and a control unit. This BMS can monitor and control the performance of upto 256 cells. The monitored battery pack performance characteristics includes: individual cell voltage, state of charge, state of health, cell temperature, leak detection, cell and pack resistance. Furthermore, the BMS can control the cell voltage and balance the cell current to prevent over current, over voltage and under voltage hence preventing the battery from operating outside its safe operating area there for increasing the life cycle of the battery.

The cooling system for each battery pack consists of a single fan provided by Johnson electric[6] in front of the battery pack and ventilation slits at the back of the pack. Furthermore, slits are present between cells in each module as can be seen in Figure 5.5a that allows air to pass through the entire battery pack. The fan is controlled by the BMS, which ensures that an optimal operating temperature is maintained. Polytetrafluoroethylene (PTFE) membrane filters provided by Nitto[7] are placed both in front of the fan and also on the ventilation slits. These filters not only prevent any dust and water particles from entering the battery pack but also provide 85% porosity, hence not hindering with the airflow. The total mass of the battery system is 103.7kg without the battery casing as that is considered to part of the structural mass. This total mass includes the cells mass, BMS and cooling fans. The total wight is 29.6% of the total mass hence meeting the power system mass requirement. Furthermore the cells have a full discharge cycle of 1000[18]. With the implementation of the cooling system and BMS this discharge cycle can be achieved without reduction in battery capacity. Hence a total of 1000 full length flights can be achieved without replacing the battery pack. With 500 flights a year the requirement PAT-UR-SAFE-04 of 2 year maintenance free can be fulfilled.

The verification of this sizing method is split into two: firstly verifying the series configuration and secondly verifying the parallel configuration. For series configuration, Equation 5.3 is derived from Kirchhoff's voltage law[20]. This law states that the sum of voltage in a closed circuit should be zero. This can be verified by a unit test, if the required motor voltage is zero then the number of cells in series should be zero. When tested in the tool the result was confirmed to be correct. Similar unit tests are performed for the parallel configuration sizing. For Equation 5.9 if $P_{motor} = 0$ then $N_p = 0$. This was tested in the tool and the result was confirmed to be correct. For Equation 5.11 if $E_{mission} = 0$ then $N_p = 0$. This was tested in the tool and the result was confirmed to be correct. As the results of all unit tests adhere to the expected out come hence the equations are verified.

To validate the method reference data form E-sprit HK36 electric aircraft is taken[21]. For electric aircraft the following data was extracted: $V_{motor} = 650$, $V_c = 3.6$, $C_{max} = 2.8$,$Q_{cell} = 3.5Ah$,$\eta = 0.93$, $P_{motor} = 74.57kW$ and $E_{mission} = 28.58kWh$. After implementing the extracted data in the tool it is calculated that 180.5 cells are required in series configuration. Furthermore, 12.5 cells are required in parallel configuration to meet the maximum power requirement and 13.6 cells are required in parallel configuration to meet the endurance requirement. The battery system used in the reference aircraft

[5] *S-BMS*. URL: `https://lithiumbalance.com/products/s-bms/` (visited on 01/18/2021)

[6] Johnson. *CFM-EV30*. URL: `https://www.johnsonelectric.com/en/features/custom-battery-cooling-fan-module-for-hybrid-and-electric-vehicles` (visited on 01/19/2021)

[7] Nitto inovation lab. *Temish*. URL: `https://www.nitto.com/eu/es/about_us/brand/promotion/innovation/temish.html` (visited on 01/19/2021)

consists of 180 cells connected in series and 14 cells connected in parallel. This is in line with the configuration calculated using the sizing tool, hence the tool is validated.

5.5. Noise Generation

To ensure that the system meets the maximum sound level requirement of $75dB$, it is vital to identify the main components in the production of noise. The single largest noise generator for this vehicle would be the propulsion system, specifically the propellers. To limit the scope of this analysis, it will concern only the noise generated by the propellers due to aeroaccoustic effects, only the noise generated by the (interaction of) the propellers. Noise due to external interference such as the beams is ignored, as it would require a much more detailed mesh to be present.

Previously the noise was modeled in a more general way by only basing the sound pressure level on the tip speed of the propeller. Now that more details on the propeller are known, this approach can be replaced by one that is more generalised for horizontally-aligned rotors, the so-called Davidson & Hargest equation, as seen in Equation 5.13. Originally, this equation was made with helicopters in mind. To ensure that this equation would work on a wide range of vehicles, which would hopefully include the vehicle being designed as well, it was validated using both helicopters and drones. For both cases, it is assumed that $C_b = 0$, as no sufficient data could be found for either validation cases. For the helicopter comparison, the Rotorschmiede VA115 was used. This helicopter also uses coaxial rotors. The error in SPL with experimental data with the Davidson & Hargest approach was $+8\%$ with the assumption of noise doubling due to double rotors, and assuming horizontal cruise speed. An analogy to the smaller drone scale was also made by validating the equation to a DZP30 off-the-shelf contra-rotating coaxial model aircraft propeller. Here, the error was -16%. Here the axial speed was assumed to be zero. Again, the vehicle that is being designed is not quite a helicopter nor a drone, but it comes close- and Davidson & Hargest does hold considerably well even on a smaller scale.

In this equation, v_F is the forward velocity, and $v_T = M_T a$ is the wing tip velocity as stated in Equation 5.14 (where a is the speed of sound and ω is the rotational speed of the propeller in RPM. This equation only gives the noise for a single propeller; The thrust must be divided over all the different disks as determined before in subsection 5.1.1. For a coaxial set at the relatively low RPMs that this device will operate on, a conservative estimate of $3dB$ should be added for the increase in noise due to coaxial interference [22]. As a total of 4 sets of coaxial propellers are used, the sound generated is $6dB$ higher than what comes out of this equation.

$$SPL = 20logT + 20log\sqrt{v_T^2 + v_F^2} - 10logS - 38.7 + C_b \tag{5.13}$$

$$M_{tip} = \frac{\pi D \omega}{60a} \tag{5.14}$$

At a rotational speed of 2400 RPM, leading to a tip speed mach number of 0.476, and a horizontal speed equal to the cruise speed of $40km/h$, the resulting sound pressure level equals $74.92dB$ at a distance of 500 ft.

5.6. Range and Endurance

Previously, it had been assumed that the addition of a horizontal component in the thrust to counter drag to fly at a cruise speed was negligible compared to the thrust required to keep the vehicle aloft. The upward pointing propellers would have to continuously actively counteract gravity directly. This is comparable to helicopters, where the maximum endurance would be hovering in the air, and maximum range can be achieved by going at near top-speed, until at some point drag becomes a bigger factor than the vertical upkeep. This means that the difference between flight profiles for maximum range and maximum endurance are minimal (except for the covered distance) [23]. For this personal air transportation vehicle with its very limited cruise speed of $40km/h$, this means that at all times it is desirable to fly at this speed.

To accurately asses the range and endurance of this vehicle exactly however, the power required for vertical levitation alone is hence not enough- The horizontal component, although small, must still be taken into account.

As the equation relating the power draw of the propeller its generated thrust does not specifically state that it can also be used to calculate the power draw for the horizontal component of the thrust generated, this is checked in two ways; once by making the assumption that this equation can be used this way directly by composing both thrust vectors into one larger vector, and once by assessing the energy required for horizontal flight separately and then adding it to the power draw.

In both cases, the horizontal thrust is there to counter the force of drag. This force is calculated using data from the aerodynamics department using the drag equation $D = 0.5\rho v^2 S C_D$, with $S \cdot C_D = 0.717$. The vertical thrust to be provided is simply equal to the weight distributed over the different actuator disks.

The first calculation assumes that the slight angle that the propellers function at does not affect its ability to generate thrust from a set power: the new thrust can be calculated simply using $T = \sqrt{D^2 + L^2}$. This is then used in the equation relating the thrust generated and power used as stated in Equation 5.1, and processed the same way as before by compensating for efficiencies and the power draw of auxiliary and support systems. This yields a total power usage of $64.483kW$. The total endurance can then be obtained by $t_{endurance} = \frac{E}{P}$, after which the range follows from $s_{range} = v_{cruise} t_{endurance}$.

The second approach of calculating this separates the power draw and the power required for horizontal translation. The former stays constant. It is known that the theoretical minimum amount of energy expended to cover a distance is $E_h = Ds$. Setting this range equal to the $30km$ requirement yields a total amount of energy, which can be subtracted from the energy stored in the batteries, after which the remaining endurance and range can be calculated similar to the previous approach. Knowing that the power draw for hover equals 64.475 kW and the energy required to cover the distance is $1.626MJ$, it is determined that the energy left for hovering is $174.08MJ$.

In the current configuration, the endurance for the first calculation is 2689.7 seconds, and for the second calculation it is equal to 2674.8 seconds. It is expected that the second calculation would give a lower number, as even though this is the 'ideal' case, the composition does not improve the conversion efficiency of the propellers due to a higher thrust being generated. In comparison, the endurance for the pure hovering case is also equal to 2704.2 seconds. In all cases, the requirement of a 45 minute flight time is met.

5.7. Charging

The internal propulsive power system works on a voltage of $63V$, and the auxiliary power system at $24V$. These two (separate) power systems need to be charged between uses. Charging is done by taking electricity from the local power grid and transfering it to the batteries. The electric grid in europe operates on a $50Hz, 240V$, DC current. An AC-DC conversion as well as voltage scaling need to be performed. It was decided to go with conventional open standards for electrically charged vehicles to be able to make use of existing charging and access points. Summarised, the current charging infrastructure consists of variable voltage DC suppliers, or slow direct interfaces. The former is faster and does not require an AC-DC converter to be on-board, but it is much more expensive, and fast-charging can damage the batteries. The latter work slower and require an AC-DC converter, but are abundant and inexpensive in terms of infrastructure cost. Fast-chargers can always be used (even if an AC-DC is in place, it can easily be bypassed. This section focuses on the technical sides of the charging process. For a more detailed overview of the operational aspects of charging and its infrastructure, please refer to section 9.6.

The question that must be answered is whether it is worth investing space and mass for an AC-DC converter to be able to access the low-power infrastructure as well. For this, an AC-DC unit was sized based on literature [8]. For application in this vehicle, the AC-DC would weigh $1.2kg$, and be dimensioned as $14 * 25 * 4cm$. This added weight means slightly more battery needs to be added as well. However, relative to the total system mass, this is only a slight addition. The additional freedom and deployability the addition of this system would give would be much greater than the slight decrease in weight, and hence it was decided to add such a vehicle-carried AC-DC converter to the charging system.

The AC-DC converter communicates with the battery controller to ensure the right voltage and currents are supplied. If a DC source is directly connected to the system, it shall detect this and relay the power and communications directly to the battery controller.

[8] Elcomsys. *Mil Grade AC-DC Compact Power Supply 30W – 3kW reference*. URL: `https://www.elcomsys.sg/mil-grade-ac-dc-compact-power-supply-30w-3kw/` (visited on 01/25/2021)

5.8. Sensitivity Analysis

A sensitivity analysis has been performed on the tool used to size the power and propulsion systems. This is a summary of what has already been reported in previous reports in this series. For more information on how these sensitivities were tested, please refer to the previous reports in this series.

Ultimately, the tool takes a system configuration as input and yields power requirements, power and propulsion subsystem component masses and their dimensions, and performance characteristics. Out of these the total power system mass fraction and noise generation are most indicative of the system's workability. The input parameters that affected the total power system mass fraction the most are (rated from most influential to least) the rotor diameter, the total system mass, the flight time, and the battery energy density. For the noise level, the most influential factors are (rated from most influential to least) the rotor diameter, the rotor RPM, total system mass, the cruise speed.

5.9. Risk Analysis

To improve the operability and reliability of the system it is important to identify the risks that accompany technologies and components applied impose. For each of these potential problems and failure modes, drivers, likelihood, and severity are identified to form a general risk. Detection strategies to identify these problems are also outlined. The identified failure modes can be found in Table 5.4 and their detection strategies in Table 5.5. These risks can be accepted, but ways around them can also be sought to mitigate the risks by either decreasing their likelihood or severity (or ideally, both). The mitigation strategies identified for the failure modes in Table 5.4 are listed in Table 5.6.

Table 5.4: Failure modes analysis for the power, propulsion and performance subsystems.

Risk ID	Failure Mode	Drivers	Likelihood	Severity
TR.PP.TP-1	Forced stop	Debris, objects	4	1
TR.PP.TP-2	Shaft misallignment	Bearing failure, deformation	2	3
TR.PP.TP-3	Motor overheating	Motor overload, Wrong supply voltage	2	3
TR.PP.TP-4	Controller failure	Short circuit, physical damage	1	5
TR.PP.TP-5	Motor short circuit	Wear on winding insulation	4	5
TR.PP.S-1	Propeller Collision	Debris, objects	4	3
TR.PP.TP-6	Propeller detachment	Gust loads, environmental decay	1	5
TR.PP.TP-7	Folding system failure	Improper unfolding	1	5
TR.PP.TP-8	Propeller stall	Wind gusts, wrong propeller setting	2	4
TR.PP.S-2	collision with ground	Landing, take-off	3	4
TR.PP.TP-9	propeller deformation	fatigue	1	1
TR.PP.TP-10	Battery fire	Overheating	2	4
TR.PP.TP-11	Battery overcharging	Leaving in the charger for too long	5	1
TR.PP.TP-12	Thermal runaway leading to explosion	Collision with the ground	1	5
TR.PP.TP-13	contamination	Environmental intrusion	2	2
TR.PP.TP-14	Terminal oxydation	Humidity	1	3
TR.PP.TP-15	Early battery aging	Heavy use	4	2

Table 5.5: Detection strategies for the identified risks.

Risk ID	Failure Mode	Detection strategy	Detection
TR.PP.TP-1	Forced stop	RPM monitoring, motor voltage spike, torque increase	1
TR.PP.TP-2	Shaft misallignment	RPM monitoring, voltage drop	2
TR.PP.TP-3	Motor overheating	Temperature sensor measurement	1
TR.PP.TP-4	Controller failure	Mismatch between power output and requested power	2
TR.PP.TP-5	Motor short circuit	Mismatch between power output and requested power	2
TR.PP.S-1	Propeller Collision	RPM monitoring, motor voltage spike, torque increase	2
TR.PP.TP-6	Propeller detachment	RPM monitoring, voltage drop	2
TR.PP.TP-7	Folding system failure	Checking folding system state	3
TR.PP.TP-8	Propeller stall	Torque drop	3
TR.PP.S-2	collision with ground	RPM monitoring, motor voltage spike, torque increase	1
TR.PP.TP-9	propeller deformation	Torque RPM mismatch to internal data	2
TR.PP.TP-10	Battery fire	Temperature sensor measurement	1
TR.PP.TP-11	Battery overcharging	Charging system voltage regulator	3
TR.PP.TP-12	Thermal runaway leading to explosion	Temperature sensor measurement	1
TR.PP.TP-13	contamination	Battery output voltage and current comparison to age model	4
TR.PP.TP-14	Terminal oxydation	Battery output voltage and current comparison to age model	4
TR.PP.TP-15	Early battery aging	Battery output voltage and current comparison to age model	1

Table 5.6: Mitigation strategies for the identified risks

Risk ID	Mitigation Strategy	Change in Likelihood	Change in Severity
TR.PP.TP-1	Flying protocols	2	0
TR.PP.TP-2	Regular inspection, self-diagnosing of motor performance	1	1
TR.PP.TP-3	Surge protection, performance limitations	1	0
TR.PP.TP-4	Controller redundancy	0	3
TR.PP.TP-5	Regular inspection, self-diagnosing of motor performance	2	2
TR.PP.S-1	Flying protocols	2	0
TR.PP.TP-6	Emergency Landing	0	2
TR.PP.TP-7	Failure detection and immediate stop of propeller	0	2
TR.PP.TP-8	Stall recovery protocal, stall condition avoidance	1	1
TR.PP.S-2	Landing clearance checking, system self-leveling	1	1
TR.PP.TP-9	Pre-flight diagnostics	1	0
TR.PP.TP-10	Self-diagnosing battery management, temperature control	1	1
TR.PP.TP-11	Charger system that disengages upon full load	4	0
TR.PP.TP-12	Active collision detector and circuit breaking of battery system	0	3
TR.PP.TP-13	Sealing batteries from environment, inspection	1	0
TR.PP.TP-14	Inspection and cleaning	0	1
TR.PP.TP-15	Limiting depth of discharge	2	0

6
Structures and Materials

In this chapter, the process of designing the load carrying structure is described.In addition to designing the structure, the materials are selected. The load carrying structure is constructed out of multiple parts. Some of these parts need actuators, presented in this chapter as well.

6.1. Materials and properties

In the midterm report the material selection was dialled down to Aluminium and Composites. Quite soon in the detailed design phase a decision had to be made between these two materials. In this decision not only material and mechanical properties were discussed, but also the cost, sustainability and production. Composites is the better option purely looking at it from a structures standpoint. It has a higher strength, is lighter and can be designed for strength and stiffness in the direction that you want. However in the bigger picture Aluminium is a cheaper option, is better recyclable and reusable and is much simpler in production. Since the start of the process as a team we have hammered on the fact that the vehicle should be as sustainable as possible and we are also bound to some cost requirements. Therefore it was decided to continue the detailed design with Aluminium as the main material. The table below shows the different materials used in the structure and an overview of their properties and characteristics[1][2].

Table 6.1: Materials overview [16]

Material	**Density** [kg/m3]	**E-modulus** [GPa]	**Yield strength** [MPa]	**Tensile strength** [MPa]	**Shear strength** [MPa]	**Bearing strength** [MPa]	**Price** [EUR/kg]
Al 7075-T6	2770	70	480	560	330	510	4.5
AL 6061-T6	2700	68.9	276	310	207	386	2.25

The 6061-T6 Aluminium is the most used in the design. The 7075-T6 is only used in the landing gear and the user module frame, since these will be highly loaded structures and the strength properties of 7075-T6 are better.

6.2. Beam design

The beams are an important part of the structure. The beams have to withstand the forces originating from the motors. The beams will be mainly in bending. In order to withstand all the loads, a hollow structure is chosen. The beams are slanted towards the end, to optimise in terms of weight. An equation is derived to find the location along the beam where the bending stress is the highest. This is not at the root, due to the slant. This equation is derived on the hand of the book Mechanics of Materials from Pearson [24]. This equation was constructed for a solid beam, so the Moment of Inertia needed an update. Other than that, the equation used in the book was made for a beam with a height at the root being three times the height at the end. In the equation constructed, the height was left as parameter a. A local coordinate system was used in the design of the beam. The beam was modelled in Python, based on the following free body diagram.

[1] ASM Matweb. *Aluminium 6061-T6; 6061-T651*. URL: `http://asm.matweb.com/search/SpecificMaterial.asp?bassnum=MA6061T6`

[2] John Mitchell. *7075-T6 aluminium: overview & properties*. URL: `https://www.engineeringclicks.com/7075-t6-aluminium/` (visited on 01/18/2021)

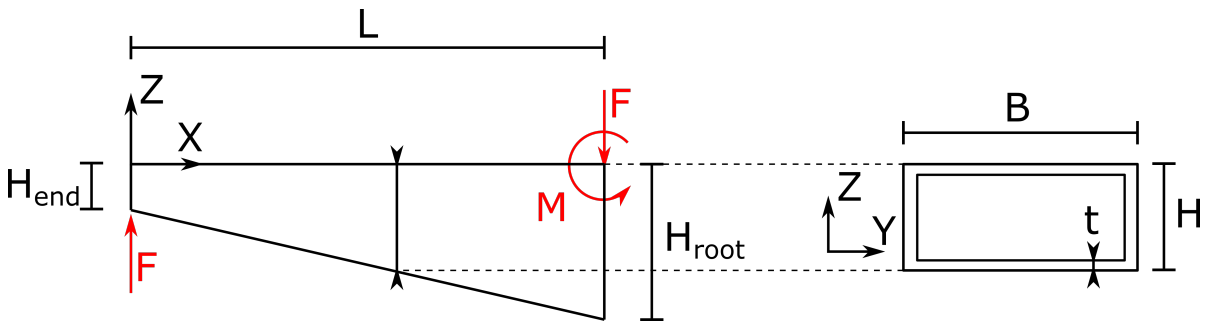

Figure 6.1: Beam free body diagram

The derivation started with the flexure formula, with c the maximum distance from the normal axis.

$$\theta = \frac{Mc}{I} \tag{6.1}$$

The Moment, c and h are defined as follows:

$$M = T \cdot x, \quad c = \frac{h}{2}, \quad h = \frac{h0}{L}((a-1) \cdot x + L) \tag{6.2}$$

Where L is the length of the beam and a is the fraction of H_{root} and H_{end} and x is the x-position on the beam. The area moment of Inertia equation for a rectangular hollow section is the final value that needs to be known in order to be able to calculate the normal stress. The area moment of Inertia is varying as the cross-section is varying.

$$I = \frac{BH^3 - bh^3}{12} \tag{6.3}$$

Now, the location with the highest occurring stress can be easily determined and the value can be calculated. A plot of the normal stress is showed.

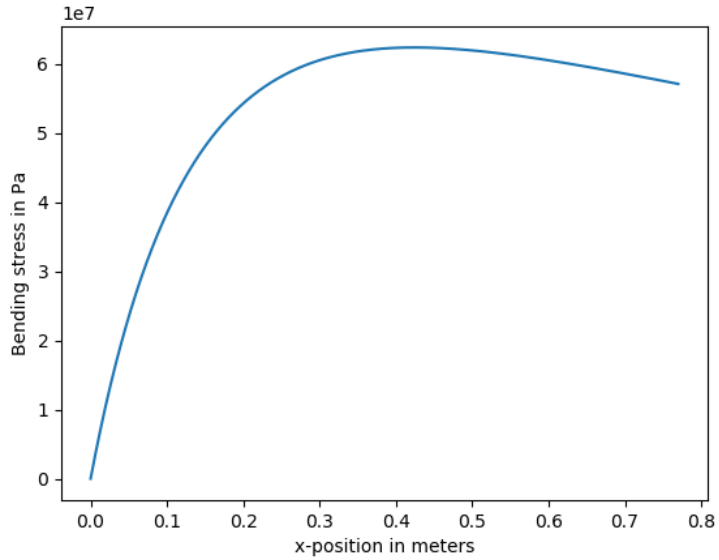

Figure 6.2: Normal stress in the beam.

As can be seen in the figure, the maximum normal stress does not occur at the root of the beam. This is a result of the varying cross-section of the beam. To check if the maximum shear stresses are

higher than the stresses that the material can resist, the maximum shear stress is calculated. The shear stress is calculated via the following equation:

$$\tau = \frac{V_{max} Q}{2 I t_{flange}} \tag{6.4}$$

V_{max} represents the maximum shear force, equal to the thrust force. t_flange represents the thickness of the beams in the flanges, equal to 2 mm. Q and I are functions of the x-position. Q is defined as follows:

$$Q = \frac{B}{2} \cdot (h + t_{webs})^2 - (\frac{B}{2} - t_{flange}) \cdot h^2 \tag{6.5}$$

The maximum shear stress is $70.8MPa$, which is well below the shear strength of Aluminum 6061T6. The shear distribution is presented in the plot below:

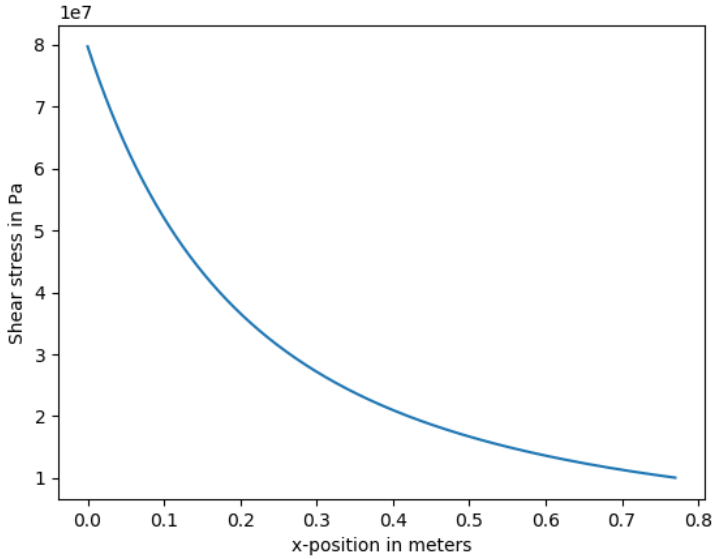

Figure 6.3: Shear stress in the beam.

The Von Mises stress is also calculated, when the maximum shear stress is used, it still does not exceed the material properties.

$$\theta_{VonMises} = \sqrt{\theta_{max}^2 + 3\tau_{allow}^2} \tag{6.6}$$

A safety factor of 1.5 is used, which is a commonly used value in Aerospace Engineering when Aluminum 6061T6 is used. According to the FAA part25.303, the safety factor is taken as 1.5, as there is no specification on the design [25].

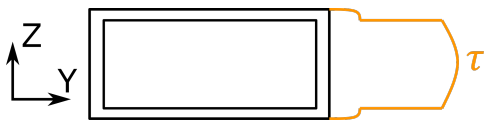

Figure 6.4: Shear stress distribution over the cross-section, with H varying.

Table 6.2: Resulting dimension of the beam design.

Beam Property	Value
Length R	$0.76m$
Wall thickness t	$0.002m$
Height at root	$0.021m$
Height at end	$0.008m$
Mass of the beam	$1.009kg$

The deflection in the beam is calculated under the maximum forces. This result in the maximum deflection. In order to do this, the following relation was used:

$$\frac{d^2w}{dx^2} = \frac{M}{E \cdot I} \tag{6.7}$$

In this equation, both the moment and the area moment of Inertia are a function of the x-position on the beam. Integration is done via Python, which gave a deflection of $0.0639m$ which is a reasonable value considered the loads. The deflection does not exceed the ground clearance.

6.3. Hinge design

The arms of the rotorcraft are to be retracted to fit inside 1 cubic meters. Therefore, the design includes a hinge between each beam and the battery casing. This hinge allows for rotation around 2-axis. The hinge shall be made from the same material as the beam, thus sharing the same properties.

The loading of the hinge is as shown in Figure 6.5. As done earlier, a safety factor of 1.5 has been included to the maximum loads to size it to that value accordingly. These final design properties can be found in Table 6.3. The stresses displayed in the table are for normal conditions. The hinge translates the vertical shear force (originating from the propeller lift) from the beam to the battery casing. On top of that, the hinge and its two bolts should withstand the bending moment induced by the propeller lift over the beam length. The hinge is therefore analysed on bearing stress, bolt shear stress and normal stresses due to bending.

The bearing yield strength of AL6061 is $386MPa$ as can be seen in Table 6.1. This property can be guaranteed for "Edge distance/pin diameter = 2.0". The shear strength of the bolt is $207MPa$ and the yield strength for the normal stresses has been taken as $276MPa$.

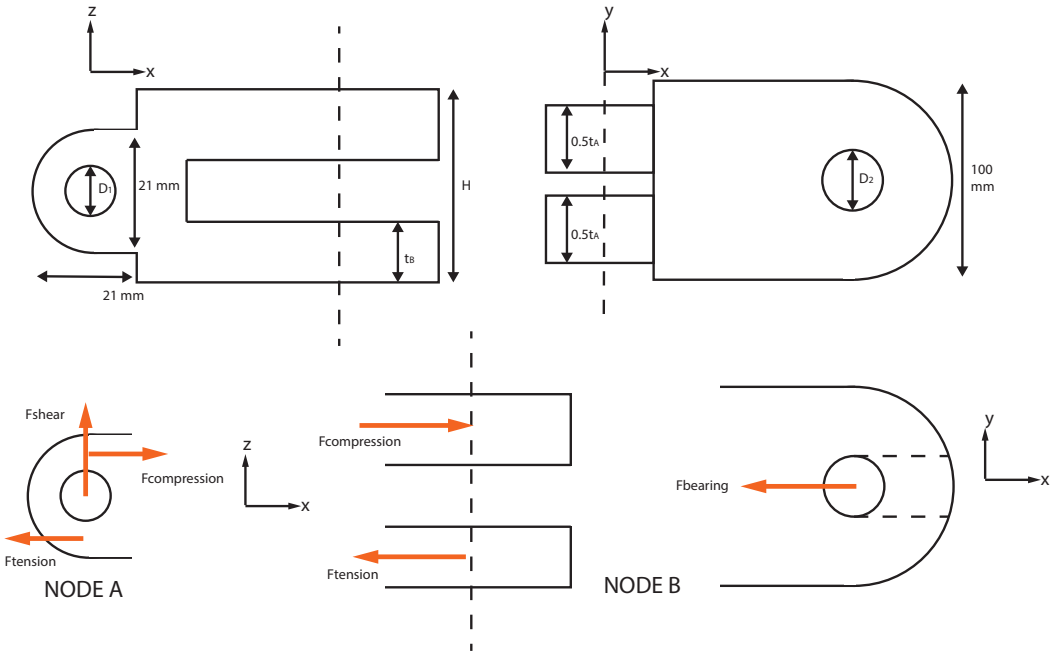

Figure 6.5: Free-body diagrams of the hinge: Node A and B

The equations used for the structural analysis of the hinge can be found below.

$$\sigma_{normal} = \frac{F_{tension}}{A} \qquad \sigma_{bearing} = \frac{F_{bearing}}{Dt} \qquad \tau_{bolt} = \frac{4 \cdot F_{shear}}{\pi D^2} \tag{6.8}$$

6.3.1. Hinge node A

As the height of the hinge is the same as for the beam, the bolt diameter and the bearing thickness t_A are left to size, looking at Figure 6.5. As the edge distance is fixed by the beam height of $21mm$, this gives a pin diameter D_1 of $4.2mm$. For this diameter, the shear stress in the bolt does not exceed a value $56MPa$ and therefore other design limiting factors have to be considered. The equation above explains how we can find the bearing stress. As the bearing stress is a function of the bearing load (in Figure 6.5 labeled as F_{shear}) over the bearing area, an expression for the minimal thickness has been obtained. For node A, the bearing load proved to not be a limiting factor. Looking at the normal stresses at node A (derived for the tension and compression caused by the lift force over the moment arm), a certain bearing thickness for the surface area was required. The result was a thickness (in this case a width) of $t_A = 40.8mm$.

6.3.2. Hinge node B

Again, the bolt diameter has been fixed with the edge distance relation shown above. As the width of the beam is $100mm$, a diameter D_2 of $20mm$ has been found. Next, the height of the flanges and their thicknesses t_B are to be sized. The shear stress in this bolt comes from the normal stresses in the hinge top or bottom flanges. These loads have also been taken as bearing loads, to size the flange thickness. So to size the flange thickness, we look at bearing and normal stress. After multiple iterations, the shear stress of the bolt proved to be the limiting factor. As the bolt diameter is already maximised, the maximum tension/compression load on this bolt came down to roughly $65.0kN$. This load has been used to size the thicknesses of the flanges and their offset, which was limited by the bearing stress. The height that was needed to get this load was 29 mm and the corresponding thickness (limited by the bearing stress) was $8mm$.

Table 6.3: Final results for the hinge in Figure 6.5

Hinge Property	Value
Diameter 1 D_1	$4.2mm$
Diameter 2 D_2	$20mm$
Thickness node A t_A	$40.8mm$
Thickness node B t_B	$8mm$
Hinge Mass (1 of 4)	$0.44kg$
Normal stress node A	$183.8MPa$
Normal stress node B	$63.7MPa$
Bearing stress node A	$9.0MPa$
Bearing stress node B	$254.7MPa$
Shear stress bolt A	$37.2MPa$
Shear stress bolt B	$129.7MPa$

6.4. Load-carrying battery design

The battery casing is designed to be the load carrying structure of the product. It carries the shear forces and bending moments of the beam as well as the weight of the entire system. As the battery cells can not be stacked, two levels had to be made. A vertical web has been added to carry the loads of the landing gear. An overview of the cross-section can be found in Figure 6.7. As the cross section is rather complicated for structural analysis, a few simplifications have been made:

- All the loads along the y-axis have been collected on the x-axis and shown in Figure 6.6.
- The single shear force V_z in Figure 6.7 stems from the shear force distribution of Figure 6.6. As can be seen, it varies along the battery length.

- The cross-section will be treated as a 2-square-multicell as shown on the right-hand side of Figure 6.7.

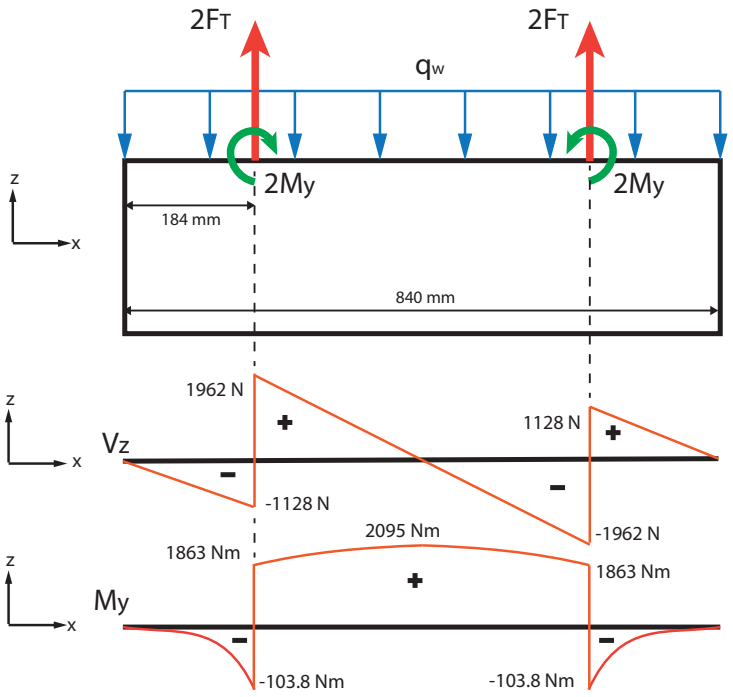

Figure 6.6: Free-body diagram, shear force diagram and bending moment diagram of the battery-casing

All the outer dimensions of the battery casing have been fixed inh the conceptual design of the battery. Only the thickness is left to size. For this, the thickness is sized by either the maximum allowable shear stress, maximum allowable normal stress or maximum allowable Von-Mises stress (all including a safety factor of 1.5). Next to that, deformation of the battery case was to be considered as well, to protect the battery cells from damage (as they should not be load carrying). The first step was to determine the shear force distribution and the corresponding bending moment diagram. The magnitudes given on Figure 6.6 include the 1.5 safety factor on the maximum loads. These have been found as follows: The beam translates the propeller thrust to the battery and is noted as F_T for each beam in Figure 6.6. The weight is distributed over the battery length.

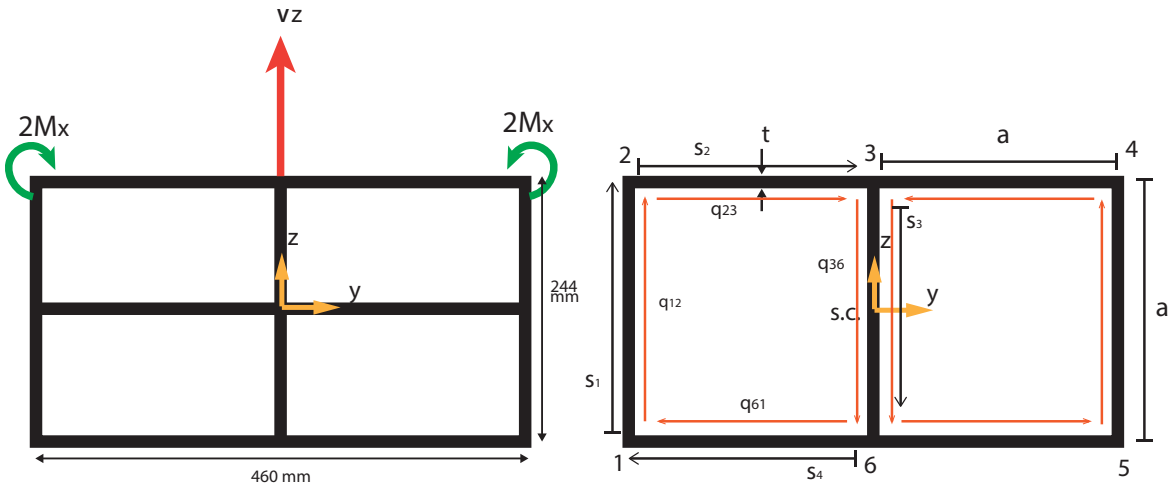

Figure 6.7: Free-body diagram of the battery cross section

The moment diagram has been used to determine the normal stresses in x-direction. The location of

maximum shear also proved to be the location of maximum von-mises stress, as this location also has an high bending moment. The location of maximum bending moment M_y has no contribution of shear force. For the shear stress calculations, the cross-section is assumed to be thin-walled. A cut has been made on between point 1 and 6 on Figure 6.7. The base shear flows have then been calculated with Equation 6.9.

$$q_{b_{0,1}} = \frac{-V_z I_{zz} - V_x I_{xz}}{I_{xx} I_{zz} - I_{xz}^2} \int_0^{s_1} tz\, ds_1 - \frac{V_x I_{xx} - V_z I_{xz}}{I_{xx} I_{zz} - I_{xz}^2} \int_0^{s_1} tx\, ds_1 \tag{6.9}$$

Taking the moment of the shear flows, expressed as M_b, about point 3 simplifies the calculation of the redundant shear flow q_0 using the expression below.

$$-2M_x + M_b + 2A_m q_{s,0} = 0 \tag{6.10}$$

Adding the redundant to the base shear flows and dividing the results with the thickness gives a shear stress per flange. The location of maximum shear is between point 1 and 2 (or due to symmetry 4 and 5) on the y-axis. Sizing the battery case thickness to the 3 aforementioned stresses resulted in a value of less than 1 mm. Predictions of this thickness were made on its performance in elastic deformation, concluding such a thickness is not feasible. Verification has been conducted using the analysis tool on CATIA, which resulted in a range of 5-10 mm in translational deformation. To get an impression (without actual deformation values), see Figure 6.8.

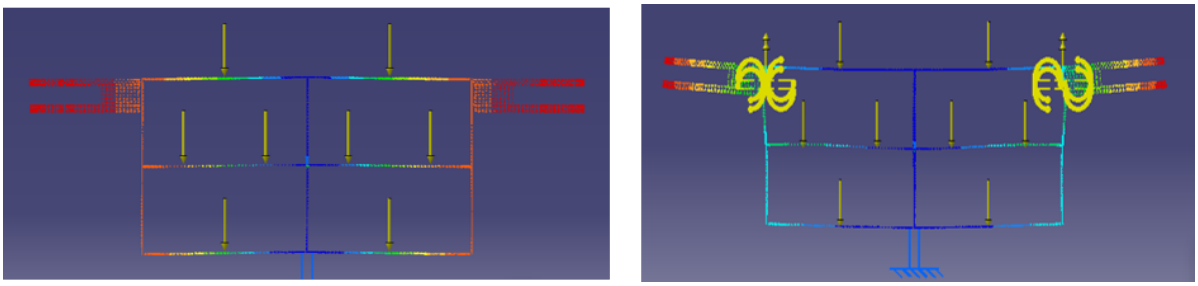

Figure 6.8: Deformation impression for a thickness of 0.75 mm while landed (left) or under maximum load (right)

Earlier, the design decision has been made to prevent the battery casing of loading the cells. Therefore, the clearance between the battery casing and the cells should take up the deformation. Increasing the thickness decreases the clearance but also the deformation. As a result, the expression used to find the optimum clearance/thickness combination, Equation 6.11, has the battery height (h), the cell height (h_{cell}), the thickness (t) and the clearance (C).

$$h - 2 \cdot h_{cell} = 4C + 3t \tag{6.11}$$

Using CATIA V5 to calculate the deformations, the optimum has been found. This, as well as stress results for this thickness are presented in the table below:

Table 6.4: Final results for the battery casing in Figure 6.7

Battery casing properties	**Value**
Thickness	$2.0mm$
Clearance top/bottom	$4.5mm$
Clearance sides	$13.5mm$
Mass	$9.5kg$
$\sigma_{x_{max}}$	$24.2MPa$
τ_{max}	$16.0MPa$
σ_{vm}	$36.8MPa$

6.5. Landing Gear

It is determined that the system should have a set of landing gear that is fixed to the device to allow for a tipover margin and extra safety during crash landings.

The main design case is the crash landing, where the energy of a power-off landing should be absorbed by the landing gear. From the CS27 small rotorcraft regulations by the European Aviation Safety Agency (EASA), it is determined to design the gear for a drop test from $0.33m$ [26]. Using the direct conversion from potential gravitational energy to kinetic energy, it is determined that this corresponds to an impact velocity of $2.55m/s$. The landing gear is designed to withstand this drop test, without permanent deformation. Thus the energy of the impact should be absorbed withing the yield strength limits of the chosen material.

Due to the limited space available for the landing gear, it is decided to size a simple helicopter skid landing gear. This configuration is shown in Figure 6.9. The size limitations, due to the volume requirement, are a length of $840mm$, a width of $920mm$ and a height of $90mm$.

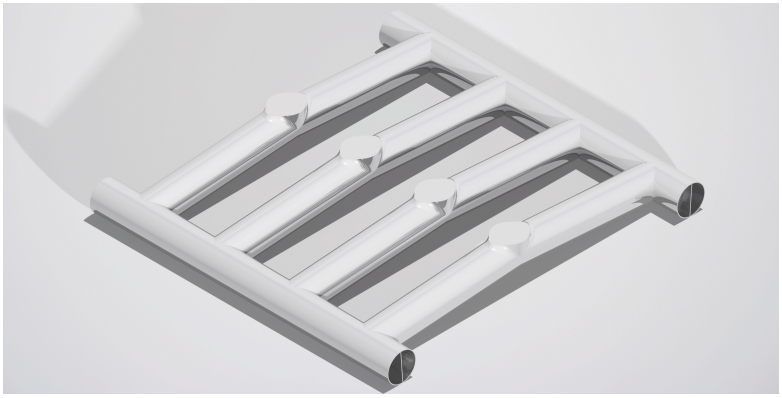

Figure 6.9: The landing gear designed for the system.

The next step is to determine the work and energy relations. This requires setting up the free body diagram and deformation diagram of the load case in Figure 6.10. The legs of the gear are modelled with cantilever beams under an angle, experiencing an impact force at the tip that has a shear and axial component in the beam.

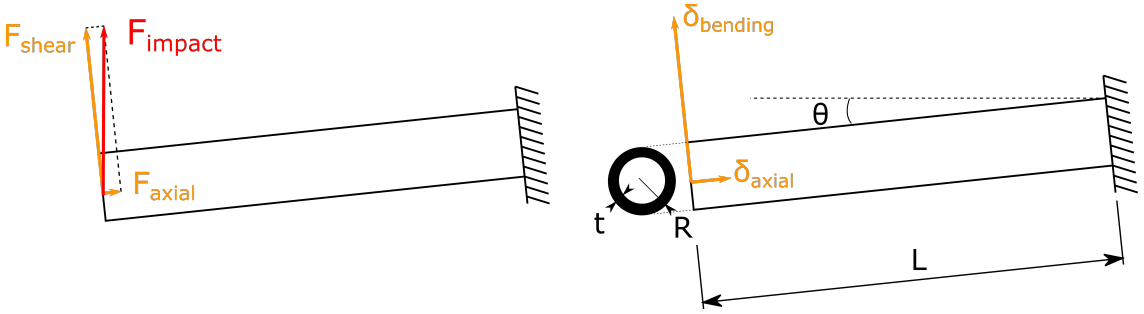

Figure 6.10: Landing gear free body diagram and deformation diagram.

Using the diagrams above, an energy balance can be set up for the impact. Since use is made of 8 legs, the impact energy is equally distributed over those. As seen in the free body diagram, there is an impact force acting on the beam. This force is split into its shear and axial components. Use is made of the deflection equations for both force components in Equation 6.13 to achieve Equation 6.14. The equation is then solved for this impact force, which is shown in Equation 6.15.

$$F_{shear} \cdot \delta_{bending} + F_{axial} \cdot \delta_{axial} = \frac{1}{2} \cdot m \cdot V^2 \tag{6.12}$$

$$\delta_{axial} = \frac{F_{axial} \cdot L}{A \cdot E}, \qquad \delta_{bending} = \frac{F_{shear} \cdot L^3}{3 \cdot E \cdot I} \tag{6.13}$$

$$F_{impact}^2 \cdot \left(\frac{L^3 \cdot cos^2(\theta)}{3 \cdot E \cdot I} + \frac{L \cdot sin^2(\theta)}{A \cdot E} \right) = \frac{1}{2} \cdot m \cdot V^2 \tag{6.14}$$

$$F_{impact} = \sqrt{\frac{m \cdot V^2}{2 \cdot \left(\frac{L^3 \cdot cos^2(\theta)}{3 \cdot E \cdot I} + \frac{L \cdot sin^2(\theta)}{A \cdot E} \right)}} \tag{6.15}$$

This singular impact force is then again expanded its components, which are used to solve for the maximum internal stresses and deflections at the unsupported end of the cantilever beam. These deflections and stresses are defined in Equation 6.13 and Equation 6.16.

$$\sigma_{axial} = \frac{F_{axial}}{A} \qquad \sigma_{bending} = \frac{F_{shear} \cdot R \cdot L}{I} \qquad \tau_{max} = \frac{F_{shear} \cdot Q_{max}}{2 \cdot I \cdot t} \tag{6.16}$$

To achieve a feasible design, the geometry of the beam cross-section is set as a hollow circular section, as seen in Figure 6.10. Due to the sizing limitation, the length of the beam is determined by the cross-section size and the placement angle θ. The dimensions of the cross-section and the placement angle are iterated until the internal stresses ($\sigma_{max} = \sigma_{axial} + \sigma_{bending}$ and τ_{max}) are lower than the yield values, including a safety margin of 25%. The final beam sizing is presented in Table 6.5.

Table 6.5: Resulting landing gear beam properties from the impact analysis.

Beam Property	**Value**
Beam Length L	$0.419m$
Placement Angle θ	$1.37°$
Cross-section Radius R	$40mm$
Wall thickness t	$11.0mm$
Landing gear mass	$24.43kg$

Between the legs, beams are added to act as skids. It is assumed that these do not carry significant loads and are thus chosen to be hollow circular tubes with the same radius as the leg beams and a thickness of $2mm$. A plate of the same thickness is put in the centre of the skid tubes to add support for the user to step on top. The final design of the landing gear is shown in Figure 6.9

6.6. User Module Frame Design

To shield the user from the environment, there is a user module. This user module consists of 3 main structural elements: the skin, the windshield and a frame. This last component requires some design work. Due to the size constraints and required volume to fit a person and certain subsystems, the external sizing is completely set, as shown in Figure 6.11 and Table 6.6 As the another important function of the user module is to keep the user safe during a crash, the frame is designed to withstand the impact without permanent deformation. Similar to the landing gear, a drop from $0.33m$ is chosen as the design case, with the main difference being that the system has flipped over.

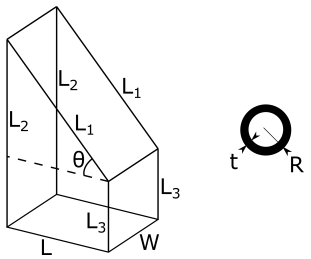

Figure 6.11: User module frame configuration.

Table 6.6: Dimensions of the module frame.

Dimension	**Length** $[m]$
Length L	0.840
Width W	0.500
Angled Beam Length L_1	1.288
Long Beam Length L_2	1.775
Short Beam Length L_3	0.778

It is assumed that only the vertical parts of the frame absorb the impact, meaning the horizontal members of the structure are ignored. This leaves 6 load carrying members, split in 2 separate structures. These 2 structures, in this case, absorb half of the impact energy. The free body diagram for this load case is represented in Figure 6.12. It shows the overall loading and the loading of each of the frame beams. On the right are the deformation diagrams used for the further analysis. Important to note is that the system is not in equilibrium, which would not be the case in real life. Impacts are dynamic situations in which deformations happen. There is an assumed force equilibrium, however, to simplify the calculations.

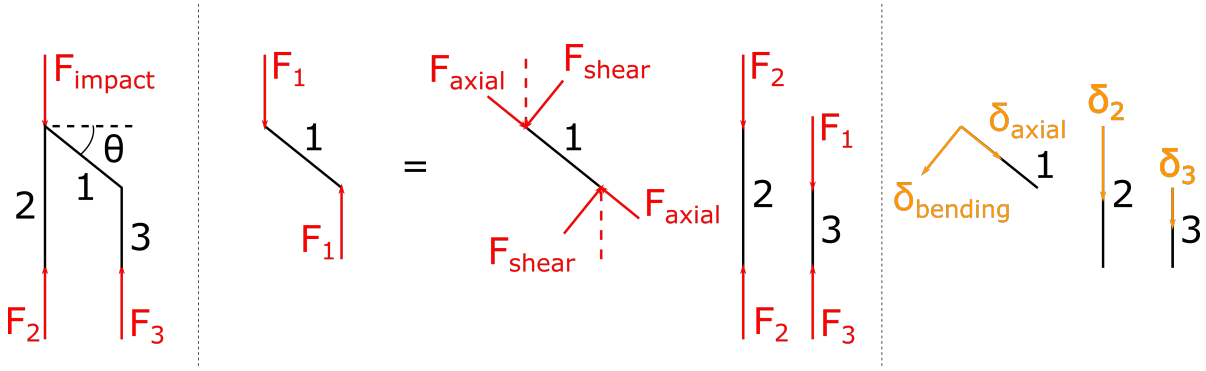

Figure 6.12: User module structure free body diagrams and deformation diagrams.

Before an energy balance is set up, compatibility equations are worked out to determine the distribution of the impact force F_{impact} over the 2 sides of the structure (beam 2, and beams 1 and 3). It is assumed that the deformation of the beam 1 is downward, as this is the acting direction of the force on that beam. This is not entirely accurate, but is an acceptable assumption for energy calculations. It is also noted that $F_1 = F_3$, $F_{shear} = F_1 \cdot cos(\theta)$ and $F_{axial} = F_1 \cdot sin(\theta)$. The compatibility equation is defined in Equation 6.17. From now on, the compatibility factor c from this equation is used for brevity. Similar deflection equations can be used to the ones for the landing gear, as the partial load cases are equivalent.

$$\delta_2 = \delta_1 + \delta_3 = \sqrt{\delta_{bending}^2 + \delta_{axial}^2} + \delta_3$$

$$\frac{F_2 \cdot L_2}{A \cdot E} = \sqrt{\left(\frac{F_{shear} \cdot L_1^3}{3 \cdot E \cdot I}\right)^2 + \left(\frac{F_{axial} \cdot L_1}{A \cdot E}\right)^2} + \frac{F_3 \cdot L_3}{A \cdot E}$$

$$F_2 = F_3 \cdot c = F_3 \cdot \frac{A \cdot E \cdot \left(\sqrt{\left(\frac{L_1^3 \cdot cos(\theta)}{3 \cdot E \cdot I}\right)^2 + \left(\frac{L_1 \cdot sin(\theta)}{A \cdot E}\right)^2} + \frac{F_3 \cdot L_3}{A \cdot E}\right)}{L_2} \tag{6.17}$$

The next step is to set up the energy balance for this system in the selected load case. Use can again be made of the free body diagram in Figure 6.12. Similar to the landing gear, the energy balance reads as follows:

$$F_{shear} \cdot \delta_{bending} + F_{axial} \cdot \delta_{axial} + F_2 \cdot \delta_2 + F_3 \cdot \delta_3 = \frac{1}{2} \cdot m \cdot V^2$$
$$F_3^2 \cdot \left(\frac{L_1^3 \cdot cos^2(\theta)}{3 \cdot E \cdot I} + \frac{L_1 \cdot sin^2(\theta) + L_2 \cdot c^2 + L_3}{A \cdot E} \right) = \frac{1}{2} \cdot m \cdot V^2$$

$$F_3 = \sqrt{\frac{m \cdot V^2}{2 \cdot \left(\frac{L_1^3 \cdot cos^2(\theta)}{3 \cdot E \cdot I} + \frac{L_1 \cdot sin^2(\theta) + L_2 \cdot c^2 + L_3}{A \cdot E} \right)}} \tag{6.18}$$

The solution of the energy balance equation results in the force in beam 3. Using the compatibility equation, the force in beam 2 can be determined and with the relations between F_3, F_1, F_{shear} and F_{axial}, the other internal forces are found. These forces can then be used to calculate the internal stresses in the frame, using the following equations:

$$\sigma_{axial} = \frac{F_{axial}}{A}, \quad \sigma_{bending} = \frac{F_{shear} \cdot R \cdot L_1}{I}, \quad \tau_{1,max} = \frac{F_{shear} \cdot Q_{max}}{2 \cdot I \cdot t}, \quad \sigma_2 = \frac{F_2}{A}, \quad \sigma_3 = \frac{F_3}{A} \tag{6.19}$$

$$\sigma_{1,max} = \sigma_{axial} + \sigma_{bending} \tag{6.20}$$

Since the cross-section dimensions are the only variables, these are iterated until all the internal stresses are lower than the yield stress of the Aluminium 7075-T6, which the frame will be made from. A safety margin of 25% is used. These iterations result in Table 6.7.

Table 6.7: Resulting dimension of the impact analysis for the user module frame.

Beam Property	Value
Radius R	$20mm$
Thickness t	$2.5mm$
Frame Mass	$8.27kg$

6.7. Deployment

The deployment of the vehicle has been explained in this section, which was required to fit inside the volume requirement. Starting off with the actuator research in subsection 6.7.1.

6.7.1. Actuators

For the automated rotation in the deployment of the vehicle, each hinge contains an actuator providing the necessary torque for this. Figure 6.13 shows the rotation that the actuators are responsible for.

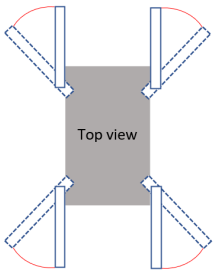

Figure 6.13: Actuator rotation movement

To determine the torque necessary for this rotation, a rotational equation of motion needs to be set up. The free body diagram and kinetic diagram can be seen in Figure 6.14 where $K = I_P \alpha$. α is the rotational acceleration and I_P the mass moment of inertia (MMOI) of the beam from point P. P is the

point where the beam is connected to the hinge and the centre of mass of the beam is assumed to be at the end where the motor and propellers are.

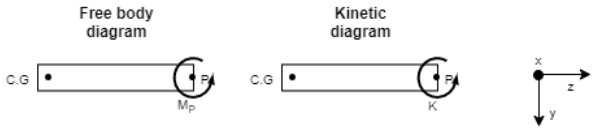

Figure 6.14: FBD and kinetic diagram actuator

For calculating the mass moment of inertia, the beams were estimated as hollow cylinders and the motors and propellers as disks. The mass moments of inertia for these shapes are as follows in Equation 6.21. The MMOI is taken from the end of the cylinder and also the edge of the disk.

$$I_{cylinder} = \frac{2mL^2}{3} \qquad I_{disk} = \frac{3mr^2}{2} \tag{6.21}$$

With this the MMOI of the complete beam around the X-axis at point P can be calculated. Using Figure 6.14 an equation of motion can now be set up. Assuming the friction in the hinges is neglected. This means the torque necessary is only based on the product of the MMOI and the angular acceleration.

$$\sum M_x : I_p \cdot \alpha = M_p \tag{6.22}$$

The chosen actuator (PA-R-205-6) from Pegasus actuators has a rotational speed of $1.833 rad \cdot s^{-1}$ and to perform the rotation in the desired 10 seconds it would need an acceleration of $0.1833 rad \cdot s^{-2}$ [3]. With $I_p = 7.821 kgm^2$, the necessary torque for this rotation is $1.433 Nm$, for which the chosen actuator is perfect. It has a rated torque of $1.8 Nm$ giving some margin for small effects like friction and air resistance of the beam in the rotation.

6.7.2. Deployment steps

In this section the different steps in deployment of the vehicle are described. In the retracted (parking) state, the vehicle looks like the right picture in Figure 6.15. The deployment goes according to the following steps.

[3] Pegasus actuators. *PA-R-205-6 actuator*. URL: `https://www.pegasus-actuators.com/product/r-205-6.html`

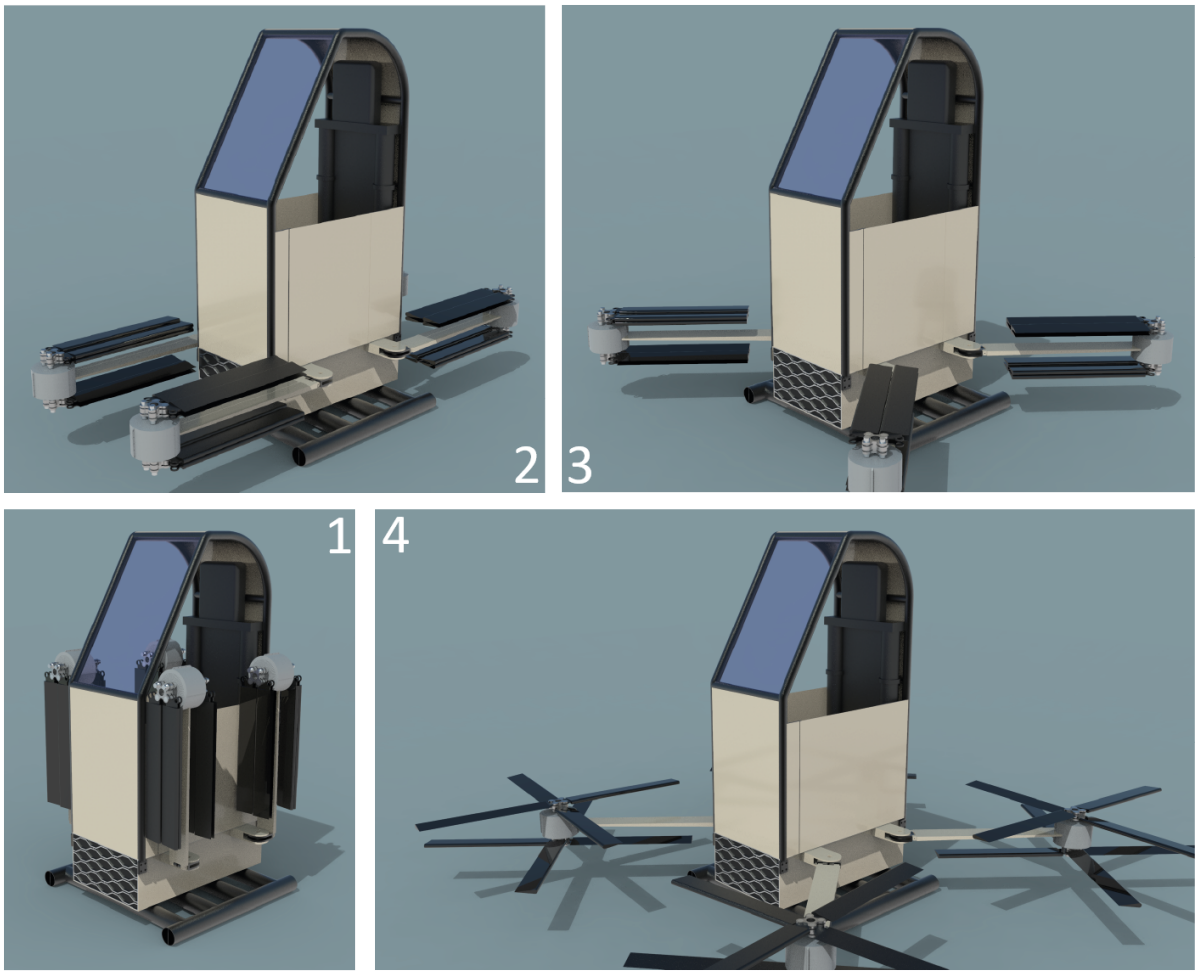

Figure 6.15: Vehicle deployment schematics clockwise order (starting bottom left).

1. The user approaches the vehicle and selects it on the app on the mobile device. The user can plan the route and the vehicle will communicate if it is able to fly that route with the current battery capacity.
2. If the user chooses to fly with this vehicle, they take one of the beams and bends them straight downward and does this for all the beams. The vehicle now looks as in the middle picture in Figure 6.15
3. The user now has space to enter the vehicle through the door on the side. Luggage can be put under the seat and the user will strap him/herself in the seat.
4. Once the user is ready for take-off, the actuators will rotate the beams outwards, as seen in the middle and left picture of Figure 6.15.
5. The beams are now in place and the propellers will now unfold and the vehicle is ready for take-off.

This is the order of steps in the deployment, when landing this sequence will take place in reverse. In subsection 6.7.1 we know it takes 10 seconds for the beams to make the horizontal rotation. The complete deployment (steps 1-5) should be achievable within 2 minutes. It is estimated that this is possible when the user works in a normal calm pace. This cannot be confirmed for sure, for this physical testing would need to be done with a prototype. Then actual timed runs can take place to see if the system can deploy within 2 minutes.

6.7.3. Vehicle volume

The final retracted configuration is limited to a ground projected surface area of $0.77m^2$, of which the dimensions are $0.84mx0.92m$. The floor projected area before retraction is $9.38m^2$, meaning the retracting saves the public area 91.8% of its original area. The resulting volume is just below the 1 cubic meter, as can be seen in Figure 6.16. This value has been found with the use of CATIA V5.

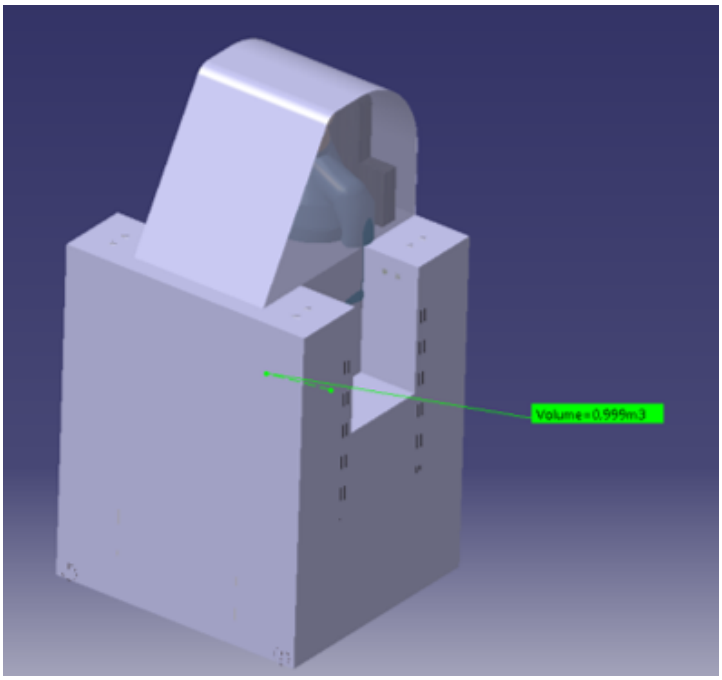

Figure 6.16: Volume of the retracted vehicle

6.8. Sensitivity Analysis

A good understanding of the parameters on the outputs is useful in any design. Therefore, sensitivity analysis has been conducted on the structural design.

6.8.1. Beams

While working on the modelling of the beams, different parameters were changed in order to find the optimum. The outcome was more sensitive to some parameters than others. The thickness of the walls and height of the root had a big influence on the design, as they contribute to the area moment of Inertia, which is the equations most sensitive parameter.

6.8.2. hinge

As explained in section 6.3, two sides of the hinge had to be designed and lots of the dimensions were already fixed. The free variables were the thicknesses described in section 6.3 and the height in node B. Conducting a sensitivity analysis on these parameters, only the normal stress and bearing stress have to be examined. Multiplying the thickness by a factor 0.1 resulted in these stresses (which can be seen in Table 6.3) to increase by a factor of 10, meaning they are inversely correlated. As the bearing stress is the limiting factor in node B, and the normal stress in node A, these thicknesses could cause for unreliable results for these two load cases. However, as a safety factor has been applied of 1.5 this can be neglected.

6.8.3. Load-carrying battery-casing

For the battery casing, as designed in section 6.4, the only variable used was the thickness. Changing this variable by multiplying it with a factor of 0.1 resulted in the following changes in stresses, compared to the values in Table 6.4.

Table 6.8: Sensitivity of the stresses for Figure 6.7.

Battery casing properties	Value	ratio new/old
Thickness	$0.2mm$	0.1
$\sigma_{x_{max}}$	$235.5MPa$	9.7
τ_{max}	$160.3MPa$	10
σ_{vm}	$364.1MPa$	9.9

On average, the stresses are inversely correlated to the thickness according to Table 6.8. This is no cause for concern, as the correlation means that no unexpected behaviour would occur.

6.8.4. Landing gear

The dimensions of the landing gear are inter-related in a complex manner, so a sensitivity analysis on the effects of changing the free variables is done. It is found that a change in placement angle θ or cross-section radius R results in highly non-linear behaviour of the resulting stresses. For both parameters, an optimal point is found through iteration, as explained in section 6.5. The wall thickness on the other hand has predictable behaviour, where an increase in thickness results in a decrease of internal stresses.

6.8.5. User module frame

Since the only free variables in the user module frame design are the cross-sectional radius and thickness, these are varied to gather the effect. It is noticed that the effects on the deflection and internal stresses are inversely related to both. The mass of the frame is quadratically related to both factors, without an optimal point in the design range. Due to this combination of relations with the output parameters and the fact that no optimal points exist in the range where the stresses are low enough, the radius and thickness are both to be minimised in the design.

For both the landing gear and user module frame, the material properties are taken at the low end of the given range [16]. Due to this, the design has the potential to be lighter. Due to time constraints, the exact potential is not determined, as this requires finding the new optimal point of the design. From intuition, it is estimated that this could make the design around 10% lighter. It is chosen to not pursue this lighter design, as the processes used for manufacturing could take the aluminium from its peak performance.

6.9. Verification and Validation

The verification and validation that have been conducted throughout the structural design can be found in this section.

6.9.1. Beams

The verification process contains two processes, namely unit testing and integration testing. Unit testing is incorporated in the script during the modelling of the beams. This is the first check for mistakes. If all unit tests are passed, integration tests are performed, to check if the unit tested modules work together properly. Values for which the outcomes are known or easily calculated by hand are put in. These values are compared to the outcomes of the model, in this way, the model is verified. After some surprising results, a few mistakes were found in the integration of the separate modules. Fixing these mistakes resulted in a proper working script.

As the equations of the beams are based on the book of Pearsons Mechanics of Materials [24], the values used in the example can be filled out in the equations created. The difference between the equation of the book and the equation used, is that some values are parametrised in order to find the optimum solution for the beams. As the values used in the textbook are filled in as parameters, this must give the same outcome as presented in the textbook. Validation is done in this way. The results had the same outcome and in this way, the method is validated. This shows that the model is a good representation of reality.

6.9.2. Hinges
The hinge calculations are really straight-forward. The load of the thrust force only had to be translated into the 3 stresses calculated: bearing stress, shear stress in the bolt and normal stress. In the first stage: hand calculations were conducted. After creating the tools, these values were compared. Additionally, the tools were subjected to unit-tests. Breaking down the tool to check smaller parts of the tool. An assumption was made on the normal stress calculations: calculating the normal loads has been done assuming the thrust force acts on the same line as the compression load displayed in Figure 6.5. A maximum deviation of $4.2mm$ could occur, which would only decrease the load. Concluding this is no cause for concern.

6.9.3. Load-carrying battery-casing
The design of the load-carrying battery-casing had multiple steps. Each step has been verified, starting with the internal loads: first method to verify the internal loads on the structure has been done with hand-calculations. A second verification on this aspect has been included with the help of an online tool on bending and shear forces.

The stress calculation tools that were used in the detailed design originate from the conceptual design [12]. These tools were verified by means of an online beam bending tool, where the results were a maximum deviation of the normal stress of $6.3 * 10^{-4}\%$ and a maximum deviation in shear stress of 0.0719%. Some tweeking of the tool to apply it for the battery-casing was verified by means of hand-calculations.

The moment of inertia calculations have been verified by means of disecting the cross-section into multiple surfaces to which the combination of steiner' terms would result in the same moment of inertia's.

As mentioned in the V&V procedures, Catia V5 has been used to verify the design as well. In the case of the battery-casing, the tools used for the battery-casing can be verified by comparing the calculated von-mises stress of Table 6.4 with the Catia V5 output on that expect location. The result was a decrease of 15.8 %. As the design has been simplified in the tool to only two cells, it is completely logical to receive a higher stress than the original cross-section in Catia V5. Deeming the tools sufficiently verified.

6.9.4. Landing gear
The implementation of the landing gear calculation is first verified to check for any mistakes in the tool. This is done with both unit tests of the individual steps to get to results. Some errors are corrected with these unit tests. Next is the integration testing of the entire process of determining the internal stresses. Some of these tests are done with hand calculations of simple cases and others are zero tests to check whether inputting zeroes has the expected result.

Since the calculations are based on exact equations, only the simplification of the connection to the device and the ground contact effects should be validated. This is outside of the scope of this project, as it requires either finite element methods or physical testing. This is the reason for introducing a safety margin to the final calculations.

6.9.5. User module frame
The verification of the user module frame is done similarly to that of the landing gear, due to the similar tool to determine the results. During the unit testing and integration testing, errors of the tool are eliminated. For validation, only one assumption is checked, namely that the deformation of the slanted beam is in the exact direction of the impact force. This is used to determine the compatibility equation and is therefore very important. Due to the relatively small scale of the deformation, it is said that this assumption holds for this stage of the design. Similar to the landing gear, there is a need for either a finite element simulation or physical testing to do final validation.

6.10. Risk analysis
The risks identified in Table 6.9 are identified as important risks to analyse. They are separated per structural component and for each possible driver(s) are stated for each failure mode. In the last two columns the likelihood and severity of each risk are given on a scale of 1 to 5 as presented in chapter 10.

Table 6.9: Failure modes analysis

Item	Risk ID	Failure mode	Drivers	Likelihood	Severity
Beams	TR.SM.S-1	Fatigue	Load cycles	3	4
	TR.SM.S-2	Impact	Debris, objects	2	4
	TR.SM.S-3	Excessive deflection	Beam stuck in flight	2	3
	TR.SM.S-4	Ductile fracture	Excessive loads	3	4
	TR.SM.S-5	Brittle fracture	Excessive loads	3	4
	TR.SM.TP-1	Buckling	Compression stresses	3	2
	TR.SM.TP-2	Corrosion	Moisture	3	3
	TR.SM.TP-3	Thermal shock	Temperature differences	1	3
Landing gear	TR.SM.S-6	Rods break	Heavy landing	4	4
	TR.SM.TP-4	Skids permanent deflection	Heavy landing	3	3
	TR.SM.S-7	No grip on landing surface	Rain, snow, ice	3	3
	TR.SM.TP-5	Corrosion	Moisture, grinding on ground	5	3
User module	TR.SM.S-8	Windshield crack	Collision	4	4
	TR.SM.C-1	Door damage	User mishandling, collision	2	3
	TR.SM.TP-6	Frame deformation	User mishandling, collision	1	4
	TR.SM.TP-7	Seat breaks	User mishandling, degradation	2	3
	TR.SM.S-9	Frame beaks fully	Heavy collision	1	5
Battery casing	TR.SM.TP-8	Deformation	Heavy landing	4	2
	TR.SM.TP-9	Fracture	Incorrect landing	3	5
	TR.SM.TP-10	Buckling	Heavy landing	3	3
	TR.SM.S-10	Thermal schock	Battery fire	1	5
Hinges	TR.SM.TP-8	Deformation	Heavy landing	4	2
	TR.SM.TP-9	Fracture	Incorrect landing	3	5
	TR.SM.TP-10	Buckling	Heavy landing	3	3

All the risks in Table 6.9 are either too likely, too severe or both to take in the use of the vehicle. Therefore risk mitigation strategies were defined and are presented in Table 6.10. For each risk it is determined how to detect the technical failure and again on a scale of 1 to 5 it is estimated how difficult it is to detect the failure. The new likelihood and new severity are after mitigation.

Table 6.10: Risk mitigation analysis

Item	Risk ID	Detection strategy	Detection difficulty	Mitigation strategy	New Likelihood	New Severity
Beams	TR.SM.S-1	SHM	4	SHM, design for fatigue	2	3
	TR.SM.S-2	Inspection	1	Use impact resistant material	2	2
	TR.SM.S-3	Strain measurements	3	Pilot training	1	3
	TR.SM.S-4	SHM	2	SHM, emergency landings	1	3
	TR.SM.S-5	SHM	2	SHM, emergency landings	1	3
	TR.SM.TP-1	Inspection	1	SHM	1	2
	TR.SM.TP-2	Ultrasonic waves	2	Coating	2	1
	TR.SM.TP-3	Strain measurements	4	Increase fracture toughness	1	2
Landing gear	TR.SM.S-6	Inspection	1	User training/autonomous	3	3
	TR.SM.TP-4	Inspection	1	User training/autonomous	2	2
	TR.SM.S-7	Weather forecast	2	Clean landing zones, user warnings	2	3
	TR.SM.TP-5	Ultrasonic waves	3	Treat material with coating	2	3
User module	TR.SM.S-8	Inspection	1	Use impact resistant material	3	2
	TR.SM.C-1	Inspection	1	User training	2	2
	TR.SM.TP-6	Inspection	2	Design stiff frame structure	1	2
	TR.SM.TP-7	Insperction	2	User warnings	2	3
	TR.SM.S-9	Inspection	1	Easy vehicle exit route	1	3
Battery casing	TR.SM.TP-8	Strain measurements	1	User training/autonomous	2	1
	TR.SM.TP-9	Inspection	3	User training/autonomous	1	2
	TR.SM.TP-10	Inspect vertical flanges	2	User training/autonomous	1	1
	TR.SM.S-10	Temperature sensors	3	Cooling, material treatment	1	3
Hinges	TR.SM.TP-8	Inspection	3	Use of safety factors in design	3	2
	TR.SM.TP-9	Inspection	3	Use of safety factors in design	3	2
	TR.SM.TP-10	Inspection	4	User training, safety factors in design	2	2

Some risks to look into a bit more detail. TR.SM.S-4 and 5. These failure modes are difficult to mitigate in terms of severity. It is given a 4 on the scale since it would be a big problem, but the vehicle would not crash instantly. Therefore as a mitigation strategy, SHM is used to detect cracks that could be the source of fracture on time. An emergency landing can still be performed with this failure, so that is chosen as a mitigation strategy to decrease the severity.

7 Aerodynamics

During the project, the aerodynamic forces are an important factor for both the performance and the stability of the system. To support the work of other departments, a tool for the analysis of the aerodynamic forces and the centre of pressure is created. The aerodynamic model, its implementation and the verification and validation are described in this chapter.

Before any other work is done however, the Reynolds is determined to ensure flow similarity. The Reynolds number is first calculated using the sea level air density $\rho = 1.225 kg/m^3$, the flow velocity $V = 40 km/h = 11.1 m/s$, a characteristic length of $1.89 m$ and the dynamic viscosity $\mu = 1.818 * 10^{-5} kg/ms$ [27]. This results in a Reynolds number $Re = 1.414 \cdot 10^6$.

7.1. Model Description

Aerodynamics of systems similar to the one in this project are usually determined using flow analysis. Due to the short span of the project, it is not feasible to execute computational fluid dynamics to achieve results. Because of this, a simple aerodynamic model model is created. This model uses a simplified geometrical representation of the system and simplified flow interaction calculations.

A reference frame is set up first. To calculate aerodynamic forces, the reference frame is only important for the relative positioning and the output of the centre of pressure. The reference frame and free body diagram is shown in Figure 7.1.

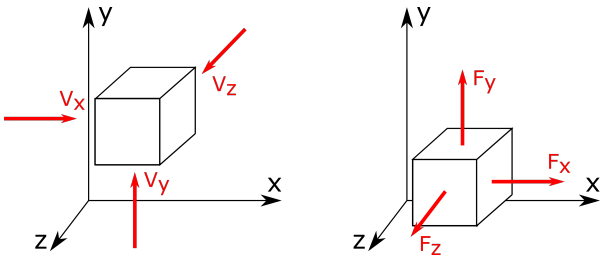

Figure 7.1: Reference frame and free body diagram for the aerodynamic model of the system.

Next, the geometry of the system is simplified using parts with primitive shapes of which the drag coefficients are well researched. These parts are placed parallel to the reference frame axes, as data for these parts at angles of attack is not widely available. An overview of these shapes, drag coefficients and their respective drag equations is shown in Table 7.1. The values for the drag coefficients are found in literature for the appropriate Reynolds number range that applies to this system [28, 29, 30, 31].

Table 7.1: Drag coefficients and drag equations for the geometric elements used in the aerodynamic model. The orientation vector of the cylinder is perpendicular to the circular surfaces.

Element	$C_D[-]$	**Drag Equation** $D = x[N]$
Sphere	0.15	$1/2\rho V^2 \cdot C_D \cdot \pi R^2$
Cylinder (Perpendicular to orientation vector)	0.4	$1/2\rho V^2 \cdot C_D \cdot 2LR$
Cylinder (Parallel to orientation vector)	0.8	$1/2\rho V^2 \cdot C_D \cdot \pi R^2$
Cuboid	0.8	$1/2\rho V^2 \cdot C_D \cdot L_1 L_2$
Disk	0.05	$1/2\rho V^2 \cdot C_D \cdot \pi R^2$

Since some of the geometrical parts are in one another's wake, flow interactions will occur. It would require flow analysis to calculate exact interactions, which is omitted as said above. Since the major occurring interaction is wake flow, a correction factor is introduced that is based on the ratio of local flow velocity to global flow velocity (V/V_{flow}), caused by the wake of the parts upstream from a certain part.

The velocity ratio mentioned is based on literature [32]. From this literature, an interpolation is set up based on the values for the ratio at different downstream distances. It is also kept in mind that only the area of a part that is obscured by the upstream part is influenced by the wake. To this end, the obscured area $A_{obscured,part}$ is determined and the correction factor is then calculated by averaging the velocity ratio over the reference area. This correction factor is shown in Equation 7.1.

$$\textit{Correction factor} = \frac{\left(\left(\frac{V}{V_{flow}}\right)^2 - 1\right) \cdot A_{obscured,part} + A_{perpendicular,part}}{A_{perpendicular,part}} \tag{7.1}$$

Using this information, the aerodynamic forces of the system are calculated by summing the forces of the individual parts multiplied by the correction factor for flow interaction.

Another aerodynamic property that is determined is the centre of pressure of the system. Since the aerodynamic forces are determined in the axis directions of the reference frame, the centre of pressure is split in 3 positions, corresponding to the components of the aerodynamic force. It is determined using the aerodynamic moments of the individual parts of the model, where it is assumed that the centres of pressure of the parts are their geometric centres. The calculations are shown below.

$$\vec{COP}_{F_x} = \left(0, \frac{\sum \bar{y}_{part} \cdot F_{x,part}}{F_x}, \frac{\sum \bar{z}_{part} \cdot F_{x,part}}{F_x}\right)^T \tag{7.2}$$

$$\vec{COP}_{F_y} = \left(\frac{\sum \bar{x}_{part} \cdot F_{y,part}}{F_y}, 0, \frac{\sum \bar{z}_{part} \cdot F_{y,part}}{F_y}\right)^T \tag{7.3}$$

$$\vec{COP}_{F_z} = \left(\frac{\sum \bar{x}_{part} \cdot F_{z,part}}{F_z}, \frac{\sum \bar{y}_{part} \cdot F_{z,part}}{F_z}, 0\right)^T \tag{7.4}$$

It should be noted that this model uses some critical assumptions and thus validation of the model should be done. The centre of pressure cannot be validated at this stage of the design as no adequate data is available from literature. Due to the fact that no single centre of pressure can be determined with the current model, it is known that this approximation is not accurate and use should be carefully considered by other departments.

7.2. Model Implementation

To use the model above, it is implemented into the design process. The first step is to appropriately represent the system with the available parts. A schematic of this representation is shown in Figure 7.2. For the aerodynamic force in y-direction, F_y, the rotors are neglected as they are themselves force generators in that direction. In the figure, the point from which the centres of pressure are measured is the indicated origin of the reference frame.

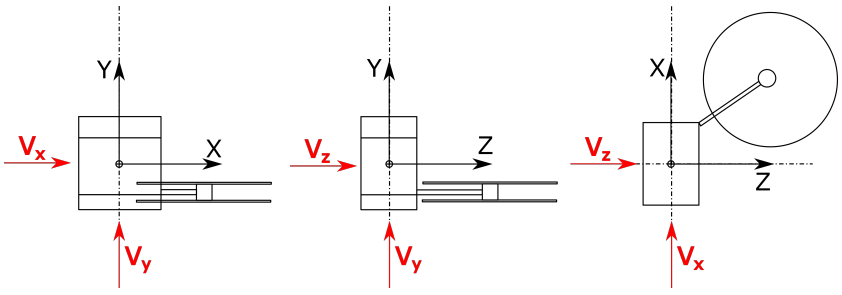

Figure 7.2: Representation of the system used in the aerodynamic analysis. Not drawn to scale.

The model is implemented in python 3.8 and the system representation is used as an input. Due to this implementation into a programming language, verification is needed to check the functioning of the tool with respect to the aerodynamic model. The output for the aerodynamic forces is set to be the drag area, rather than the actual drag at a set velocity. This is done to aid the stability and control department in their analysis at different flight conditions. The drag of the different part and their respective correction factors are also output for verification purposes. The results of the tool are presented in Table 7.2.

Table 7.2: Aerodynamic model output for the system. The centres of pressure are given as vectors with respect to the reference frame in Figure 7.2.

Flow direction	$C_D A\ [m^2]$	$COP\ [m]$
x	0.717	$(0, 0.031, 0)^T$
y	0.874	$(0, 0, 0)^T$
z	1.079	$(0, 0.086, 0)^T$

7.3. Verification and Validation

Due to using a model for the aerodynamic forces and implementing this in a tool, it is required to execute verification of the tool and validation of the model. The methods to do this and the results for this model and tool are presented in this section.

7.3.1. Verification

Verification is done in 2 main steps: unit tests and integration tests. Unit tests are done using the python unittest module, where each individual function of the tool is tested against a known input-output pair. These unit tests are set up to test the edge cases, nominal cases and out-of-bounds cases of the functions. Integration tests are done by using simple input cases, where the expected output can be calculated without a tool. These cases are designed to work within the bounds of the tool to test the nominal functioning of the tool. Edge cases and out-of-bounds cases are not used in integration tests, as these cases are already covered by unit tests.

While developing the tool, the unit tests are created to catch issues as early as possible. The code is adjusted until all unit tests pass. While executing the code with the system representation and with the validation case, errors are still caught and extra cases are added to the unit tests accordingly. The precision of the functions is also determined during verification to be 3 decimal places.

7.3.2. Validation

To check the model against reality, validation of the model through the tool is executed. The aerodynamic model is compared to wind tunnel data of a known input, in this case a cyclist mannequin [33]. The representation of this validation case in the model is shown in Figure 7.3 This validation case is chosen for its similar Reynolds number and flow velocity. The geometry of the validation case is also suitable to be simplified to use the available parts of the model. Large errors, in the order of 10% to 50% are expected due to the highly simplified flow interactions and geometry. As alluded to before, the centre of pressure is not validated, as no adequate data is readily available for use. For this reason, the results should only be used as an indication, not an absolute. The calculations are deemed reasonably good, since the model only involves bluff bodies.

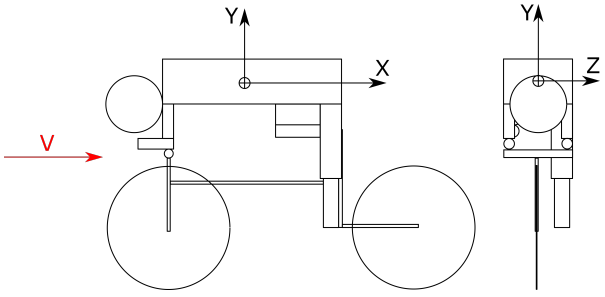

Figure 7.3: Model representation of the aerodynamics validation case. Not drawn to scale.

During the validation, certain parameters with a given range are adjusted to better fit the model to reality. After these adjustments, final results for the validation case are obtained. These are compared to the experimental wind tunnel data [34] in Figure 7.4. In reference [34], a quadratic fit is created of the wind tunnel data with respect to the velocity. This is also plotted against the model output to check the quadratic nature of the aerodynamic force in the model in terms of the velocity.

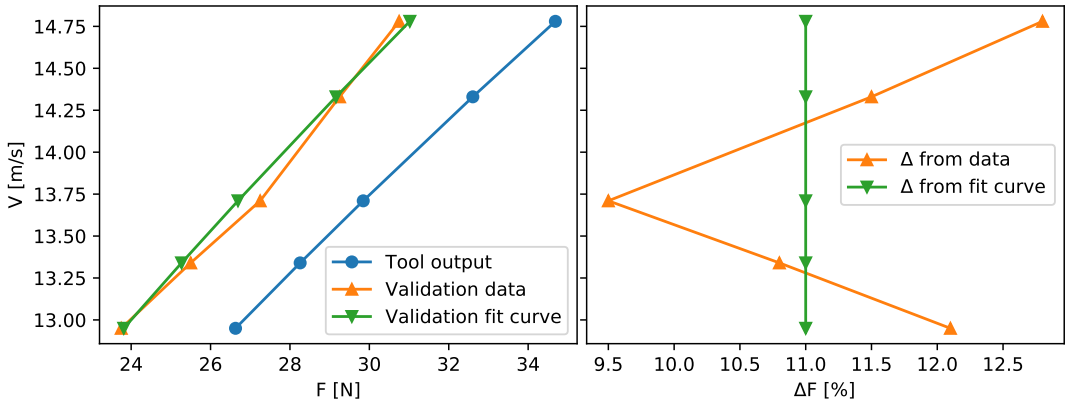

Figure 7.4: Results of the validation of the aerodynamic force tool.

From these results, it can be noticed that the error from the wind tunnel data varies between 9.5% and 12.7%. The error from the data fit curve is constant at 11.0%. These differences can be explained by the inexact nature of the aerodynamic model and the inaccurate estimation of the flow interaction. The model is not adjusted to have an exact match with the data fit curve, since the validation case contains a lot of flow interaction. This would mean that an overestimation is expected and an exact match would not work in other use cases. Due to the validation errors, the error range of the tool is estimated at $\pm 15\%$.

7.3.3. Sensitivity Analysis

Since the aerodynamics tool executes a highly simplified calculation of the system aerodynamics, the sensitivity of the aerodynamics to the input parameters is only analysed qualitatively. A quantitative analysis would only be meaningful with a higher fidelity flow simulation.

Quantitatively speaking, the dimensions of the system have a direct influence on the aerodynamic forces. Any increase in frontal surface area would linearly scale the magnitude of the force in the perpendicular flow direction to that surface. The user module is the largest contributor to these forces and is thus subject to create the largest changes in overall aerodynamic force. The sizing of the motor arms on the other hand, does not influence the aerodynamic forces significantly. They do, however, have the potential to significantly change the centre of pressure of the system.

This concludes the work from the aerodynamics department for this design phase. In the future of the project, a more elaborate aerodynamic analysis should be executed. This can be done with computational fluid dynamics and validated with wind tunnel tests of models and prototypes. Analysis of the effects of gust in urban environments is also left for future research, due to time constraints. A better aerodynamic design of the user module should also be considered. This is not deemed as high a priority due to the low flight velocities experienced by the system.

8

Stability and Control

This chapter details the design of the Stability and Control subsystem. In section 8.1 the used reference frames are explained. section 8.2 introduces the means of control of the system. In section 8.3 the control plant is described and the dynamics of the aircraft, as well as the motor input, are modelled. Furthermore, section 8.4 argues what type of sensors should be used to measure the state and any particularities related to their placement. The control architecture and the loop design is then given in section 8.5. Furthermore, the controller and hardware selection is documented in section 8.6. The controller is implemented in section 8.7 and the closed loop system characteristics are presented. After performing a sensitivity analysis in section 8.8, verification and validation procedures are discussed (section 8.9) and future work for the control system is discussed (section 8.10). Finally, a risk analysis is performed in section 8.11.

8.1. Coordinate Systems and Reference Frames

For all mentions of coordinate systems in this chapter refer to Figure 8.1. All coordinate systems and transformations are right-handed and they are detailed in this section.

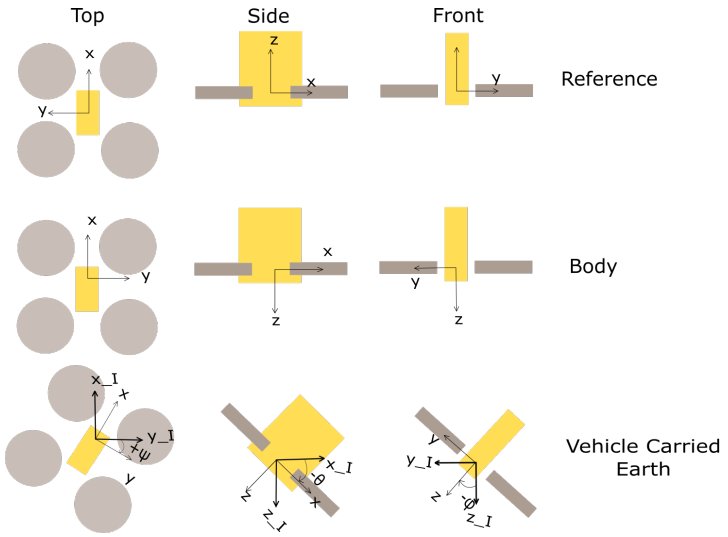

Figure 8.1: Reference frames for the vehicle

A CAD model of the vehicle is constructed and assembled in CATIA. In this model the reference axis system is a right handed system with x pointing to the front of the aircraft and z pointing up. The origin of the coordinate system is an arbitrary point in the assembly defined by CATIA. The Centre of Gravity (COG) and Mass moment of inertia (MMOI) of the system were calculated with respect to this reference frame: the Vehicle Reference frame (VR).

A transformation from the Vehicle Reference Frame to the Body Reference Frame (B) is done by a translation to the COG location and a half rotation about the x-axis, using transformation matrix $T_{VR->B}$. The Body frame is defined as follows: the origin is located at the COG, the x-axis points forward, the y-axis points to the right and the z-axis downward. This frame allows for the calculations of moment arms. The equations of motion are derived with respect to this frame.

A final transformation can be done from the Body Frame to the Vehicle Carried Earth Reference (V_{ce}) Frame. This reference frame is assumed to be inertial, as the flat, non-rotating earth assumption

is made. This frame is also important for navigation as ground velocity and position can be obtained from it.

The euler angles (ϕ, θ, ψ) are defined as the rotations between V_{ce} and B, about the Z, Y, X directions in that order. The euler angles are used to describe the angular orientation of the vehicle. The inverse of this matrix describes the final rotation [35].

8.2. Control Means

Controlling the translation and much of the rotation of a coaxial quadcopter is essentially the same as with a conventional quadcopter. The thrust differential between the front rotors and the rear rotors is used for pitching, and the thrust differential between the right set of rotors and the left set of rotors is used for rolling. These control means are coupled with a translation in the body y-direction and x-direction, respectively.

In a conventional quadcopter, yawing motion is achieved by reducing the RPM of diagonally-placed rotors, while increasing the RPM for the remaining rotors. However, in the case of 4 sets of twin coaxial rotors the strategy for control is no longer changing the RPM of diagonal rotors. This would not yield the desired yawing result as the upper rotors spin in the opposite direction of the lower rotors (refer to Figure 8.4 for a visualisation of this). A positive angular acceleration in the body z-axis (yawing) is then achieved by increasing the RPM of all lower rotors and decreasing the RPM of the upper rotors.

8.3. Plant Description

The plant of the control system consists of the motor and propeller model, the coaxial quadcopter dynamics model and the sensor model (Figure 8.2). The signals coming from the processor will be fed into the motor controller which in turn are fed to the motor, which generates force and torque inputs for the coaxial quadcopter dynamics model. Finally, the sensors measure the current state of the system. Note that for the purpose of this project, the sensors are not modelled and it is assumed that the states of the system can be observed perfectly. All components of the plant are detailed in this section.

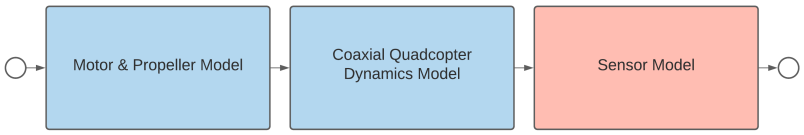

Figure 8.2: The Plant of the control system and its components

8.3.1. Motor and Propeller Model

The inputs for the motor controllers are signals generated by using Pulse-width modulation (PWM). For the purpose of the controller design the input signal of the motor block is assumed to have a linear relationship with the driving torque and force that the propeller generates. A linear relationship is approximated by regression as is presented in Figure 8.3b.

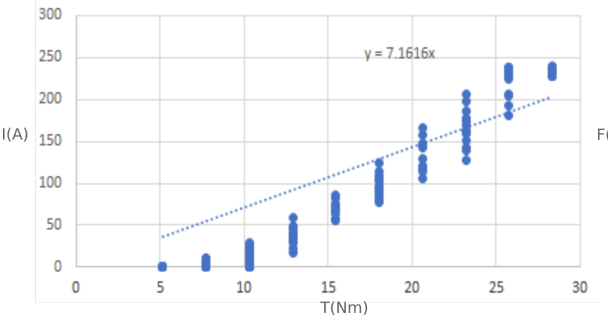

(a) The driving torque versus the signal current.

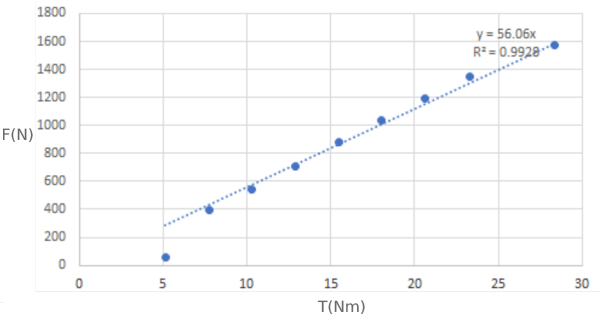

(b) The driving torque versus the rotor thrust.

Figure 8.3: Linear approximation of motor model.

$$I = 7.16 \cdot T \tag{8.1}$$

$$F_{prop} = 56.06 \cdot T \tag{8.2}$$

The output of the motor and propeller model are the linearised thrust forces and driving torques of the propellers. They are subsequently fed into the state space system of the coaxial quadcopter dynamics model.

8.3.2. Coaxial quadcopter dynamics

In order to model and describe the dynamics of the system, the equations of motion (EOM) are derived in the body frame. As there is simultaneous translation and rotation of the frame, the chain rule for derivatives must be applied to Newton's second law, in order to arrive at the translational EOM (Equation 8.3) and the rotational EOM (Equation 8.4) [1] [35].

$$\vec{F} = m \cdot (\dot{\vec{v}}^b + \vec{\omega_n}^b \times \vec{v}^b) \tag{8.3}$$

$$\vec{M} = I^b \cdot \dot{\vec{\omega}}_n^{\,b} + \vec{\omega_n}^b \times (I^b \cdot \vec{\omega_n}^b) \tag{8.4}$$

In these equations $\vec{v} = \begin{bmatrix} u & v & w \end{bmatrix}^T$ is the linear velocity vector and its time derivative $\dot{\vec{v}}$ is the linear acceleration. Similarly, $\vec{\omega_n} = \begin{bmatrix} p & q & r \end{bmatrix}^T$ is the angular velocity and its time derivative $\dot{\vec{\omega}}_n$ is the the angular acceleration vector. Finally, the inertial terms m and I^b describe the total mass of the system including the user and the Inertia Tensor, respectively. The superscripts indicate the reference frame in which the variables are expressed.

The total force vector consist of the body forces F^b_{body}, the gravity force F^b_g, and the aerodynamic force F^b_a (Equation 8.5). F_{body} and F_a are already defined in B, but F_g is first transformed from V_ce to B.

$$\vec{F} = \begin{bmatrix} 0 \\ 0 \\ -(F_1 + F_2 + F_3 + F_4 + F_5 + F_6 + F_7 + F_8) \end{bmatrix} + \begin{bmatrix} F_{a_x} \\ F_{a_y} \\ F_{a_z} \end{bmatrix} + T_{V_{ce}->B} \cdot \begin{bmatrix} 0 \\ 0 \\ m \cdot g \end{bmatrix} \tag{8.5}$$

The total moments can be obtained in a similar fashion. They are broken up into the body moments and the aerodynamic moments (Equation 8.6 and Equation 8.7). Gravity does not have component in the moment equation as it effectively acts through the COG. For the definition of the lower and the upper rotors and their spinning direction refer to Figure 8.4. It is assumed that the thrust force of the lower rotors effectively act at the same location as their upper counterparts.

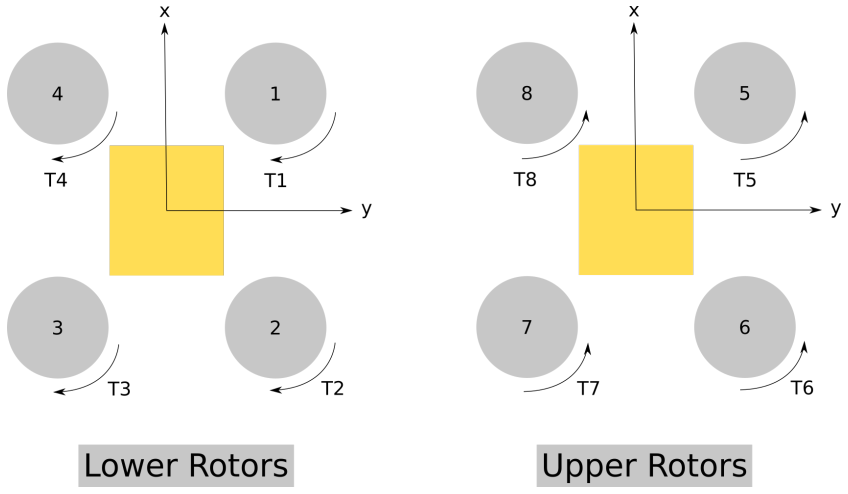

Figure 8.4: The naming convention of the rotors and their spinning direction and torque (T_i).

[1] Charles Tytler. *Modeling Vehicle Dynamics – Quadcopter Equations of Motion*. URL: https://charlestytler.com/quadcopter-equations-motion/ (visited on 12/27/2020)

$$\vec{M_{body}} = \vec{p_{FR}} \times (\vec{F_1} + \vec{F_5}) + \vec{p_{BR}} \times (\vec{F_2} + \vec{F_6}) + \vec{p_{BL}} \times (\vec{F_3} + \vec{F_7}) + \vec{p_{FL}} \times (\vec{F_4} + \vec{F_8}) + \begin{bmatrix} 0 \\ 0 \\ C_{FT} \cdot (F1 + F2 + F3 + F4 - F5 - F6 - F7 - F8) \end{bmatrix} \tag{8.6}$$

$$\vec{M_a} = \vec{p_{cp_A}} \times \begin{bmatrix} F_{a_x} \\ 0 \\ 0 \end{bmatrix} + \vec{p_{cp_B}} \times \begin{bmatrix} 0 \\ F_{a_y} \\ 0 \end{bmatrix} + \vec{p_{cp_C}} \times \begin{bmatrix} 0 \\ 0 \\ F_{a_z} \end{bmatrix} \tag{8.7}$$

Where the thrust forces $\vec{F_i} =< 0, 0, -F_i >$ and Equation 8.2 yields $C_{FT} = \frac{1}{56.06}$. Position vectors of the rotors are indicated by their relative location (for instance FR stands for Front Right).

Substituting these terms and performing the products yield the nonlinear equations of motion of the coaxial quadcopter in B; Equation 8.8 and Equation 8.9.

$$m \cdot \begin{bmatrix} \dot{u} + q \cdot w - r \cdot v \\ \dot{v} - p \cdot w + r \cdot u \\ \dot{w} + p \cdot v - q \cdot u \end{bmatrix} = \begin{bmatrix} F_{a_x} - m \cdot g \cdot sin(\theta) \\ F_{a_y} + m \cdot g \cdot cos(\theta) \cdot sin(\phi) \\ F_{a_z} - F_{total} + m \cdot g \cdot cos(\phi) \cdot cos(\theta) \end{bmatrix} \tag{8.8}$$

$$I^b \cdot \begin{bmatrix} \dot{p} \\ \dot{q} \\ \dot{r} \end{bmatrix} = \vec{M_a} + \vec{M_{body}} - \begin{bmatrix} p \\ q \\ r \end{bmatrix} \times (I^b \cdot \begin{bmatrix} p \\ q \\ r \end{bmatrix}) \tag{8.9}$$

And finally the kinematic equations that convert angular acceleration in the body frame to the inertial frame are given by Equation 8.10 [35].

$$\begin{bmatrix} \dot{\phi} \\ \dot{\theta} \\ \dot{\psi} \end{bmatrix} = \begin{bmatrix} p + sin(\phi) \cdot tan(\theta) \cdot q + cos(\phi) \cdot tan(\theta) \cdot r \\ cos(\phi) \cdot q - sin(\phi) \cdot r \\ (sin(\phi) \cdot q + cos(\phi) \cdot r) \cdot sec(\theta) \end{bmatrix} \tag{8.10}$$

It is important to note that a singularity exists in Equation 8.10 for $\theta = \pm 90°$. However, a pitch angle of this magnitude is not expected to occur in the flight envelope and it is assumed that it does not.

8.3.3. Model Linearisation

The equations derived in the previous section can be used for nonlinear simulation, using MATLAB in combination with Simulink (simulation software which is part of the MATLAB package). However, designing flight control systems is more conveniently done using linear plant models. For this purpose, the equations are linearised around steady symmetric flight conditions. The influence of this step will be further analysed in section 8.9. The linearisation is expected to only yield valid results at small angle deviations. A requirement for the controller implementation is thus generated: the euler angles must not exceed $5°$ of deviation during the flight profile.

The trimming points that are chosen for the design of the control system are identified as *Cruise* ($40 km/h$ at a constant $20m$ altitude) and *Hover* (no velocity). The state of the system at both conditions is found by using the trimming tool in the nonlinear Simulink model (for verification of this tool, refer to section 8.9). The VTOL phase can be considered to be at hover condition. As such, these trimming points account for a large part of the flight envelope. This leads to two different linear systems for which controllers are designed. Both of these systems are expressed in the state space form.

8.3.4. Linear State Space Form

The state space representation of the linearised systems are of the following form.

$$\dot{\vec{x}} = A \cdot \vec{x} + B \cdot \vec{u} \tag{8.11}$$

$$\vec{y} = C \cdot \vec{x} + D \cdot \vec{u} \tag{8.12}$$

With the state vector ($\vec{x}$) and the input vector ($\vec{u}$) defined as follows.

$$\vec{x} = \begin{bmatrix} u & v & w & p & q & r & \phi & \theta & \psi \end{bmatrix}^T \tag{8.13}$$

$$\vec{u} = \begin{bmatrix} F_1 & F_2 & F_3 & F_4 & F_5 & F_6 & F_7 & F_8 \end{bmatrix}^T \tag{8.14}$$

Note that the state-space system is only valid for a certain Take-off weight (TOW) and COG location; it has to be computed for every user weight. This is part of the calibration procedure. The COG limits in VR are presented in Table 8.1. In order to account for the 95 percentile of the population (for more details pertaining to human size research, refer to the Midtem Report [12]).

Table 8.1: The COG limits for different types of users.

User type	user weight (kg)	Luggage (kg)	$\bar{x}$ (m)	$\bar{y}$ (m)	$\bar{z}$ (m)
Light	50	0	-0.0294	0	-0.7343
Light	50	10	-0.0324	0	-0.7363
Heavy	100	0	-0.0344	0	-0.6768
Heavy	100	10	-0.0369	0	-0.6802

A similar linearisation is done for the cruise condition and the system is derived. The poles and zeros of both systems is plotted by a MATLAB script. The open loop systems are unstable as they both have positive poles as can be found in Figure 8.5. Stabilisation of the vehicle is done by closing the control loop and designing the controller, as is detailed in subsequent sections.

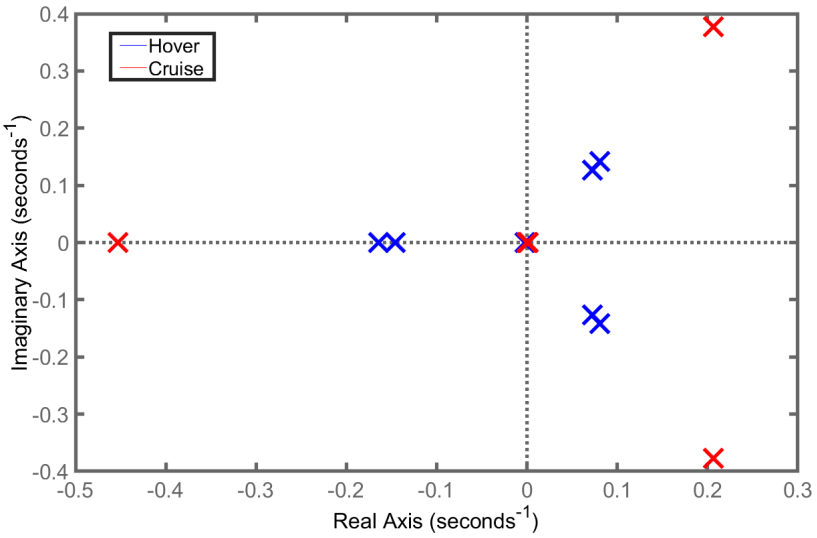

Figure 8.5: The pole map of the open loop system linearised at hover and cruise conditions.

8.4. Sensors, Controllability & Observability

To guarantee arbitrary pole placement and that all states can be reached, the system must be controllable. For an n-dimensional continuous linear time-invariant system (LTI) the controllability matrix is given by Equation 8.15 [36][37]. The rank of the controllability matrix must be equal to the size of the control input vector $\vec{u}$, in order to have full controllability.

$$CTRL = \begin{bmatrix} B & A \cdot B & A^2 \cdot B & \dots & A^{n-1} \cdot B \end{bmatrix} \tag{8.15}$$

Besides controllability, it is also important to be able to measure the system state. This can be checked by comparing the rank of the observability matrix to the size of the state vector. For LTI systems (n-dimensional) the observability matrix is given by Equation 8.16 [37].

$$Obs = \begin{bmatrix} C \\ C \cdot A \\ C \cdot A^2 \\ \vdots \\ C \cdot A^{n-1} \end{bmatrix} \tag{8.16}$$

The rank of the controllability and observability matrices were checked using a MATLAB script and the resulting systems are both controllable and observable.

8.4.1. Sensor selection

Sensors are selected to comply with observability and to measure the navigational states that would allow the most direct adjustments by the user.

The desired state measurements are the following:

$$y = \begin{bmatrix} X & Y & h & u & v & w & p & q & r & \phi & \theta & \psi \end{bmatrix}^T, \tag{8.17}$$

The first three states are used directly for the VTOL and navigation of the aircraft; while the rest of the inputs are used to provide full state feedback.

A multitude of sensors could be used to determine the same desired state measurement. In cases that warrant these a filter such as a complimentary or a Kalman filter could be employed to fuse the separate signals and synthesise the desired measurement (The implementation of filters is left to future of the project, as explained in section 8.10). An example is when the terms are calculated using dead reckoning. One caveat of using dead reckoning is that random noise in the integrated measurement causes random walk in the estimated state output; in this case the measurement could be combined with a slower but more accurate measurement to get the state.

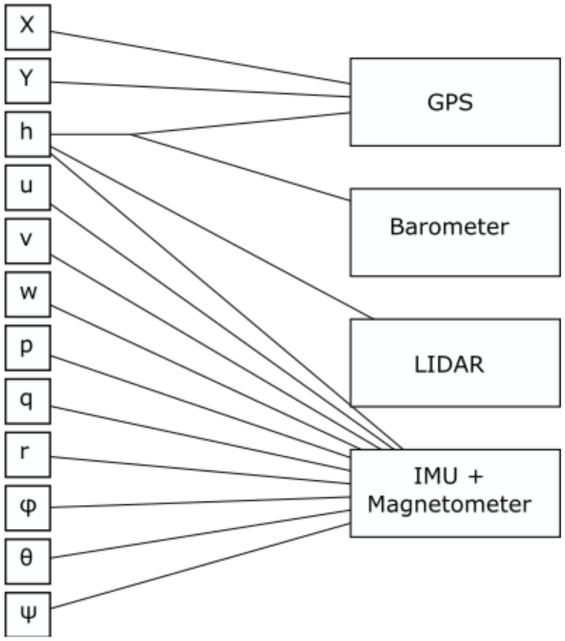

Figure 8.6: The states and the sensors used in measuring them.

At this stage it is important to mention the integration of the aircraft with the mobile device that is used to control it, since smart mobile devices come with various sensors that could be used to obtain navigational parameters. A modern smartphone is equipped with an inertial measurement unit (IMU), a magnetometer, a barometer, sometimes a LIDAR sensor, a camera, and a GPS sensor. This set of sensors in theory covers all the state measurements.

However, the non-navigational states are essential for controlling the inherently unstable vehicle and it was decided to include an IMU (that has a built-in magnetometer), a barometer, a LIDAR sensor and a GPS sensor in the design. This is due to the variability of the sensor components from smartphone to smartphone. Besides, the positioning of the sensors can not be done freely when they all come in the smartphone (especially LIDAR pointing). GPS is included primarily because using the barometer yields indirect altitude measurements and for the functioning of the safeguard system.

The X, Y geo-locations are gathered from a GPS module. The altitude measurement is measured from multiple sources: the barometer provides mean sea level altitudes and combined with a topo-

graphic map and the X, Y location measurements can be transformed into altitude. This measurement is prone to errors in the topological map and due to pressure variations because of weather fronts. The LIDAR sensor is used to measure the distance from the vehicle to the nearest obstruction below the vehicle; this measurement works the best when the ground is the nearest obstruction but is prone to fluctuations in an urban environment. The IMU measures accelerations in all directions, using dead reckoning the acceleration measurement can be converted into positional change measurements. All the other states are obtained from the IMU in a similar fashion.

8.5. Control Architecture and Loop Design

The system makes use of two different control schemes:

- VTOL
- Cruise

The VTOL control scheme allows positional control of the vehicle facilitating landing and takeoff in cross-wind situations and the positioning of the vehicle on the ground [38].

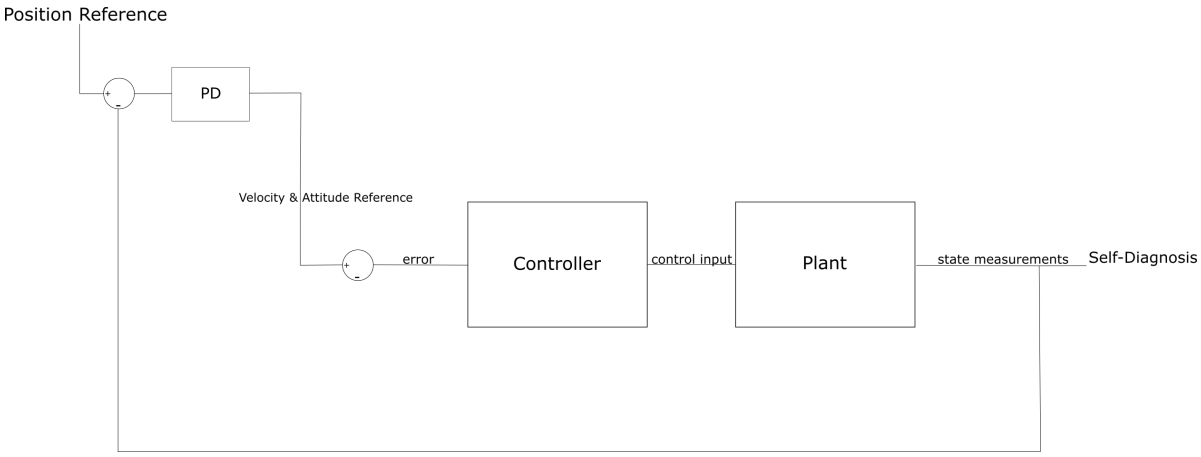

Figure 8.7: The VTOL control scheme.

The Cruise control scheme implements velocity control throughout the operational speed envelope by means similar to gain scheduling[39]; allowing the vehicle to speed up with small angular deviations. In practice, this can be thought of as the underlying gears in an automatic car.

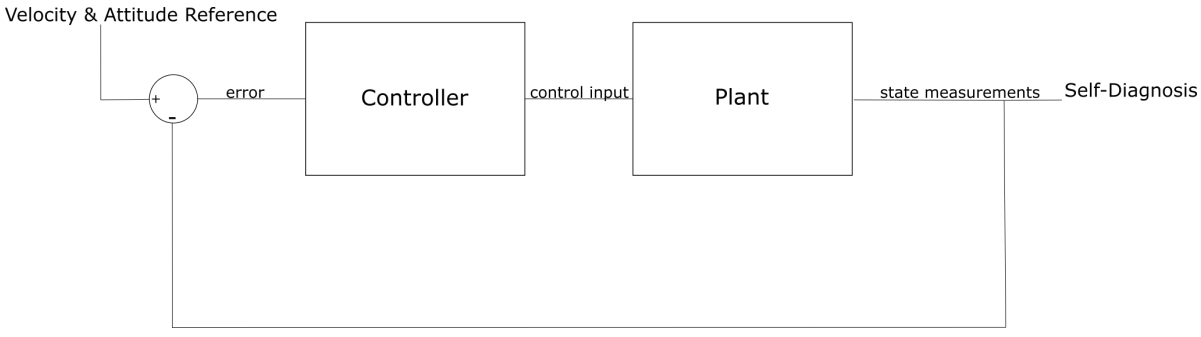

Figure 8.8: The Cruise control scheme.

8.6. Controller & Processing Hardware Selection

The control system consists of hardware and the control software. There are multiple options for linear controllers and processor units. In the following sections these options are discussed and compared.

8.6.1. Controller Selection

Three different control law strategies are compared and contrasted to find the most suitable choice for the application. These are: PID Control, Linear Quadratic Regulator (LQR) and Model Predictive Control (MPC). Once the selection is made the internal parameters (gains, weights, etc. where they would be applicable) are designed.

Several underlying assumptions for the comparison are made. Firstly, A PID controller architecture would be comprised of a PID controller for each control input or a set of at least four PID controllers and an additional control mixing algorithm. The MPC controller architecture would implement an SSMPC algorithm from the family of MPC algorithms. The LQR architecture would implement the solution to the quadratic cost function which is solved just before each flight using the Algebraic Riccati Equation.

The PID control architecture would come with an additional control mixing algorithm which has to be tuned/calibrated for the user weight variation along with the PID controllers. The multitude of the PID controllers also pose a big question mark on how the tuning is going to be done. Furthermore the PID controllers do not allow for the implementation of bounds or the penalisation of control input magnitudes. On the other hand the architecture is easy to implement and not very costly in terms of computation.

The LQR method allows for the controller gains to be tuned optimally with the use of a quadratic cost function which guarantees a minimum solution and is quick to implement. The main difficulty comes in the determination of the weighting matrices Q (state penalty weights) and R (input penalty weights); this is especially true given the linearisation points all correspond to a nonzero input state which makes optimisation of the total control input unclear. On the other hand once the gain matrix is calculated the control is computationally very cheap and stability is guaranteed.[40] The MPC framework allows for optimal control to be implemented over a prediction horizon, making it especially suitable for trajectory tracking tasks.[41] The downside is that the control matrix size grows with prediction horizon and sampling rate, making it the most expensive algorithm of the three. An advantage of MPC is that it allows more freedom in the selection of the optimisation problem (cost function). The determination of the additional control and prediction horizon values make the implementation less clear. Additionally the implementation outputs a smooth control signal which might be important for some actuators but also causes worse disturbance rejection compared to LQR.[42]

Table 8.2: Simple trade-off for the controller selection.

Metric	PID	MPC	LQR
Computational Cost			
Ease of Tuning			
Penalisation of Inputs			

As a result of its ease of implementation, penalisation options and low computational cost the LQR controller has been selected for this application. For the outer loop controller in the VTOL controller scheme a single PD type controller with output saturation ensuring the maximum speed requirement is not exceeded is selected to perform the conversion from the position error to a velocity reference.

8.6.2. Processor Selection

The type of the desired processor is the first decision to be made in the design of a processor. For a Real-time Operating System (RTOS), a general purpose COTS processor (microcontroller or microprocessor) along with digital signal processors (DSP) for fast mathematical operations are initially to reduce development time and improve flexibility in changes after the product is on the market. When the algorithms used have matured an application specific integrated circuit (ASIC) type processor may be developed to decrease the per unit cost, power usage, and increase reliability.[43]

8.7. Controller Implementation

For an LQR design the system's performance index is characterized by a cost function (J) that the controller is supposed to minimise. This cost function is presented in Equation 8.18 [44].

$$J = \int_0^\infty \left[x^T Q x + u^T R u\right] dt \tag{8.18}$$

This cost is minimised by the closed loop controller gain matrix found by solving the Algebraic Riccati Equation:

$$A^T P + PA - PBR^{-1}B^T P + Q = 0 \tag{8.19}$$

where P is an unknown n by n symmetric matrix.

$$K = -R^{-1}B^T P \tag{8.20}$$

where K is the optimal gain solution to the optimisation problem.[45] Q is the diagonal state weighting matrix and R is the diagonal control weighting matrix. Through trial-and-error the weights of the matrices are found. For every trial, the state outputs were checked if acceptable and the input force deviations were checked. The cost for the control inputs was determined to be equal for all rotors. This results in R being an identity matrix multiplied by a single weight.

8.7.1. VTOL

Below the Q and R matrices of the LQR controller and the proportional and derivative gains for the PD controller are presented for the VTOL phase.

$$Q_{VTOL} = \begin{bmatrix} 1000 & 0 & 0 & 0 & 0 & 0 & 0 & 0 & 0 \\ 0 & 1000 & 0 & 0 & 0 & 0 & 0 & 0 & 0 \\ 0 & 0 & 1000 & 0 & 0 & 0 & 0 & 0 & 0 \\ 0 & 0 & 0 & 1000 & 0 & 0 & 0 & 0 & 0 \\ 0 & 0 & 0 & 0 & 1000 & 0 & 0 & 0 & 0 \\ 0 & 0 & 0 & 0 & 0 & 1000 & 0 & 0 & 0 \\ 0 & 0 & 0 & 0 & 0 & 0 & 1 & 0 & 0 \\ 0 & 0 & 0 & 0 & 0 & 0 & 0 & 1 & 0 \\ 0 & 0 & 0 & 0 & 0 & 0 & 0 & 0 & 1 \end{bmatrix} \tag{8.21}$$

$$R_{VTOL} = 0.1 \cdot I_8 \tag{8.22}$$

Where I_n is the n-dimensional identity matrix.

$$K_{Proportional} = 0.7 \tag{8.23}$$

$$K_{Derivative} = 0.5 \tag{8.24}$$

8.7.2. Cruise phase 1

Below the Q and R matrices of the LQR controller are presented for Cruise 1 phase.

$$Q_{hover} = \begin{bmatrix} 100 & 0 & 0 & 0 & 0 & 0 & 0 & 0 & 0 \\ 0 & 100 & 0 & 0 & 0 & 0 & 0 & 0 & 0 \\ 0 & 0 & 100 & 0 & 0 & 0 & 0 & 0 & 0 \\ 0 & 0 & 0 & 10000 & 0 & 0 & 0 & 0 & 0 \\ 0 & 0 & 0 & 0 & 10000 & 0 & 0 & 0 & 0 \\ 0 & 0 & 0 & 0 & 0 & 10000 & 0 & 0 & 0 \\ 0 & 0 & 0 & 0 & 0 & 0 & 100000 & 0 & 0 \\ 0 & 0 & 0 & 0 & 0 & 0 & 0 & 100000 & 0 \\ 0 & 0 & 0 & 0 & 0 & 0 & 0 & 0 & 10000 \end{bmatrix} \tag{8.25}$$

$$R_{hover} = 100 \cdot I_8 \tag{8.26}$$

8.7.3. Cruise phase 2

Below the Q and R matrices of the LQR controller are presented for the Cruise phase 2 flight phase.

$$Q_{cruise} = \begin{bmatrix} 100 & 0 & 0 & 0 & 0 & 0 & 0 & 0 & 0 \\ 0 & 100 & 0 & 0 & 0 & 0 & 0 & 0 & 0 \\ 0 & 0 & 100 & 0 & 0 & 0 & 0 & 0 & 0 \\ 0 & 0 & 0 & 10000 & 0 & 0 & 0 & 0 & 0 \\ 0 & 0 & 0 & 0 & 10000 & 0 & 0 & 0 & 0 \\ 0 & 0 & 0 & 0 & 0 & 10000 & 0 & 0 & 0 \\ 0 & 0 & 0 & 0 & 0 & 0 & 100000 & 0 & 0 \\ 0 & 0 & 0 & 0 & 0 & 0 & 0 & 100000 & 0 \\ 0 & 0 & 0 & 0 & 0 & 0 & 0 & 0 & 10000 \end{bmatrix} \tag{8.27}$$

$$R_{cruise} = 50 \cdot I_8 \tag{8.28}$$

8.7.4. Closed Loop System Characteristics

After the addition of the controller and closing the loop of the system, the control and stability characteristics change significantly. The resulting system is asymptotically stable with a worst case disk margin of greater than 2.5 dB and phase margin of 16 degrees. The performance of the system is depicted in this section.

The climb profile for the VTOL controller is presented in Figure 8.9a and the acceleration in this phase is given in Figure 8.9b. Note that the maximum acceleration is lower than $1g$.

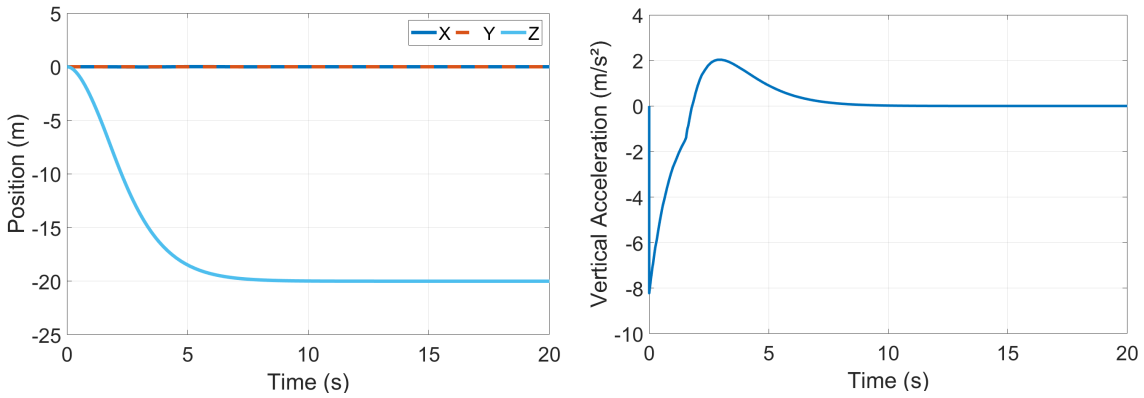

(a) The VTOL position profile, given a control input of 20m altitude.

(b) The acceleration during VTOL.

Figure 8.9: Results from the VTOL simulation.

When the cruise altitude is reached, there is a transitional phase between hover and cruise conditions, identified as the cruise phases, displayed in Figure 8.10a and Figure 8.10b. The first half of the acceleration is done using the controller designed for the hover condition. Note that the initial condition for velocity in Figure 8.10a is 0, as the initial condition corresponds to hover. The second cruise phase is performed using the controller designed for cruise conditions. The initial condition here corresponds to the final condition of the first cruise phase (as the model is linearised about the cruise velocity).

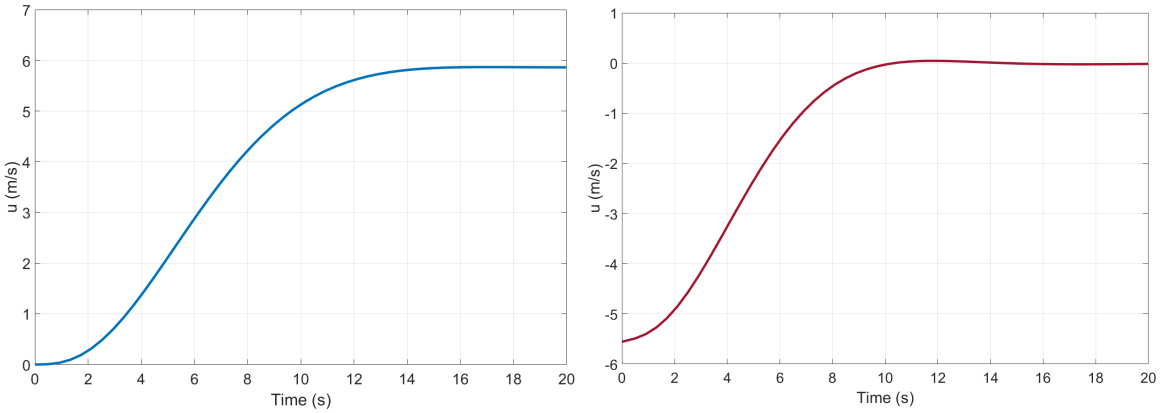

(a) The forward velocity during the first cruise phase as a function of time.

(b) The forward velocity for the second cruise phase as a function of time.

Figure 8.10: The cruise phases expressed as forward velocity in B.

In Figure 8.11 the pitch angle θ is plotted against time during the two cruise phases. Note that the angle decreases (pitching downward) in order to gain forward acceleration. Eventually θ increases again and reaches the steady state. The requirement for the linearisation of the models set in subsection 8.3.3 is complied with, as the magnitude of θ never exceeds $5° = 0.087rad$ or $5deg$.

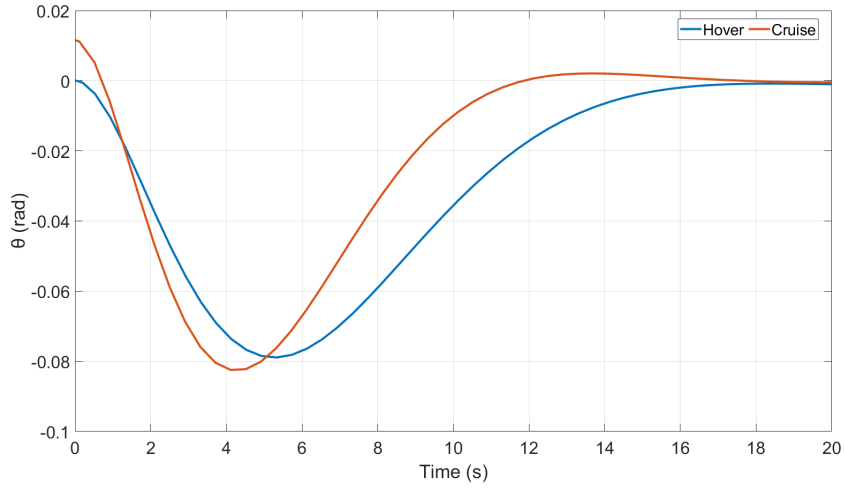

Figure 8.11: The pitching angles during the cruise phases.

The real part of the poles of the closed-loop systems are now all negative, as presented in the pole maps of the hover and cruise conditions (Figure 8.12). Hence, the closed-loop system is stable. This confirms compliance with $PAT - SYS.C - FUNC - 01$.

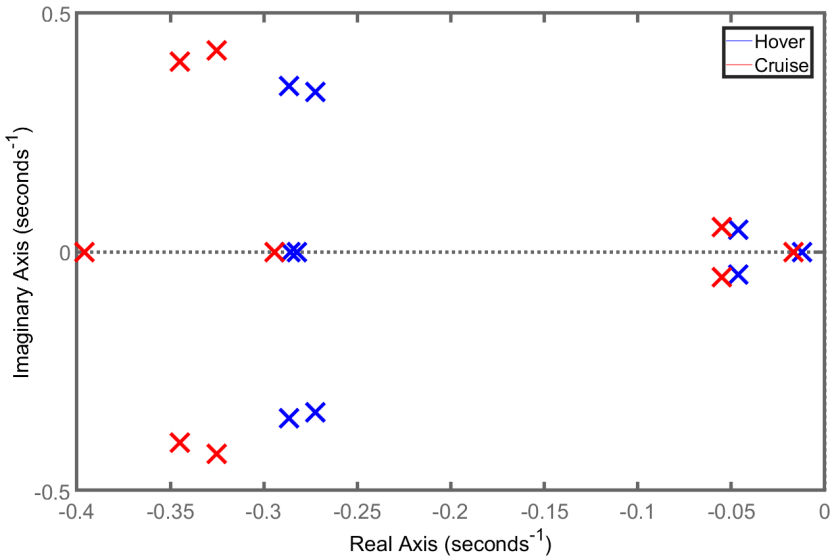

Figure 8.12: The pole map of the closed-loop system linearised at hover and cruise conditions.

8.8. Sensitivity Analysis

In order to gain an understanding to the sensitivity of the design parameters of an LQR controller and a PD controller, a sensitivity analysis is performed for the following parameters: the velocity overshoot, the settling time, and the maximum deviation in pitch angle. This must be done for the positional hover controller, the hover controller, and the cruise controller.

8.8.1. Hover and cruise

The approach to the sensitivity analysis of the hover and the cruise controller is based on taking the Q- and R-matrix of the original LQR controller design and investigating what the sensitivity is to the overshoot of the forward velocity, the settling time of the velocity, and the maximum deviation from the steady state θ for a given control input. These parameters are chosen as the overshoot and the settling time are a measure of performance for acceleration to cruise condition. The maximum magnitude of θ is also an interesting parameter to analyse for sensitivity, as a requirement was set for linearisation.

The sensitivity is tested by altering the weights for the Q-matrix and the R-matrix given in section 8.7. The first three diagonal entries in the Q-matrix correspond to the penalisation of velocity-error. The middle three entries correspond to that of the angular rates and the last three correspond to that of the euler angles. When analysing the sensitivity to changing a state's penalisation, all three entries of that state are altered. They are either divided by 10 or multiplied by 10 while all the others are kept constant. Finally, the results are logged in Table 8.3 (hover) and Table 8.4 (cruise). They are noted as the absolute deviation of the parameter from the original controller implementation in the form $(result_{weight/10}; result_{weight \cdot 10})$.

Table 8.3: The sensitivity analysis for the hover condition controller design.

	Overshoot $[m/s]$	**Settling Time $[s]$**	**Max. θ Deviation $[rad]$**
Speed Error Weights	0;+0.56	+27.01;+6.56	+0.038;-0.042
Angular Rate Error Weights	0;0	+16.35;+16.35	-0.001;+0.001
Angle Error Weights	-0.38;0	+7.35;+28.5	-0.025;+0.025
Delta Control Force Weights	0;+0.163	+36.35;+13.35	-0.025;+0.025

Table 8.4: The sensitivity analysis for the cruise condition controller design.

	Overshoot [m/s]	**Settling Time [s]**	**Max. θ Deviation [rad]**
Speed Error Weights	-0.021;+0.080	-1.91;-3.88	+0.008;-0.035
Angular Rate Error Weights	0;+0.003	+0.02;-5.08	0;+0.002
Angle Error Weights	-0.009;-0.044	+13.23;+19.97	-0.010;-0.3671
Delta Control Force Weights	-0.044;+0.3805	+0.53;+3.96	-0.006;-0.004

It is found that the controller design for both hover and cruise is not very sensitive to changing the speed error weights as the maximum deviation of -0.38 m/s is relatively small.

However, the settling time is quite sensitive to changing the weights. The maximum deviation is +36.35 s means that it would take an additional 36.35 seconds to reach the reference velocity, which is a significant loss of performance.

The maximum magnitude of θ of the original design is already close to the linearisation requirement. Thus significantly negative deviations could cause unreliable results.

8.8.2. VTOL

The sensitivity analysis for the VTOL controller was done similarly as it features an LQR controller as well. Additionally the PD controller is analysed for sensitivity by altering the proportional gains and the derivative gains by 50%. For this controller the maximum angles were an order of magnitude lower than the 5° limit; therefore only the overshoot and settling time metrics are presented.

Table 8.5: The sensitivity analysis for the VTOL controller.

	Overshoot [m]	**Settling Time [s]**
Speed Error Weights	0;+2.2	+1.5; -0.7
Angular Rate Error Weights	0;0	0;0
Angle Error Weights	0;0	0;0
Delta Control Force Weights	0;0	0;0
Proportional Gain	+0.2;+0	-2;+8.3
Derivative Gain	0;+0.021	+1.9; -1.6

It can be seen that the speed error costs, the proportional gain and derivative gain cause the most change in performance while the performance change associated with the remaining costs are not noticeable. This is expected as without a disturbance the angles and angular rates hardly change during the VTOL phase.

8.9. Verification and Validation

The MMOI and COG estimations have been verified with the use of hand calculations and a more simplistic estimation case. The COG estimate can be updated as more details are known and validated by measuring the weight of the aircraft on multiple scales on a level surface and at a slanted surface. The MMOI estimates can be validated per component by further analysis, and for the vehicle with in-flight measurements during flight testing.

As discussed in subsection 8.3.3, linearisation was done at the hover and cruise conditions. The trimming tool in Simulink was verified by calculating the steady state input forces for the hover condition by hand. The same was done for finding the trim steady state values.

MATLAB was used for the linearisation of the equations of motion. The equations were represented symbolically in MATLAB using its symbolic toolbox. The Taylor series function in MATLAB was used for the linearisation of all equations simultaneously. This function was verified by performing one of the linearisations by hand.

Finally, the simulation was done using Simulink blocks. The following Simulink blocks were used and verified one by one and within the system, by logging the input and output signals:

Built-in Simulink functions:

PD, Constant, Integral, Derivative, Mux, Demux, Sum, Gain (both matrix multiplication and SISO), LTI System, Divide, Invert, Matrix Multiply, and Cross Product.

Custom MATLAB functions

- $BodytoVCE$: Transformation matrix of a positional vector from B to V_{ce}.
- $VCEtoBody$: Transformation matrix of a positional vector from V_{ce} to B.
- $VRtoBody$: Transformation matrix of a positional vector from VR to B.
- $pqrtoeuler_{dot}$: Transformation matrix of the kinematic relationship of angular velocity.
- $sumF_{body}$: Summation of all body forces.
- F_{abody}: aerodynamic force calculation.
- M_{abody}: aerodynamic moment calculation.
- $M_{thrust_{body}}$: moment caused by thrust forces calculation.

All custom MATLAB functions were tested using unit tests as well and altered if necessary.

8.10. Future Work

The control system has now been designed in some level of detail. However, various assumptions and simplifications have been made along the way. In order to obtain a more reliable design, more accurate design must be performed. The next steps to be taken in the project development are listed here.

- **Design Transition Between Phases and Schemes**
  The transition logic from the VTOL control scheme to the Cruise control scheme, and the transition between the two gain sets in the cruise control scheme has to be designed and tested.
- **Discretization of the System**
  The system must be discretized in order to be implemented in hardware, the effects of discretization must be tested.
- **Testing of Control Loop with the Non-linear System Model**
  The linearised models have already been tested against the non-linear model with linearised actuators. The nonlinear dynamics of the actuators (motor-controller+motor) should be tested and modeled and the system stability should be verified. At every stage the control system should be tested with the non-linear model.
- **Modelling of Sensors, Sensor Noise, and Disturbances**
  Disturbances such as gusts and noise such as sensor noise should be modelled and accounted for.
- **Design of the Filters Used in Combining Sensor Measurements**
  Filters to combine several measurements should be designed to get the robust and accurate readings of the system state.
- **Further Development of the Gain Scheduling System**
  More linearisation points along the operational envelope can be used to increase performance and reliability.
- **Integration with the Safeguard System**
  The Safeguard System sets constraints in order to prevent the breach of no-fly zones; this system has to be integrated within the current architecture.

- **Integration with the Self-Diagnosis System**
  Emergency procedures for in-flight emergency prevention have to be better defined. The hardware or software implementation of the system must be better defined.
- **Hardware-in-the-loop Testing**
  Physical tests with sensors and actuators may be conducted without the processor but with an external computer to gain more insight into the interactions and overall system dynamics.
- **Development of the UI and testing connectivity with the mobile device**
  The mobile device must be integrated, the UI for the user controls have to be designed and tested separately in simulation and together with the entire system.
- **Testing with the MCU+DSP H/W**
  A complete control subsystem stress test must be done and all possible functions tested.
- **Monitoring and Maintenance of the Operational System in the Market**
  The system shall be monitored for the duration it is operated, any problems that arise must be fixed and performance could be possibly increased.
- **Development of ASIC Processors**
  To improve safety, reliability and cost less flexible yet better performing and cheaper (per unit) ASIC processors may be designed and certified once product maturity has been reached.

8.11. Risk analysis

The results of the FMEA for the Control and Stability subsystem are presented in Table 8.6 and Table 8.7. In Table 8.6 the failure modes are identified and assessed for likelihood (L) and severity (S). Also the main drivers of the failure modes are identified. Subsequently, in Table 8.7 the failure modes are given a detection level (D) that indicates the difficulty of detection based on the detection strategy that is chosen. Mitigation plans are formed and the new L- and S-values are estimated.

Table 8.6: The failure modes and their properties found through the FMEA for the Control and Stability subsystem.[46] [47]

Item	**Risk ID**	**Failure Mode**	**Drivers**	**L**	**S**
Processor	TR.CS.S-1	Control System Failure, Loss of vehicle control	Processor Failure	1	5
	TR.CS.S-1.1	Processor Failure due to loss of pin contact	Fretting	1	5
	TR.CS.S-1.2	Processor Failure due to Overheating	Hot operating condition/ low thermal insulation/ high calculation load for long periods	1	5
	TR.CS.S-1.3	Processor Freezing or performance loss	Unstable Input power	1	4
	TR.CS.S-1.4	Unpredictable Processor Behaviour, possibly fatal	Electromagnetic Interference from other components	1	4
Connections	TR.CS.S-2	Loss of Signal OR Unacceptable Signal Noise OR False Signal	Connection Failure	2	4
	TR.CS.S-2.A	Interruptions of Signal	Cable Conductor, In-jacket Breakage	1	4
	TR.CS.S-2.B	False Signal	Short to ground/ Hot Short	1	5
	TR.CS.S-2.C	Signal Noise due to high resistance at contact	Corroded, worn-out or cracked Connector	1	3
	TR.CS.S-2.D	Open Circuit	Insulation Jacket Damage	1	5
	TR.CS.TP-2.E	Increased risk of mechanical failure mode occurence	Torsional Deformation	2	1
	TR.CS.TP-2.F	Signal Noise due to electro magnetic interference	Shielding Losses	4	2
Sensors	TR.CS.S-3	Partial (Switch to alternative control laws) /Full Control Sytem Failure Depending on Sensor	Sensor Failure	1	5
	TR.CS.S-3.A	Sensor Failure - No reading or reading out of bounds	Obstruction, physical damage, sensor specific electronic failure	2	4
	TR.CS.S-3.1	GPS System Failure - No geolocation, no position control during hover	GPS Satellite (GNSS) Signal Loss	5	2
	TR.CS.TP-3.3	Lidar altitude reading momentary deviation	Object passing underneath vehicle	5	3
	TR.CS.S-3.4	Barometer MSLA to altitude conversion bias	Weather pattern pressure deviations	4	2
Software	TR.CS.S-4	Control System Failure, Loss of vehicle control	Software Failure	1	5
	TR.CS.S-4.1	Processor crashes	Illegal pointers due to firmware	1	4
	TR.CS.S-4.2	Processor Failure	Memory stack overflow due to firmware	1	4
	TR.CS.S-4.3	Drift in certain calculation outputs	Rounding Errors	5	2
Input Device	TR.CS.TR-5	Vehicle Automated Landing Sequence Initiated	Input device failure	1	4
	TR.CS.S-5.A	Vehicle slows done and goes into hover mode	Input Device Touch Display Malfunction	1	2
	TR.CS.S-5.1	Vehicle slows done and goes into hover mode until interruption over	Input Device Interruption (received call, application exit etc.)	5	2

Table 8.7: The mitigation strategies found through the FMEA for the Control and Stability subsystem.

Item	Risk ID	Detection strategy	D	Mitigation Strategy	New L	New S
Processor	TR.CS.S-1	Pre-flight electronic check	2	Triple Modular Redundancy with a Command-Standby-Monitor lane setup	1	5
	TR.CS.S-1.1	Pre-flight electronic check	5	PCB Natural Frequency 200 Hz, Mounting Standoffs	1	5
	TR.CS.S-1.2	Processor self-diagnosis	1	Implement active air/water cooling solution if necessary	1	5
	TR.CS.S-1.3	Input power monitoring	2	Use of a dedicated power grid separate from the high power grid.	1	3
	TR.CS.S-1.4	-	5	Shielding of the processor unit	1	3
Connections	TR.CS.S-2	Pre-flight electronic check	2		1	3
	TR.CS.S-2.A	-	4	No more than TBD degree deviation during cable routing, procedures not to overbend cables during assembly	1	4
	TR.CS.S-2.B	Pre-flight electronic check	4	Choice of thick enough isolating layer surrounding cable conductor, good isolation between cable and connector	1	5
	TR.CS.S-2.C	Pre-flight electronic check	2	Match Plating material, maximize distance between differing voltage potential connections, Use mezzanines and hermetic seals	1	3
	TR.CS.S-2.D	Pre-flight electronic check	1	No sharp edges traversed by cables, limit cable movement and loads on cables	1	5
	TR.CS.TP-2.E	Post-assembly check	3	Procedures to avoid torsion of cables during assembly, careful design and testing of cables that traverse joints	1	1
	TR.CS.TP-2.F	-	5	Use of shielded cables for high power component connections	1	1
Sensors	TR.CS.S-3	-	5	Redundant sets of sensors, mobile sensor backups	1	4
	TR.CS.S-3.A	Pre-flight electronic check	3	Sensor and Vehicle Stress Testing	2	3
	TR.CS.S-3.1	Inspect signal	1	Switch to dead reckoning positional control	5	1
	TR.CS.TP-3.3	Inspect signal	2	Combination of lidar and barometer measurements, filters	5	2
	TR.CS.S-3.4	Inspect signal	3	Combination with lidar sensor and perhaps use of local ground level pressure measurements or predictions	3	1
Software	TR.CS.S-4	Full system testing	4	Self detection and a separate safety software running on redundant processor core to land the vehicle	1	5
	TR.CS.S-4.1	analysis/testing	5	Extensive firmware testing and development	1	4
	TR.CS.S-4.2	analysis/testing	5	Extensive firmware testing and development	1	4
	TR.CS.S-4.3	analysis/long period testing	5	introduction of deadbands	5	1
Input Device	TR.CS.TR-5	Inspect signal, connection self check	2	Automatic landing sequence	1	3
	TR.CS.S-5.A	-	4	-	1	2
	TR.CS.S-5.1	Input device event message	1	-	5	2

9 Operations

In a previous design stage, reported in the project plan [1], the choice was made for a rentable system instead of a retail system due to feasibility of the mass requirement and audience preference on ownership. A renting system brings all kinds of challenges, as locations must be made for rental distribution. The idea is created to use vertiports, where users can retrieve and bring back vehicles, also allowing to make stops at specific landing zones explained in the vertiport section. In addition, communication, user interface, no-fly zones and flight training are discussed. To start, an operational flow diagram is presented to show a big-picture view of operations.

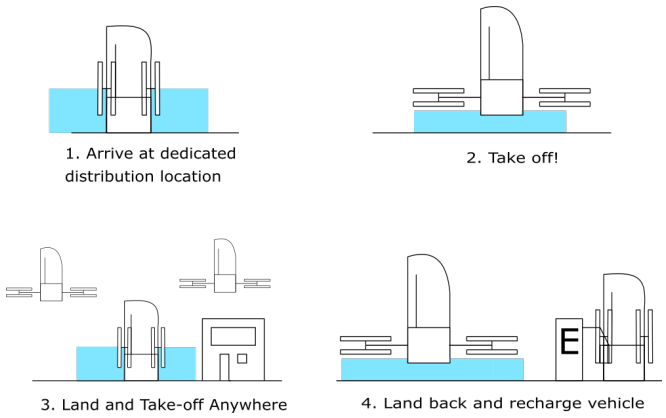

Figure 9.1: Business Rental Idea

9.1. Operational Flow Diagram

The flow of operations is presented in Figure 9.2.

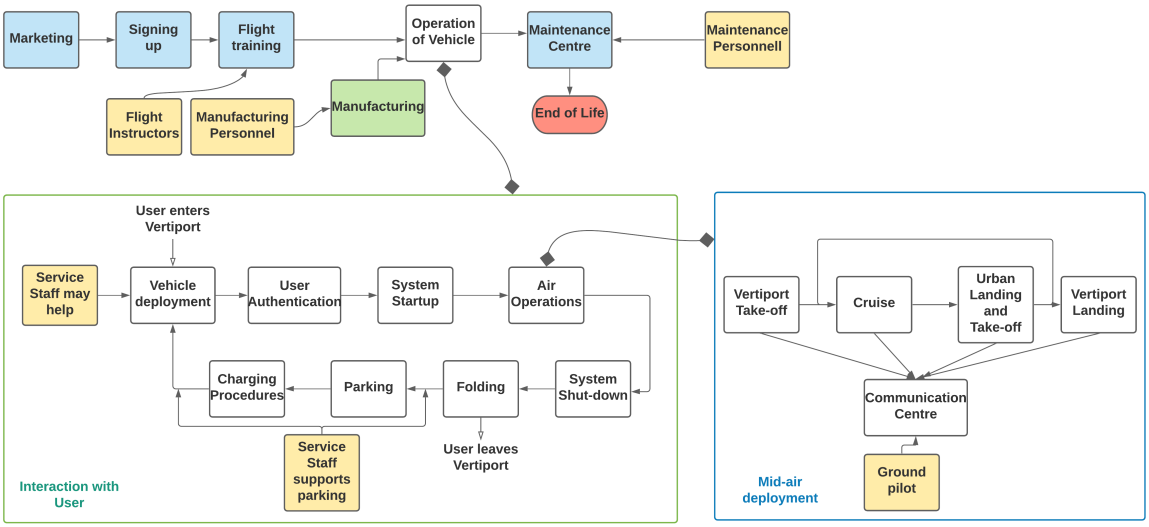

Figure 9.2: The operational flow diagram of the system

9.2. Communication

As found in public surveys and research on personal air transportation and the requirement that the user controls the vehicle on its own with help of automation, some kind of pilot needs to be able to take control of the vehicle in case the user experiences difficulties. Research suggests a ground pilot [48], a pilot that keeps an eye on multiple vehicles and can intervene when the user is in need of help. The use of a ground pilot means that communications need to be set-up. Various communication methods are possible, among which are satellite, VHF (Very high frequency) radio and 4g/5g mobile network. Satellite is an expensive option and not necessary as ground stations are a cheaper option. 4g/5g has the advantage of a high bandwidth and hence the possibility of much data to transport. Although research is underway of using 4g/5g for vehicle control from the ground, it is new and perhaps unreliable technology. For less critical functions it is an option. VHF Radio is used regularly in aviation and supplies a reliable communication method. Hence, VHF is used for critical subsystems, such as ground control. 4g/5g may be used for non-critical subsystems. A diagram for communications is given below:

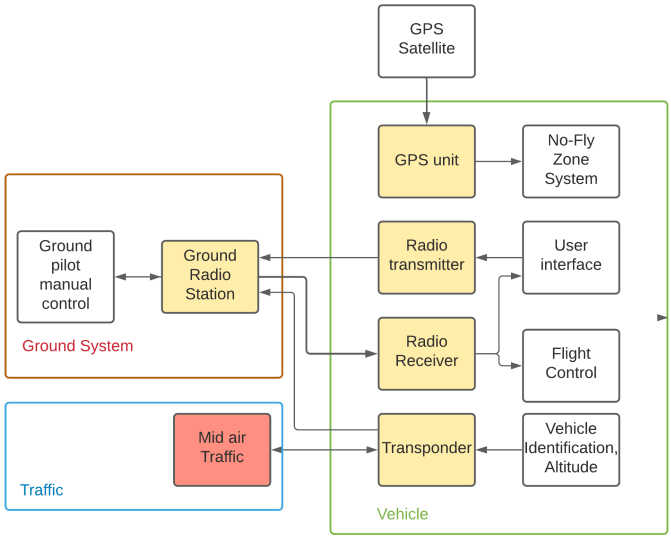

Figure 9.3: Communication flow diagram

9.3. No-Fly Zones

One requirement is that the vehicle should avoid no-fly zones by having knowledge on aerial legislation and can update this, and checking that with its current position. Aerial legislation is in Europe determined by the EASA and categorises airspace from A to G. Airspace class A is highly controlled by air traffic control and is hence not suitable for our system, as the user is responsible for its position. Class G is defined until 200m above ground level and is hence suitable for our system, as this is not controlled by ATC. Attention should be given to airports as there are constraints on where to fly. In addition, there are no-fly zones such as military terrains. These areas must also be prohibited. The straightforward method for position determination is GPS. One such a device is a safeguarding system, a small box consisting of a GPS sensor in combination with a system that checks predefined no-fly locations with its GPS location [49]. Combining these functions, the aircraft is able to keep the user from no-fly zones. There are two options for intervening. Only a warning might be given, in combination with good training where not to fly. On the other hand, a link with the control system can make it physically impossible to fly near these zones. This does have the consequence that for example there is little space to avoid collisions when on this border. The most viable option is to combine them, giving a warning when approaching such an area and make it impossible to physically fly there.

9.4. User Interface

Requirements for user interface are that a smartphone must be used for user interaction, and that the user needs to be able to control the vehicle. A user module is designed for these purposes. For the placement of the module, it is needed that it does not obstruct the view, but however is in the close vicinity [50]. The location is therefore desired to be right in front of the user, placed just higher than the elbows of the user.

For the design of the user module, the following information must be present: airspeed, navigation (including location), altitude, communication options to ground pilot, system diagnosis information, and VTOL activation. Communications with the ground would consist of regular communications (e.g. voice or text) and emitting a distress call to ask for assistence (e.g. button/lever/voice). The smartphone is relied on as little as possible, as the reliability of the smartphone is unkown in terms of a software or hardware malfunctioning of the smarthone. Hence, the smartphone provides a means of control (e.g. touch of buttons on screen) and navigation on screen. Additionally, the vehicle must be controllable by the user panel (e.g. joystick/buttons) for back-up in case of smartphone failure.

From these functions and making the displays reasonably big for legibility, an approximation can be made for the size of the user panel, found to be 40x14x5 cm.

Additionally, a camera is placed underneath the vehicle, presenting the downward view during VTOL for the user. The controls for the users themselves will be straightforward, as the control system manages the complex movements. Flight training will make sure this is achieved, talked about more in the next section.

9.5. User Flight Training

Due to the fact that the user primarily controls the aircraft and the fact that, although much control is automated, many piloting tasks are not or partly automated. For these tasks, user training is necessary. The goal of this section is to list all learning goals for the user, including training methods for each learning goal. First, however, three learning categories are described and it is explained which learning categories are preferred in this training.

At the start of the design, an important concept trade-off parameter was the amount of automation. Automation means less control is given to the user and hence, the user can make less mistakes, making the aircraft safer. However, there are many disadvantages on too much automation; the system might get unnecessary complex, increasing development and production costs significantly. Even more, automation might prevent small mistakes, such a mistake would be flying too high on final approach. The big dangers comes however from the user becoming complacent or loosing attention. This leads to mistakes on so-called 'high level' tasks, an example might be flying too far over the destination and hence loosing too much fuel. In conclusion, a trade-off must be made between automation and amount of control.

The characteristics of this specific design and user operations are the starting point of user training. The vehicle consist of 4 sets of co-axial rotors, guided by a control system. The control system allows the user for control in speed direction in the horizontal plane, and control in altitude. As specified in section 9.1, other user tasks consist of deployment of vehicle, authentication, system start-up, route planning, VTOL procedures, safety procedures and communication procedures. These tasks have to be learned by flight traing prior to using the vehicle.

9.5.1. Learning categories

Specific learning categories can be specified. The method of Skills, Rules and Knowledge is helpful, as explained in the midterm report:

'In general, any training consists of three learning categories : Skills, Rules and Knowledge [51]. Skills refers to muscle memory in which neural pathways to muscles are trained to automatically sense feedback of sensations and control muscles, needed for continuous control. It takes relatively large amount of time to learn this, however once learnt is not easily forgotten.

Rules consist of recognising situations and apply the correct procedures. Typical procedures can be procedures in start up, landing approach or standard emergency procedures. This discrete way of controlling needs to be trained and automated, in which choosing the correct procedure is critical. The choice is made with help of knowledge, the next type.

Knowledge is abstract knowledge, which can be technical knowledge of the aircraft, tactics for

emergencies or planning strategies. Knowledge is critical in unfamiliar situations, as the user needs knowledge to understand the bigger picture and think about how the problem could be solved, improvising a solution. Only relying on rules cannot be used when an improvisation of the user is needed, knowledge on dealing in that situation guides the behaviour and choices of the user. Even more, it is critical that the user is aware of the severity of an unknown situation, except for much experience, knowledge is the basis for new information.

For flight training, tasks requiring skills should be automated as much as possible, increasing safety. Hence, vehicle flight control is automated, allowing the user to control with simple horizontal and vertical control. As such, VTOL is heavily guided by the control system, and with the help of a camera, it is made as simple as possible. Automating more complex systems, such as traffic management, is hard too do and increases the complexity greatly, allowing the user to loose attention. Hence, procedures and knowledge is the point of focus. This way of thinking is backed up by research [48], calling it 'simplified vehicle operations', first automating basic controls. After years of use and development in technology, more systems can be automated, such as traffic control, VTOL etc.

9.5.2. Learning goals

When the level of automation is known, a look can be taken at the user operations, leading to the learning goals of the training. These learning goals can be found in Table 9.1, as well as proposed learning methods and aspects to take into account for the design, categorised by learning type.

9.5.3. Learning Methods

From the learning goals listed in Table 9.1, methods to learn these can be thought off. As can be seen in the table, many goals are knowledge related goals, meaning the user must learn this knowledge and know when to use it. For this, a textbook, reader of information video is suitable. As learning knowledge can be experienced as hard/boring, efforts should be made to make it exciting and/or interactive, for example with personal guidance. For procedural learning, mock vehicles are a viable option. A mock cockpit can be used to learn landing and start-up procedures, while a mock vehicle can be used for practising deploying the vehicle. For skills, active continuous control must be practised. Since the vehicle allows only one user, a real life flight instruction with a flight instructor is not an option. Hence, a flight simulator with simulator software must be used for cruise control and navigation practice.

9.5.4. Logistics of Flight Training

A separate facility is recommended for multiple vertiports, containing the mock vehicles, flight simulators and flight instructors to support the learning method. As similar to a driver's license, the user can pay for this him/herself. As visible in Figure 9.2, flight training takes place after signing up, and before user operation. After of completion of flight training, the user receives a pass to authorise itself to the system, for example with a key or card. Information of the user must be stored, and are with the users personal authentication available to the rental system. One special piece of information is the user's weight, measured in the training centre. Its information is important towards the control system and for determining if the system is over its weight limits.

Table 9.1: For user flight training, all steps for normal user operation including the learning goals, method and difficulty / required level needed.

	Learning Goals	What to learn	Type of learning	Learning method	Difficulty / level needed
Vehicle Deployment	Visual inspection for damage	Learn function of windscreen and rotors	Knowledge	Text/video	Normal
	Pull down rotor beams manually	How to put safely pull down beam with no damage	Procedure	Practice	Normal
	Put rotors into place	How to put safely assemble rotor with no damage	Procedure	Practice	Normal
	Enter Vehicle	When to enter safely and how to apply seatbelt	Procedure	Practice	Easy
System Start-up	Start up system , key/card to authenticate	Learn startup procedure, Know how key/card works	Knowlege, Rules	Text, video and mock cockpit	Easy
	Rotate beams to correct place	Learn Beams rotate procedure	Procedure	Practice with Mock Vehicle	Normal
	Enter navigation route	Learn how navigation works	Knowledge	Mock cockpit with navigation device	Normal
	System self-check procedure	Learn self-check activation, what to do in case of failure	Knowledge	Text/video	Normal
Vertical Take-off	Check airtraffic clear	Practice watch techniques	Procedure	Flight simulation	Hard
	Communicate take-off	Learn and practice communication on user screen	Knowledge, Procedure	Practice with instructor	Normal
	Final system self check	Learn self-check activation, what to do in case of failure	Knowledge	Practice mock cockpit	Normal
	Perform Take-off procedure	Practice procedure and safety procedures	Procedure	Flight simulation	Normal
Cruise	Perform flight control	Learn muscle control of vehicle, including flight boundaries	Skills	Flight simulation	Hard
	Follow Route	Learn to operate route middle of flight, visual see where user is	Skills	Flight simulation	Hard
	Be able to communicate with ground personell	Practice ground personell comms	Procedure	Practice with instructor	Hard
Vertical Landing	Identify Landing site, Check if landing site is clear	Learn where landing zones habbit check for clear runway	Knowledge, Skills, Procedure	Flight Simulator, Video	Normal
	Communicate landing	Learn to always communicate landing	Procedure	With instructor	Hard
	Perform landing procedure	Learn and practice procedure	Procedure	Mock cockpit, Flight simulator	Normal
System shut-down	Shut-down procedure	Learn startup procedure	Knowlege, Rules	Text and Practice	Easy
	Exit vehicle	When to exit safely and how to use seatbelt	Procedure	Practice mock cockpit	Easy
Un-deployment	Disassemble rotors	How to safely disassemble rotor with no damage	Procedure	Practice with mock vehicle	Normal
	Push rotor beams up	How to push rotorbeams up with no damage	Procedure	Practice with mock vehicle	Normal
	Visual Inspection of damage	Learn function of windscreen and rotors	Knowledge	text/video	Easy

Table 9.2: For safety procedures user flight training, all steps for normal user operation including the learning goals, method and difficulty / required level needed.

	Learning Goals	What to learn	Type of learning	Learning method	Difficulty / level needed
Safety Procedures	Unexpected landing	Procedure for unexpected landing	Procedures	Mock cockpit	Normal
	Handling weather conditions	When to choose to do emergency vertical landing	Knowledge	Video, text	Normal
	Procedures for subsystem failure	Learning procedures for all important subsystem failures	Knowledge, Procedures	Video, text, Flight simulation	Hard

9.6. Charging

As battery charging and charging technicalities are covered in the power and propulsion chapter, this section will look at charging infrastructure options. This starts at charging at the vertiports. Looking at the car charging infrastructure, two types of charging are possible: fast charging with high power (order of 40kW), or regular charging (order of 8kW - 22 kW). Since fast-charging delivers a high power and thus allows for quick charging time, it is generally not good for the lifetime of batteries. Hence, fast charging is not recommended for regular daily use. This means charging at a lower power is needed, significantly increasing charging time unfortunately. This means it is chosen to charge vehicles while parked, requiring overnight charging as an option. This requires a larger fleet size to deal with peaks in demand and the possibility for every parking space a manner of charging. The upside is that one can use the low voltage infrastructure (order of 100V), instead of the medium voltage infrastructure (1kV). Low voltage is also advantageous in costs compared to medium voltage infrastructure, as high voltage requires much more construction costs due to a small transformation house needed to lower the voltage (Roughly 1,000 euros instead of 100,000 euros per vertiport).

9.7. Vertiports

Vertiports are very similar to heliports in aspects of safety and requirements. Therefore, regulations such as ICAO provide information on vertiport requirements [52]. Relevant requirements are the size for final approach and take-off areas (FATO) and safety areas. The FATO is area for the vehicle to land on, while the safety area should be clear of objects. According to regulations (EASA source), FATO area should be at least 0.8 times the highest dimension, and the safety area at least 3 meter from the FATO, also found in the vertiport map below. Note that this area requirement takes into account all weather conditions for helicopter vehicles.

The size of the vertiport depends on the size of a vehicle and the number of vehicles to take-off and land simultaneously and all other components, such as maintenance shop, communication centre and costumer service.

The fleet size is an important parameter, since waiting times highly increase if demand is higher than supply, due to flexibility in handling higher demand. This effect is higher for shorter distances and lower air speeds [11]. This source found as well that this effect is very high at 10-20 vehicles and 'nearly covered' at 100 vehicles per vertiport. However, sources also mention that handling more than 20 vehicles can be complex [53]. In conclusion, fleet size of around 100 is more efficient than less, where special consideration should be given in fast storage, deployment and charging handling.

As 500 flights per year per vehicle is a requirement, it means that on average, $500/365 = 1.37$ flights need to be able to take place everyday per vehicle. $n = 200$ vehicles per vertiport is used, with the assumption that 1.37 flights per day are needed. the additional assumptions are made that that 80% of vehicles are used and flight procedures on vertiports take in total 8 min, and that all VTOL procedures take in total 5 hours per day, the next simple calculation shows the an approximation of simultaneous VTOL procedures.

$$N_{simultVTOL} = \frac{n \cdot 1.37 \cdot \%_{useddaily}}{N_{hoursopened} * 60} = 3.6 \tag{9.1}$$

This means that according to the approximation, At least 4 VTOL spaces are needed on the vertiport

for the desired VTOL capacity. Assuming all VTOL operations take 5 hours instead of a full day is done in order to design for some flexibility.

From the expected dimensions of VTOL pads, parking and charging, a vertipad concept can be constructed. In this concept, the vehicles are stored in the centre, with landing pads and communication plus small maintenance around. Another shape can be thought off, however this picture only presents one configuration. As the needed area is the main factor, any other viable configuration is possible.

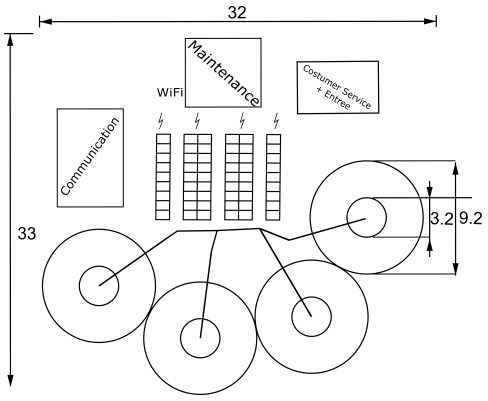

Figure 9.4: Possible vertiport concept, dimensions given in meters

For long term maintenance, a centre for maintenance must be constructed, operating for multiple vertiports. With the requirement that maintenance is done every two years, in the long term this means that the number of vehicles needed in a year is more or less spread over this time period. This may lead to an estimation of the number of maintenance centres. This is used in cost estimation, and is estimated on 1 maintenance centre per 2000 vehicles, leading to ten vertiports per maintenance centre.

For transporting the vehicle between parking and VTOL area, several systems can be thought off. One option is inspired on automated parking lots below ground. where an automated system transports the car to the parking space. Such a system might be used, however is very complex and expensive. another option is transporting the vehicle via a simple structure on wheels, where service workers can transport the vehicle between parking and VTOL. This method is preferred, however does require extra personnel. The design of such a vehicle can be simple: A platform with wheels big enough for supporting the bottom structure is needed, in combination with a elevation system to elevate the vehicle from the ground. Simply put, it is a pallet hand truck [1] optimised for the vehicle's weight and size.

9.8. Urban VTOL Sites

The dedicated vertiports are not the only locations suitable for VTOL operations. The vehicle must also be able to land in various other places in urban areas, such as parking spaces found on roofs of buildings. Good examples of suitable locations might be parking spaces on roofs, already known at IKEA or big shopping centres. Other buildings can also be adjusted into VTOL locations. For VTOL locations not on roofs, it is important in terms of bystander safety that no bystanders can accidentally come to close. This is done first off all by the system by notifying its surroundings with sounds and lights. For storing the vehicle, transporting methods can be similar to the one used in vertiports, by use of a pallet handtruck[2].

In terms of clearance to its surroundings, the control system is capable of staying within a radius of 1.5m. As the diagonal dimension of the vehicle is 3.8m, a total diameter of 7 meters is needed for clearance. When wind gusts are taken into account, a diameter of 9 meters is necessary.

[1] Mennens. *An example of pallet handtruck: Hand pallet truck HU 25-115 Silverline*. URL: `https://www.mennens.nl/en/products/hand-pallet-truck-hu-25-115-silverline-p253517` (visited on 01/25/2021)

[2] Mennens. *An example of pallet handtruck: Hand pallet truck HU 25-115 Silverline*. URL: `https://www.mennens.nl/en/products/hand-pallet-truck-hu-25-115-silverline-p253517` (visited on 01/25/2021)

10
Risk Management

The vehicle that is being designed features various components that have the potential for failure. Besides the technical performance and the safety aspect of risk management, the cost will be analysed as well. The risk identification and assessment will be done on a system level and on a subsystem level. This is because a portion of the failure modes can be traced back to specific components and others deal with the interaction between subsystems.

10.1. Risk Identification and Assessment

In this section risk identification and assessment is detailed for the different risk types. Technical performance and safety are treated separately from cost, as these are analysed in different manners. However, generally the likelihood (L) and severity (S) of risks are defined similarly for all risks. In Table 10.1 the general approach to the quantification of likelihood is tabulated. This quantification is done based on the amount of times an event is expected to occur per vehicle life time. This estimation is based on the state of technology, the complexity of the system and other considerations that differ per specific risk. In Table 10.2 the method of quantifying the severity of risks is presented (including some examples of consequences) [54].

Table 10.1: Likelihood quantification

Quantifier	Occurence
1	Once in 50-100 life times
2	Once in 20-50 life times
3	Once in 1-20 life times
4	1-5 times per life time
5	5-10 times per life times

Table 10.2: Severity quantification, with examples of consequences for every risk type

Quantifier	Influence	Safety	Technical Performance	Cost	Scheduling
1	Very low	Small injury	one component fails	€10-100	1-4 hrs
2	Low	Medium injury	Several components fail	€100-€1000	1-2 days
3	Medium	Several injuries	Subsystem fails	€1000-€10000	3-4 days
4	High	Serious injury	Several subsystems fail	€10000-€100000	5-7 days
5	Very high	Several serious injuries	Entire system fails	€100000-€200000	1-2 weeks

10.2. Technical Performance and Safety Risk

The risk identification and assessment on a subsystem level is done by doing a Failure Modes and Effects Analysis (FMEA) by every technical department. An FMEA is of importance for various reasons. It provides a basis for assessing performance levels and fault-detection mechanism. The FMEA also acts as an effective mechanism of evaluating failure effect on human safety and environment [0]. The analysis that is done is a combination of a standard FMEA and the risk analysis that was done so far in the design. Specifically this means that the risk properties are extended by adding a detection level. This is a number in the range of 1 to 5 that describes the detectability of a certain failure mode in operation. The estimation of the detectability is done intuitively based on the method of detection. A detection level of 1 means that the failure mode is easily and reliably detected, whereas a detection level of 5 indicates that there is no possibility for detection. All the FMEAs performed are reported in

a dedicated section of every department. The subsystem-specific technical risk IDs are of the form $TR.\{DEPARTMENT\}.\{RISKTYPE\} - \{NUMBER\}$.

Since the Aerodynamics department only did an analysis of the design and does not feature components that have the potential of technical failure, this department is excluded from this analysis.

10.3. Cost Risk

In chapter 15 the cost is broken down into manufacturing cost, development cost and operational cost. Different types of cost estimations were performed and the uncertainty differs greatly. For instance, for manufacturing, some components are directly bought from external suppliers and their price is either publicly known or an official quote was delivered by the supplier. No additional safety factors or margins are required in this case. In other cases there was a lack of knowledge and statistical data was used for estimation and thus adding margins is a suitable way of mitigating cost risk.

10.3.1. Manufacturing cost

The manufacturing cost is estimated by summing up the expected cost of all the components in the vehicle. For the estimation of component cost an inventory sheet of all the system's components was made. All components from all departments are listed including its properties such as cost, mass, life time and manufacturing methods. After summing up the inventory cost a margin is added in order to account for uncertainties.

10.3.2. Development cost

As there are many uncertainties pertaining to development, its cost is very difficult to estimate. Hence, an analogy is done based on the Lilium Jet1 to get a very rough estimate of development cost. The estimation is done mostly based on the salary rate of the engineers working on the project. The growth of the team over time is taken into account. Additionally, a margin is added per person in order to account for extra cost.

10.3.3. Operational cost

The operational cost is broken down into vertiport-related cost, charging cost, infrastructure connection cost and maintenance centre-relate cost. For each, an appropriate margin is added between 20 % and 50 %, based on the cost uncertainty. This results in different profit scenarios, of which the worst case scenario has to comply with the requirements.

10.4. General risk and Subsystem Interaction

Performing an FMEA for all departments takes into account the risks related to the specific subsystems. However, additional failure modes are possible. Earlier in the design general technical risks were identified and assessed. A portion of these were used to generate requirements for the system. Others became irrelevant after performing the trade-off, as preliminary design choices were made, or performing the FMEA already identified more specific subsystem risks.

Besides pre-existing risks, the interaction between subsystems (including self-diagnosis) is investigated more thoroughly. As this also concerns system-wide risk, the identified risks are added to the general risk log tabulated in Table 10.3. The general risk IDs are of the form $TR.G.\{RISKTYPE\} - \{NUMBER\}$.

Table 10.3: The general technical risk log including their types, description and drivers.

ID	Risk Types	Description	Drivers	L	S
TR.G.SC-1	Scheduling	System design cannot be finished during allocated period	Complex design, Team-related issues, Planning failure	3	5
TR.G.TP-1	Technical performance	The mass budget defined in an early design stage cannot be satisfied	Heavy design, mass budget too strict	3	4
TR.G.S-1	Safety	System is used for flying in a no-fly zone	Small vehicle: little to no detection	2	4
TR.G.S-2	Safety	Civilians are in danger because of moving parts/heat during takeoff and landing	Urban mobility, lift generation required	2	4
TR.G.C-1	Cost	The requirement for a rental cost of 5000 euro a year cannot be satisfied	Expensive technology, unforeseen repair costs	2	5
TR.G.TP-2	Technical performance	Time of deployment is above 2 minutes	Limited lift generation, weather conditions	3	4
TR.G.S-3	Safety	User tries to fly above 20 meters altitude.	Curiosity,ability to avoid buildings, busy air traffic	2	4
TR.G.TP-3	Technical performance	System is not capable of elevating user	User is too heavy	3	4
TR.G.S-4	Safety	Strong wind at sea level has a large impact on the lightweight system	Strong winds, lightweight system	4	4
TR.G.TP-4	Technical performance	Subsystem design not verified and/or validated	Time pressure, poor execution	2	4
TR.G.TP-5	Technical performance	Requirements are contradicting	Insufficient overview of requirements, communication error	2	5
TR.G.S-5	Safety	User in danger as a total system failure occurs	System crashes, system hits obstacle, Control computer crashes	1	5
TR.G.TP-6	Technical performance	One of the subsystem fails during flight	Poor subsystem design, damage taken during flight	1	4
TR.G.C-2	Cost	Several users treat the system without care: damage, unclean interior	Careless attitude, rental system	3	3
TR.G.S-6	Cost	The crashworthiness of the design is expected to be insufficient	No safety measures in place, low container strength, high likelihood of post-crash fire	3	3

Table 10.4: The mitigation strategies for the general risks including the their types, description and property change.

ID	Mitigation Types	Mitigation Description	Property Change (L,S)
TR.G.SC-1	CTC and CMO	Opt for a simpler design choice that still satisfies requirements. Make sure the schedule is respected and that slight deviations are discussed	(0,-2)
TR.G.TP-1	CTC and CMO	Opt for lighter design (materials, structures). Reconsider budget and contingency values	(-1,-2)
TR.G.S-1	CMO	User gets signals from software when close to no-fly zone. User controls are overruled in case of (almost) entering no-fly zone.	(-1,-4)
TR.G.S-2	CTC and CMO	Opt for design choice with a smaller amount of dangerous side-effects. Indicate a landing/takeoff by using warning signals: audio/light signals. System can only do ground maneuvers with a TBD m radius of clearance	(-1,-2)
TR.G.C-1	CTC and CMO	Replace expensive parts of system with cheaper alternatives (materials, software etc.)	(-1,-2)
TR.G.TP-2	CTC and AMR	Change propulsion device such that it generates more lift. Lower drag by minimising top-down surface area.	(-2,-1)
TR.G.S-3	CTC and CMO	System should stop ascending when 20m altitude is reached (override user controls).	(0,-3)
TR.G.TP-3	CTC and CMO	Opt for a design with stronger lift capabilities. Make system only available to people under 100 kg.	(-1,-2)
TR.G.S-4	CTC and CMO	Opt for a stable design. System should not start when weather conditions are not adequate (scale of beaufort).	(-3,0)
TR.G.TP-4	CMO	Team should be made aware of importance of verification validation.	(-1,-1)
TR.G.TP-5	CMO	Both requirements are redefined or one of the requirements is discarded if deemed unnecessary.	(0,-3)
TR.G.S-5	CTC	Means of protection from rain and obstacles implemented.	(0,-2)
TR.G.TP-6	CTC	Means of user protection from large impact with ground or obstacle implemented.	(0,-2)
TR.G.C-2	CMO	Emergency procedures initiated.	(1,-2)
TR.G.S-6	A	All users are registered and have to leave contact information. Users will be fined in case of unacceptable behaviour.	(-2,0)

10.5. Risk Mitigation

Mitigation plans are devised by the departments originating from the FMEA and for the general technical risk log. In this section the general risk log and the results from the FMEA will be treated separately. For details of the FMEA-related mitigation plans refer to the individual chapters of the departments.

10.5.1. General risk

For the general risks, the types of risk mitigation plans and their abbreviations are presented in Table 10.5. The mitigation plans of all the risks are tabulated in Table 10.4.

Table 10.5: Risk mitigation strategies and their consequence on risk properties

Mitigation Category	Consequence
Acceptance (A)	Unchanged properties
Change technology choice (CTC)	Decrease likelihood or severity
Change manner of operating (CMO)	Decrease likelihood or severity
Add margins of redundancy (AMR)	Decrease likelihood

10.5.2. FMEA

In order to see the expected effect on the properties, the pre-mitigation risk map is presented in Table 10.6 and the post-mitigation risk map is presented in Table 10.8. The estimation of the likelihood and the severity are presented on the horizontal axis and the vertical axis, respectively. The risk IDs are tabulated based on their properties. This means that the total expected risk loss is largest at the bottom right of the risk map. The cells are colour-coded based on overall expected loss. The legend for the colour scheme can be found in Table 10.7.

Table 10.6: The pre-mitigation risk map resulting from the FMEA

		Likelihood				
Severity		1	2	3	4	5
	1	TR.PP.TP-9	TR.CS.TP-2.E		TR.PP.TP-1	TR.PP.TP-11
	2	TR.CS.S-5.A	TR.PP.TP-13, TR.SM.TP-1, TR.SM.C-1		TR.PP.TP-15, TR.SM.TP-8, TR.CS.TP-2.F, TR.CS.S-3.4	TR.CS.S-3.1, TR.CS.S-4.3, TR.CS.S-5.1
	3	TR.PP.TP-14, TR.SM.TP-3, TR.CS.S-2.C	TR.PP.TP-2, TR.PP.TP-3, TR.SM.S-3, TR.SM.TP-7	TR.SM.TP-2, TR.SM.TP-4, TR.SM.S-7, TR.SM.S-8, TR.SM.TP-10, TR.G.C-2, TR.G.S-6	TR.PP.S-1, TR.SM-TP-13	TR.SM.TP-5, TR.CS.TP-3.3
	4	TR.SM.TP-6, TR.CS.S-1.3, TR.CS.S-1.4, TR.CS.S-2.A, TR.CS.S-4.1, TR.CS.S-4.2, TR.CS.TP-5, TR.G.TP-6	TR.PP.TP-8, TR.PP.TP-10, TR.SM.S-2, TR.CS.S-2, TR.CS.S-3.A, TR.G.S-1, TR.G.S-2, TR.G.S-3, TR.G.TP-4	TR.PP.S-2, TR.SM.S-1, TR.G.TP-1, TR.G.TP-2, TR.G.TP-3	TR.SM.S-6, TR.G.S-4	
	5	TR.PP.TP-4, TR.PP.TP-6, TR.PP.TP-7, TR.PP.TP-12, TR.SM.S-9, TR.SM.S-10, TR.CS.S-1, TR.CS.S-1.1, TR.CS.S-1.2, TR.CS.S-2.B, TR.CS.S-2.D, TR.CS.S-3, TR.CS.S-4, TR.G.S-5	TR.G.C-1, TR.G.TP-5	TR.SM.S-4, TR.SM.S-5, TR.SM.TP-9, TR.SM-TP-11, TR.SM-TP-12, TR.G.SC-1	TR.PP.TP-5	

Table 10.7: The risk map legend.

Colour	Loss
	Very small
	Small
	Medium
	Large

Table 10.8: The post-mitigation risk map resulting from the FMEA

		Likelihood				
		1	2	3	4	5
Severity	1	TR.PP.TP-9, TR.PP.TP-11, TR.SM.TP-10, TR.CS.TP-2.E, TR.CS.TP-2.F	TR.PP.TP-1, TR.SM.TP-2, TR.SM.TP-8	TR.CS.S-3.4		TR.CS.S-3.1, TR.CS.S-4.3
	2	TR.PP.TP-2, TR.PP.TP-4, TR.PP.TP-12, TR.PP.TP-13, TR.PP.TP-14, TR.SM.TP-1, TR.SM.TP-3, TR.SM.C-1, TR.SM.TP-6, TR.SM.TP-9, TR.CS.S-5.A	TR.PP.TP-15, TR.SM.S-2, TR.SM.TP-4, TR.SM-TP-13	TR.SM.S-8, TR.SM-TP-11, TR.SM-TP-12		TR.CS.TP-3.3, TR.CS.S-5.1
	3	TR.PP.TP-3, TR.PP.TP-6, TR.PP.TP-7, TR.PP.TP-8, TR.PP.TP-10, TR.SM.S-3, TR.SM.TP-7, TR.SM.S-9, TR.SM.S-10, TR.CS.S-1.3, TR.CS.S-1.4, TR.CS.S-2, TR.CS.S-2.C, TR.CS.TP-5	TR.PP.TP-5, TR.PP.S-1, TR.PP.S-2, TR.SM.S-7, TR.SM.TP-5, TR.CS.S-3.A	TR.SM.S-6		
	4	TR.CS.S-2.A, TR.CS.S-3, TR.CS.S-4.1, TR.CS.S-4.2	TR.SM.S-1			
	5	TR.CS.S-1, TR.CS.S-1.1, TR.CS.S-1.2, TR.CS.S-2.B, TR.CS.S-2.D, TR.CS.S-4				

11 Sustainable Development

”Sustainable development is development that meets the needs of the present without compromising the ability of future generations to meet their own needs[55]”. This definition highlights the fact that the world is running out of fossil fuels[1]. Hence, the need for sustainable design solutions is increasing more than ever. The ongoing and upcoming energy transition from non renewable resources, i.e. fossil fuels, to renewable resources such as wind and solar energy with hydrogen storage is becoming a trend for both the industry and for governments. In fact, the greenhouse gas emissions must be reduced by 40% (from 1990 levels) and 32% of the energy resources used should be renewable by 2030, according to the European Commission[2]. Moreover, the European Union aims to be climate-neutral by 2050. This means that the general economy should have net-zero greenhouse gas emissions[3]. Following these guidelines, it is necessary to take into account sustainable insights and solutions for the final design. Although the aforementioned emission goals, environmental sustainability is not a stand alone factor for achieving a sustainable product. Sustainability can only be attained when there is balance between environmental, economic and social sustainability, as can be seen in Figure 11.1[4].

Figure 11.1: The three pillars of sustainability: economy, humanity and ecology.

This chapter ensures that the vehicle is sustainable enough to meet the regulation that are set for the future. For the environmental aspect, this will be done by a Life Cycle Assessment (LCA), that will be explained in section 11.1, section 11.2 and section 11.3. The results of this analysis, with sensitivity analysis of these results are presented in section 11.4 and section 11.5 respectively. Furthermore, the end of life solution are discussed in section 11.6. Also, the economical and social aspect regarding

[1] Gioietta Kuo. *When Fossil Fuels Run Out, What Then?* URL: https://mahb.stanford.edu/library-item/fossil-fuels-run/ (visited on 01/15/2021)
[2] European Commission. *2030 climate and energy framework*. URL: https://ec.europa.eu/clima/policies/strategies/2030_en (visited on 01/15/2021)
[3] European Commission. *2050 long-term strategy*. URL: https://ec.europa.eu/clima/policies/strategies/2050_en (visited on 01/15/2021)
[4] University of Tartu. *Introduction to environmental auditing in public sector*. URL: https://sisu.ut.ee/env-intro/book/1-1-sustainable-development (visited on 01/15/2021)

sustainability are described in section 11.7 and section 11.8. Lastly, in section 11.9, advise is given on possible approaches on how to increase sustainability for future design phases.

11.1. Goal and Scope Definition

Before defining the goal and scope of the assessment, it should be clear what a LCA is and why it should be performed.

11.1.1. Introduction to LCA

A LCA is a cradle-to-Gate approach which provides a better understanding in the environmental aspects of a product throughout its life cycle[56]. In this chapter, a LCA is performed on the personal air transportation vehicle that is designed. The LCA is performed in order to both identify (section 11.2) and quantify (section 11.3) the potential impacts of the life cycle of the product. This includes the impact of all processes during life from raw material extraction to transportation of goods to waste management. Although the LCA should theoretically cover every process, defining processes in such minuscule detail is beyond the scope of this design stage. Therefore, simplifications and assumptions, that will be explained in section 11.2 and section 11.3, are made for being able to perform the analysis with the available software.

11.1.2. Applied Software

OpenLCA is the software that is used for performing the LCA. The reason of this selection is simple, namely because this type of software is freely available for everyone. GaBi or Solidworks could also be used. Despite slightly more resources available compared to OpenLCA, the costs for both are significantly higher, hence these are not suitable for this analysis. OpenLCA features various well-known databases, such as ELCD, Ecoinvent and Environmental Footprints, which all contain enough data to perform the intended analysis.

11.1.3. Goal and Scope Definition

The use of fossil fuels in the automotive industry is a world wide problem, both regarding the manufacturing processes and the emissions during the operational phase. The batteries in the vehicle nullify the latter, i.e. the direct emissions during operation are almost zero and no use will be made of fossil fuels on board for combustion. It should be noted that the electricity used for powering the vehicle should come from renewable energy sources. However, indirect emissions will still be expelled during the manufacturing, assembling and transporting of all components, especially the batteries[5]. Thus, the indirect emissions and their possible reduction possibilities seems to play the crucial role throughout the life time of the vehicle. *The goal of this LCA is to identify the processes that have the largest impact on the environment, hence need to be improved or revised before the product comes onto the market.* When identified these so-called bottlenecks, suggestions will be provided to reduce the environmental impact of these processes. For the scope of the analysis, details of the product system that will be used, must be established for the preventing of false calculations, hence conclusions. These details are guidelines throughout the LCA and include the system function, functional unit and the system boundaries[56]. The system function consists of transporting a person safely from one place to the other in an urban environment, whereas the usage of a single vehicle throughout the estimated life time can be seen as the functional unit. The system boundaries that are being considered during this study are the following:

- The analysis includes the following steps of a product life cycle: raw material extraction, manufacturing and processing of the raw materials into parts or components, the packaging and production of the materials used for packaging, the transportation of the goods and components to plants and transport to the final assembling destination,
- As the LCA is performed based on a Cradle-to-Gate process, the End of Life (EOL) solutions will not be taken into account. Elaboration on those solutions can be found in section 11.6.

[5] Hans Eric Melin. *Analysis of the climate impact of lithium-ion batteries and how to measure it*. URL: `www.transportenvironment.org` (visited on 01/15/2021)

- The outcome of the LCA will be considered both for the life cycle of one functional unit, i.e. one vehicle, and for the estimated total number of vehicles that will be produced on average per year.
- The LCA is based on indirect emissions that arise from the usage of the product system, i.e. the vehicle.

The majority of the processes within a product system do have a MIMO (Multiple Input Multiple Output) structure. (Co-)product allocation is needed to divide the input and output flows to the desired and useful outputs. More information regarding allocation can be found in section 11.2[56].

11.2. Inventory Analysis

In this section, a description is given for all the material flows that are present in the product system. Focus is also laid on explaining the product system in more detail together with the corresponding assumptions and simplifications. The inventory analysis is the basis for the impact assessment performed in section 11.3.

11.2.1. Life Cycle Inventory Approach

For the Life Cycle Inventory (LCI) approach, the attributional modelling method is selected rather than the consequential modelling method. As the goal of the LCA is to identify emission bottlenecks in the production process of the vehicle, it is sufficient to only depict the potential impact of the product system on the environment, rather than identifying and subsequently anticipating on consequences of adjustments of processes on other processes, both in up- and downstream directions[57]. For this phase of the design, it is sufficient to perform a static analysis.

11.2.2. Inventory List

A next step would be to create an inventory list, based on the final design. Once all components and parts have been thoroughly selected or designed, their characteristics are needed for the LCA. Important features for those components are the mass, the material and the manufacturing method. In Table 11.1, the inventory list can be seen, with all the relevant information that will be needed to perform the LCIA. Based on this inventory, assumptions and simplifications will be applied to reduce the amount of detail that would be required in OpenLCA. Also, the relative short time available to both learn the software and performing the LCA is a limiting factor, hence a justification to simplify the following things already:

- Only the final mass of the components will be taken into account. No distinction is made regarding the quantity. For example, no difference in footprints exist between 8 motors having a mass of 32kg and 1 motor having a mass of 32kg.
- Some components have not been taken into consideration for the LCA. No data is found on the BMS, the connector, the USBCOM5 and the seat. Therefore, they are neglected for the LCIA. Moreover, the measuring instruments (Lidar sensor, IMU, Barometer and GPS) are not used throughout the LCA. This has three reasons, namely one being the fact that their mass is at least a factor 10 smaller than the other components. It is assumed that the contributions to the environment are small compared to others, even though the components are generally made from expensive materials and therefore more costly to produce. Also, the architecture of these measuring instruments are complex and consisting of many smaller units. Integrating these units into the LCA is beyond the scope of this design phase, both in intricacy and in time available. Lastly, none of these instruments are found in one of the available databases from OpenLCA

Based on the inventory from Table 11.1, a product system is made with processes that should be connected with each other. The essence of such a process depends on inputs, often coming from previous processes in sequential processes, and on output flows, that will be inputs for a possible next process. Even though a LCIA could be performed on a single process, the aim is to get results for the entire product system. To achieve this, a flow diagram is made and is shown in Figure 11.2. This diagram acts as both a starting point and a reference for performing the LCIA. Within Figure 11.2, the distinct colouring represents the different categories of the life cycle in question going from Cradle-to-Gate.

Table 11.1: Inventory used for performing the LCA

Department	Component	Mass [kg]	Material	Manufacturing method
Power	Battery cells	101.12	-	Provided by Sion Power
	BMS	0.592	-	Provided by MGM Compro
Propulsion	Propeller blades	9.72	Aluminium	Hot closed die forging
	Motors	32	-	Provided by MGM Compro
	Propeller hubs	2.8	Stainless steel	Low pressure die casting
Structures	Beams	5.712	Aluminium	Cold roll forming, welding
	Hinges	4.896	Aluminium	Hot closed die forging, drilling
	Battery casing	9.5	Aluminium	Electron beam welding
	Landing gear	24.43	Aluminium	Extrusion
	Wind shield	4.5	Glass	Make and temper glass
	Module frame	8.56	Aluminium	Extrusion
	Front and top skin	1.58	Aluminium	Rubber forming
	Back, left and right skin	4.06	Aluminium	Sheet metal forming
Other	Lights	-	-	LED production

To analyse the impact of the production of each component, the entire production systems analysed. It can be seen in Figure 11.2 that components such as motors and battery system only comprise of one process. These processes are stand alone system process hence do not require an input. For battery production, data set for Lithium metal battery production system is not available so the production system for lithium-ion battery is used. As both battery technologies have similar composition, hence this assumption can be justified. The battery production process take into account the fallowing steps: raw material acquisition, transpiration of raw material, pre-processing of raw material, manufacturing of all battery components and assembly of the battery packs including the battery management system. Similarly, the electric motor production process takes into account all processes from the raw material acquisition till the assembly of the motor. Furthermore transportation used during each step of the production system is also considered. For windshield production, two processes are used first the production of uncoated glass and then tempering of this uncoated glass to make safety glass. Production of uncoated glass takes into account: raw material production, transportation, electricity and infrastructure used for final production. Data for lamination process after tempering the glass is not available hence this process is not considered.

For all the components made from aluminium, production of aluminium ingots is used as the starting process. This process takes into account the acquisition of raw material for aluminium production, transportation of raw material, intermediate processes for aluminium production and formation of aluminium ingot. These ingots are then used for different parts manufacturing process. Each part manufacturing process also takes into account the transportation of ingots to the manufacturing facility and remelting of the scrap metal to be used again. Data for alloying of aluminium is not available hence production process of aluminium ingots of high purity is used.

For production of lights, data for high power single bulb is not available so production process of THT LED is used. Furthermore each light module consist of 10 THT LED's. A total of 10 light modules with 100 THT LED's are considered. The production process take into account all step from the acquisition of the raw materials till the assembly of the light module.

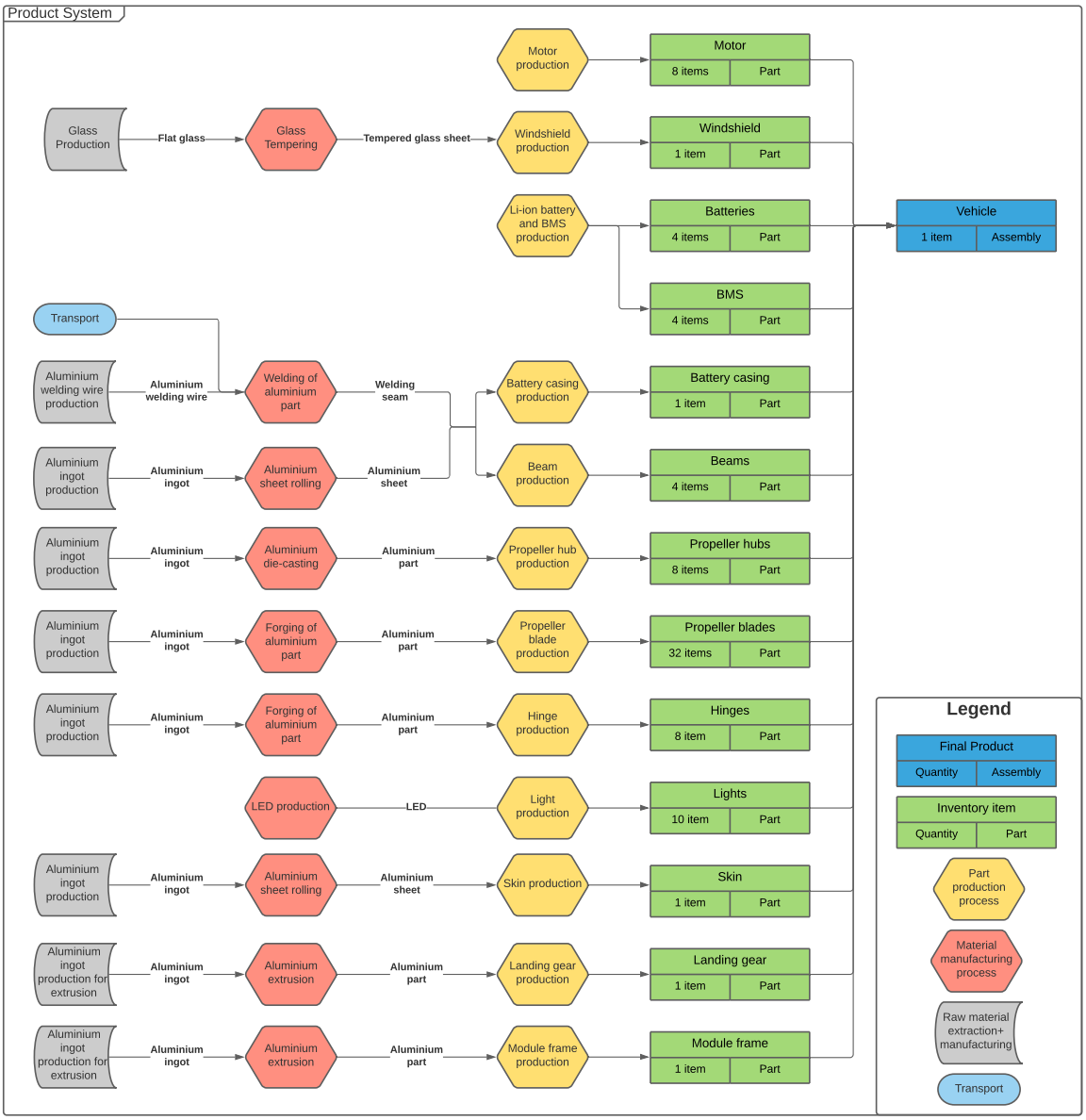

Figure 11.2: Flow diagram of the product system being studied including all relevant processes

11.3. Life Cycle Impact Analysis (LCIA)

The LCIA is generally seen as the most important segment of the LCA. In this section, the LCIA methodology will be explained followed by the results.

11.3.1. LCIA methodology

The LCI (section 11.2) should be thoroughly coupled with the generation and interpretation of the results. A Life Cycle Impact Assessment (LCIA) provides this missing link. LCIA translates emissions and resource extractions into a limited number of environmental impact scores[6]. Within OpenLCA, several LCIA methods are available. Use is made of the (Product) Environmental Footprints (PEFs). This method is developed by both the European Commission and European Council and was aimed to "establish a common methodology on the quantitative assessment of environmental impacts of prod-

[6]RIVM. *LCIA: the ReCiPe model*. URL: `https://www.rivm.nl/en/life-cycle-assessment-lca/recipe` (visited on 01/16/2021)

ucts, throughout their life-cycle[7]." The PEF database covers many categories that are important for the life cycle, namely agricultural products, energy carriers and technologies, materials production, systems and transport services[8]. Although EOL treatment is also a category of this database, it will not be used for the analysis as the Cradle-to-Gate cycle is considered and the goal is to identify possible environmental impact bottlenecks for the production. All rights from the datasets go to the following providers: European commission, Thinkstep, Quantis, CEPE ecoinvent, Ecoinvent, Fefac, Cycleco and RDC[58]. The PEF LCIA is a so called Mid-point indicator. Those midpoints give more information about single environmental impacts, whereas End-point indicators give the impact on a higher level, hence less detailed[9]. It is desired to gain knowledge about specific environmental impacts and analyse how they change with varying the inputs. For this reason, a Mid-point analysis is preferred, rather than an End-point analysis.

11.3.2. Environmental Potentials

In total, 19 environmental indicators can be analysed using PEF. However, not all indicators are an area of interest. The Global Warming Potential (GWP) is subdivided in three categories, namely biogenic, fossil and land use global warming. The summation of the three will be used as an indication for GWP. The Acidification Potential (AP), freshwater Eutrophication Potential (fEP), the Ozone Depletion Potential (ODP) and the Human Toxicity Potential (HTP) have already been defined as important parameters in the Midterm Report[12]. Moreover, the freshwater Ecotoxicity Potential (fETP), Land Use Potential (LUP). Water Scarcity Potential (WSP), the Fossils Resource Use (FRU) and the Photochemical Ozone Formation Potential (POFP) are particularly interested. These indicators will be used to quantify the environmental impacts and this can be used as a reference for the sensitivity analysis in section 11.5. An overview of all the used indicators with their definition and units is given in Table 11.2 and Table 11.3 [58].

Table 11.2: Environmental potentials that are used in the LCIA with their definition and unit type 1/2

Impact Category	**Definition**	**Unit**
GWP	Defines how much energy from 1 kg of a certain greenhouse gas will be absorbed by the atmosphere, relative to the emissions of 1 kg of CO_2[59].	kg CO_2 eq.
AP	Potential that is based on the contributions of SO_2, NO_x, HCl, NH_3 and HF to the potential acid deposition, such as acid rain. The AP is expressed in 1 kg of gas contribution compared to 1 kg of $SO2$[59].	mol H+ eq.
fEP	Potential that is based on the contribution of phosphorus atoms to the environment, which can cause over-fertilisation of water. The fEP is expressed in environmental impact of 1 kg of substance compared to 1 kg of P[59].	kg P eq.
fETP	Potential that is based on the effect of chemicals on organisms that are living in the water. The fETP is expressed in Comparative Toxic Unit for aquatic eco-toxicity. The CTUe is calculated by multiplying the potentially affected fraction of species over a period of time with the freshwater volume with the mass of chemicals emitted[a].	CTUe
ODP	Potential that is based on the contribution of the so called CFCs to the depletion of the ozone layer. The ODP is expressed relative to the depletion potential of CFC-11[59].	kg CFC-11 eq.

[a] Laura Golsteijn. *How to Use USEtox Characterisation Factors in SimaPro*. URL: https://pre-sustainability.com/articles/how-to-use-usetox-characterisation-factors-in-simapro/ (visited on 01/19/2021)

[7] European Commssion. *Environmental Footprint pilot phase*. URL: https://ec.europa.eu/environment/eussd/smgp/policy_footprint.htm (visited on 01/19/2021)

[8] European Commssion. *Environmental Footprint pilot phase*. URL: https://ec.europa.eu/environment/eussd/smgp/policy_footprint.htm (visited on 01/19/2021)

[9] RIVM. *LCIA: the ReCiPe model*. URL: https://www.rivm.nl/en/life-cycle-assessment-lca/recipe (visited on 01/16/2021)

Table 11.3: Environmental potentials that are used in the LCIA with their definition and unit type 2/2

Impact Category	Definition	Unit
LUP	Potential that is based on using, occupying, reshaping and destroying natural land for human purposes. The LUP is measured in point, which is the smallest unit of measure and used for measuring size[60].	pt
WSP	Potential that is based on the amount of water that is being used to dilute toxic elements emitted into the water. The WSP is expressed as the number of cubic meters of water that is used[a].	m3 water eq.
FRU	Potential that is based on the depletion of natural fossil fuel resources and is expressed in the amount of MegaJoules that is used[b].	MJ
HTP	Potential that is based on the contribution of gases, which are toxic for human beings (both gases that can cause cancer and gases that cannot cause cancer). The HTP is expressed in Comparative Toxic Unit for human beings (CTUh, 1.4-dichlorobenzene)[59].	CTUh
POFP	Potential that is based on estimating airborne particles for forming atmospheric oxidants. It is also being known as an indicator that estimates the ozone depletion near the earth surface, where-after smog can arise. The POF is expressed in kg Non Methanic Volatile Organic Compounds, i.e. in kg NMVOC[61].	kg NMVOC eq.

[a] Luc Hillege. *Impact Categories (LCA) – Overview*. URL: `https://ecochain.com/knowledge/impact-categories-lca/` (visited on 01/19/2021)

[b] Luc Hillege. *Impact Categories (LCA) – Overview*. URL: `https://ecochain.com/knowledge/impact-categories-lca/` (visited on 01/19/2021)

11.3.3. LCIA results

Combining the process diagram for all the components in Figure 11.2 together with the impact categories mentioned in Table 11.2 and Table 11.3, the LCIA can be performed. OpenLCA gives the environmental footprint results for all the different processes, based on their mass, material and production process. Those production processes are traditional productions methods, hence no sustainable processes have been used. This has been done for two reasons, first of all within the datasets from OpenLCA, almost no data was available on sustainable production processes. It is neither useful nor equivalent to compare apples and oranges. For this reason, the old fashioned processes are used as all the parts can be inserted into the program. Then second, comparing similar processes (apples and apples), a valid product system can be made, on which bottlenecks can be easily found and production alternatives for those severe impact processes can be established. This is done in section 11.4.

Table 11.4: Results of the Cradle-to-Grave impact analysis for the vehicle.

Impact Category	Reference Unit	Li-ion Batteries	Electric Motors	Other Components	Total
GWP	kg CO2 eq.	787.45	123.27	919.26	**1829.99**
AP	mol H+ eq.	12.75	1.90	3.65	**18.30**
fEP	kg P eq.	2.33	0.31	7.47E-03	**2.66**
fETP	CTUe	1158.56	194.32	63.12	**1416.00**
ODP	kg CFC-11 eq.	4.69E-05	5.92E-06	3.12E-07	**5.31E-05**
LUP	pt	6799.77	771.71	3294.57	**10866.05**
WSP	m3 water eq.	372.58	53.55	87.75	**513.87**
FRU	MJ	6549.01	625.84	13396.18	**20571.03**
HTP	CTUh	6.3E-04	1.2E-04	4.26E-05	**7.92E-04**
POFP	kg NMVOC eq.	3.97	0.65	1.73	**6.35**

The results in Table 11.4 are for the entire product system described in Figure 11.2. All the components and processes have been taken into account. Three groups are made to analyse the results, namely the environmental impact from the Li-ion batteries, from the electric motors and from other com-

ponents. These other components can again be found in Figure 11.2. Generally, the potentials for the latter group is (much) smaller than for the first two groups. There is no need to analyse the contribution of each (component) process separately as they are small compared to the contribution of the batteries and motor. A closer look on the results in combination with interpretation can be found in section 11.4.

11.4. Interpretation and Discussion of Results

In this section, a more detailed look over the results are given, together with interpretation. Next, an answer with discussion regarding the goal stated in section 11.1 will be provided. Lastly, alternatives will be given to avoid those bottlenecks.

11.4.1. Interpretation and discussion of Results

Looking more adjacent to the results of the different groups in Table 11.4, some remarks can be made. As the group consisting of the remaining components gives not a clear view on the single components contributions, this group has to be compared to the first two groups. Only then one can identify if it is needed to further investigate the impact contribution of single components. For the AP, the production of the batteries contributes 3.5 times as much to the impact, compared to all the other components together. For the fEP, fETp, ODP, LUP, WSP, HTP and POFP, computed that the batteries contribute 311.9, 18.4, 150.3, 2.1, 4.2, 14.7 and 2.3 times more than for all the remaining components. Therefore, it will be assumed that for those impacts the battery production is the limiting process and the contribution of single components does not have to be considered. However, for two impact categories, namely for the GWP and for the FRU, the impact for the other components is significantly larger then for the batteries and motors. Hence, it is worth to dive deeper into the contribution of the single components to the impact category. In Figure 11.4 and Figure 11.3, the impact contributions of the other part production processes can be seen.

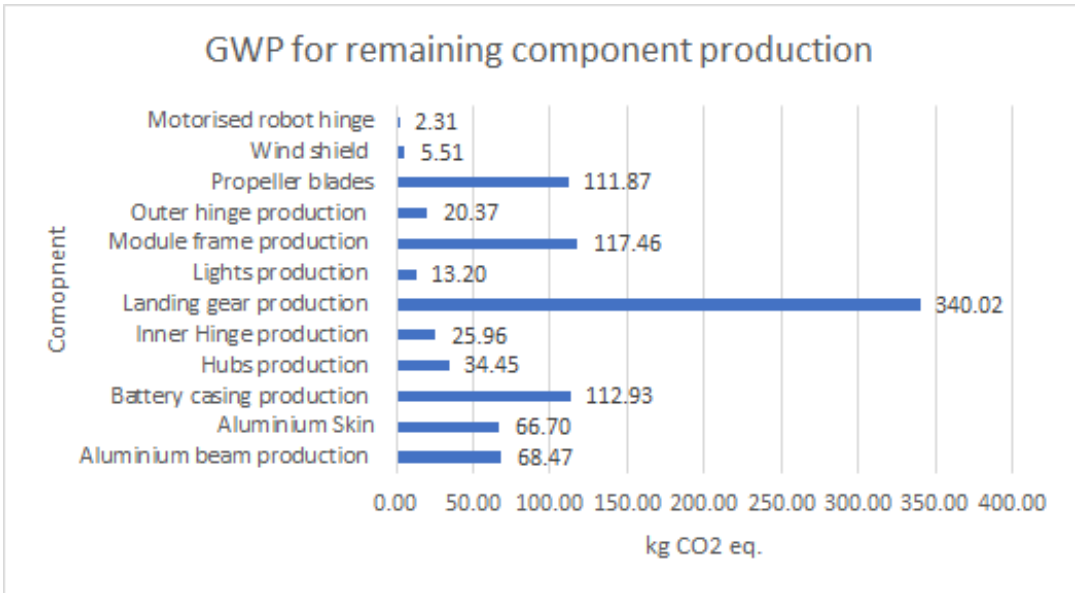

Figure 11.3: GWP for the specified single components that are part of the group 'Other Components'

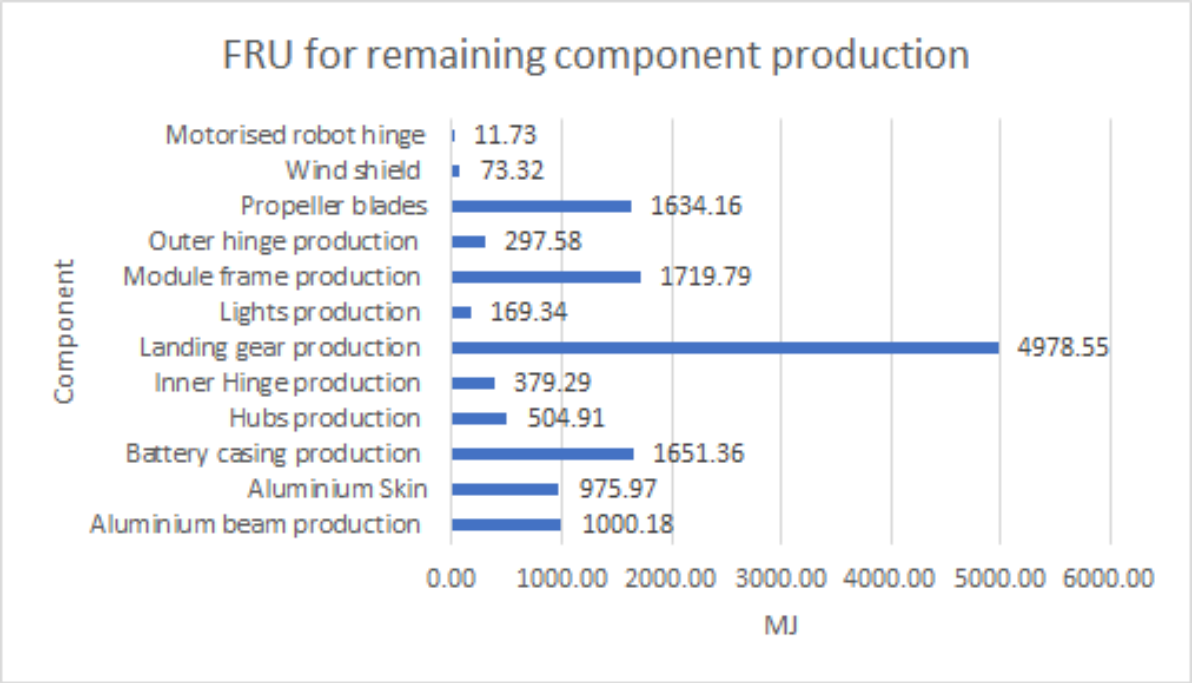

Figure 11.4: FRU for the specified single components that are part of the group 'Other Components'

Comparing the battery and motor production, the battery production has the highest GWP and FRU impact. If the results from Figure 11.3 and Figure 11.4 are studied, the landing gear comes out to be the main bottleneck together with the battery production process. The GWP for the battery production is still 2.3 times bigger than for the landing gear production. Moreover, the FRU for the battery production is 1.3 times bigger than for the landing gear. Coming back to the goal of the LCA, the bottlenecks are found for the product system. By far, the battery production process has the largest impact on the different aspects of the environment, compared to other components. From the remaining components, the landing gear production does have a relative large impact contribution. Alternatives should be found to avoid these bottlenecks and eventually the environmental footprint should be reduced compared to the initial results (Table 11.4).

11.4.2. Comparison with Competitors

The results presented in the previous section can be used to compare the rent-a-copter with other competitive vehicles that are currently onto the market. Unfortunately, other air transportation vehicles can not be used for comparison as almost no data is available due to the new and competitive niche market. Moreover, (big) drones will not be used as too as their mission is different that for the rent-a-copter. Conventional and electric cars do bring people from A to B in an urban environment, hence they are more suitable for comparison. In Table 11.5, the GWP from rent-a-copter is shown together with the average GWP of a conventional and electric car. The reduction in GWP is also given when is switched from one of the two classic transportation types to the newer rent-a-copter transportation.

Table 11.5: The rent-a-copter compared to other competitive urban transport types.

Vehicle	GWP	Unit	Reduction GWP rent-a-copter w.r.t. the other vehicles
Rent-a-copter	60.6	Kg CO2 eq per km	-
Conventional Car	252		76%
Electric Car	150		52%

Obviously, a comparison that is fully consistent can never be made. Comparing something that flies to something that rides, something that transports human beings to something that transports goods or something that weights 300kg to something that weights 1000kg, can never be fully covered. However,

with some assumptions and clearly stating the differences within the comparison, the results can be considered valid enough for this phase of the design. Firstly, for the two types of urban transports used in the comparison, the life time of the vehicles is taken as 10 years. For electric car it is assumed that the life time of the battery is equal to life time of the car, hence a single battery is used during the entire life time. This can not be assumed for rent-a-copter as it is required to change the battery after 2 years as mentioned in subsection 5.4.5. For this reason the environmental impact of a total of 5 batteries are taken into account for the life time of rent-a-copter. For conventional cars, environmental impact of production of car and tail pipe emissions are taken into account. Furthermore, for electric cars the environmental impact of production of car and the production of electricity used throughout the life time of the car is taken into account. For rent-a-copter the environmental impact of production of vehicle and the production of electricity through wind energy is taken into account. The assumption of electricity production through wind energy is in line with the requirement PAT-UR-SUST-07 which states that the energy used by the system shall be generated by sustainable means. The impact of electricity generation is modelled in OpenLCA, which subsequently adds this to the total LCA of rent-a-copter. By underlining the differences in LCA models of the competitive transport types and making justified assumptions to remove the differences present it is made sure that a fair comparison can be made.

11.5. Sensitivity Analysis

Sensitivity analysis is performed to check the influence of bottleneck components, as mentioned in section 11.4, on the GWP. The analysis is done using OpenLCA, where the mass of components under investigation are changed to give the resulting output environmental impacts. As it can be seen in Figure 11.5 the percentage mass of each component is decreased and is plotted against the percentage reduction in the total GWP. It can be seen that the influence of mass reduction of each component on GWP is linear. This can be attributed to the fact that LCA for each component is done relative to a standard mass of that component, so change in mass has a linear influence.

Figure 11.5: Influence of weight reduction of components on total GWP

A reduction in 21.5% in total GWP can be achieved by a reduction of 50% battery mass. For landing gear and motor a reduction in 50% mass leads to a reduction in 9.3% and 3.4% of GWP respectively. Hence it can be concluded that battery system has the highest influence on the total GWP. As the battery system and motor system are fixed for the mission requirements so it can not be altered. For this reason the end of life solutions for these system is the only way the environmental impact can be

decreased. For landing gear production, the GWP production can be decreased by 92% if ingots made from recycled aluminium are used instead of high purity first stage aluminium. This decision can have adverse impact on the performance of the landing gear which can be assessed in detail in the later stages of the project.

11.6. End of Life Solutions

As mentioned in section 11.5 end of life solutions are important to reduce the environmental impact of not only complex components such as battery and motors but also simple components such as landing gear. For end of life solution at this point, recycling of the components is considered.

Lithium batteries are recycled in three ways; physical dismantling, hydrometallurgy and pyrometallurgy. At a battery pack level physical dismantling is used to remove metals from the casing and cell connections. Furthermore, in hydrometallurgy the materials present in the battery are selectively dissolved in a chemical solvent so the metals can be separated in a leachate and removed. This process can be used alone or it can be used with the combination of pyrometallurgy to increase the efficiency of the metal removed. Both processes are relatively cheap as they do not require high cost equipment. Using these processes around 4.8kg of material can be recycled from a 8kg battery pack. This gives lithium batteries a recycling percentage of 60%[62]. The materials recycled includes aluminium, steel, copper, nickel, polypropylene and lithium.

For recycling of permanent magnet DC motor first rotor, stator, windings and magnets are disassembled. These disassembled parts are then sorted to separate parts containing only metals and parts containing both metals and rare-earth magnets(NdFeB)[63]. The disassembled parts containing only metals are either reused directly or are melted to be used as a raw material. Parts that contain both metals and rare-earth magnets are first shredded and then sorted to remove different materials. Using this method 93% of the motor material can be recycled or reused. Materials recovered using this recycling method includes, electrical steel, non-electrical steel, aluminium, copper and rare-earth magnets[63].

Rest of the components are made from aluminium alloy and can be melted to make aluminium ingots which can then again be used to make parts. Almost 95% of the aluminium can be recycled. As mentioned in section 11.5 using these recycled ingots the GWP can be decreased by almost 92%. Using the end of life solutions mentioned 61% of the material can be recycled or reused.

11.7. Economic Sustainability

As mentioned in the introduction of this chapter, not only the environment is needed to achieve sustainability. The economical aspect of the product needs to be assessed as well. This will be done qualitatively rather than quantitatively as has been done for the environmental part. Economic sustainability can be viewed from two different perspectives, which both will be assessed for the Rent-a-copter in question.

The first consideration is referring to the continued success of the Rent-a-copter over a certain period of time, i.e. how successful will the vehicle be in the future[10]. This potential is mainly dependent on two factors, namely the competitors that are and will be on the market and the features of the product in combination with the return of investment. As described in chapter 2, it is important to identify the gap in the market in order to act according this missing gap. This will enhance the economic sustainability, because investing in a product that is already on the market is simply not worth it. High constant costs are needed to join this niche market and it is even more ambitious to make profit over a period of time as first the costs need to be covered. However, the marking gap discovered in chapter 2, namely the personal, renting aspect, makes it for investors more attractive to invest as this product can generate and take the lead in this new niche market. Moreover, features of the design make it also interested to invest money in, such as modularity of components and the small size. The fact that parts can be easily replaced when failure occurs, makes it an interesting product for the long term.

Secondly, economic sustainability can be seen as the economic development that does not influ-

[10] Jane Courtnell. *Economic Sustainability For Success: What It Is And How To Implement It*. URL: `https://www.process.st/economic-sustainability/` (visited on 01/24/2021)

ences the environmental or social sustainability negatively[11]. If rent-a-copter appears to be a success, the production of the vehicle will increase as the demand for more vehicle will increasing. Although this scale in manufacturing is often seen as attractive, to make more profit, cautiousness should be taken as scaling goes hand in hand with more emissions being emitted. Therefore, manufacturing methods shall be chosen, where an increase in production does not proportionally lead to a larger environmental footprint. Besides, the increase in economic welfare should not lead to negligence of social aspects within a company. When the return of investment is achieved, explained in section 15.3, the salary of the people directly involved should rise together with the increase in profit. In this way, the workers are motivated to accomplish more ambitious goals in the future and thrive the rent-a-copter.

11.8. Social Sustainability

The last category of sustainability that needs a closer look is the social sustainability. Social sustainability is directly related to the impact of the design process and the final product on the community it operates in. This includes all engineers working on the project, everyone working in corporations and customers which includes rental companies and passengers[12]. For the users of the rent-a-copter, safety and comfort are of importance. Safety can be assured by protecting the user against environmental conditions and by informing about the possible risks during flight and how these risks have been mitigated. More on this can be found on the risk analysis, which is present throughout the entire report. Also the comfort within the vehicle is a dominant factor in the early stages of the rent-a-copter. One does not want to have physical complaints after flight, resulting in atrocious reviews. More on safety and reliability can be found in subsection 12.5.1 and subsection 12.5.4. The product should be easy to access and also the waiting times should not be too long, hence the availability (subsection 12.5.2) is a relevant factor. For the ground personnel that are performing the maintenance and part of the assembling, rules should be made to protect them from potential dangerous situations during those processes, which is further discussed in subsection 12.5.3. Furthermore, the noise of the vehicle should also be taken into consideration. Noise disturbance is extremely annoying and it is undesired that bystanders do to get hearing damage. As the noise requirement of 75dB is achieved, no hearing damage will occur and the vehicle can be seen as socially sustainable in that area[12].

11.9. Future Recommendations

In the beginning of this chapter, the goal of the LCA was determined. In the followed sections, a methodology and the steps are discussed before performing the LCA. Then, the results give enough information regarding the objective in section 11.1. The bottlenecks, namely the battery and the landing gear, have been identified. These components have the biggest impact on the environment and a mass reduction would lead to significant savings in emissions. Both the economic and social sustainability have been discussed as well, leading to the general assessment of sustainability for the rent-a-copter.

Rent-a-copter can be seen as a sustainable product in all the three aforementioned categories. To travel one kilometer with the vehicle, the total emissions exhausted, both indirect and direct, are less than for a conventional and electric car. It is a fast and quiet solution for ever increasing urban traffic congestions, making it socially sustainable. Lastly, the new niche market of this personal, rental air transportation transport vehicle makes it interesting and worthy to invest money in, hence being economic sustainable too. A balance of the three categories results in a sustainable product, which is for now being achieved.

Despite the rent-a-copter being sustainable enough for the current market, the environmental regulations are becoming stricter every year, making the vehicle perhaps not sustainable enough for the future market. Therefore, extra (future) analysis is ought to be performed in order to ensure that the rent-a-copter will be sustainable in the future and be more competitive on the market. This includes the following points:

- The LCA in this report was performed to identify bottlenecks in the production of the rent-a-copter. Although these bottlenecks have been found and the LCA was performed successfully, possible

[11] KTH. *Economic sustainability*. URL: `https://www.kth.se/en/om/miljo-hallbar-utveckling/utbildning-miljo-hallbar-utveckling/verktygslada/sustainable-development/ekonomisk-hallbarhet-1.431976` (visited on 01/25/2021)

[12] Centers for Disease Control and Prevention (CDC). *What Noises Cause Hearing Loss?* URL: `https://www.cdc.gov/nceh/hearing_loss/what_noises_cause_hearing_loss.html` (visited on 01/25/2021)

alternative manufacturing processes for those bottlenecks should be investigated. Subsequently, a new LCA should be performed to investigate and prove that the influence of the new processes have a positive effect on the environmental potentials, hence reduce the general environmental footprint of the vehicle.

- Some simplifications and assumptions have been made for some components of the vehicle due to the database limitations in OpenLCA. A next analysis could include these components with more detail, hence obtaining more reliable results than with simplifications.
- The comparison with other vehicles is based on the emissions of a vehicle in its entire life cycle. However, as already mentioned in subsection 11.4.2, it is not possible to fairly compare different vehicles with different purposes. A subsequent analysis could include an identical LCA, based on similar simplification, if present, on the three vehicles, namely the rent-a-copter, a conventional and electrical car. After the results have been gathered, the numbers should be normalised to get a better insight in the differences in EF for all the vehicles. Comparison could be made on the basis of the environmental footprint per kW of power, per kWh of energy, per kg of mass or per km driven.
- The social sustainability has been qualitatively described. Further analysis could be done to quantify the various influences of the rent-a-copter on human beings. A human development factor could be introduced and this factor can then be used to compare the rent-a-copter with other vehicles.
- Lastly, use is made of rather traditional production processes. The main reason for this is that these processes are available in OpenLCA. A next analysis could focus also on alternative manufacturing processes, such as additive manufacturing.

12
Final Design

12.1. Requirement Compliance

Now that there is a final design, it is important to look back and see if it meets all the requirements. In an elaborate process at the start of the project from the customer needs, a list of requirements was set up. The final design should adhere to all these requirements in order for the team to deliver a successful concept to the customer. The list of requirement along which the final concept was designed is presented in section 3.2. In Table 12.1 all requirements are presented with their ID and checked for compliance.

Table 12.1: The Requirements Compliance matrix

Requirement ID	Complied with	Compliance proof	Requirement ID	Complied with	Compliance proof
PAT-UR-PERF-04	Yes	section 5.6	PAT-SYS.S-FUNC-02	Yes	section 6.6
PAT-UR-PERF-03	Yes	subsection 6.7.3	PAT-SYS.S-FUNC	Yes	chapter 6
PAT-UR-PERF-02	Yes	section 12.2	PAT-SYS.S-CONS-05	Yes	chapter 6
PAT-UR-PERF-12	Yes	section 9.4	PAT-SYS.S-CONS-04	Yes	chapter 6
PAT-UR-PERF-08	Yes	subsection 8.7.4	PAT-SYS.S-CONS-03	Yes	chapter 6
PAT-UR-05	Yes	section 9.5	PAT-SYS.P-FUNC-01	Yes	section 9.8 section 9.7 chapter 10
PAT-UR-01	Yes	chapter 9	PAT-SYS.P-FUNC-02	Yes	section 5.4
PAT-SYS.O-FUNC-02	Yes	section 5.7	PAT-SYS.O-FUNC-01	Yes	section 9.8 subsection 11.2.2
PAT-SYS-FUNC-10	Yes	subsection 13.2.3	PAT-UR-SUST-03-01	Yes	chapter 5
PAT-SYS-FUNC-03	Yes	section 3.1	PAT-SYS.O-CONS-04	Yes	section 9.8
PAT-SYS-CONS-05	Yes	subsection 11.4.2	PAT-SYS.O-CONS-02	Yes	chapter 13
PAT-SYS.O-CONS-03	Yes	section 9.7 section 9.8	PAT-SYS.O-CONS-01	Yes	section 9.5
PAT-SYS-FUNC-16	Yes	section 12.2	PAT-SYS.C-FUNC-11	Yes	subsection 8.7.4
PAT-UR-SUST-07	Unknown		PAT-SYS.C-FUNC-10	Yes	subsection 8.4.1
PAT-UR-SUST-01	Yes	section 5.5	PAT-SYS.C-FUNC-09	Yes	section 8.6
PAT-UR-SAFE-06	Yes	section 6.6	PAT-SYS.C-FUNC-07	Yes	section 8.6
PAT-UR-SAFE-07	Yes	section 6.6	PAT-SYS.C-FUNC-03	Yes	subsection 8.4.1 section 9.3
PAT-UR-SAFE-08	Yes	section 6.6	PAT-SYS.C-FUNC-01	Yes	subsection 8.7.4
PAT-UR-SAFE-04	Yes	See subsection 12.5.3, section 5.4	PAT-SYS-PROD-04	Yes	section 11.6
PAT-UR-SAFE-01-02	Yes	section 9.3	PAT-SYS-PROD-03	Yes	chapter 14
PAT-UR-SAFE-01-01	Yes	section 9.3	PAT-SYS-PROD-01	Unknown	
PAT-UR-PROD-01	Yes	chapter 15	PAT-SYS-FUNC-23	Yes	section 3.1
PAT-UR-PERF-13	Yes	section 5.7	PAT-SYS-FUNC-22	Yes	section 9.1
PAT-UR-PERF-12-02	Yes	section 9.4	PAT-SYS-FUNC-20	Yes	chapter 5
PAT-UR-SAFE-09	No		PAT-SYS-FUNC-19	Yes	chapter 13
PAT-UR-PERF-09	Yes	section 5.4	PAT-SYS-FUNC-18	Yes	section 3.1
PAT-UR-PERF-06-02	Yes	section 3.1section 9.1	PAT-SYS-FUNC-12	Yes	section 5.6
PAT-UR-PERF-06	Yes	subsection 6.7.2	PAT-SYS-FUNC-09	Yes	section 3.1
PAT-UR-PERF-05	Yes	section 5.2, section 5.6	PAT-SYS-FUNC-02	Yes	section 8.4
PAT-UR-PERF-01	No		PAT-SYS-FUNC-01	Yes	section 3.1
PAT-UR-COST-01-01	Unknown	subsection 15.1.1	PAT-SYS-CONS-03	Yes	section 9.7
PAT-UR-COST-01	No		PAT-SYS-CONS-04	Yes	subsection 8.7.4
PAT-UR-07	Yes	section 9.7	PAT-UR-SAFE-06	Yes	section 9.5
PAT-UR-06	Yes	Figure 12.1	PAT-SYS-PROD-04-02	Yes	section 11.6
PAT-UR-04	Yes	section 9.1section 9.5	PAT-SYS-PROD-08-01	Unknown	
PAT-UR-02	Yes	chapter 9	PAT-SYS-PROD-08-02	Yes	section 6.1
PAT-SYS-PROD-08-03	Yes	section 5.4			

Some of the requirements are not complied with. PAT-UR-SAFE-09 is the first one and the team found out for such a device it is not feasible to make it self-desinfecting. The final design is not a completely closed structure, so airflow is possible in the structure. Also in the operation it is more feasible to have the vehicle cleaned by ground staff, than add a complex self-desinfecting system. PAT-UR-PERF-01 was partially not met. The system is able to transport 1 person, however it is not ideal to transport a baby too. The luggage compartment ended up below the user seat so the vehicle has no specific area designated for a baby to come aboard. PAT-UR-COST-01 PAT-SYS-PROD-01 and PAT-SYS-PROD-08-01 are requirements where it could not be determined if it was met. In the selection for manufacturing process for parts, the most sustainable options were selected, but to gain a good insight on how sustainable the total system manufacturing process is, a more elaborate analysis is necessary and information would be necessary that cannot be obtained at this stage of the design. For example

depending on where the vehicle factory will be located, the building's electricity could be renewable energy or whether the packaging material will be made from recycled materials, this cannot be said at this stage.
In the current cost analysis the development cost of the system is included, but the breakup of development cost is not. Therefore PAT-UT-COST-01-01 can not be checked for compliance, as this cost breakdown will be defined later. For PAT-UR-SUST-07 also it is not possible to determine what energy provider will be contracted for the charging stations. This is something outside of the scope of this phase of the development process.

12.2. Mass Budget

A mass budget had been set up to guide the sizing process of the vehicle and to give an overview of the distribution of mass in the finished product. The final mass budget can be found below in Table 12.2

Table 12.2: The mass budget for the final vehicle configuration

Component	Mass [kg]
Contingency	17.4
Main motors	30.4
Battery	100.2
Landing gear	24.43
User + Luggage	110
ACDS and Sensors	2
Flight computer	2
Seat	7
Cabling	2.5
Wind shield	4.5
Propellers	5.76
Load-carrying battery casing	9.5
Battery auxiliary systems	9.5
Propeller connection beam	5.71
Vehicle skin	5.64
Hinges and connectors	4.9
Vehicle frame	8.56

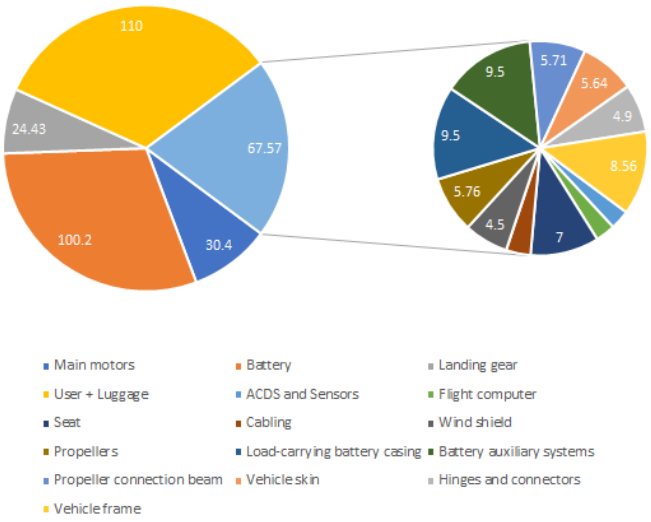

12.3. Vehicle Systems

In this section, an overview of several systems that are present in the vehicle is given. These systems are crucial during the operation, hence an elaboration can not be omitted. First, the electrical system will be explained, followed by the data handling system. Also, the hard- and software systems will be described.

12.3.1. Electrical Power System

Figure 12.1 shows the Electrical Block Diagram (EBD) for the vehicle. It is subdivided into various categories, as can be seen by the indicated colouring. The grey boxes represent the power supply system. The power for the entire vehicle will be provided by two battery types, namely the propulsion system battery pack and the auxiliary battery pack. The first mentioned will generate the power for both the BMS and the propulsion system through the motor controllers. The BMS needs electricity in order to provide power for the cooling fans in the battery packs. Besides, the small fans need to be actively controlled by the BMS. On the other side, the motor controllers are controlling the rpm and torque of the motors, which on their means convert the electricity into mechanical energy for driving the propellers. As already mentioned, the motor controllers and motors are perfectly coupled, i.e. custom made by MGM Compro for the mission. More information regarding the motors and batteries can be found in section 5.2 and section 5.4, respectively. The light blue boxes represent the power control components. These components regulate the voltage for the desired instruments (modulators) and motors (motor controllers). The propellers are driven by the electrical energy from the motors and are presented by the

dark blue boxes. Then, the power that is being modulated by the modulator is needed for 4 categories. The first category is related to structural features, namely that power is needed for the interrogater (data acquisition system), which allows the reading of a sensor network, such as strain gauges[1]. Moreover, electric motorised robot hinges are needed for one of the folding directions of the beams, hence they need electricity. Secondly, for the yellow system, several instruments are present in the vehicle that should provide the user with flight information, namely position, speed, altitude and navigation. GPS, IMU, Lidar Sensor and the barometer will provide this information. The latter three are working on a comparable voltage level and are therefore integrated together on a board package, whereas GPS has it own board and separate power supply. The processor receives the input from the boards and processes it. Therefore, electricity is needed too. although the red boxes have the same function as the yellow boxes, they are only being used if the instruments during flight fail. The instruments on the mobile device are back ups in case of failure or malfunction. Lastly, other instruments, such as lights, the flight computer and a back up flight computer, need power. These instruments are coloured orange. The communication system, consisting of a radio, should also receive electricity to communicate with the ground or with other vehicles.

12.4. Configuration/external lay-out

On the next 2 pages, the technical drawings of the system can be found. The first one is the deployed state of the system, the second one is for the retracted state of the system. These drawings only include the most important dimensions which are relevant to the public space.

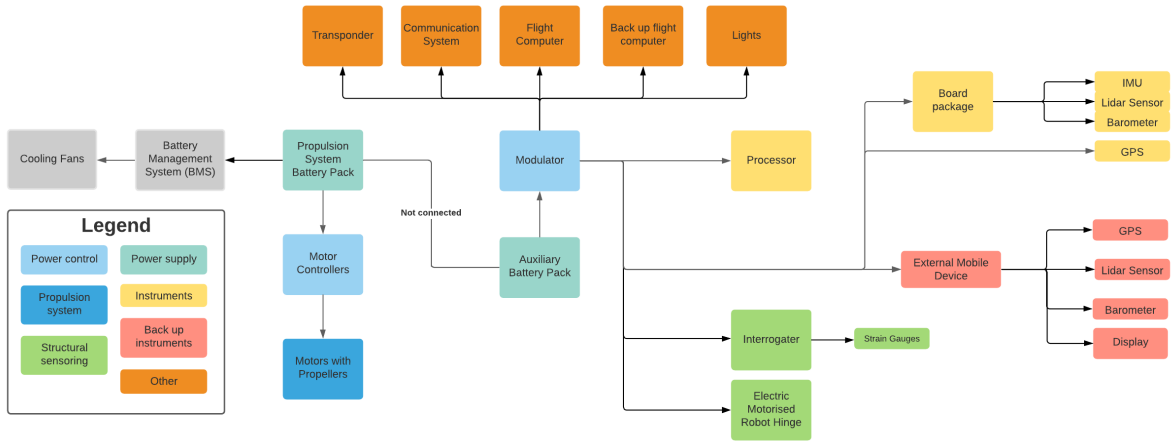

Figure 12.1: Electrical block diagram of the electrical power system

12.4.1. Data Handling System

The data handling diagram of the system is presented in Figure 12.2. The data handling within the system is enclosed in the square shape and the primary control computers are further detailed at the top of the diagram.

[1]HBM. *Optical Interrogators and Data Acquisition Modules*. URL: `https://www.hbm.com/en/2322/optical-interrogators/` (visited on 01/18/2021)

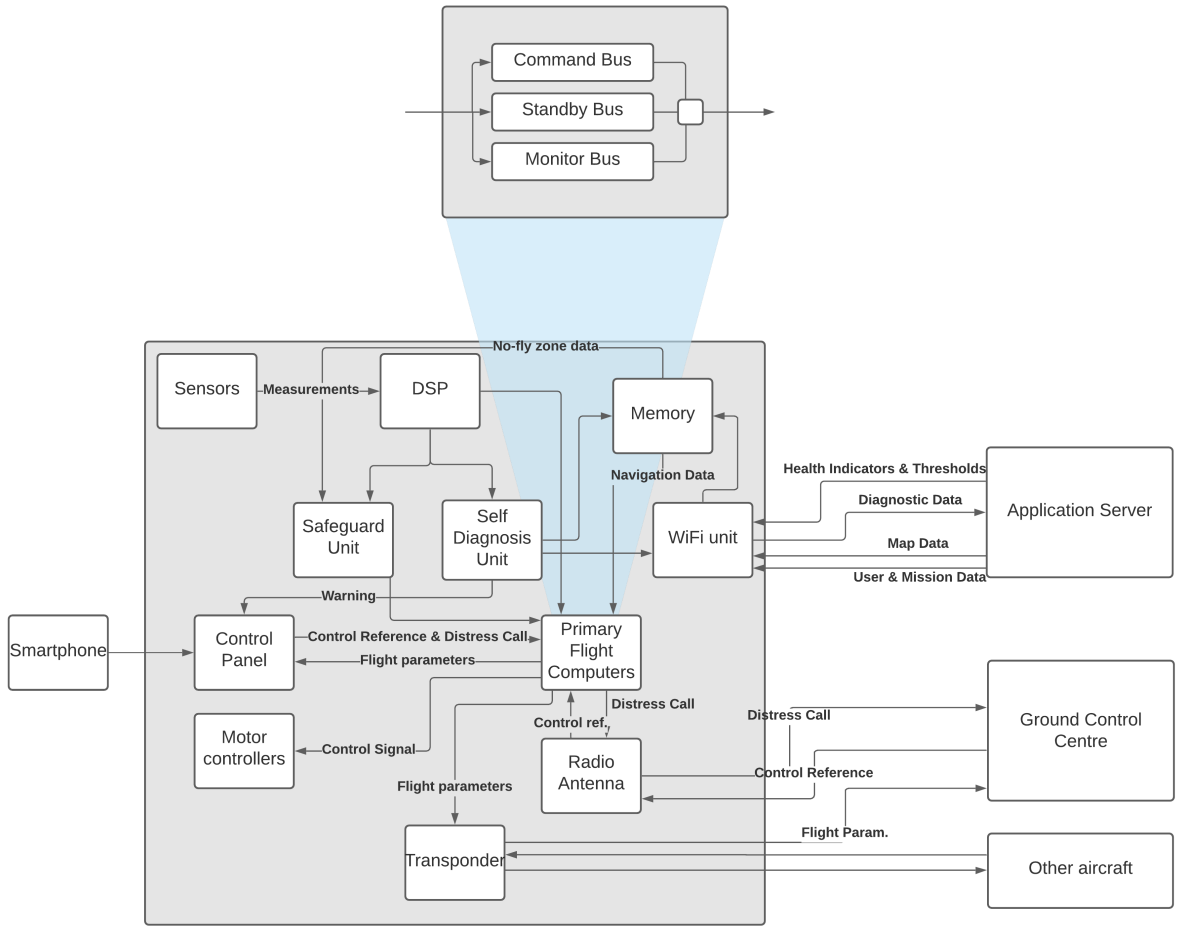

Figure 12.2: The data handling diagram of the vehicle, including its interactions with other systems.

12.4.2. Hardware and Software Systems

The final system features various hardware and software components. Figure 12.3 shows the hardware diagram of the system, including both components and their interactions. A similar diagram can be made for the software of the system. This is presented in Figure 12.4.

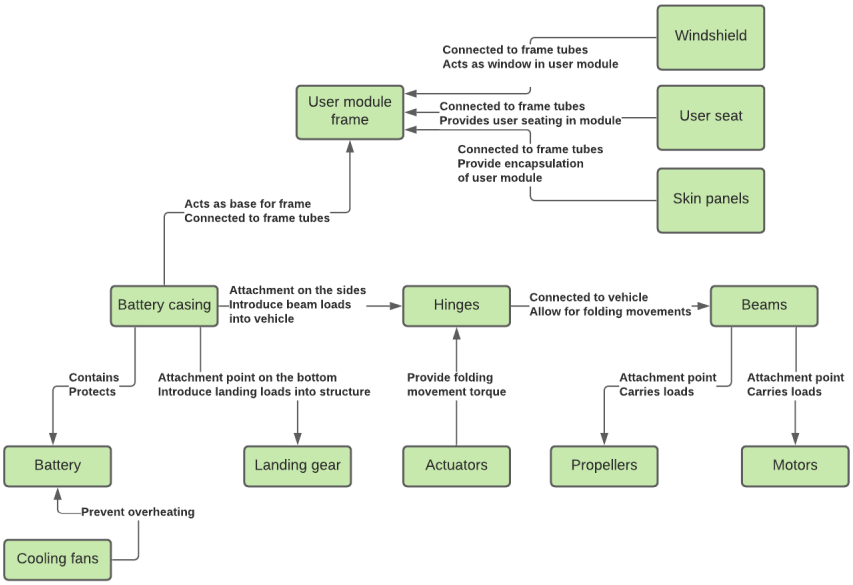

Figure 12.3: The system hardware diagram including the interaction between components.

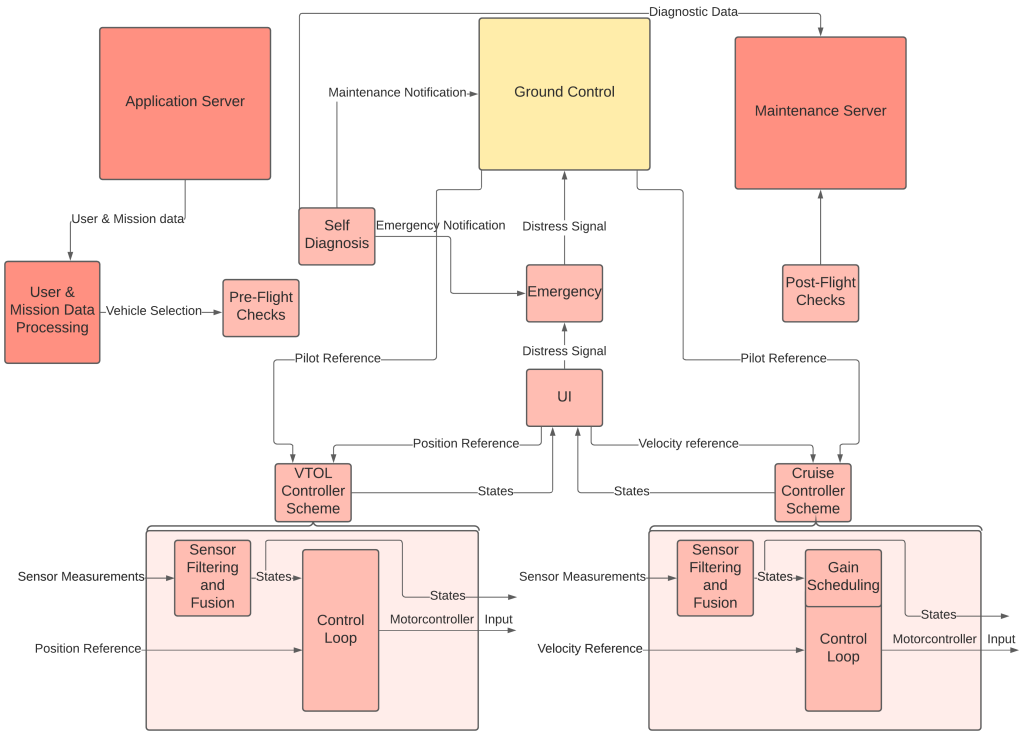

Figure 12.4: The system software diagram including the interaction between components.

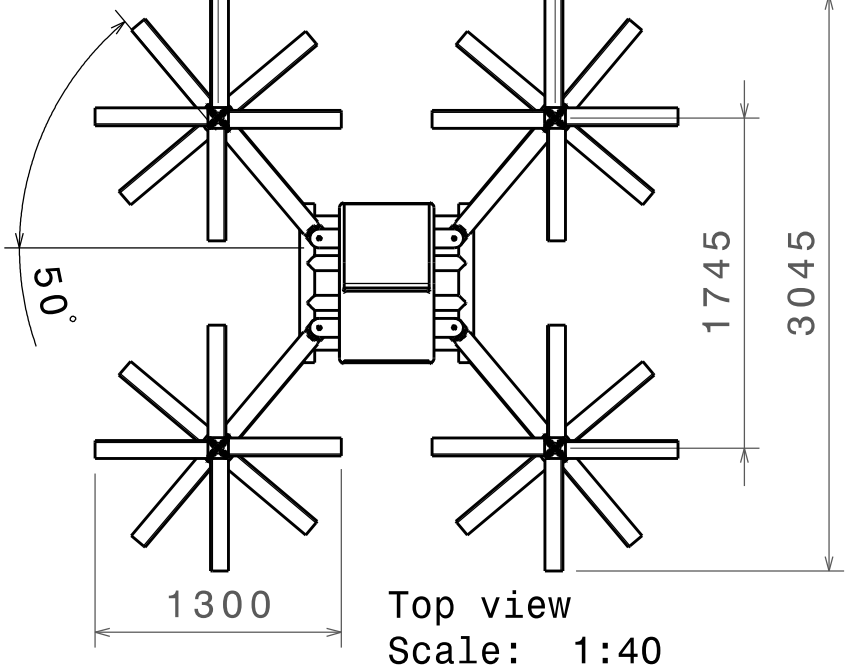

Top view
Scale: 1:40

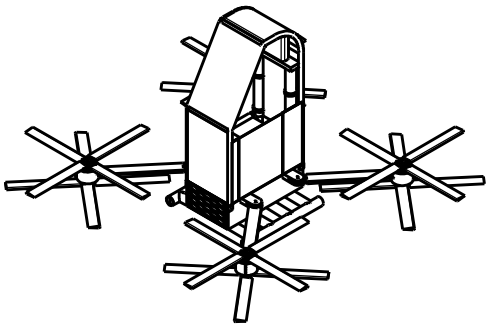

Isometric view
Scale: 1:60

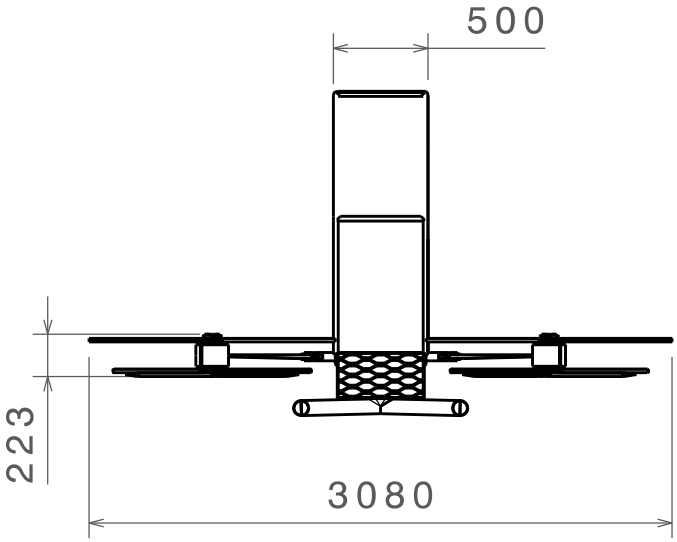

Front view
Scale: 1:40

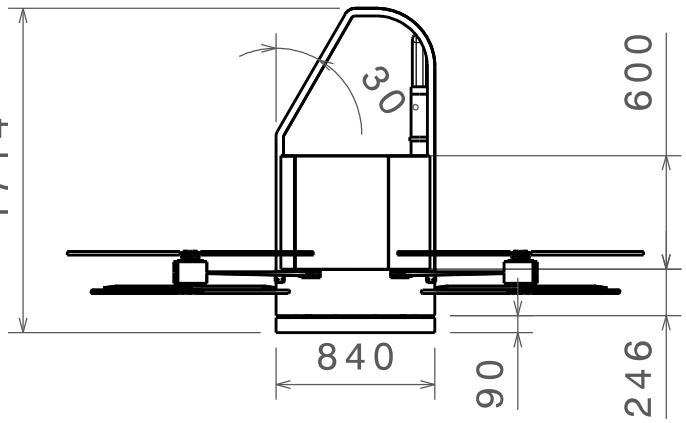

Right view
Scale: 1:40

RENT-A-COPTER

DRAWING TITLE

DEPLOYED CONFIGURATION

DRAWN BY: DSE/GROUP5	DATE: 25-1-2021	SIZE: A4	DRAWING NUMBER: Open_Final_assembly	REV: X
CHECKED BY: XXX	DATE: XXX			
DESIGNED BY: XXX	DATE: XXX	SCALE 1:40	WEIGHT(kg) 219.72	SHEET 1/1

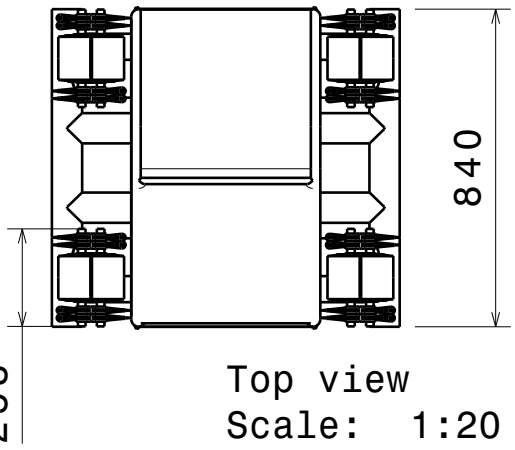

Top view
Scale: 1:20

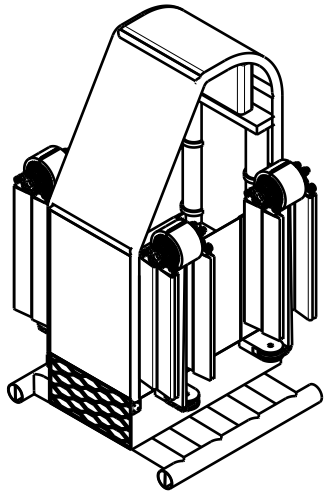

Isometric view
Scale: 1:30

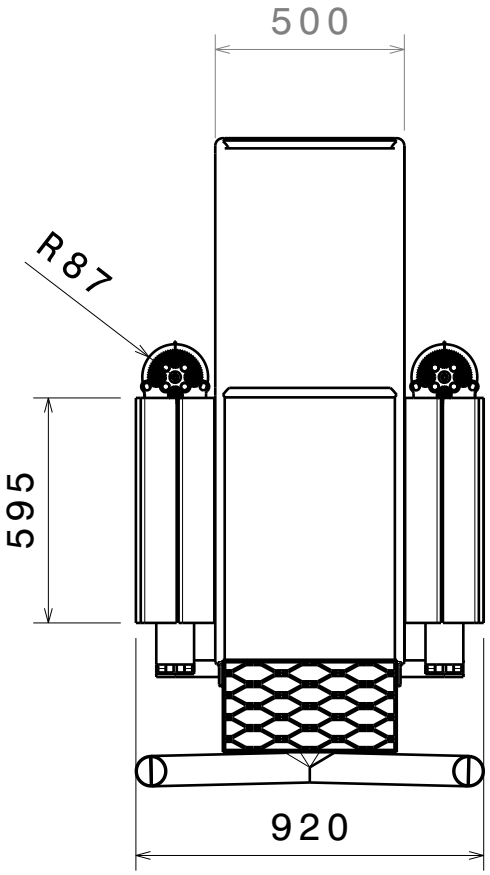

Front view
Scale: 1:20

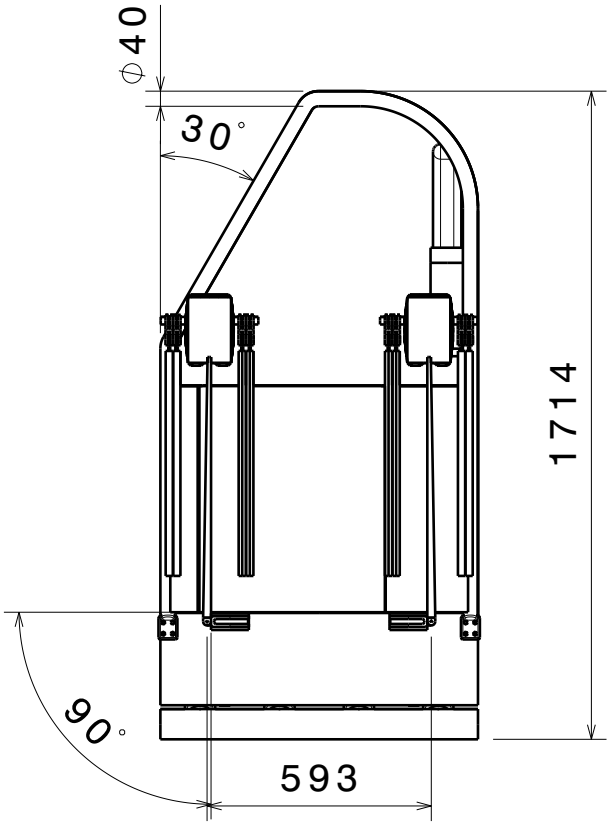

Right view
Scale: 1:20

RENT-A-COPTER

DRAWING TITLE

RETRACTED CONFIGURATION

DRAWN BY: DSE/GROUP5	DATE: 25-1-2021			
CHECKED BY: XXX	DATE: XXX	SIZE: A4	DRAWING NUMBER: Final_assembly_closed	REV: X
DESIGNED BY: XXX	DATE: XXX	SCALE: 1:20	WEIGHT(kg): 219.72	SHEET: 1/1

12.5. RAMS-Analysis

Before producing the product in question, it is vital to identify significant causes of loss in availability. Moreover, there may be some components that can limit the production throughput or anticipation is needed on components that may fail, predicted or unexpectedly, during operation[2]. A Reliability, Availability, Maintainability and Safety Analysis (RAMS) ought to be performed in order to gain more understanding in these four aspects. This section elaborates on all the aforementioned aspects.

12.5.1. Reliability

The first of the 4 that is discussed, is the reliability of the entire system. It can be considered as the assurance that the vehicle should perform its intended function, without failure, for a given period of time in a specified environment[64]. The reliability of all the components should be according to today's standard and should meet national and European regulations. The vehicle is mainly made of aluminium and as the rent-a-copter flies slower than a conventional aircraft and the range is smaller than an electrical car, this material can be seen as reliable for the mission of the rent-a-copter. As personal air transport is a new market, it is hard to base the reliability on already existing vehicles. However, some systems can be assessed.

The power system should be extremely reliable as the batteries are positioned directly under the user. Overheating of these batteries will have catastrophic consequences as the main structure is made out of aluminium. To increase the reliability, a cooling system is integrated in the batteries, such that each pack can be thoroughly cooled. This form of cooling is active, hence needs power from the auxiliary batteries. Besides, there is redundancy in the battery system. The probability that all batteries fail at the same time is negligible as 4 packs are connected in parallel. The rent-a-copter is still able to fly with the failure of one battery pack, i.e. on three working battery packs.

Additionally, the rent-a-copter does not have fuel tanks. This means that fire due to the contact of a spark with the fuel in the tanks is avoided. When a flame does occur during flight, the vehicle does not explode because of the fuel present in the tanks.

Lastly, the reliability of the instruments should be discussed. Sensors that are integrated on board, such as IMU, GPS, barometer and the LIDAR sensor, do provide the user with enough and redundant flight information. Although the probability is really low, it may occur that the flight instruments are malfunctioning or give false information. To avoid a crash, the user can connect his or her mobile device to provide the system the information that comes from sensors in the mobile device. This will make sure that the user is able to land with reliable information on speed and altitude, for example.

12.5.2. Availability

Availability is defined as "the probability that a repairable system or system element is operational at a given point in time under a given set of environmental conditions[3]." In the case of the Rent-a-Copter this aspect depends highly on the maintainability and the reliability of the system. The system must be available for a large number of people in the cities. The most important thing here is the location of the vertiports.

It was found from market research that it is crucial to build vertiports at train stations or close to them. This makes it possible for users to combine public transportation with the usage of a Rent-a-Copter.

For vertiports placed on the roofs of buildings, a public access route must be available for the user in order to reach the vertiport, as many buildings in the city centre are not accessible for all people.

Per vertiport a sufficient amount of vehicles should be available. In the beginning of starting the rental system, the vehicle availability is expected to be relatively small, as branding and the growth is still in progress. subsequently, as detailed in section 15.3, scaling is required to make profit and return on investments. The availability will increase with the scaling of the company.

[2] ARMS reliability. *RAM Analysis*. URL: `https://www.armsreliability.com/page/services/our-services/ram-analysis` (visited on 01/21/2021)

[3] Paul Phister and David Olwell. *Reliability, Availability, and Maintainability*. URL: `https://www.sebokwiki.org/wiki/Reliability,_Availability,_and_Maintainability#Maintainability` (visited on 01/21/2021)

12.5.3. Maintainability

Generally, maintainability can be defined as the ”probability that a system or system element can be repaired in a defined environment within a specified period of time[4].” There exists no such thing as a general type of maintenance, but it can be subdivided into several categories. Figure 12.5 shows the subdivision of the maintenance categories. Maintenance can be divided into two categories, namely planned and unforeseen maintenance. Reactive (breakdown) maintenance is maintenance that has to be done after a component fails. Corrective maintenance implies the ability to fix a component that is not working properly anymore and opportunistic maintenance is being performed when there is an unexpected stop in production[5]. On the other side, there is planned maintenance. Preventive maintenance is maintenance, while the vehicle is still working properly, that is regularly performed to decrease the uncertainty of failure[6]. It is also possible to predict maintenance based on data analysis and statistics on components and is called predictive maintenance[7]. Lastly, improvement maintenance is maintenance aimed to identify improvements on components.

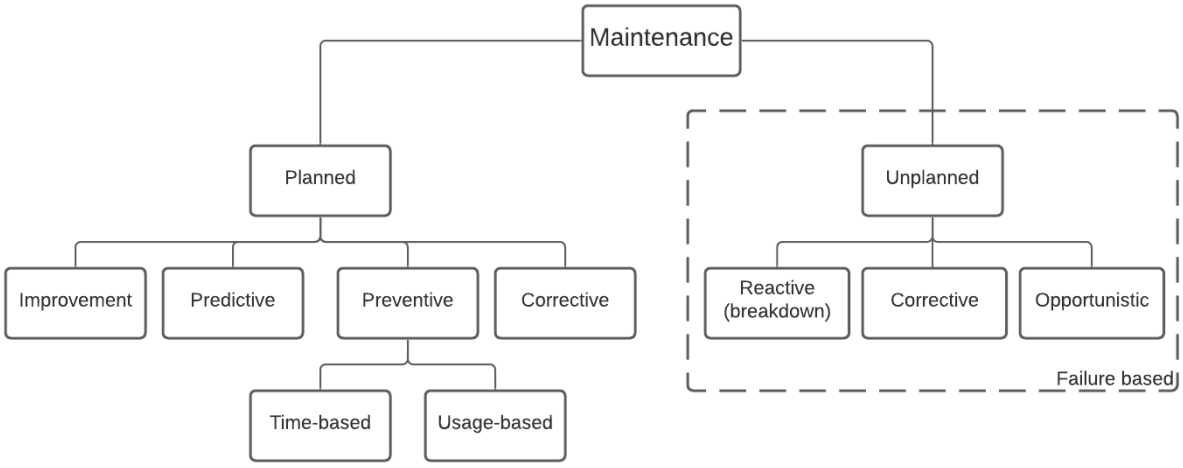

Figure 12.5: The different types of maintenance that can occur.

Now that the relevant maintenance types have been mentioned and discussed, the vehicle can be qualitatively assessed. Following the maintenance requirement, the vehicle should be maintenance free for 2 years. This is achieved for the rent-a-copter and therefore the first two years no maintenance have to be performed, except for some minor regular inspections. After those two years, some components need to be replaced or maintained. Starting with the battery: the batteries have a lifetime of approximately two years. This means that after 1.5 year, preventive based maintenance should be performed to see how the batteries are behaving. This will be predictive maintenance after two years as that is the estimated lifetime. In general, for an operational time of 10 years, the batteries need to be replaced five times. The four beams, connecting the motors with the body, are all identical and are therefore modular. If damage occurs at one of the 4 beams, they can easily be replaced with a spare one. Also, when the product is at the end of its life and a beam is still functioning like it use to do, it can be re-used in a new vehicle. It then probably needs regular (preventive) maintenance or inspection in the first two operating years of the rent-a-copter. The inner and outer hinges are free of maintenance in the first two years too, but needs to be thoroughly checked after this period as they experience high bending bending and shear stresses from the upward forces produced by the propellers. For the motors, regular preventive inspections need to be performed on the bearings after each 500 hours of working[0]. This is for normal weather conditions. During severe rain, the motors have to be checked

[4]Paul Phister and David Olwell. *Reliability, Availability, and Maintainability*. URL: https://www.sebokwiki.org/wiki/Reliability,_Availability,_and_Maintainability#Maintainability (visited on 01/21/2021)

[5]Fiix. *Unplanned Maintenance*. URL: https://www.fiixsoftware.com/unplanned-maintenance/ (visited on 01/21/2021)

[6]Fiix. *Preventative Maintenance*. URL: https://www.fiixsoftware.com/maintenance-strategies/preventative-maintenance/ (visited on 01/21/2021)

[7]Fiix. *Predictive Maintenance*. URL: https://www.fiixsoftware.com/maintenance-strategies/predictive-maintenance/ (visited on 01/21/2021)

even more regularly as the bearings are more vulnerable in those conditions. The motor controllers need to be inspected after 2000 active hours of operation and the capacitors need to be replaced. The skin and the wind shield should be yearly inspected, if no emergencies or failures occur, and it can be assumed that they do not need major replacements during their life. For the propulsion system, the wires should be regularly checked as well as the possible forming of corrosion on the components and the possibility of loosen contacts between the components.

12.5.4. Safety

During the design of the vehicle various safety issues were discussed. All components are analysed for safety. Here user safety and environmental safety are distinguished. A breakdown of the safety considerations in the design is presented in Figure 12.6.

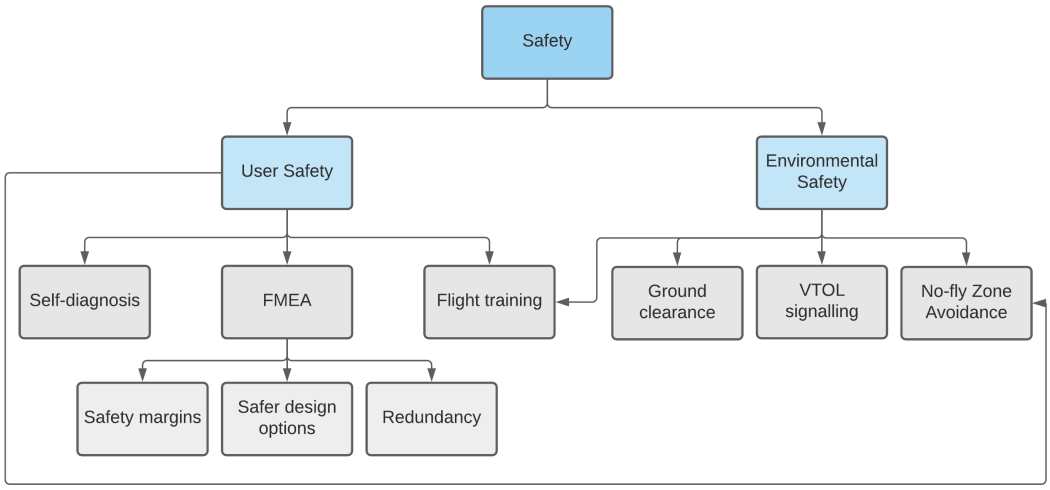

Figure 12.6: The breakdown of all the safety measures related to the system.

As was explained in chapter 10, all departments did an FMEA in order to identify the most important technical performance- and safety concerns of technical components. Mitigation plans are devised in order to maximise safety. These plans include certain technical design choices, production methods, adding safety margins, and redundancy. User safety and environmental safety are both considered here.

The system features a self-diagnosing system, which is detailed in chapter 13. Although an important reason for including this in the design is decreasing the maintainability of the design, it also increases the user safety. The user is less likely to step into a poorly functioning vehicle when the system is self-diagnosing.

One of the most important characteristics of the vehicle design is that it is *personal* transport; the users pilot themselves. This requires the user to learn how to safely fly. In section 9.5 the importance of proper flight training is emphasised. Additional attention is paid to making the flight training engaging, in order to keep user safety high. Besides user safety, environmental safety is also positively affected by flight training, as the user is unlikely to do damage to his/her surroundings if properly trained. Furthermore, the ground clearance and the signalling during VTOL that were set in section 9.8 increases environmental safety.

After receiving proper flight training the user is expected to pilot the system safely. However, suddenly changing weather conditions or other unforeseen circumstances could distress the user. For this purpose, a distress call can be made to the ground station. If necessary, a ground pilot can override controls (for a description of how this data is handled, refer to Figure 12.2).

13
Self Diagnosis System

This chapter includes the discussion and the design of the self diagnosis functions of the vehicle.

13.1. Rationale & Definitions

In currently operational safety-critical systems the overwhelming design strategy to combat risk and uncertainty involves the allocation of sufficiently large safety margins in calculations, the use of redundant components, and the design of fail-operational systems. The high performance required (especially relating to mass) from aerospace systems limits the use of the mentioned strategies and lead to the operational approaches of scheduling frequent inspections and periodic replacement of parts. With the current improvements in sensing technology and computation, a real-time self monitoring vehicle can be designed to replace the need for frequent inspections, to identify faults when they occur, to predict failure into the future, and to integrate with a degradation aware part replacement schedule. Resulting in a less costly, more sustainable, and safer system overall.

Before venturing further into the specifics of the system a few definitions must be clarified:

13.1.1. Failure, Damage and Self-Diagnosis

Components and systems can fail in many different ways with many different effects. The distinction between failure, damage/degradation and fault that we have identified is whether the component or system can still perform its function: Damage and degradation could cause deviation in performance but the system could still perform its functions. Likewise a fault in a system could be detected and corrected for or be sufficiently small to not cause failure.

Self-diagnosis, in turn, involves the monitoring of the system state including the damage/degradation and faults using health indicators.

13.1.2. Conceptualisation

Self diagnosis is a method that can be implemented at different levels. The conceptualised self-diagnosis system will only incorporate level 1: ”is the (sub)system failing or not?”. In different subsystems health indicators will be chosen for the most critical components. Multiple thresholds may be set in the form of Emergency Thresholds and Maintenance Thresholds.

A central learning system may then be constructed to provide thresholds for, and form the combined health indicators using health history data and health indices from other operating aircraft. If the Maintenance Threshold values are exceeded the Maintenance Server is contacted so the maintenance of the vehicle can be promptly scheduled. If the Emergency Thresholds are exceeded Ground Control is alerted and immediate measures are taken to ensure passenger safety. The differing prediction horizons of each health indicator may lead to various types of measures being taken. Furthermore, for the critical components selected the determination of these thresholds should be done ahead of the launch of the vehicle as failure of these components may lead to life-threatening events. In the coming sections the self diagnosis health indicators per subsystem are explained.

13.2. Self Diagnosis per Subsystem

In this section the integration of the self-diagnosing system within the design that is defined so far is explained. For every subsystem the self-diagnosis aspect is discussed and design choices are made.

13.2.1. Control and Stability

As the system being controlled is inherently unstable, the design involves high reliability components and a redundant architecture. Due to the fail-operational nature of the design, the faulty components

can be identified as part of self-diagnosis during flight, without compromising the mission.

The first components to consider are the processor and the software running inside it. Modern multi-core processors such as the one chosen for the initial launch have many built in self-diagnostic features. Since the current plan involves a switch to an ASIC processor, this discussion will also cover desired capabilities whether they are all present in the initial chosen processor or not.

The processor has triple modular hardware redundancy to ensure that the system is tolerant to hardware related faults. Subsequently, if multiple processor cores are used a dual core lock-step setup with the second core running identical calculations with a slight delay (to prevent transient errors from causing a fault[1]) can be implemented and the comparison of the two results may be used as a diagnostic. A similar approach can be pursued for the real-time operating system software running: a supervisor process and a number of redundant calculation processes may be launched at startup along with communication channels between them. The active process may then be tasked with producing a ”heartbeat” signal and the redundant processes may take over when the heartbeat signal fails to come. When a thread faults, the supervisor process must be alerted; and the alert data can also be used as a diagnostic. The supervisor thread could be thought of as a software watchdog unit that detects thread deadlocks and starvation[2]. Additionally, an on chip memory management unit may be included to prevent cross thread data corruption. Illegal attempts at overwriting data along with memory quota breaches can be used as a diagnostic. These health indicators come with little to no implementation cost since they are already present to ensure the reliability and safety of the subsystem. Furthermore these indicators are very specific about the location and type of fault which makes them excellent health indicators.

Since the control system already requires the collection of state data via sensors it is also worth discussing how the measured states may be used for less local yet free diagnostics. One such health indicator might be the controller output and the vehicle dynamics being compared to expected pairs to determine propulsive faults or degradation. This could perhaps lead to the design of an adaptive control architecture in the future of the project. Another indicator may be the comparison of separate sensor measurements of the same state to determine sensor health. The breadth of data collected from a network of such vehicles might be used in contribution to various weather and wind related research in an urban environment, after some processing.

13.2.2. Power and Propulsion

For the power and propulsion subsystems, the main components that have a large amount of modes and chances of failure are the batteries, the motors, motor controllers, and the propellers. These different components will be looked at in detail; first, modes of failure are discussed. These are then translated into health indicators, from which sensors and reporting systems are made.

The batteries are there to supply adequate power to the rest of the system. For this it needs to have adequate voltage to power the system’s load, capacity to sustain this load for a long enough time. If the battery fails to supply adequate power, it has failed as a subsystem entirely. If the voltage is too low, the current is too low, or if the battery stops supplying energy entirely because of internal failure the battery does not function properly. These can be caused by battery degradation over its life, overheating, thermal runaway, short circuiting, or any other mode of cell failure.

Current performance can be assessed by comparing the current voltage, power, and current read-outs to those being demanded from the cell. If supplied voltage is zero, this could be indicative of a failed battery or failure in the connection between the battery and the measuring point. If it is too low, the battery could be old or broken. The battery must run in operable conditions in terms of temperature, as high temperatures are often the result of internal failure. High temperatures can also end in critical failure, so it is important this state is closely monitored. These factors indicate current performance and a prediction of future performance, and hence can be considered good health indicators. Finally, the battery must be able to perform this over multiple loading cycles, so the history of these values are indicators for battery health as well. If the current voltage is much lower than the ones in previous cycles (and lower than what was projected), this could signify this battery is degrading fast.

[1] Richard Quinnell. *Designer’s Guide: Safety-critical processors - Electronic Products*. 2018. URL: https://www.electronicproducts.com/designers-guide-safety-critical-processors/#

[2] Embedded Staff. *Safety-Critical Operating Systems - Embedded.com*. 2001. URL: https://www.embedded.com/safety-critical-operating-systems/

The battery, as an array of cells, is comprised of different cell groups. All of these cells can fail individually, and for gains in maintenance it is beneficial to know where the failure has occurred, as to being able to service specific cells instead of the entire battery array. Doing this on a complete per-cell basis would require a lot of extra sensors, but dividing the monitoring over these cell groups still begets most of the benefits of this approach. The exact configuration and division of these groups is out of the scope of this paper, and must be researched further. For the self-diagnosing system, this means that battery health is assessed on these group basis. These groups are all connected to the battery controllers, which will report the data to the self-diagnosing system.

The voltage per group is logged using voltage meters in the battery controller, as is its corresponding current (and power). The temperature is checked with a probe as well and sent to the battery controller. Comparing current power and voltage readouts with data from previous flights and internal statistical models, the current charge and maximum charge of the battery can be determined, and projected into the future to estimate remaining lifetime.

As for the motors: note that every motor operates essentially independently. This is required for the applied method of using differential thrust for control. This means that every motor must be assessed individually, with their own references. The motor must be able to convert electrical power into a rotation of a certain speed at a specific torque. Failure modes here are getting stuck, failure to transfer load over the axle (axle failure) to the propeller, and failure to generate enough rotation, either by degradation or internal failure (such as slipping). The engine itself can also be damaged- this itself often shows in its performance as well, but some failure modes are easier identified by heat buildup.

Checking how well the motor performs its tasks can generally be done by comparing the engine RPM and input power to that of engine input power. The ratio of axle power to input power (the power factor) is therefore a good health indicator. This can be determined by keeping track of several other parameters: RPM, torque (which together are the axle power), and input power are therefore good performance indicators, and hence health indicators if the input power is also known. The value of the power factor is variable dependent on the power supplied, and will always be lower than 100% because of internal losses. For a properly functioning motor, this relation is known, as can be seen in the power curves in Figure 5.3. Note that the exact values will be slightly different with the propeller load compared to this controlled environment test, and that accurate curves will have to be generated experimentally for this specific vehicular application. It must also be noted that during spin-up, the performance does not necessarily coincide with the expected value do to latency and inertia. Hence, this reading is only usable in a steady state when the power is constant and some settling time has been allocated.

Another effect present in motors can be exploited for diagnostics as well: Voltage sag and voltage surge (voltage dip and voltage swell in American English) are very short fluctuations in the voltage supplied often caused by changes in load of the system. Starting to turn a motor from standstill causes a sag, and stopping a motor causes a surge. The exact duration and intensity of these surges are dependent on the nature of the change in load. A motor that is stuck will experience a larger sag during startup, a small sag will occur when a small object enters the propellers. A propeller breaking off will cause a very large surge, whereas shutting down the motor will cause a minimal surge. The characteristics of a surge can be combined with other data present to identify what caused it.

These health indicators can also be used to identify issues with the propeller. Hence, the power ratio and voltage fluctuations will also be referenced in the part dedicated to that analysis.

As engines running hot often go coupled with failure, temperature is a health indicator too.

The RPM will be counted using a tachometer. By measuring the interval between activations, the tachometer will be able the measure the rotational speed of the axle. The torque will be measured using a decoupled dynamometer, allowing simultaneous reading and operation of the motor. The input power is determined using a current meter and a voltage meter placed directly in front of the engine. Alternatively, the power setting from the motor controller can be used to get the corresponding power from it directly. This loses some redundancy (it is not possible to determine if the motor controller or the motor itself has failed), this reuses the capabilities of the controller, saving weight and cost in the process. The temperature of the motor will be determined using temperature sensors.

13.2.3. Structures and Materials

Disassembly in order to inspect the system and inspecting it by hand, requires a certain amount of time and money. Reducing this will result in lower cost. Self-diagnosing structures are regarded as smart

structures. Health indicators are placed either on or in the structure to be aware of the health of the structure. Structural Health Monitoring, SHM, is used in order to make the structure self-diagnosing. Such a system compares states, of which the initial state is referred to as the undamaged state. Several techniques are available, based on different principles. SHM is divided in five categories, where the first is the least detailed and complex, the fifth the most. The categories are: Existence, Location, Type, Extent and Prognosis. As with many systems, the more complex, the more expensive. In this design, the structure will monitor if it is damaged, so category one. To have a structure containing SHM, sensors, actuators and a computer are needed. The sensors are placed at places on the beams where the first damage is expected.

A number of companies are contacted in order to acquire some information on prizes and different systems. A few companies responded, with different results. Some offered a product, without mentioning prizes, others gave access to their web shop. After consulting an expert in self-diagnosis, all options are regarded as too expensive or complex for the designed vehicle. The SHM system will be developed by the team. Regarding the beams, the following is chosen: strain gauges are placed on the beams where the highest stresses are experienced. These locations are determined in section 6.2. If the strain gauges exceed a certain threshold, the system alarms the user that it requires further inspection. Next to this system, ultrasonic structural health is used. The benefit of this, is that the probability of detection curve can be adapted to the conditions it is operated in. When the structure is known to be undamaged, the noise level can be detected and the threshold for damage can be adapted [67]. The system developed will have the same type of architecture as the PAMELA SHM, developed by AERNNOVA [3]. The piezoelectric transducers producing an ultrasonic wave, which is interfering with the properties of the structure and is reflected back. If damage has occurred, the trajectory is changed, which is measured by the piezoelectric elements. This data is processed afterwards and compared to the healthy state. In this way, the system can detect the damage and possibly locate it.

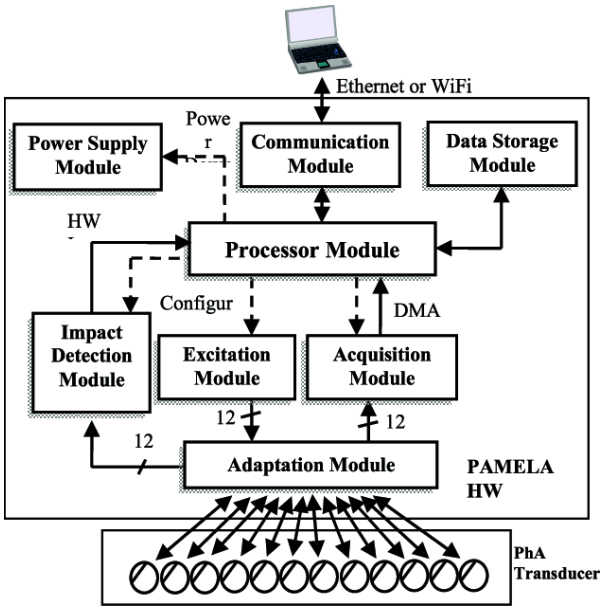

Figure 13.1: Diagram of the hardware of PAMELA III

The benefit of this system is that only 1 side with piezoelectric elements is needed per beam, reducing the power required to a minimum. Other than that, the damage is found any time, not only when it is occurring [4]. This means, damage to the system that happened when the system was not in use is also found by this system. The costs of this system are incorporated in the development costs.

[3] P.M. Monje et al. *Integrated Electronic System for Ultrasonic Structural Health Monitoring*. URL: `http://oa.upm.es/20571/1/INVE_MEM_NADA_136958.pdf` (visited on 01/19/2021)

[4] P.M. Monje et al. *Integrated Electronic System for Ultrasonic Structural Health Monitoring*. URL: `http://oa.upm.es/20571/1/INVE_MEM_NADA_136958.pdf` (visited on 01/19/2021)

14
Production Plan

Now that there is a complete final design, it is important to look how this vehicle can be produced. For different components and parts the manufacturing processes are described and explained. Like in the whole design, the sustainable approach to this project is continued in the set-up of the production plan. This chapter starts with section 14.1 as a general overview of the flow of parts into sub-assemblies into main assemblies to final integration and quality control. The part manufacturing is explained in section 14.2, then in section 14.4 the sub-assemblies, section 14.5 the main assembly and finally in section 14.6 and section 14.7 the total system integration and quality control respectively.

14.1. General overview

Figure 14.1 Shows by colour coding the different phases of the production process. The ”A” bubble indicates a short stage of inspection and testing as part of overall quality control between every phase. If for example a part is tested and not good enough, it is rejected and the process goes back to part manufacturing.

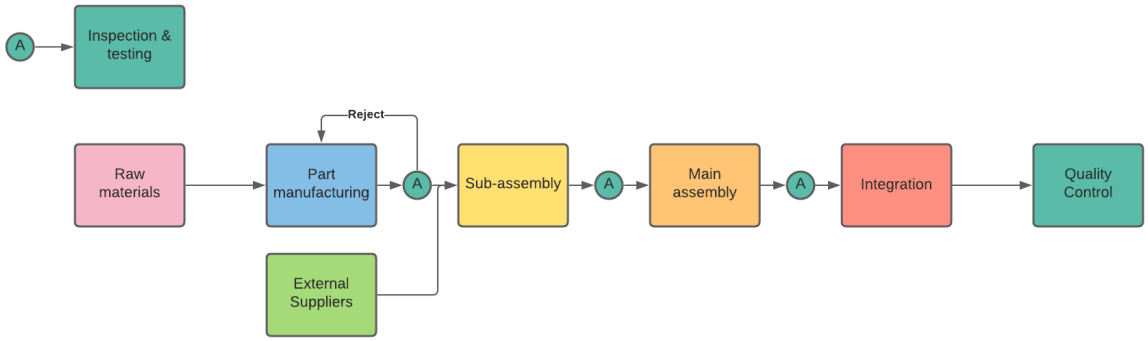

Figure 14.1: General flow of the production of the system.

The colour coding in Figure 14.1 correspond to the colours of the blocks in Figure 14.2. The diagram shows which parts and components are combined in each sub-assembly and consequently which sub-assemblies form the main assemblies. To ensure modularity in the design the choice has been made to divide the main assembly into the arm assembly and the body assembly. Every vehicle will need 4 arms, which are all identical and not specific front left, back right arms for example. The body assembly then contains the rest of the system, where the user module is first constructed separately, so that as a whole it can be replaced easily in vehicles.

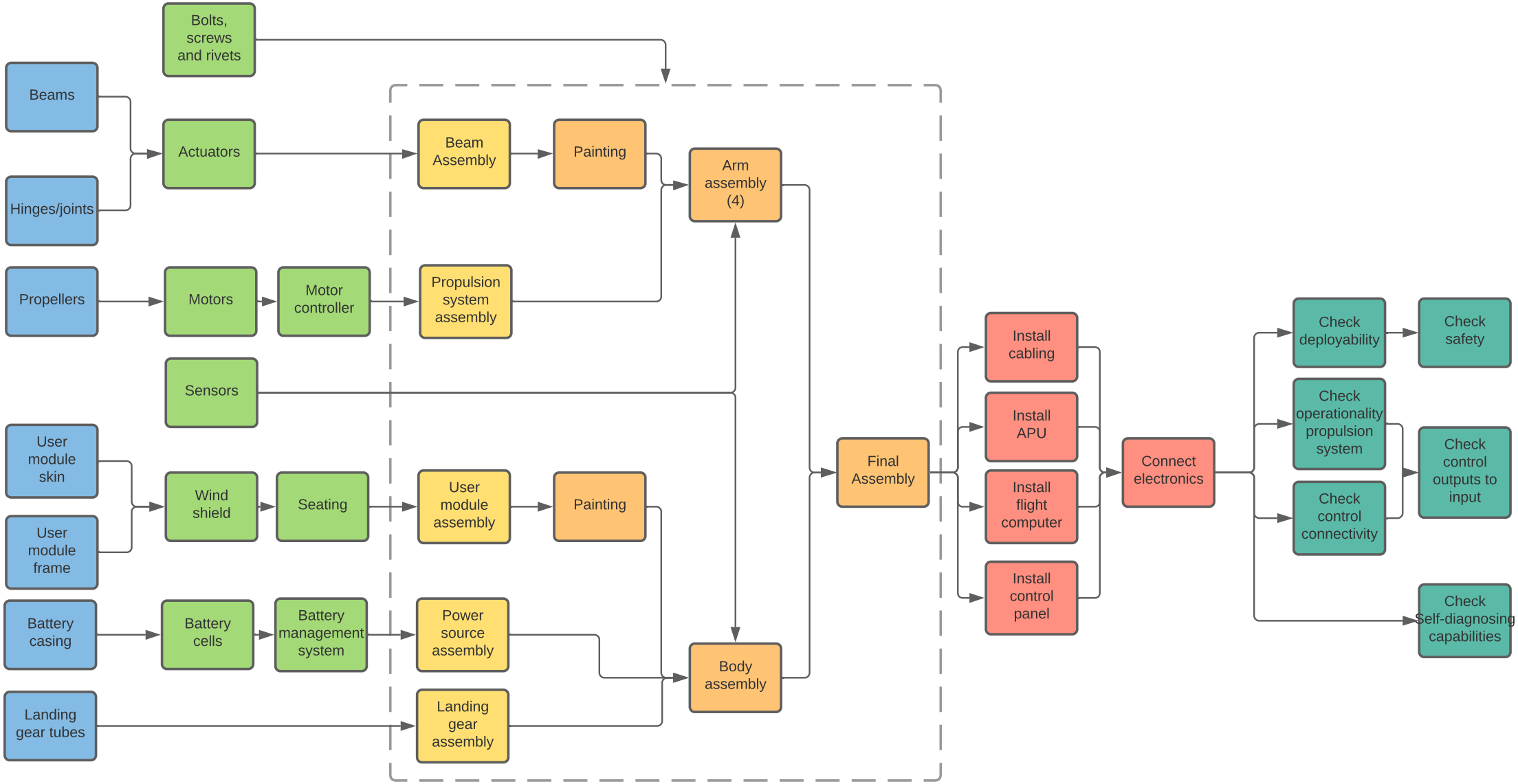
Bolts, screws and rivets
Beams
Actuators
Hinges/joints
Beam Assembly
Painting
Arm assembly (4)
Propellers
Motors
Motor controller
Propulsion system assembly
Sensors
User module skin
User module frame
Wind shield
Seating
User module assembly
Painting
Battery casing
Battery cells
Battery management system
Power source assembly
Landing gear tubes
Landing gear assembly
Body assembly
Final Assembly
Install cabling
Install APU
Install flight computer
Install control panel
Connect electronics
Check deployability
Check safety
Check operationality propulsion system
Check control outputs to input
Check control connectivity
Check Self-diagnosing capabilities

Figure 14.2: Production flow diagram

14.2. Part manufacturing

In this section the manufacturing processes of the different parts are described and explained. For the self-constructed parts, they are made through batch production, so the parts are made in batches and for the production of each vehicle or for maintenance new parts can be retreived from there.

14.2.1. Beams

Production of the beams is less self-explaining as thought at first glance. This is mainly because the varying cross-section. The beams are made of Aluminium, which is folded around a template. After uncoiling, the edges are milled and rolls are formed. In this design, a template is used around which the sheet is formed, this process is called cold forming. The edges are welded together.

14.2.2. Beam-body actuator hinges

As the hinges translate the loads from the beam to the battery, they are under heavy loads. Their simple design allows for forging of the flanges to then weld them together. Welding is cost effective, however forging is not. The benefit of forging is that the grains of the material align, making the structure stronger. In between the forging and welding, the material has to be subjected to machining, to drill the required diameters of the bolts.

14.2.3. Propellers

Due to the fact that they need to fold, the propellers are made of 2 main components: the hub and the blades. These both have to be produced. Both require different methods due to their shape and material differences. The amount of waste is lowered by using low waste processes, as the production series for the propellers are large.

Firstly, the blades are produced using a hot closed die forging process. Due to the geometry and material choice for the blades, this method is best suited. The process is also well suited for the large required batch size of $32,000$ blades per year to meet the required production rate. The cost of the process is also well suited for the system under design. Finishing processes will be required to refine and weatherproof the blades.

The hubs are made of a high strength stainless steel. Due to its shape and the batch size of 8000 hubs per year, a low pressure die casting process is well suited. Some finishing processes, such as creation of holes and general refining processes will still be required.

The propellers are by far the most exposed part of the vehicle. At their relatively high cost it is preferable that they don't break at all, but they do have the highest associated risks in occurrence for the power and propulsion subsystem. A strategy must be employed to get the vehicle back in operational quickly. As the system has multiple propellers (all consisting of multiple rotor blades), this is a good candidate for the application of modularity. The propellers themselves consist of 4 of the same propeller blades attached to the folding system. The propeller blades are mounted to this folding system with a certain freedom anyway, so making this the attachment point for the blades in a modular sense is relatively simple. In the case of a broken propeller blade, this singular blade can be dismounted from the folding base and a new one can be inserted. As the propellers varry very heavy loads however, it is important that this connection is solid; In this case, the modularity of the system is compromised in the traditional sense a bit in that specialised tools will be required to replace a propeller to make sure that the heavy joints are properly secured. This does double as a safety feature for theft however, as the propeller blades are very much exposed at all times, even during stowage.

14.2.4. User module skin

The user module skins are metal sheets for which sheet metal forming processes can be used. The cheapest solution, which is applicable due to the low complexity of the sheets, is rubber forming [68]. Rubber forming uses a universal rubber die to push the metal against male or female die. Due to symmetry, only 2 dies need to be made with one machine, making it a cheap solution. There are 5 sheets, of which one requires this process. The other sheets do not require a curvature.

14.2.5. Battery System

The cells inside the battery modules are connected using nickel-plated copper bus bars, as this provides least amount of resistance and high corrosion resistance[69]. Furthermore this bus bar is connected to the battery cell terminals using ultra sonic welding as these welding joints provide the least amount of electric resistance in comparison to other forms of joining methods[69]. The modules are connected together using removable terminal wires provided by Sion power[1]. These wire can handle the output voltage and current of the battery pack, further they can also be removed easily to replace the battery modules. Each battery pack is also connected to battery management system provided by Lithium balance[2]. The BMS (battery management system) consists of a monitoring unit and a control unit. This BMS can monitor and control the performance of upto 256 cells. The monitored battery pack performance characteristics includes: individual cell voltage, state of charge, state of health, leak detection, cell and pack resistance. Furthermore, the BMS can control the cell voltage and balance the cell current to prevent over current, over voltage and under voltage hence preventing the battery from operating outside its safe operating area there for increasing the life cycle of the battery.

As is covered in section 5.4, the batteries are organised in groups that are monitored to diagnose their health or other issues. In the event of full component failure, this is also pointed out. This aids in indicating when replacement of the batteries is necessary. If all the batteries were connected in one large grid, this would mean that the entire battery would need to be replaced or every individual cell would have to be checked manually to find the fault. In the grouped organisation, it is much easier to narrow down which exact batteries will need replacement. Combining this with batteries that can be removed and replaced instead of fixing them in the frame of the vehicle entirely means that only a single group of batteries can now be replaced in the event of a detected failure, making it significantly more attractive to repair a vehicle instead of scrapping it. This increases the operational lifetime as well as maintenance costs, at the price of increased build cost.

14.2.6. Landing gear

The landing gear is a structure made from round aluminium tubes with specialised cross-sections to meet the impact requirements of the system. These tubes are produced using hot metal extrusion, as this is the only metal forming process that allows for the forming of longer hollow sections. Multiple moulds are required to create the cross-section of the skid to allow for the extra supporting plate through the centre of the tube.

14.2.7. User module frame

The user module frame is produced in a similar fashion to the landing gear, as it is also constructed from hollow tubes. These tubes are thus made using hot metal extrusion and cut to specification. The tubes are also bent to achieve the shape of the user module and windshield. End plates are attached for the final assembly of the system.

14.3. External suppliers

For some of the parts, there is no need to make a manufacturing plan and it is more convenient that those are being supplied by external partners. In this subsection, the external suppliers will be mentioned and explanation will be given on the parts that will be provided for the project.

14.3.1. MGM Compro

The motor and the motor controller are complex systems and it is difficult to come up with a detailed manufacturing plan for those components. Therefore, it has been decided that the aforementioned parts will be supplied by a third party, namely MGM Compro. ”MGM is a company that focuses on the development and manufacturing of state of the art solutions in the area of electric motors for industrial applications and Electric Vehicles (EVs)”[3]. Not only they import and produce motors, but also propulsion systems, motor controllers, battery management systems, batteries and industrial chargers. For the vehicle, MGM Compro provided us with almost all the electronics. Only the batteries will be supplied by another company, that will be mentioned in REFERENCE SUBSECTION. The motors needed for the

[1] *Modular Power Packs*. URL: `https://sionpower.com/products/s` (visited on 01/18/2021)
[2] *S-BMS*. URL: `https://lithiumbalance.com/products/s-bms/` (visited on 01/18/2021)
[3] MGM compro. *About us*. URL: `https://www.mgm-compro.com/` (visited on 01/08/2021)

driving the propellers are custom made by MGM, based on our input variables as already explained in REFERENCE 3P SECTION[4]. Also the motor controller, which suits the motor perfectly, will be provided by MGM[5]. Other components such as cables and connectors will also be chosen and delivered by MGM depending on the system requirements. Hence, these components will be manufactured externally and a self-made production plan is not needed. Although the battery cells will not be provided by MGM due to the fact that a last change in battery structure would lead to major different structural properties, the battery management system will be delivered by MGM[6]. Once again, special thanks to Mr. J. Kovaricek, S. Svec and MGM Compro for the assistance and helpfulness regarding the power system design choices!

14.3.2. Sion Power®

As mentioned in subsection 14.3.1 the battery management system, connectors and cabling is provided by MGM Compro but the battery cells used are provided by Sion Power. Sion Power manufactures and tests licerion lithium metal cells which delivers highest combination of energy density and specific energy[18]. With over 20 years of research and development Sion power has developed Licerion cells which are being currently used in high altitude pseudo satellites. These cells are selected for their compact size and ideal life cycle as mentioned in section 5.4. As the cells are manufactured and packed into modules externally so a self-made production plan is not needed.

14.3.3. KD fasteners Inc.

The production of standard and custom rivets and bolts will also be made by an external supplier. Rivets and bolts are needed to fasten the user module to the battery casing, to attach the propeller to the motor and to attach the landing gear to the battery casing. KD Fasteners could provide those fasteners for the vehicles. KD Fasteners is a company that is specialised in the manufacturing of nuts and bolts in both standard and metric designs[7]. KD Fasteners has also been selected due to its various material possibilities.

14.3.4. Seating

The seat that was chosen for the system is the commercially-certified, lightweight, rugged and crash-worthy BAE S3000 [8].

14.3.5. Windshield

The wind shield will be made from laminated glass which is stronger than regular and tempered glass. Another benefit is that laminated glass doesn't shatter when fractured but stays in place due to the film. As the windshield area will not have to be curved, it can be easily cut to a specific size and inserted onto the vehicle. The laminated glass will be custom cut to a size of 600x500x60mm. This can be done in-house using standard size glass panels as the tool and machining requirements for this process are simple. However, to aid in lean manufacturing, it is preferable to custom order glass panels of this size at companies who provide them to make sure there is less glass waste.

14.4. Sub-assembly

In the beam assembly the hinges and actuators are installed on the beams. Since all beams go through the same rotations and deployment movements, they can all be assembled the same way and only in the final assembly will it be determined which beam becomes a left front beam for example. The other two structural sub-assemblies are the user module and landing gear. The landing gear tubes are already cut to the specification of the landing gear. The appropriate holes are cut as well, to allow for proper assembly. The leg and skid tubes are then assembled using fastener plates and rivets. The

[4]MGM compro. *Electric Motors*. URL: https://www.mgm-compro.com/kategorie-produktu/electric-motors/ (visited on 01/08/2021)

[5]MGM compro. *Motor Controllers*. URL: https://www.mgm-compro.com/brushless-motor-controllers/ (visited on 01/08/2021)

[6]MGM compro. *Battery Management Systems*. URL: https://www.mgm-compro.com/bms/ (visited on 01/08/2021)

[7]KD Fasteners. *Supplier of Standard and Metric Fasteners*. URL: https://www.kdfasteners.com/ (visited on 01/08/2021)

[8]BAE Systems. *S3000 Lightweight, Crashworthy Rotorcraft Utility Seat*. URL: https://www.baesystems.com/en/download-en/20190408151308/1434555685514.pdf (visited on 12/15/2020)

whole landing gear can then be integrated into the assembly of the body. Similar to the landing gear the user module frame tubes are connected using fastener plates and the skin attached using rivets.

The propulsion and power source are seen as two separate sub-assemblies, because the propulsion system is attached to the beams, and like this the complete arms can be assembled separately and the same counts for the power source sub-assembly. The propulsion system assembly consists of the propellers which are attached to the MGM Compro motors and motor controllers. In the power source sub-assembly process, the battery cells are grouped into 4 modules and with the battery management system placed into the battery casing.

14.5. Main assembly

The final assembly is made form the two main assemblies: the arms and the body. The User module, power source and landing gear sub-assemblies are stacked and connected to become the body assembly. For the arm assembly for each beam a propulsion system sub-assembly is connected. For both these main assemblies, a start on laying out the cabling is made. The arms for example are hollow and the propulsion system cabling is installed durin this assembly phase.

14.6. Integration

In the integration phase the rest of the cabling is installed, together with the control panel and flight computer. Then all the electronics are connected to each other such that they can communicate as described earlier in subsection 12.4.2.

14.7. Quality control

After the whole vehicle has been assembled and all systems set-up, extensive testing is done. For the motors, MGM Compro was able to provide test data to the team, so the motor outputs can be tested against that. The arms are tested for smooth deploy-ability and subjected to factory load and deflection tests. The control system is tested on the ground and in test flights, together with the readings from the self-diagnosis health indicators. The exact procedures and test performed on the vehicle are not defined yet, this is outside of the scope of this phase of the project. When test flights are being performed, the essential things to test before putting the product in use can be better defined, so this is done at a later stage.

15 Cost Breakdown and Return on Investment

This chapter aims to estimate the costs and incomes of the business concept, and from this determine the years to accomplish break-even, also showing the return on investment.

15.1. Costs

Costs are subdivided into operational costs and development costs. Costs may be one-time/initial costs, or yearly costs. Production costs are presented under vertiport costs, as it is considered that every vertiport has $n = 200$ vehicles.

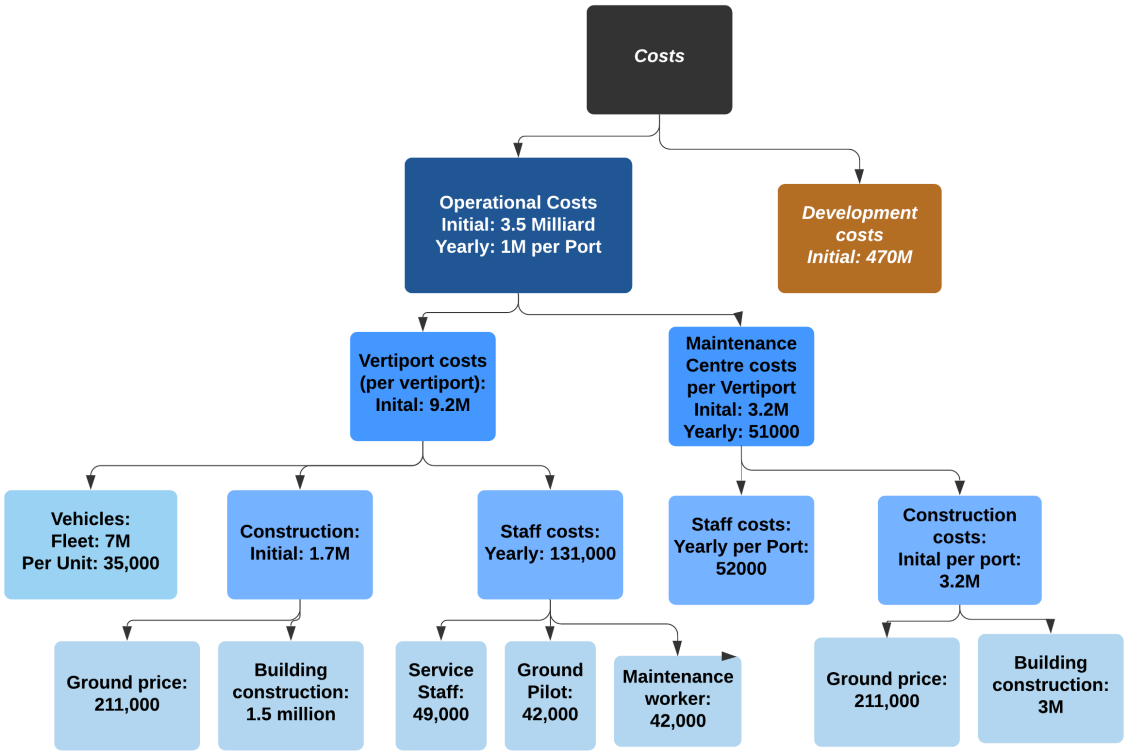

Figure 15.1: The Cost Breakdown structure.

15.1.1. Development costs

The development cost of the system is hard to estimate, as it is a very novel product and concept. Therefore, a cost estimation by analogy is done to get a very rough estimate of development cost. The analogy is based on the Lilium Jet[1], for its similarities and its readily available information about the size and timing of the project. Based on Lilium and other similar projects, it is determined that the

[1] Lilium GmbH. *Learn more about Lilium*. URL: `https://lilium.com/about-us` (visited on 01/13/2021)

development will take $10\ years$. The size of the team is also based on Lilium Jet, but is assumed to be smaller due to the fact that this product will use more off-the-shelf components.

There is still a need for assumptions on multiple aspects. A $€150/hr/person$ rate for the engineering hours of the development team is assumed with an added $€50/hr/person$ for other costs, such as office space, taxes, etc. An assumed growth of the size of the team based on the timing of the development is also assumed. It is also assumed that each employee works $235\ days$ per year. The cost for prototypes and testing equipment is not explicitly included. It is, however, assumed to be covered by the amount for extra costs.

The result of the estimation of the development cost is presented in Table 15.1. This table also breaks down this cost over the $10\ years$ of development for clarification. The result is deemed realistic, as it is less than most large aerospace projects, while being in the same order as the funding received by Lilium [2]. It should be noted that this is a very rough estimation due to the many assumptions, and needs to be further researched. For this reason, margins are implemented in the return on investment calculations. The best case scenario is a margin of -10%, which is based on the fact that over estimations in aerospace projects do not happen often and are usually very small. A worst case margin is set at $+50\%$, also based on analogy with historic aerospace projects.

Table 15.1: Evolution of the development team size and yearly cost over the development period.

Development Year	**1**	**2**	**3**	**4**	**5**	**6**	**7**	**8**	**9**	**10**	**Total**
Development Team Size	10	25	25	50	50	100	100	150	250	500	-
Development Cost [M €]	3.76	9.40	9.40	18.8	18.8	37.6	37.6	56.4	94.0	188	473.76

15.1.2. One-time Operational costs

One time operational costs considers the construction of the vertiports, construction of maintenance centres and production costs. Production costs is elaborated on in the next section.

Vertiport Construction Costs Construction costs takes into account the ground price, charger infrastructure costs, small maintenance shop costs and general the construction of vertiport. They are listed in Table 15.2. Construction costs are found from the company Lilium as analogy [3]. For the maintenance centre, it is assumed every 8 vertiports have 1 maintenance centre.

Charging stations cost In order to charge the vehicles in its parking space, 200 medium power chargers are needed and a connection to the infrastructure is needed.

Table 15.2: One-time vertiport costs, per vertiport

	Mean	**Best Case**	**Worst Case**
Total ground cost (200 eu/m2)	€ 211,200	€ 75,600	€ 406,800
Construction cost	€ 1,500,000	€ 1,000,000	€ 2,000,000
Medium Voltage Infrastructure Connection[a]	€ 3,000	€ 2,500	€ 3,500
Maintenance centre costs per port (0.13 centres/port)	€ 375,000	€ 125,000	€ 625,000
Production costs all vehicles	€ 7,000,000	€ 5,600,000	€ 8,400,000
Total One time Vertiport Costs	**€ 9,289,200**	**€ 6,962,300**	**€ 11,676,500**

[a] JoulZ. *Joulz charging solutions*. URL: `https://joulz.nl/` (visited on 01/25/2021)

15.1.3. Production costs

Production costs were analysed in an inventory shown in Table 15.3, analysing all separate components. The production of the component is included as well. As the total components cost is 31,261 €,

[2] Lilium GmbH. *Learn more about Lilium*. URL: `https://lilium.com/about-us` (visited on 01/13/2021)
[3] *Lilium Intercity and regional connectivity*. URL: `https://lilium.com/journey` (visited on 01/18/2021)

an estimate of €35,000 for total production costs.

Table 15.3: Production cost breakdown for one vehicle, based on all subcompenents, including manufacturing

Departments	Component	Cost p.p. [euros]	Quantity [-]	Total Costs [euros]
Power				
	Battery cells	10	640	6144
	Motor Controller	953	8	7624
	Battery management system	270	4	1080
Propulsion				
	Propeller blades	113	8	906
	Motor	1200	8	9600
	Propeller hubs	51	8	407
Structures				
	Beams	22	4	88
	Inner Hinge	41	4	162
	Outer hinge	41	4	162
	Battery casing	21	1	21
	Motorised robot hinge	1026	4	4104
	Landing gear	150	1	150
	Wind shield	160	1	160
	Module frame	158	1	158
	Front skin	150	1	150
	Top skin	150	1	150
	back skin	3	1	3
	Left/right skin	3	2	6
Stability & Control				
	Lidar sensor	130	1	130
	IMU (includes magenetometer)	38	1	38
	Barometer	5	1	5
	GPS	14	1	14
Total costs				**31261**

15.2. Yearly Profit per Vertiport

This section analyses the incomes and yearly costs consisting of staff and reduction of vehicle value.
Income Incomes come solely by the incomes of the user, in which they pay for a certain time period for a vehicle. The following payment system is though off:

- Per hour : €5 ($1/4$ from daily fee, to assume more than 4 hours is a daily rent)
- Per day : €20 (Fixed due to client requirement)
- Per week-end : 35 € (2x day with 5 € discount)
- Per Working-week : 90 € (5x day with €10 discount)
- Yearly subscription : €5000 (Fixed due to client requirement)

The next step is to assume a certain distribution of these pricing options. After that, for the yearly option, an estimation must be made how much is the subscription is used, or in other words how many people 'share' one vehicle on average. This is assumed to be 5 person as a guesstimate, as car sharing service Greenwheels shares 24 persons per car [4]. For this system, it is less as users might rely on using the vehicle almost daily. A user might use it multiple days per week, or don't use it much in the first place.

[4] *Greenwheels, Corporate car sharing*. URL: `https://www.greenwheels.nl/en-us/business` (visited on 01/18/2021)

Staff Costs Looking at staff, three types are analysed: Service staff, Maintenance staff and ground pilot staff. To asses the costs, salary, holiday pay and employee insurance were taken into account. For service staff, Dutch gross minimum wage was assumed, being 1700 per month. For maintenance and ground pilots, 3000 monthly gross salary was assumed. Assuming full-time work, the following staff costs were found:

Table 15.4: Staff Costs, including gross salary, 8% holiday pay and staff insurance

	Monthly	Yearly	n Available
Salary Service Staff	€ 2,022.75	€ 24,273.00	2
Salary Ground Pilots	€ 3,448.33	€ 41,380.00	1
Salary Maintenance Staff	€ 3,448.33	€ 41,380.00	1
Total Staff costs	€ 10,942.17	€ 131,306.00	

Vehicle Reduction in Value As also assumed mainly on the battery and motors in subsection 11.4.2, the vehicle is expected to last at least 10 years. This leads to a reduction in value of 3500 € per year.
Energy Charging Costs Looking at the costs per kWh (assumed 0.23 € [5]) and using the entire battery capacity of 48.9 kWh, the price of an entire charge is 11.15 €. This is not part of the cost breakdown, as the user pays separately for battery charging.

Yearly Profit per Vertiport The total yearly vertiport costs and incomes are summarised in the next table. It leads to a yearly profit of almost 3 million €.

Table 15.5: Yearly costs, per vertiport

	Mean	Best Case	Worst Case
Income	€ 4,000,000.00	€ 4,500,000.00	€ 3,500,000.00
Yearly Personell costs Vertiport	€ 262,612.00	€ 262,612.00	€ 262,612.00
Maintenance Center Staff	€ 51,725.00	€ 51,725.00	€ 51,725.00
Reduction in Vehicle Value	€ 700,000.00	€ 350,000.00	€ 1,050,000.00
Profit Yearly	**€ 2,985,663.00**	**€ 3,835,663.00**	**€ 2,135,663.00**

15.3. Return of Investment

When knowing the profit per year for one vertiport, one can look at after how many years and how many vertiports, intitial costs are balanced with yearlt profit. reaching a break even point.

15.3.1. Scaling

In order to make profit and balance the high investment (building vertiports and development), scaling up is critical. As the production of at least a 1000 units each year is a requirement, it creates the opportunity to scale-up. It is assumed that, with 200 vehicles per vertiport, a number of 5 vertiports are created each year.

Aside from production, other bottlenecks of growth are investment money for vertiports, and areas where market demand is high enough. Already discussed in chapter 2, it is suggested that markets are possible, though hard to predict.

For looking at the break even point, the investment costs can be plotted against the best, worse and mean case of profit. Figure 15.2 shows that for the expected 'mean' case, it is 12 years. One option to shorten the period until profit is to increase production, letting the company grow even more. As shown in Figure 15.3, when producing 5000 vehicles each year, profit is made after 8 years.

[5] DutchNews.nl. *After a €30 rise in January, Dutch energy prices among highest in EU*. URL: `https://www.dutchnews.nl/features/2019/05/after-a-e30-rise-in-january-dutch-energy-prices-among-highest-in-eu/` (visited on 01/19/2021)

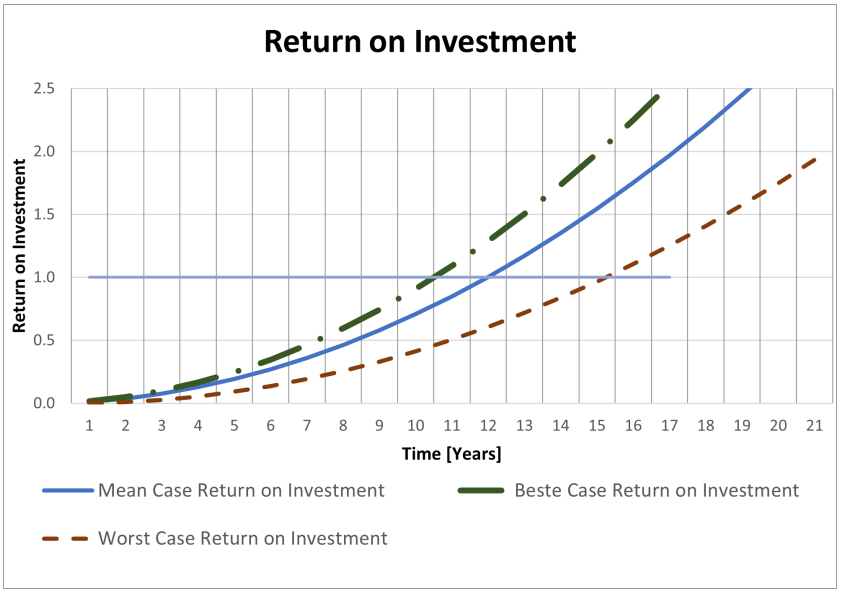

Figure 15.2: Return of investment after number of years for 1000 units produced per year

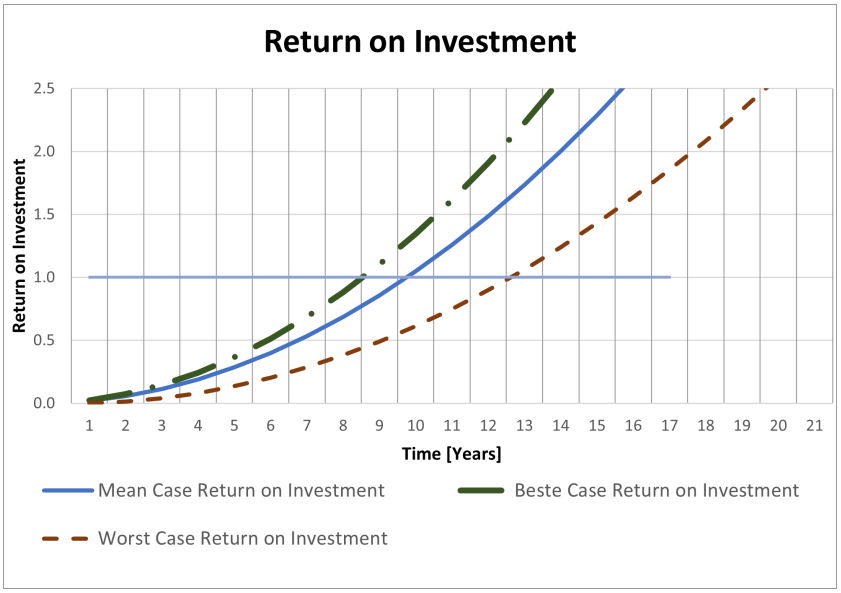

Figure 15.3: Return of investment after number of years for 5000 units produced per year

16
Future of the Project

Since this report is the last one for this project, it is important to look at what is ahead to complete the design and get the system into service. A design and development logic is set out first, to get a sense of all the tasks to be executed. These tasks are then planned over the estimated development period of 10 years.

16.1. Design and Development Logic

During this project a conceptual design has been worked out, that has to be worked out further into a product to go into service. Firstly, the conceptual design has to be worked out into a preliminary design. Similar methods to this report's can be used to get to that step. The steps after the preliminary design are laid out in Figure 16.1 and explained in this section.

After finishing the preliminary design, it is time to work this out into a detailed design. Multiple steps are to be executed and iterated to achieve this.

Firstly, the models from the preliminary design have to be worked out further to get increase the certainties of the system. These detailed models can then be run through numerous simulations. These simulations include aerodynamic flow analyses, structural analysis and control simulations. These simulations will then serve to assess the performance of the system in terms of the requirements.

After this performance assessment, an iteration of the design may be required, as not all requirements are met. This is kicked off by a revision of the trade-offs and then going back into creating detailed models. When all requirements are found to be met in the performance assessment, iterations may be halted. At this point the detailed design milestone is reached and the next phase of the further development can be started.

With the detailed design, a production plan can be set up. The first step in this second stage is to determine the production methods required to manufacture and assemble the parts of the product. With the production methods determined, tools needed for these methods can be found or specially designed. It is desirable to use existing tools to lower cost needed for design and worker training. Specially designed tools also have the downside of less universal maintenance options later in the product's lifecycle. The final step is to actually plan the production. This involves laying out the logistics, order of operations and production line layout among other aspects.

With a detailed design and production plan in place, a series of testing and validation action are to be taken. This is an important phase, as it will show that the design works as intended and is able to comply to all requirements. Firstly, one or multiple prototypes are to be produced. The amount of prototypes is highly dependant on the amount and nature of the intended tests to be done. With the prototype(s), tests are executed and the results can then be used for validation of the product.

At this point, the validation might show that there is still need to iterate the design, for the physical product to meet the requirements. The performance is then to be reassessed and the detailed design process should be repeated from that point. In case the validation does pass, a final design is achieved, which can be moved to the certification stage of the process.

The certification process is an important step for any aerospace vehicle, as it proves the correct functioning and safety to authorities and plays an important role in future operations. A flight test campaign is to be executed that proves all aspects to achieve airworthiness. During these tests, the documentation for certification should be filed as well. After these steps, either the certification of the product is received or the design should be iterated on once more.

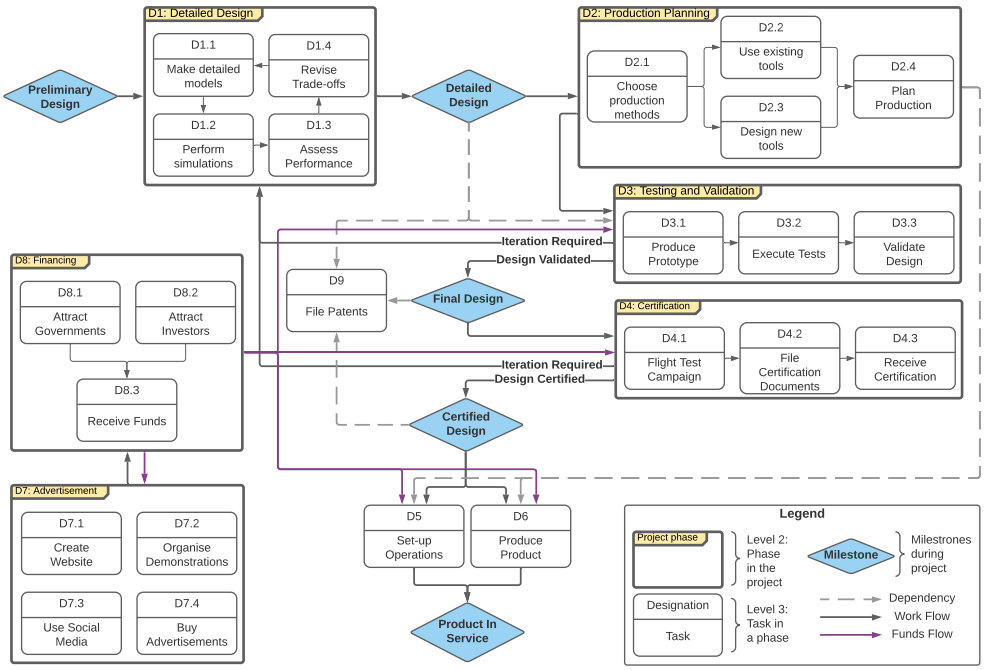

Figure 16.1: Flow diagram of the design and development logic.

With the now certified product design, the operations can be set up and full production can be started. The operations that have been previously described, require a few steps of their own to get in order. Infrastructure needs to be built and personnel has to be hired and trained. The production is to be done according to the latest production plan. After these steps, the product can go into service.

During the design phases, it is important that the system is properly documented. This is needed for both the production and certification. It is also important to file patents for newly invented or designed mechanisms, to keep the competition from using important design aspect of the product. Documentation is a continuous task and should be tracked properly.

Another continuous task is advertisement for the product. There are a multitude of ways to do advertising in the modern age. A website should be created to convey detailed information to potential customers and other stakeholders of the product. Social media can be used to keep people up-to-date on current progress of the project and to attract customers and investors. Advertisements can also be bought to reach a wider public and get them warmed up to the advantages of the using the system. Lastly, demonstrations can be organise to show the potential of the system. This is a method for later in the development process, as it requires a functioning product.

All this advertisement is aimed mainly at attracting costumers, but also at attracting governments and investors to spark their interest. The goal is to receive funds to continue the development process. These funds are primarily needed to afford the production of prototypes, testing equipment, the initial set up of operations and the initial production.

This is a surface level plan on how to get from the end of this project to an actual product in service. As mentioned in subsection 15.1.1, this process is estimated to take around 10 years. All the steps mentioned above are planned over these years in the next section.

16.2. Project Gantt Chart

The logical order of tasks to be performed during the 10 year development is presented below. Here, each vertical divider represents a month. 9 years have been scheduled between the period of February 2021 till February 2030 giving the development 1 year extra in case of delay or scheduling errors. For the details of the production plan, see chapter 14 as the production is a continuous production line.

D&D

D1: Detailed Design
- D1.1: Make detailed models
- D1.2: Perform simulations
- D1.3: Assess Performance
- D1.4: Revise trade-offs
- Detailed Design

D2: Production planning
- D2.1: Choose production methods
- D2.2: Use existing tools
- D2.3: Design new tools
- D2.4: Plan production

D3: Testing & validation
- D3.1: Produce prototype
- D3.2: Execute tests
- D3.3: Validate design
- Final Design

D4: Certification
- D4.1: Flight test campaign
- D4.2: File certification documents
- D4.3: Receive certification
- Certified design

D5: Set-up operations
- D5.1: Build maintenance center
- D5.2: Build communications center
- D5.3: Build vertiports
- D5.4: Set-up user-training
- D5.5: Hire employees
- D5.6: Train employees

D6: Produce product
- D6: Production (max. 1000 units - See production plan)

D7: Advertisement

D8: Financing
- D8.1: Attract government
- D8.2: Attract investors
- D8.3: Receive funds: design and prototype
- D8.3: Receive funds: flight test campaign
- D8.3: Receive funds: Operations/production

D9: File patents
- D9: File patents
- Product in service

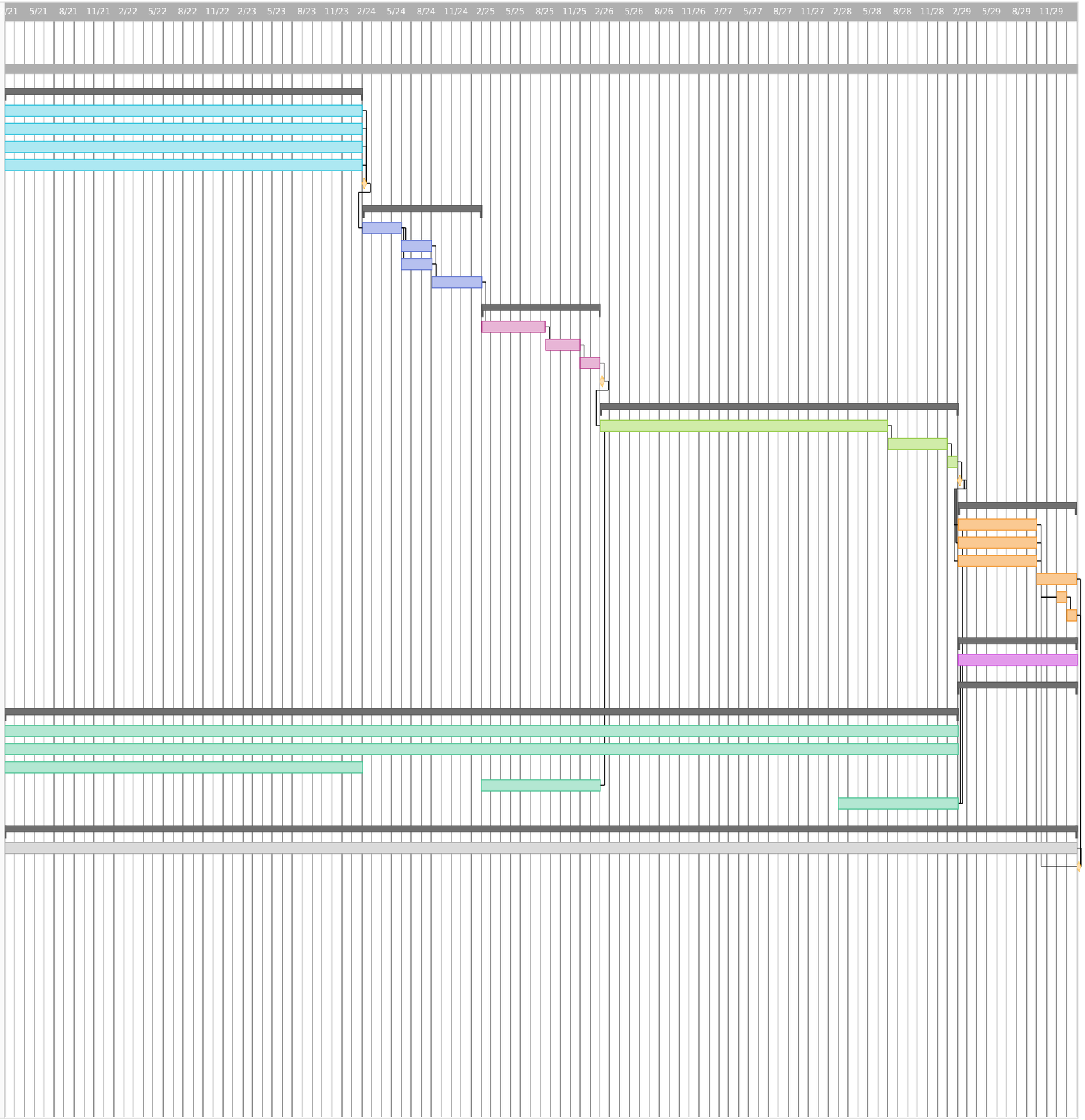

Bibliography

[1] DSE Fall 2020 group 5. *Project Plan - Personal Air Transportation*. 2020.

[2] Giovanni Huisken. “Inter-urban short-term traffic congestion prediction”. In: (2006).

[3] European Environment Agency. *Is passenger transport becoming more efficient?* Occupancy rates of passenger vehicles. 2015.

[4] A Kampert and J Nijenhuis. *The Dutch and their Cars (Nederlanders en hun auto’s)*. 2017.

[5] Davide Pu. “Zip Vehicle Commuter Aircraft Demand Estimate: a Multinomial Logit Mode Choice Model”. In: (2014).

[6] Raoul Rothfield. “Initial Analysis of Urban Air Mobility’s Transport Performance in Sioux Falls”. In: (2018).

[7] *MOBILITY SERVICES REPORT 2020, Statista Mobility Market Outlook*. 2020.

[8] Colleen Reiche, Rohit Goyal, and Adam Cohen. “Urban Air Mobility Market Study”. In: (Nov. 2018).

[9] Porsche Consultancy. *The Future of Vertical Mobility, Sizing the market for passenger, inspection, and goods services until 2035*. 2018.

[10] Emergen Research. *Urban Air Mobility Market By Component (Infrastructure, Platform), By Operations (Piloted, Autonomous, Hybrid), By Range (Intercity, Intracity), and By Region, Forecasts to 2027*.

[11] K. O. Ploetner and C. Al Haddad. *Long□term application potential of urban air mobility complementing public transport: an upper Bavaria example*. 2020.

[12] DSE Fall 2020 group 5. *Midterm Report - Personal Air Transportation*. 2020.

[13] W. Z. Stepniewski and C.N. Keys. *Rotary-Wing Aerodynamics (Dover Books on Aeronautical Engineering)*. Dover Publications, 1984.

[14] Alessandro Bacchini and E. Cestino. “Electric VTOL Configurations Comparison”. In: *Aerospace* 6 (Feb. 2019), p. 26. DOI: 10.3390/aerospace6030026.

[15] C.P. Coleman. “A Survey of Theoretical and Experimental Coaxial Rotor Aerodynamic Research”. English. In: (1997).

[16] Granta Design Limited. *CES Edupack software*. Cambridge, UK. 2019.

[17] J. T. Warner. *The handbook of lithium-ion battery pack design: Chemistry, components, types and terminology*. Elsevier Science, 2015.

[18] NASA Aerospace Battery. *650 Wh/kg, 1400 Wh/L Rechargeable Batteries for New Era of Electrified Mobility*. 2018.

[19] Jeffrey D. Sinsay et al. *Air Vehicle Design and Technology Considerations for an Electric VTOL Metro-Regional Public Transportation System*. 2012.

[20] Dr. Zian Qin. *Introduction To Electrical Power Engineering*. 2020.

[21] Tianyuan Zhao. *Propulsive Battery Packs Sizing for Aviation Applications*. May 2018.

[22] Ryan Mckay, Michael Kingan, and Sung Tyaek Go. “Experimental investigation of contra-rotating multi-rotor UAV propeller noise”. In: (Nov. 2019).

[23] Federal Aviation Administration. *Helicopter Flying Handbook (FAA-H-8083-21B)*. FAA Self-published, 2020. URL: https://www.faa.gov/regulations_policies/handbooks_manuals/aviation/helicopter_flying_handbook/media/hfh_ch07.pdf.

[24] R.C. Hibbeler. *Mechanics of Materials*. Pearson, 2014.

[25] Federal Aviation Administration. *PART 25 AIRWORTHINESS STANDARDS: TRANSPORT CATEGORY*. FAA Self-published, 2020. URL: https://www.engineerstoolkit.com/Airworthiness.

[26] European Aviation Safety Agency. “Certification Specifications for Small Rotorcraft CS-27”. In: (2012).

[27] R. B. Montgomery. “Viscosity and thermal conductivity of air and diffusivity of water vapor in air”. In: *Journal of Meteorology* 4.6 (Dec. 1947), pp. 193–196. ISSN: 0095-9634. DOI: 10.1175/1520-0469(1947)004<0193:VATCOA>2.0.CO;2. eprint: https://journals.ametsoc.org/jas/article-pdf/4/6/193/3691666/1520-0469(1947)004_0193_vatcoa_2_0_co_2.pdf. URL: https://doi.org/10.1175/1520-0469(1947)004%3C0193:VATCOA%3E2.0.CO;2.

[28] E. Achenbach. “Experiments on the flow past spheres at very high Reynolds numbers”. In: *Journal of Fluid Mechanics* 54.3 (1972), pp. 565–575. DOI: 10.1017/S0022112072000874.

[29] A. Roshko. “Experiments on the flow past a circular cylinder at very high Reynolds number”. In: *Journal of Fluid Mechanics* 10.3 (1961), pp. 345–356. DOI: 10.1017/S0022112061000950.

[30] V. Chai et al. “A model for the aerodynamic coefficients of rock-like debris”. In: *Comptes Rendus Mécanique* 347.1 (2019), pp. 19–32. ISSN: 1631-0721. DOI: https://doi.org/10.1016/j.crme.2018.10.001. URL: http://www.sciencedirect.com/science/article/pii/S1631072118302225.

[31] H. B. Jiang, Y. R. Li, and Z. Q. Cheng. “Relations of Lift and Drag Coefficients of Flow around Flat Plate”. In: Applied Mechanics and Materials 518 (May 2014), pp. 161–164. DOI: 10.4028/www.scientific.net/AMM.518.161.

[32] L. Ong and J. Wallace. “The velocity field of the turbulent very near wake of a circular cylinder”. In: *Experiments in Fluids* 20.6 (Apr. 1996), pp. 441–453. ISSN: 1432-1114. DOI: 10.1007/BF00189383.

[33] W. Terra, A. Sciacchitano, and F. Scarano. “Evaluation of aerodynamic drag of a full-scale cyclist model by large-scale tomographic-PIV”. English. In: (2016). International Workshop on Non-Intrusive Optical Flow Diagnostics ; Conference date: 25-10-2016 Through 26-10-2016. URL: http://nioplex.eu/?tribe_events=nioplex-international-workshop-on-non-intrusive-optical-flow-diagnostics.

[34] W. Terra, A. Sciacchitano, and Y. H. Shah. “Aerodynamic drag determination of a full-scale cyclist mannequin from large-scale PTV measurements”. English. In: *Experiments in Fluids: experimental methods and their applications to fluid flow* 60.2 (Feb. 2019). ISSN: 0723-4864. DOI: 10.1007/s00348-019-2677-6.

[35] J.A. Mulder et al. *Lecture Notes AE3202 - Flight Dynamics*. Unknown: Delft University of Technology, 2013.

[36] Prof. Jonathan P. How and Prof. Emilio Frazzoli. *Feedback Control Systems*. Massachusetts Institute of Technology: MIT OpenCouseWare. License: Creative Commons BY-NC-SA. Oct. 2010. URL: https://ocw.mit.edu/.

[37] Zoran Gajic. *Linear Dynamic Systems and Signals*. Unknown: Prentice Hall, 2003.

[38] Tim Clarke. “Flight Control for Rotorcraft”. In: *Encyclopedia of Aerospace Engineering*. Encyclopedia of Aerospace Engineering. John Wiley & Sons, Ltd, 2010, nil. DOI: 10.1002/9780470686652.eae266. URL: https://doi.org/10.1002/9780470686652.eae266.

[39] Chris Fielding. “Fly-by-Wire Flight Control Systems”. In: *Encyclopedia of Aerospace Engineering*. Encyclopedia of Aerospace Engineering. John Wiley & Sons, Ltd, 2010, nil. DOI: 10.1002/9780470686652.eae264. URL: https://doi.org/10.1002/9780470686652.eae264.

[40] Kevin A. Wise. “Adaptive and Robust Flight Control”. In: *Encyclopedia of Aerospace Engineering*. Encyclopedia of Aerospace Engineering. John Wiley & Sons, Ltd, 2010, nil. DOI: 10.1002/9780470686652.eae266. URL: https://doi.org/10.1002/9780470686652.eae266.

[41] Sanjiban Choudhury. *Iterative LQR & Model Predictive Control*. May 2019. URL: https://courses.cs.washington.edu/courses/cse490r/19sp/site/resources/.

[42] Andrzej Jezierski, Jakub Mozaryn, and Damian Suski. “A Comparison of LQR and MPC Control Algorithms of an Inverted Pendulum”. In: *Advances in Intelligent Systems and Computing*. Advances in Intelligent Systems and Computing. Springer International Publishing, 2017, pp. 65–76. DOI: 10.1007/978-3-319-60699-6_8. URL: https://doi.org/10.1007/978-3-319-60699-6_8.

[43] Joel Huebner. *Choices, choices, choices*. URL: http://smallformfactors.mil-embedded.com/articles/choices-choices-choices/.

[44] E. Okyere et al. “LQR controller design for quad-rotor helicopters.” In: *The Journal of Engineering* 17 (2019). DOI: 10.1049/joe.2018.8126.

[45] Sanjiban Choudhury. *Linear Quadratic Regulator*. May 2019. URL: https://courses.cs.washington.edu/courses/cse490r/19sp/site/resources/.

[46] Michael Blattau. *Design for Reliability for Connectors: A Review of Failure Modes and Mitigations*. Design for Reliability Conference. Mar. 2019.

[47] Alan C. Tribble, Steven P. Miller, and David L. Lempia. *Software Safety Analysis of a Flight Guidance System*. Tech. rep. Rockwell Collins, Inc., 2004.

[48] Akshay Mathur et al. “Paths to Autonomous Vehicle Operations for Urban Air Mobility”. In: *Annalen der Physik* (June 2019). DOI: 10.2514/6.2019-3255.

[49] *Interface Control Document for Safeguard Units*. 2020.

[50] C.D. Wickens et al. *An introduction to human factors engineering*. Pearson, 2004.

[51] J. Rasmussen. “Skills, rules, and knowledge; signals, signs, and symbols, and other distinctions in human performance models”. In: (1983). URL: https://www.iwolm.com/wp-content/downloads/SkillsRulesAndKnowledge-Rasmussen.pdf.

[52] International Civil Aviation Organization. *Aerodromes, International Standards and Recommended Practices, Annex 14, Volume II: Heliports*. 2009.

[53] Uber. *Fast-Forwarding to a Future of On-Demand Urban Air Transportation*. 2016.

[54] R.J. Hamann and M.J.L. van Tooren. *Systems engineering and technical management techniques - part I*. Delft University of Technology, 2006.

[55] Heriberto Cabezas and Urmila Diwekar. *Sustainability : Multi-Disciplinary Perspectives*. Bentham Science Publishers, 2012.

[56] Mary Ann Curran. *Life Cycle Assessment Student Handbook*. John Wiley and Sons, Incorporated, 2015.

[57] Institute for Environment European Commission Joint Research Centre and Sustainability. *ILCD Handbook: General guide for Life Cycle Assessment - Detailed guidance*. JPublications Office of the European Union, 2010.

[58] Francesca Recanati and Andreas Ciroth. *Environmental Footprint secondary data for openLCA*. 2019.

[59] A. Azapagic, A. Emsley, and L. Hamerton. *Definition of Environmental Impacts*. 2003.

[60] K. Ilacker, D Souza, and S Sala. “Land use impact assessment in the construction sector: an analysis of LCIA models and case study application”. In: *Int J Life Cycle Assess* 19 (2014), pp. 1799–1809. DOI: https://doi.org/10.1007/s11367-014-0781-7. URL: https://link.springer.com/article/10.1007/s11367-014-0781-7#citeas.

[61] European Commission. *ENVIRONMENTAL IMPACTS ANALYSED AND CHARACTERISATION FACTORS*.

[62] Xin Sun et al. “Life cycle assessment of lithium nickel cobalt manganese oxide (NCM) batteries for electric passenger vehicles”. In: *Journal of Cleaner Production* 1 (2020). DOI: https://doi.org/10.1016/j.jclepro.2020.123006.

[63] *RE-USE AND RECYCLING OF DIFFERENT ELECTRICAL MACHINES*. 2018.

[64] D.R. Kiran. “Reliability Engineering”. In: *Total Quality Management* (2017), pp. 391–404. DOI: https://doi.org/10.1016/B978-0-12-811035-5.00027-1. URL: http://www.sciencedirect.com/science/article/pii/B9780128110355000271.

[65] Richard Quinnell. *Designer's Guide: Safety-critical processors - Electronic Products*. 2018. URL: https://www.electronicproducts.com/designers-guide-safety-critical-processors/#.

[66] Embedded Staff. *Safety-Critical Operating Systems - Embedded.com*. 2001. URL: https://www.embedded.com/safety-critical-operating-systems/.

[67] Adam C. Cobb, Jennifer E. Michaels, and Thomas Michaels. "Ultrasonic structural health monitoring: A probability of detection case study". In: (Mar. 2009).

[68] Ir. J. Sinke. *Production of Aerospace Systems, Costs and Lean Manufacturing*. 2019.

[69] M.F.R. Zwicker et al. "Automotive battery pack manufacturing – a review of battery to tab joining". In: (Nov. 2020).